THE UNIVERSITY OF HULL

Identification and Functional Characterization of the Mitochondrial Adenine Nucleotide Carriers of *Trypanosoma brucei*

being a Thesis submitted for the Degree of Doctor of Philosophy

in the University of Hull

by

Carmen Priscila Pena Diaz,

Licenciada en Biologia

March 2011

Abstract

The Mitochondrial Carrier Family encloses a group of transmembrane proteins that transport metabolites across the mitochondrial inner membrane. The ADP/ATP carrier is the most widely studied MCF protein. It catalyzes the counter exchange of ADP for ATP in the mitochondrion of all eukaryotes. In the genome of the kinetoplastid parasite *Trypanosoma brucei,* three putative ADP/ATP carrier sequences (MCP5, MCP15 and MCP16) and one GDP/GTP (MCP13) entries were analyzed by sequence analyses and phylogenetic reconstruction. AACs phylogenetic reconstruction proved a strong association with yeast, funghi and plant clades, whilst separates from those AACs and from metazoans. MCP13 groups with GGCs, seems to be present only on lower eukaryotes and do not seem to present any homologues in metazoans. Gene deletion studies were performed to assess the roles of MCP5, MCP15, MCP16 and 13. A conditional double knockout cell line, with an inducible myc-tagged rescue copy was constructed for MCP5, which proves the essentiality of the protein for the parasite. Growth curves of the mutant cell line proved a growth defect phenotype in various carbon sources conditions. Mitochondrial ATP production assays were performed in the mutant cell line, in presence and absence of the inducible protein, using permeabilized cells with digitonin that confirmed the ADP/ATP transport activity of the carrier. For in-vitro activity assays, the carriers were cloned and expressed in *Escherichia coli* and *Spodoptera frugiperda,* solubilised and reconstituted into liposomes. Unfortunately, the reconstitution was unsuccessful and the conditions and methodologies are discussed.

Table of Chapters

Abbreviations

2D BN/SDS-PAGE	Two-Dimensional Blue Native/ SDS- Polyacrylamide Gel Electrophoresis
^{31}P-NMR	Nuclear Magnetic Resonance with Phosphorus 31
AAB	ATP Assay Buffer
AAC	ADP/ATP Carrier
AceCS	Acetyl CoA synthetase
ADP	Adenosine diphosphate
AMP	Adenosine monophosphate
ANT	Adenine Nucleotide Transporter
ASCT	Acetate: Succinate CoA Transferase
ATP	Adenosine Triphosphate
ATR	Atractyloside
BKA	Bonkretate or Bonkrekic acid
BLA	Blasticidin
BLE	Phleomycin
BSF	Bloodstream form
CAT	Carboxyatractyloside
CDP-Etn	Cytidine Diphosphate Ethanolamine
CIAP	Calf Intestinal Alkaline Phosphate
CL	Cardiolipin
CMP	Cytidine Monophosphate
CNS	Central Nervous System
COX	Cytochrome C Oxidase
CPI II III	Contact Points I, II and III
dA,G,TP	Deoxy Adenine Guanosine Triphosphate
DAPI	4',6-diamidino-2-phenylindole
dCTP	Deoxy-Cytidine Triphosphate
DNA	Deoxyribonucleic Acid
ECL	Enhanced Chemiluminiscence
EK	Ethanolamine Kinase
ET	Ethanolamine Phosphate Cytidyltransferase
FCCP	Carbonylcyanide p-trifluoromethoxyphenylhydrazone
FCS	Foetal Calf Serum
FRD	Fumarate Reductase
G-3-PDH	Glycerol-3-Phosphate Dehydrogenase

G6PDH	Glucose-6-Phophate Dehydrogenase
GDMP	Glucose Depleted MEM-Pros
GDP	Guanosine Diphosphate
GGC	GDP/GTP Carrier
GPI	Glycosylphosphatidylinositol
GTP	Guanosine Triphosphate
HAT	Human African Trypanosomiasis
HYG	Hygromycin
IFA	Immunofluorescence Microscopy
IgG	Immunoglobulin G
IPTG	Isopropyl-beta-D-thiogalactopyranoside
K-Pi	Potassium Phosphate
KDH	2-Ketoglutarate Dehydrogenase
KO	Knockout
KOH	Potassium Hydroxide
LB	Luria-Bertani Medium
MCF	Mitochondrial Carrier Family
MCP	Mitochondrial Carrier Protein
MEM-Pros	Minimum Essential Medium with Proline
MOI	Multiplicity of Infection
MOPS	3-(N-morpholino)propanesulfonic acid
MPglu	MEM-Pros + 5mM glucose
mRNA	Mitochondrial Ribonucleic Acid
mtDNA	Mitochondrial Deoxyribonucleic Acid
MTP	Mitochondrial Transition Pore
NAD^+	*Nicotinamide Adenine Dinucleotide Oxidized*
NADH	*Nicotinamide Adenine Dinucleotide Reduced*
NADH-FRD	NADH-Dependent Fumarate Reductase
$NADP^+$	Nicotinamide Adenine Dinucleotide Phosphate oxidized
NADPH	Nicotinamide Adenine Dinucleotide Phosphate reduced
NEO	Neomycin
Ni-NTA	Nickel-Nitriloacetic Acid
NMP	Normal MEM-Pros
O.D.	Optical Density
OGC	Oxoglutarate Carrier
ORF	Open Reading Frame

OXPHOS	Oxidative Phosphorylation
PBS	Phosphate Buffer Saline
PC	Phosphatidylcholine
PCF	Procyclic Form
PCR	Polymerase Chain Reaction
PE	Phosphatidyletanolamine
PEP	Phosphoenolpyruvate
PEX	Peroxisome Biogenesis Factor Protein
PiC	Phosphate Carrier
PL	Phospholipid
PPDK	Pyruvate Phosphate Di-Kinase
PUR	Puromycin
RNA	Ribonucleic Acid
RNAi	Ribonucleic Acid Interference
Sal1p	Suppressor of *aac2* lethality
SBCGP	Single Binding Center Gated Pore Mechanism
SDM-79	Semi-Defined Medium 79
SDS	Sodium Dodecyl Sulphate
SDS-PAGE	Polyacrylamide Gel Electrophoresis in Sodium Dodecyl Sulphate
SoTE	Sorbitol Tris EDTA buffer
SSC	Saline-Sodium Citrate buffer
SUBPHOS	Substrate-Level Phosphorylation
TAE	Tris Acetate EDTA buffer
TB	Terrific Broth
TCA	Trycarboxylic Acid
TIM	Translocating Inner Membrane protein
tRNAs	Transference Ribonucleic Acid
UCP	Uncoupling Protein
UMP	Uridine Monophosphate
UTR	Untranslated Region
VDAC-ANT-CyP-D	Voltage Dependent Anion Carrier- Adenine Nucleotide Transporter- Cyclophylin D complex
VSG	Variant Surface Glycoprotein
WB	Western Blot
WT	Wild Type

Table of Contents

Chapter I. Introduction

1. *Trypanosoma brucei* and Sleeping Sickness

Trypanosoma brucei is the causative agent of Sleeping Sickness or Human African Trypanosomiasis (HAT). It is a fatal disease for which no suitable treatment has been found and affects around 300,000 people (WHO, 2010). Around 16,000 new cases are still reported every year by the World Health Organization (WHO). *Trypanosoma brucei* is represented by three sub-species: *i.e. T.b. gambiense* and *T.b. rhodesiense*, both are human infective and cause what is known as West African and East African Sleeping Sickness, respectively (Kennedy, 2004; Rodgers, 2009). A third sub-species of the parasite *T. b. brucei*, causes Nagana in cattle, which represents a major agro industrial problem in Northern Africa, due to economical losses in the region (WHO, 2010).

The clinical manifestations of Sleeping Sickness vary according to the different forms of the disease: West African Sleeping Sickness is a chronic disease that lasts from months to years, whereas East African Sleeping Sickness has an acute course of weeks to months duration (Rodgers, 2009). 90% of Sleeping Sickness cases reported belong to the West African type, with the remaining 10% to the East African variation (Simarro *et al.*, 2008). The progress of Sleeping Sickness can be divided into two different stages. The first stage of the disease, also called the haemolymphatic stage, shows symptoms like fever, headaches and lymph nodes enlargement. The infection may also invade tissues like spleen, heart and liver, before reaching the central nervous system (CNS), where stage 2 of the disease commences (Rodgers, 2009). Stage 2 of Sleeping Sickness is characterized by the presence of parasites in the cerebrospinal fluid and the start of the disease-typical symptoms, including lethargy, sensory disturbance, confusion, disrupted sleeping patterns and coma (Steverding, 2008). For *T. b. gambiense*, stage 2 of the infections might appear months or even years after initial infection, whereas stage 2 of *T. b. rhodesiense*-related Sleeping Sickness might manifest weeks to months after initial infection, and distinction between stage 1 and 2 might not be evident (Steverding, 2008; Rodgers, 2009; Barrett *et al.*, 2007).

1.1. Drug treatments for Sleeping Sickness

The four drugs mainly used for the treatment of Sleeping Sickness are Pentamidine, Suramin, Melarsoprol and Eflornithine (Barrett et al., 2007). The efficacy of these

drugs depend on whether the infection has reached the CNS or is still in the haemolymphatic stage 1 (Rodgers, 2009). Pentamidine is used to treat stage 1 of *T.b. gambiense*-related Sleeping Sickness. Suramin, a drug used since the 1920s is limited to the early stages of the disease because of its inability to cross the blood-brain barrier, and it is used to treat the stage 1 of *T.b. rhodesiense* infections (Kennedy, 2004; Barrett *et al.*, 2007). Both Pentamidine and Suramin cause severe secondary effects on the host. Eflornithine was developed in the 1980s as an anti-cancer drug and was registered in 1990 as a treatment for *T.b. gambiense* infections in the CNS-stage of Sleeping Sickness. Adverse effects are also related with Eflornithine therapy, but are usually reversible. Typical side effects are gastrointestinal problems, unusual bleeding and weakness, pancytopenia, thrombocytopenia and convulsions (Rodgers, 2009; Simarro et al., 2008). Melarsoprol is an organic arsenical and is the only drug available that can be used to treat both *T.b. gambiense* and *T.b. rhodesiense* infections in stage 2 of the disease (Barrett et al., 2007; Rodgers, 2009). Nevertheless its side effects are also severe: tachycardia, convulsions, coma and heart failure have been reported (Barrett et al., 2007; Rodgers, 2009). It is painful to administer, destroys veins after several applications and causes an overall mortality rate of 5% (Bacchi, 2009; Kennedy, 2004). The high toxicity of the mentioned drugs is one of the main problems related to the treatments, along with emerging drug resistance (Barrett et al., 2007; Simarro et al., 2008; Rodgers, 2009; Steverding, 2008).

The pattern of resistance to the drugs is related to their mode of action on the trypanosome biology, as well as on their route of entry into the parasite. Pentamidine and its diamidines structural analogues, enter the parasite mainly through the P2 transporter (aminopurine transporter), HAPT1 (high-affinity pentamidine transporter) and LAPT1 (low-affinity pentamidine transporter) (de Koning, 2001a; de Koning, 2001b). Although its mode of action is not completely clear, the di-cationic structure of Pentamidine has been reported to bind polyanionic molecules in the cell, where it interacts with nuclear and kinetoplast DNA (Simpson, 1986; Mathis *et al.*, 2007). Pentamidine has also been reported to inhibit plasma membrane proteins, such as Ca^{2+}-Mg^{2+} ATPases (Benaim *et al.*, 1993). In-vitro cell assays observed an initial accumulation of the synthetic diamidines DB75 and DB820 (Pentamidine analogues) in the mitochondrion of *T. brucei* immediately after the drug enters the cell, where it exerts a detrimental effect on the kinetoplast (Mathis *et al.*, 2007; Wilson *et al.*, 2008). DB75 has also been found to collapse mitochondrial membrane potential and inhibit the F_1F_0-ATPase (Lanteri *et al.*, 2008).

Once this effect takes place, these compounds seem to accumulate in the acidocalcisomes (Mathis *et al.*, 2006). Pentamidine resistance of *T. brucei* has been related to substrate affinity loss of the P2 (aminopurine transporter) transporter (Barrett *et al.*, 1995; Lanteri *et al.*, 2006). Suramin, a hexacharged polysulphonated napthylamine, enters the parasite via receptor-mediated endocytosis once it is bound to serum proteins, particularly LDL (low-density lipoprotein) (Voogd *et al.*, 1993; Coppens *et al.*, 1987; Vansterkenburg *et al.*, 1993). As expected from a very charged molecule, it is incapable to cross membranes, therefore its inability to cross the brain blood barrier and its subsequently inefficacy in the treatment of stage 2 of Sleeping Sickness. Although its mode of action is not completely clear, it has been hypothesized that Suramin inhibits glycosomal enzymes (Marché *et al.*, 2000; Hanau *et al.*, 1996). Resistance to Suramin does not seem to be common in the field whereas it has been observed in laboratory conditions and in animals infected with *Trypanosoma evansii* (El Rayah *et al.*, 1999; Barrett *et al.*, 2007). The resistance to Suramin has been hypothesized to be dependent on a trypanosomal Suramin-metabolism or a host drug-extrusion system similar to the one registered for the P-glycoprotein (de Koning, 2001a; Sanderson *et al.*, 2009).

Eflornithine (difluoromethylornithine or DFMO) is one of the two drugs commonly used for the treatment of *T.b. gambiense* –related stage 2 of Sleeping Sickness. Eflornithine site of entry was debated for years, and two possible mechanisms were suggested: 1) the drug enters the parasite via passive diffusion in bloodstream form cells (Bitonti *et al.*, 1986), whereas 2) the entry of the drug is mediated through active transport, which exhibited a Michaelis-Menten-type of uptake kinetics in procyclic forms of *T. brucei* (Phillips and Wang, 1987). However, the nature of the transporter remained unclear until very recently. The transporter was elucidated when RNAi of the TbAAT6 gene (amino acid transporter 6) developed resistance to the drug (Vincent *et al.*, 2010) Eflornithine acts as an irreversible inhibitor of ornithine carboxylase, an enzyme that catalyzes the decarboxylation of ornithine for the formation of putrescine in the pathway of synthesis of polyamines (Bacchi *et al.*, 1983). Inhibition of ornithine carboxylase leads to the accumulation of S-adenosyl-L-methionine, which is condensed with putrescine for the subsequent formation of spermidine (Byers *et al.*, 1991). Eflornithine inhibits both the ornithine carboxylase from trypanosomas and humans as well, with the only difference that the human enzyme has a faster turnover rate than the one found in *T.b. gambiense*, therefore making it less susceptible to the drug (de Koning, 2001a). The difference between *T.b. rhodesiense* and *T.b. gambiense* susceptibility to Eflornithine was also found to

be related to a higher turnover, as well as a higher specific activity of the ornithine carboxylase found in *T.b. rhodesiense* (Iten *et al.*, 1997).

Melarsoprol (or MelB) is a lipophilic arsenical-based compound by far the most toxic of all the 4 mainstream drugs used for the treatment of Sleeping Sickness; its use is limited to the stage 2 of *T.b. rhodesiense* infections (Barrett *et al.*, 2007). It is the only arsenical –based compound (melaminophenyl arsenical) still in use for the treatment of Sleeping Sickness; older arsenical-based compounds used in the early 20th century are not licensed for their use in humans, and only one, MelCy, has approval for veterinary treatment (de Koning, 2001a). It has been observed that *T. brucei* and *T. evansii* strains resistant to soluble melaninophenyl arsenicals present impaired transport activity of the P2 transporter (aminopurine transporter), therefore accounting the drug entry into the cells via mediated transport (Carter and Fairlamb, 1993). Moreover, a pentamidine resistant strain lacking HAPT1 (high-affinity pentamidine transporter) was also resistant to soluble melaminophenyl arsenical compounds (Bridges *et al.*, 2007). However there is controversy amongst melaminophenyl arsenical-resistant *T. brucei* strains that displayed sensitivity to Pentamidine, which is also transported into the cell through the P2 and HAPT1 transporters (Barrett *et al.*, 2007). Therefore, an alternative route of entry had to account for the drug entry in the cells, that was either a different transporter to those described for Pentamidine, or a completely different mechanism. The activity of Melarsoprol as observed in *in vitro* studies has been suggested to move across membranes through passive diffusion, due to its largely lipophilic structure, which makes it different to older and aqueous-soluble arsenical compounds, which might make use of Pentamidine transporters for their entry in the cell (Scott *et al.*, 1997). The drug may enter the cells by passive diffusion and mediated transport (Scott *et al.*, 1997; de Koning, 2001a). Melarsoprol site of toxicity in the cell is still largely uncertain. Fairlamb *et al.* (1989) suggested that trypanothione, the glutathione version in trypanosomas, mediated the toxicity of cyclic arsenicals in the parasite. Other authors suggested that Melarsoprol inhibited glycolysis, although this hypothesis was contradicted when ATP concentrations were found to be stable after drug-mediated parasite lysis (Van Schaftingen *et al.*, 1987).

The controversies regarding drug treatments for Sleeping sickness are mostly related to the extent of toxicity of the drugs for the host, together with the emerging resistant-strains in the field. The therapies are administered in high concentrations in order to avoid rapid resistant emergence, which does not improve the cytotoxic

effects on the host. Pentamidine is administered daily at a concentration of 4 mg/kg for 7-10 days (Barrett *et al.*, 2007). Whereas the drug displays *in vitro* IC_{50} values of approximately 10nM and kills the parasites over a period of three days under these conditions, *in vivo* concentrations of the drug are several orders of magnitude higher (Miezan *et al.*, 1994; Barrett *et al.*, 2007). Suramin is administered in 5 doses, via intravenous injection at concentrations of approximately 80 mg/kg, every 3-7 days, over a period of 4 weeks (Voogd *et al.*, 1993). These concentrations contrast with the *in vitro* concentrations needed to kill the parasites (only 1 μg/kg) in a 24-hours exposure assay (Barrett *et al.*, 2007). Eflornithine is administered via intravenous injection, every 6 hours for 14 days, at a concentration of 100 mg/kg (Barrett *et al.*, 2007). The reason the treatment with Eflornithine requires such frequency is that the half-life of the drug is approximately 3.3 hours in the host's plasma (Haegele *et al.*, 1981). Melarsoprol, on the other hand, is administered once a day for 10 days, via intravenous injection, at a concentration of 2.2 mg/kg (Pepin and Mpia, 2006).

Despite the efforts, drug-resistant strains are still found in the field, particularly regarding the drugs used in stage 2 of the disease. In order to address this, several trials of combination therapies have been performed to reduce the risk of developing drug resistance and further allow lower drug doses, thereby reducing the severity of the side effects. The use of Nifurtimox, a drug used for the treatment of American trypanosomiasis (caused by *Trypanosoma cruzi*), in combination therapy trials with Eflornithine and Melarsoprol seems to be the new available alternative (Steverding, 2008; Simarro *et al.*, 2008; Rodgers, 2009; Priotto *et al.*, 2009; Jeganathan *et al.*, 2011). Nifurtimox is a toxic nitrofuran that once metabolized into nitrile derivatives by the parasite, displays high cytotoxicity for both parasite and host cells (Hall *et al.*, 2011). Other studies have focused on the combination of Suramin with known antibiotics such as minocycline as an alternative to treat early stages of CNS parasite invasion in mice (Amin *et al.*, 2008). In 2007, a promising new drug effective for the treatment of stage 1 of Sleeping Sickness, called diamidine pafuramidine (DB289), a Pentamidine analogue, had finished phase III trials. However its severe side effects, e.g. liver toxicity and renal insufficiency- caused the program to be discontinued (Wenzler *et al.*, 2009; Steverding, 2010). Encouraging results were observed in a trial with Fexinidazole, a nitroimidazole compound from the family of metronidazole, a widely used antibiotic with apparently acceptable toxicity levels. The treatment *in vitro* and *in vivo* (in mice) of *T.b. gambiense* and *T.b. rhodesiense* with fexinidazole, eliminated the parasites even at late stage 2 of the infection (Torreele *et al.*, 2010). Also the pyrazole sulphonamide compound

named DDD85646, which acts as a N-myristoyltransferase inhibitor, has proved effective in eliminating the parasite *in vitro* and *in vivo* (in mouse models), indicating another future opportunity for therapy (Frearson *et al.*, 2010).

Some of the most encouraging results regarding advances in drug therapies are the ones observed in the drug research for *Trypanosoma cruzi* (Clayton, 2010). Amongst the various compounds in the outlook for treating Chagas disease are biphosphonates (Hudock *et al.*, 2006; Sanz-Rodríguez *et al.*, 2007) and a range of ergosterol biosynthesis inhibitors (EBI) (Urbina *et al.*, 2002; Urbina *et al.*, 2004; Urbina, 2009; Urbina, 2010; Paniz-Mondolfi *et al.*, 2009; Oldfield, 2010), representatives of the most forward-looking efforts in the race against trypanosomiasis in the last decades.

2. The kinetoplastid parasite *Trypanosoma brucei*

Trypanosoma brucei is a parasitic protozoan of the order Kinetoplastidae, which also includes *Trypanosoma cruzi*, the causative agent of American Trypanosomiasis and the *Leishmani*a species (which cause visceral and cutaneous Leishmaniasis) (Simpson *et al.*, 2006; Balmer *et al.*, 2011). *Trypanosoma brucei* belongs to the genus *Trypanozoon*, altogether with *Trypanosoma evansii* (which affects camels, horses, bovids and dogs) and *Trypanosoma equiperdum* (which infects horses) (Hoare, 1972; Gibson, 2003). Other trypanosoma species, like *Trypanosoma congolense*, *T. simiae* and *T. godfreyi,* from the subgenus *Nannomonas,* are parasites of a wide range of ungulate animals, and therefore represent a group of agricultural importance due to the great economical losses related to livestock infections (Gibson, 2003; Adams *et al.*, 2010). *Trypanosoma vivax,* from the genus *Dutonella* also infects a wide range of livestock (Adams *et al.*, 2010; Osorio *et al.*, 2008). All the species described above are known pathogens to animals and are transmitted by salivarian route (except *T. cruzi* which is transmitted through faecal route) (Hoare, 1972). It is noteworthy to mention that the taxonomy of the *Trypanosoma* species is still an area of debate, since new molecular techniques for taxonomical identification have modified old parameters of classification. An interesting example of this was the use of markers such as glyceraldehyde phosphate dehydrogenase for phylogenetic studies between species of the order *Kinetoplastidae,* once the sequencing of several of their genomes was completed a few years ago (Hamilton *et al.*, 2004).

2.1. The cell cycle of *Trypanosoma brucei*

Trypanosoma brucei is transmitted between mammalian hosts by an insect vector, i.e. the Tsetse fly, a member of the *Glossina* genus (Steverding, 2008). When the Tsetse fly takes an infected blood meal, the procyclic form (epimastigote) of the parasite divides by binary fission in the midgut before migrating to the salivary glands, where it subsequently differentiates into infective metacyclic trypomastigotes (Figure 1). Metacyclic trypomastigotes are transmitted into new mammalian hosts when the fly feeds again. Once in the mammalian bloodstream, the parasite is long and slender and divides until it has reached a parasitemia peak, followed by differentiation into the non-dividing short-stumpy form (Matthews, 2005). The parasite is able to survive in the host bloodstream through antigenic variation, by expressing a repeatedly changing coat of Variable Surface Glycoproteins (VSGs) (McCulloch, 2004). The life cycle is completed when a fly bites an infected host, ingesting the parasites in its blood meal, after which they begin to divide again in the midgut (Matthews *et al.*, 2004).

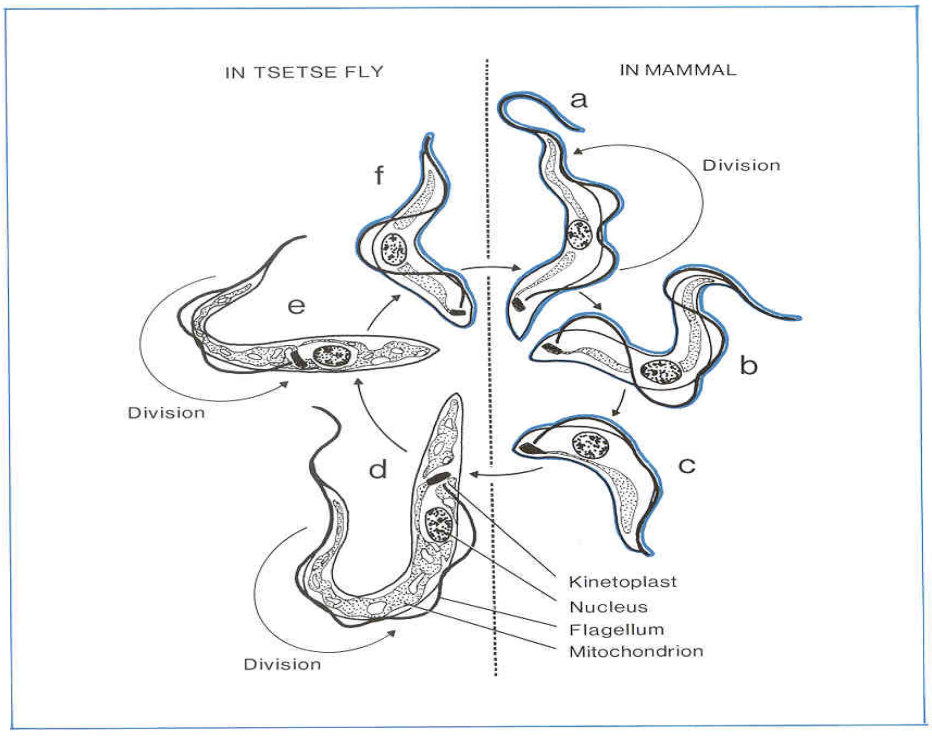

Figure 1. Schematic representation of the *Trypanosoma brucei* life cycle. After entering the mammalian bloodstream, the metacyclic trypomastigote form of the parasite (a) differentiates into the long-slender form (b), which is capable of division by binary fission. Division arrest takes place once parasitemia reaches a peak, and the parasite subsequently differentiates into the short-stumpy form (c). The short-

stumpy form trypanosome migrates to the fly midgut, where it differentiates into the procyclic form (d). The procyclic form is also capable of division by binary fission, like the long-slender bloodstream form. The procyclic form subsequently differentiates into the epimastigote form (e), which migrates to the Tse-tse fly salivary glands for their final differentiation into the infective metacyclic trypomastigote form (f). Infection of another mammalian host with metacyclic trypomastigote parasites completes the life cycle. http://www.ilri.org/InfoServ/Webpub/fulldocs/Ilrad90/Trypano.htm

The most striking changes in the morphology of the parasite throughout its life cycle are evident in the mitochondrial structure, the endocytic system and the glycosomes. When the fly ingests an infected blood meal, the short-stumpy bloodstream forms in the fly mid-gut rapidly change into procyclic forms, whereas the long-slender bloodstream form parasites die (Vickerman, 1985). These two stages, the long-slender and the short-stumpy bloodstream forms coexisting in one host is a phenomenon known as pleomorphism (Fenn and Matthews, 2007). The morphological changes are known to be triggered by temperature and pH changes, as well as the presence of citrate/cis-aconitate (Czichos *et al.*, 1986). These signals are related to the presence of a group of carboxylate transporters on the cell surface identified as PAD proteins (proteins associated with differentiation) (Dean *et al.*, 2009). The cell body length increases, particularly noticeable at the posterior end of the cell, after the kinetoplast; the mitochondrion relative volume increases from 5 to 25% and displays discoid cristae, rather than the tubular structure of the bloodstream form mitochondrion; the glycosomes become bacilliform-like structures; and the VSG (Variable Surface Glycoprotein) coat is replaced by the procyclin glycoproteins on the cell surface (Vickerman, 1985; Roditi and Clayton, 1999). The morphological changes of the short-stumpy bloodstream form into procyclic form take place within 24 hours after the ingestion of the infected blood meal, in the endoperitrophic space, at the posterior part of the fly midgut (Sharma *et al.*, 2009; Vickerman, 1985). All the changes described above translate into a metabolic shift of carbon source usage from the glucose-rich environment of the bloodstream of mammal host to the amino acid-rich fly gut (Overath *et al.*, 1986). The development of the mitochondrion is key for the parasites to perform this metabolic shift (Brown *et al.*, 1973).

The procyclic form parasites then migrate to the ectoperitrophic space of the midgut of the fly, where they continue to divide and eventually, after 9-14 days after initial infection, a series of changes commence in the morphology of the parasite's cell body (Vickerman, 1985; Gibson and Bailey, 2003). The mitochondrion volume starts reducing in volume, the cell body elongates and cell division ceases (Sharma *et al.*, 2009). These parasite forms are known as proventricular mesocyclics due to the fact that they migrate forward towards the proventriculus of the fly, and seem to be the form that further migrates towards the salivary glands of the fly, for their subsequent transformation into epimastigote forms (Vickerman, 1985). Differentiation into epimastigotes is achieved via an asymmetric division that produces two different types of daughter cells: a long and a short epimastigote cell. The most striking feature of this difference is the presence of a very short flagella in the short epimastigote, and the fact that the long epimastigote cell dies (Sharma *et al.*, 2008).

Little is known about the signalling that induces the migration towards the salivary glands and the differentiation into epimastigote and metacyclic forms (Roditi and Lehane, 2008; Sharma *et al.*, 2009). The epimastigotes are the main replicative form found in the salivary glands of the fly. One of the structural traits of this stage is the loss of the procyclin coat, which is replaced by BARP proteins (brucei alanine-rich proteins) (Urwyler *et al.*, 2007). Epimastigotes division seems to require the attachment to the epithelial cells' microvilli, via the flagellum of the parasite (Vickerman *et al.*, 1988). The differentiation of the epimastigote into pre-metacyclic form occurs meanwhile the cells are attached to the epitelium (Tetley and Vickerman, 1985). Pre-metacyclics can still divide and conserve the epimastigote coat, whereas the fully developed metacyclic trypomastigote cannot divide and display a VSG coat (Vickerman, 1985; Tetley and Vickerman, 1985; Fenn and Matthews, 2007). Only metacyclic forms are found freely detached in the salivary glands. The metacyclic trypomastigote is the infective form that enters the mammal host bloodstream.

Once the metacyclic trypomastigote enters the bloodstream of the mammal host, it swiftly re-starts its cell cycle and undergoes division (Matthews *et al.*, 2004), with a concomitant initiation of the elaborate VSG coat that confers them antigenic variation (Barry and McCulloch, 2001). This process establishes the change into the long-slender proliferative form of the parasite. The differentiation of long-slender forms into short-stumpy forms seems to be correlated to the increase in cell density,

and involves arrest of the cell cycle, as short-stumpy forms are non-dividing forms of the parasite (Reuner *et al.*, 1997). The signalling is believed to be triggered by a molecule that accumulates as the cell density increases, and was called SIF (stumpy induction factor) (Vassella *et al.*, 1997). The stumpy-form growth arrest has been hypothesized to function as a means to control the parasite growth in the mammal host, which otherwise would eliminate the host very rapidly, impeding the trypanosoma the completion of its life cycle (Tyler *et al.*, 2001).

2.2. Cell biology of *Trypanosoma brucei*

All members of the Kinetoplastidae order present certain common structural and physiological features that characterize them as such. Amongst the most interesting features of these organisms is perhaps the presence of a modified peroxisome, known as the glycosome. It owes its name to the fact that it contains the first 6-7 enzymes of the glycolytic pathway, which are normally found in the cytosol of all other eukaryotes (Opperdoes and Borst, 1977). Next to glycolysis, other metabolic pathways were identified in the glycosomes, such as the pentose phosphate pathway, purine salvage and pyrimidine synthesis, ether-lipid biosynthesis and peroxide catabolism pathway (Heise and Opperdoes, 1999; Duffieux *et al.*, 2000; Opperdoes, 1984; Hammond *et al.*, 1985; Zomer *et al.*, 1999; Hannaert *et al.*, 2003a; Tielens and Van Hellemond, 1998; Colasante *et al.*, 2006b). The glycosome was classified as a peroxisome due to its prototypical peroxisomal features (Michels and Opperdoes, 1991). The glycosome lacks DNA of its own, entailing the need to import all of its proteins from the cytosol. This import mechanism depends on conserved targeting signals, similar to those found for peroxisomal proteins from other eukaryotes (Hart *et al.*, 1987; Dovey *et al.*, 1988). The biogenesis of the glycosome depends on members of the peroxin (PEX) protein family (or its homologous in trypanosomes), which are the key to peroxisome biogenesis in other eukaryotes (de Hoop and Geert, 1992). The evolutionary origin of the glycosome is still uncertain, and different hypotheses have been proposed in the past. Ever since the glycosome was discovered, the phylogenetic relationship between trypanosomes and other species has been investigated, leading to a number of different hypothesis (Simpson *et al.*, 2006; Opperdoes and Michels, 2007). It was found recently that some of the trypanosome enzymes are rather similar (in sequence and in function) to enzymes only found in phototrophic organisms (Hannaert *et al.*, 2003b; Simpson *et al.*, 2006; Opperdoes and Michels, 2007). Since then it has been widely accepted that the glycosome might have an endosymbiotic

origin, similar to the endosymbiotic origin of other organelles like the mitochondrion, but with additional loss of the organellar DNA (Michels and Opperdoes, 1991; Vickerman and Coombs, 1999; Hannaert *et al.*, 2003a; Hannaert *et al.*, 2003b; Opperdoes and Michels, 2007). Nevertheless, the protein import mechanism used by glycosomes, as well as peroxisomes and glyoxysomes, has not been found in any prokaryote organism known to date, suggesting an independent evolution (Hannaert *et al.*, 2003a).

Trypanosomes are known to transcribe their mRNAs polycistronically. Long mRNA precursors (polycistrons) are processed into separated mRNAs, *via* trans-splicing and polyadenylation (Campbell *et al.*, 2003; Walder *et al.*, 1986). Trans-splicing is the process through which a spliced leader (SL), a 39-nucleotide small nuclear RNA, is added as a cap to the 5-'terminus of an mRNA (Parsons *et al.*, 1984; Walder *et al.*, 1986). This feature relegates gene expression regulation to post-transcriptional levels (Vanhamme and Pays, 1995). At this point mature, differences in mRNAs concentration have been detected, and 3'UTR (untranslated regions) have been shown to regulate mRNA stability (Hotz *et al.*, 1997). The only genes known to express monocistronically in trypanosomas are those encoding VSGs (variant surface glycoprotein) in the metacyclic trypomastigote. VSGs are present on the coat of the metacyclic and the bloodstream-forms, conferring them antigenic variation during infection of the mammal host (McCulloch, 2004; Alarcon *et al.*, 1994). Trypanosomas make use of RNA polymerases (RNAP) I, II and III. RNAPI, like in most eukaryotic cells, is in charge of the transcription of rRNA genes (Campbell *et al.*, 2003). However, it also performs a unique task: it transcribes the procyclins and the VSG genes (Rudenko *et al.*, 1991). The promoter sites for rRNA, VSGs and PARP (procyclin acidic repetive protein) have been characterized (Vanhamme *et al.*, 1995; Brown *et al.*, 1992; Janz and Clayton, 1994). RNAPII is in charge of the transcription of housekeeping genes (e.g., tubulin, actin and *hsp* genes) and splice leader RNA genes (Campbell *et al.*, 2003). However, promoter sites for RNAPII are somewhat rare. A bidirectional RNAPII promoter was described for the chromosome I *Leishmania major* (Martinez-Calvillo *et al.*, 2003). Another characterized RNAPII promoter is that of the spliced leader (Gilinger and Bellofatto, 2001). Very few basal transcription factors have been described in trypanosomes; most of them related to the transcription of the spliced leader (Martínez-Calvillo *et al.*, 2010), and only one basal transcription factor, universal for all three RNAP (Ruan *et al.*, 2004).

Another interesting attribute of trypanosomes is the presence of a single tubular and cristae-devoid mitochondrion in each cell, which runs elongating from the posterior to the anterior part of cell (Matthews, 2005; Matthews *et al.*, 2004). This mitochondrion bears a unique structure, the kinetoplast, which contains highly compacted mitochondrial DNA composed of mini and maxi DNA circles (Liu *et al.*, 2005; Klingbeil *et al.*, 2001; Guler *et al.*, 2008). The kinetoplast is structurally linked to the basal body of the flagellum by a protein complex that transverses the cell body and the mitochondrial membranes and is attached to the microtubule cytoskeleton (Liu *et al.*, 2005). Kinetoplast pre-RNAs undergo a unique transcription and editing process, i.e. the insertion and deletion of hundreds of urydilates and the formation of novel initiation and termination codons, before processing into the final mRNAs (Stuart and Panigrahi, 2002; Campbell *et al.*, 2003). Mitochondrial DNA replication in trypanosomatids is strictly cell-division associated due to the presence of only one mitochondrion per cell (Liu *et al.*, 2005).

An organelle of metabolic importance in trypanosomes is the acidocalcisome. These organelles are single membrane bound, electro-dense, acidic reservoirs of Ca^{2+}, PPi, poly phosphate (poly P), Mg^{2+}, K^{+}, Na^{+} and Zn^{2+} (Moreno and Docampo, 2009). Acidocalcisomes are known to possess several proton pumps, ion exchangers and aquaporins, and have been proposed to actively participate in storage, osmoregulation, pH homeostasis, and metabolism modulation (Docampo *et al.*, 2005; Rohloff *et al.*, 2004; Montalvetti *et al.*, 2004; Urbina *et al.*, 1999; Acosta *et al.*, 2004). The ATPases found in acidocalcisomes membranes belong to the plasma membrane calcium ATPase family (PMCA), without the classic calmodulin-binding domain that characterizes this group of membrane proteins (Docampo *et al.*, 2005). Vacuolar-type H^{+} -ATPase and H^{+} -PPase activities, as well as Na^{+}/H^{+} and Ca^{2+}/H^{+} ion exchangers, have also been identified in these organelles (Scott *et al.*, 1998; Hill *et al.*, 2000; Vercesi *et al.*, 1994; Vercesi and Docampo, 1996).

The presence of pyrophosphate (PPi) in the acidocalcisomes of trypanosomes has been hypothesized to play a pivotal role in the regulation of the intermediary metabolism of these parasites. Several proteins like hexokinase, pyruvate phosphate dikinase, enolase and various enzymes from the metabolism of sterols seem to be regulated and/or inhibited by pyrophosphate (Hudock *et al.*, 2006; Quiñones *et al.*, 2007; Caceres *et al.*, 2003; Acosta *et al.*, 2004; Urbina *et al.*, 1999).

2.2.1. Metabolic pathways in the glycosome of *Trypanosoma brucei*

As mentioned above, the glycosomes bear the first 6-7 enzymes of the glycolytic pathway, which will be discussed in detail in the next section. Some of the other metabolic pathways in the glycosomes of trypanosomas will be summarized in this section. One of these is the pentose phosphate pathway (PPP), a metabolic pathway for the production of NADPH that utilizes metabolite oxidation for reductive biosynthesis (Voet and Voet, 1995). NADPH is an important role in the production of reductive power, which is crucial for the parasite survival against the host's defence system (Duffieux *et al.*, 2000). The first of the enzymes that constitutes this pathway, glucose-6-phosphate dehydrogenase is exclusively found inside the glycosomes, whereas 6-phosphogluconolactonase, the second enzyme of the pathway, displays a dual localization between cytosol and glycosomes (Duffieux *et al.*, 2000). These results allocated the first part of the PPP, the oxidative PPP, inside the glycosomes, a localization that is not unique to trypanosomes, as the PPP has also been reported in mammalian peroxisomes (Hannaert *et al.*, 2003a; Antonenkov, 1989). Proteomic analysis on the glycosomal proteins of *T. brucei* allocates 6 enzymes of the PPP in the glycosomes, with all of them (except glucose-6-phosphate dehydrogenase) displaying a PTS-1 targeting signal (Colasante *et al.*, 2006b). Whereas the 6 first enzymes of the PPP are present in the glycosomes of the procyclic form of the parasite, only 2 of them could be detected in the glycosomes of the bloodstream form of *T. brucei* (Colasante *et al.*, 2006b). Although the presence of the pentose phosphate pathway in peroxisomes is not exclusive to trypanosomes, other pathways found in the glycosomes are, i.e. pyrimidine synthesis, purine salvage and gluconeogenesis (Hannaert *et al.*, 2003a).

The pyrimidine synthesis pathway has been described in detail for *Trypanosoma cruzi (*Gao *et al.,* 1999; Nara *et al.,* 2000*).* The 6 genes coding for the pathway in *T. cruzi, T. brucei* and *Leishmania* are displayed in an operon-like cluster, a unique case in trypanosomes (Gao *et al.*, 1999; Opperdoes and Szikora, 2006). In metazoans, the enzymes that constitute the pyrimidine biosynthetic pathway, are fused to form multifunctional proteins, and can their genes can be found as *pyr1-2-3* and *pyr5-6*, and *pyr4* as a monofunctional protein (Opperdoes and Szikora, 2006). In trypanosomas, the genes are separated and expressed as single functional proteins, except for *pyr5-6*. This multifunctional protein is found in the glycosomes of *T. cruzi, T. brucei* and *Leishmania* (Gao *et al.*, 1999; Colasante *et al.*, 2006b; Opperdoes and Szikora, 2006).

The purine salvage pathway, mainly represented by hypoxanthine-guanine phosphoribosyltransferase (HGPRTase), adenine phosphoribosyltransferase (APRTase) and inosine 5' monophosphate dehydrogenase, is found in the glycosomes of the procyclic form of *Trypanosoma brucei*, whereas in the bloodstream form only the first two of the above-mentioned enzymes have been detected by proteomics analysis (Colasante *et al.*, 2006b). However, in-silico analysis detected a PTS-1 signal for APRTase (Opperdoes and Szikora, 2006). Other related enzymes like adenylate and guanylate kinases are also found in the glycosomes of *T. brucei* procyclic form (Colasante *et al.*, 2006b).

Another pathway that is found partially in the glycosomes is the biosynthesis of ether-lipids. Dihydroxyacetonephosphate acyltransferase and alkyl dihydroxyacetonephosphate synthase have been identified as glycosomal, and have been characterized in *Trypanosoma brucei* and *Leishmania mexicana* (Opperdoes, 1984; Zomer *et al.*, 1999; Colasante *et al.*, 2006b; Opperdoes and Szikora, 2006; Lux *et al.*, 2000). These enzymes catalyze the first steps of the pathway of alkyl (ether) lipids biosynthesis, important precursors of phospholipids and plasmalogens, as well as the formation of glycosylphosphatidyl inositol (GPI) anchors. GPI anchors are involved in the attachment of several membrane proteins to lipid bilayers, with a key role in assembly the coat of procyclins and VSG coats, in the procyclic and in the bloodstream forms of the parasite, respectively (Ferguson, 1997; Acosta-Serrano *et al.*, 1999; Field *et al.*, 1991). GPI anchors in trypanosomas are attached via a specific α, β-unsaturated ether linkage to the outer-leaflet of the plasma membrane (Zomer *et al.*, 1999).

Another important pathway of the lipid metabolism in trypanosomes is the synthesis of sterols. 3-hydroxy-3-methyl-glutaryl-CoA reductase (HMGR) is the first step in the isoprenoid synthesis and was first characterized for *Trypanosoma cruzi*. In *T. cruzi*, this enzyme displayed a dual localization between glycosomes and mitochondria (Concepcion *et al.*, 1998), whereas for *Trypanosoma brucei* the opposite was observed (Heise and Opperdoes, 2000). However, the localization of this enzyme has been controversial, and now is widely accepted that HMGR is not localized to the glycosomes (Pena-Diaz *et al.*, 2004; Vertommen *et al.*, 2008; Ginger *et al.*, 2010). Nonetheless, mevalonate kinase, 5-diphosphomevalonate carboxylase, isopentenyldiphosphate isomerase and squalene synthase/farnesyl transferase have been found to bear a PTS-1 targeting signal, which would localize them in the glycosomes of trypanosomas (Opperdoes and Szikora, 2006). Despite the facts

that there are differences in targeting signals between the different *Trypanosoma* and *Leishmania* species, as well as contradicting reports regarding enzyme localizations, it is now widely accepted that the metabolic steps between the phosphorylation of mevalonate to the formation of squalene are indeed localized in glycosomes (Ginger *et al.*, 2010; Ferella *et al.*, 2008). This pathway has attracted a lot of attention in recent years, particularly in *Trypanosoma cruzi*. *T. cruzi* is incapable of using the cholesterol from the mammal host, which forces it to synthesize its own sterols, making this pathway a promising drug target against Chagas disease (Urbina *et al.*, 2004).

Peroxisomes are known to harbour β-oxidation of fatty acids in a wide range of cells and their metabolism is quite important in the production of ATP (Voet and Voet, 1995). However, ATP production from fatty acid metabolism does not seem to occur in trypanosomatids (van Hellemond and Tielens, 2006). After the sequencing of the genome, β-oxidation of fatty acids has been hypothesized to occur between glycosomes and mitochondria, despite the very little experimental characterization evidence found for the branch in the glycosomes (Wiemer *et al.*, 1996; Berriman *et al.*, 2005; Opperdoes and Szikora, 2006). Since then, evidence towards the *de novo* synthesis of fatty acids has been addressed (particularly in bloodstreams forms) with the concomitant localization of this pathway in the mitochondrion of *T. brucei* (Stephens *et al.*, 2007; Guler *et al.*, 2008; van Hellemond and Tielens, 2006).

A unique characteristic of the glycosomes of Trypanosomatids is the absence of catalase, known as a classic marker for peroxisomes in other eukaryotic cells. Instead of catalase, trypanosomes display a unique thiol-based peroxidase-type cascade: the trypanothione system (Muller *et al.*, 2003). Trypanothione is a bis-glutathionylspermidine conjugate that participates in the elimination of ROS species in trypanosomes (Fairlamb *et al.*, 1985). Dual localizations (glycosomal and cytosolic) have been identified for a trypanothione peroxidase in *T. brucei* and *T. cruzi*, whereas trypanothione reductase (TR), presents an exclusively cytosolic localization in *T. brucei*. (Wilkinson *et al.*, 2002; Hillebrand *et al.*, 2003; Opperdoes and Szikora, 2006),

3. The glycosome, the mitochondrion and the intermediary metabolism

Glycolysis is a universally conserved metabolic pathway present in virtually all cells, through which glucose is oxidized for ATP generation. The glycolytic pathway

consists of 10 enzymatic steps, in which there is a net gain of 2 ATP moles for every mole of glucose that enters the pathway. In virtually all eukaryotic cells, glycolysis takes place in the cytosol. Its final product, pyruvate, is then taken up by the mitochondria, where it is decarboxylated and condensed with a cofactor: Coenzyme-A, leading to the formation of Acetyl-CoA. This energy-rich intermediate is the precursor for the Tri-Carboxylic (TCA) Cycle (Voet and Voet, 1995). Under aerobic conditions, the mitochondrion provides ATP to the cell through oxidative phosphorylation. Because energy production from glucose breakdown involves oxidation, the passage of redox power has to be done through molecules that require recycling: e.g. NAD^+ and $NADP^+$. The TCA cycle has amphibolic functions, by providing substrates to other pathways for synthesis as well as oxidizing intermediates from glucose metabolism (Voet and Voet, 1995).

Trypanosoma brucei is an extracellular parasite in the mammalian and the insect hosts; these environments are rather different, representing a metabolic challenge for the parasite. Trypanosomes perform “aerobic fermentation”, a process through which final products of the anabolic pathways are not the most oxidized forms, but rather some of its intermediates (Cazzulo, 1992; Tielens and Van Hellemond, 1998; Hannaert *et al.*, 2003a). Amino acids have been described as their main carbon and energy source, especially proline, which is actively taken up by the cell, but in-vitro studies have described glucose to be the preferred carbon source of these parasites (Lamour *et al.*, 2005).

The energy metabolism of bloodstream form trypanosomes relies mainly on the formation of pyruvate from glucose, as this is the major carbon source in the mammalian bloodstream (Coustou *et al.*, 2008). Since only the first 7 glycolytic enzymes are compartmentalized in the glycosome (Figure 2), the last intermediate in the organelle is 3-phosphoglycerate, which is transported to the cytosol for the pathway to continue (Opperdoes and Borst, 1977; Hannaert *et al.*, 2003a). NADH is re-oxidized by the combined action of a glycosomal glycerol-3-phosphate shuttle and mitochondrial alternative oxidase (Kohl *et al.*, 1996; Tielens and Van Hellemond, 1998; Michels *et al.*, 2006). The mitochondrion of the bloodstream form lacks several key components and enzymes of the TCA cycle, and is regarded as “not functional”. The final product of the glycolytic pathway, i.e. pyruvate, is formed in the cytosol and is excreted into the culture medium. In contrast to bloodstream forms, procyclic forms depend mainly on mitochondrial metabolism for their energy generation: after pyruvate is formed in the cytosol, it is transported into the

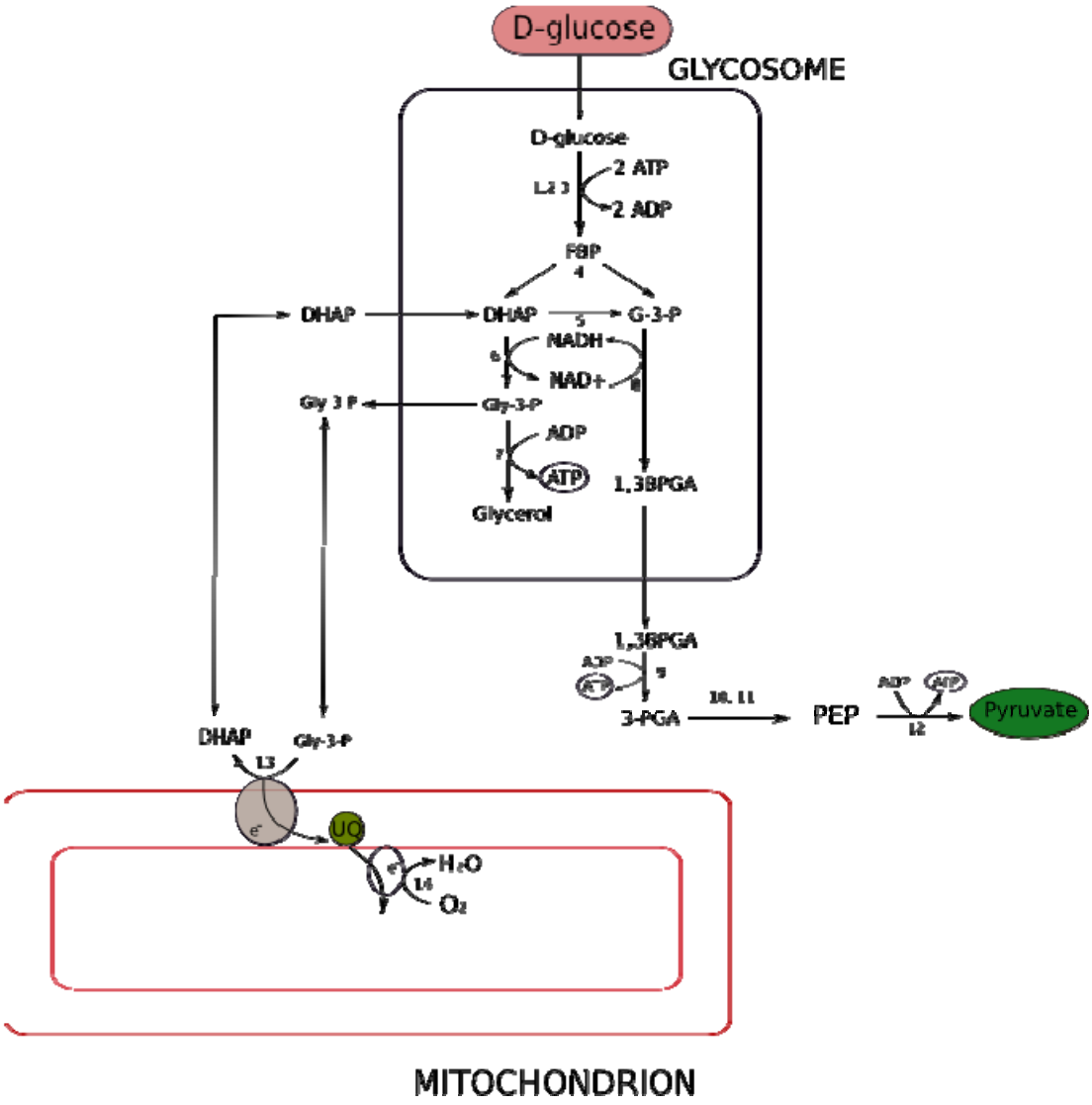

Figure 2. Schematic representation of *T. brucei* bloodstream form energy metabolism. Abbreviations: FBP: fructose 1,6 bisphosphate; DHAP: dihydroxyacetone phosphate; G-3-P: glycerol-3-phosphate; 1,3BPGA: 1,3 bisphosphoglycerate; 3-PGA: 3-phosphoglycerate; PEP: phospho*enol*pyruvate, UQ: ubiquinone. Enzymes catalyzing reactions: 1, hexokinase; 2, glucose-6-phosphate isomerase; 3, phosphofructokinase; 4, aldolase; 5, triose-phosphate isomerase; 6, glycerol-3-phosphate dehydrogenase; 7, glycerol kinase; 8, glyceraldehyde dehydrogenase; 9, phosphoglycerate kinase; 10, phosphoglycerate mutase; 11, enolase; 12, pyruvate kinase; 13, glycerol-3-phosphate oxidase; 14, alternative oxidase.

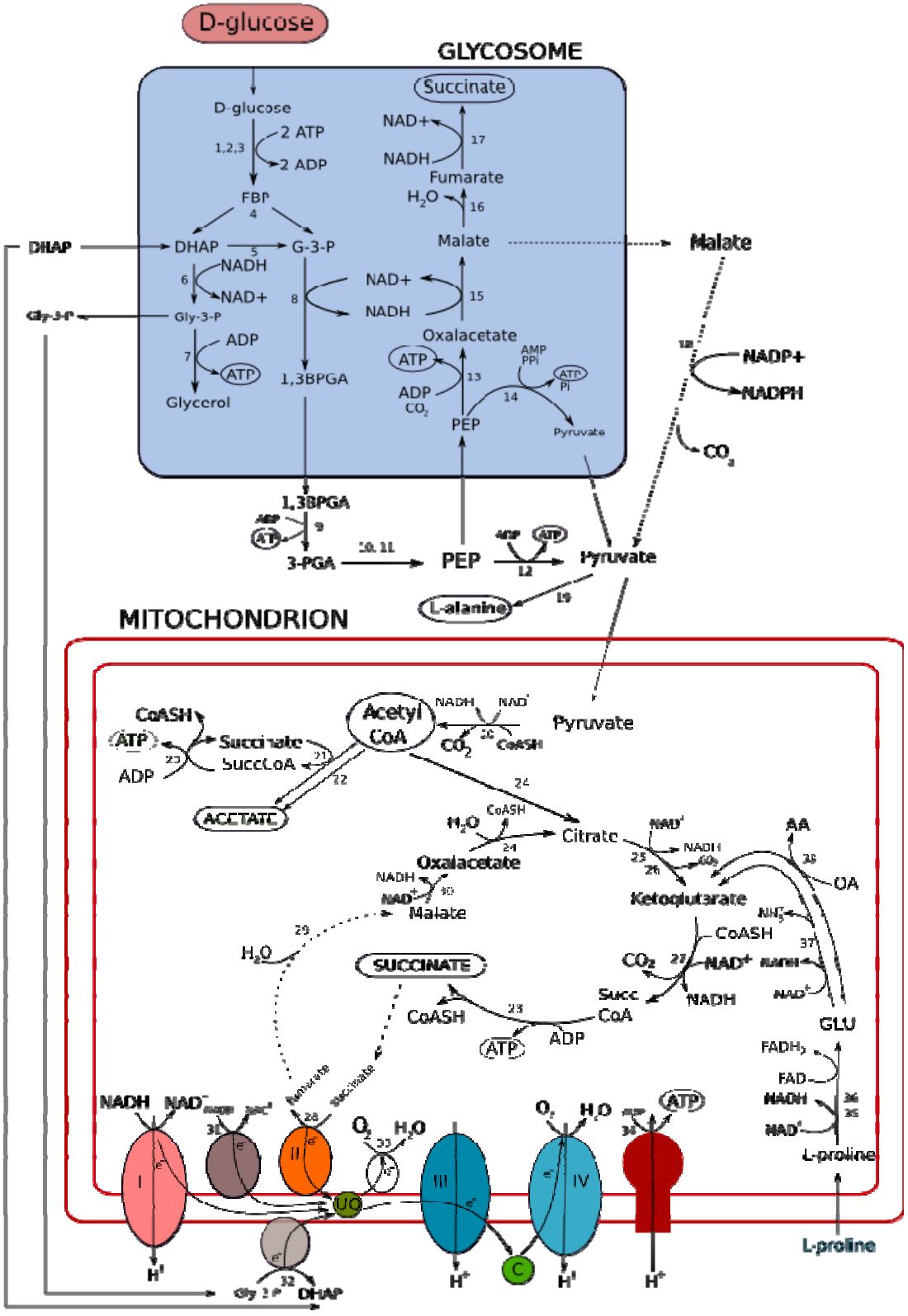

Figure 3. Schematic representation of key energy metabolism pathways from *T. brucei* procyclic form. Acetate, succinate, L-alanine and CO_2 are excreted products. Dashed lines represent steps that are supposed to happen under cultured conditions. Abbreviations: AA: amino acid; OA: 2-oxoacid; FBP: fructose 1,6

bisphosphate; DHAP: dihydroxyacetone phosphate; G-3-P: glycerol-3-phosphate; 1,3BPGA: 1,3 bisphosphoglycerate; 3-PGA: 3-phosphoglycerate; PEP: phospho*enol*pyruvate; PPi, pyrophosphate; Pi: inorganic phosphate; SuccCoA: succinyl CoA; CoASH: Coenzyme A; GLU: glutamate. Enzymes catalyzing reactions: 1, hexokinase; 2, glucose-6-phosphate isomerase; 3, phosphofructokinase; 4, aldolase; 5, triose-phosphate isomerase; 6, glycerol-3-phosphate dehydrogenase; 7, glycerol kinase; 8, glyceraldehyde dehydrogenase; 9, phosphoglycerate kinase; 10, phosphoglycerate mutase; 11, enolase; 12, pyruvate kinase; 13, phospho*enol*pyruvate carboxykinase; 14, pyruvate phosphate dikinase; 15, glycosomal malate dehydrogenase; 16, glycosomal fumarase; 17, NADH-fumarate reductase; 18, malic enzyme; 19, alanine aminotransferase; 20, pyruvate dehydrogenase complex; 21, acetate:succinate CoA transferase; 22, unknown enzyme; 23, succinyl CoA synthetase; 24, citrate synthase; 25, aconitase; 26, isocitrate dehydrogenase; 27, 2-ketoglutarate dehydrogenase complex; 28, succinate dehydrogenase (complex II); 29, mitochondrial fumarase; 30, mitochondrial malate dehydrogenase; 31, rotenone-insensitive NADH dehydrogenase; 32, glycerol-3-phosphate oxidase; 33, alternative oxidase; 34, F_0/F1 ATP synthase; 35, proline dehydrogenase; 36, pyrroline-5-carboxylate dehydrogenase; 37, glutamate dehydrogenase; 38, acetyl-CoA:glycine C-acetyl transferase; I, II, III and IV, respiratory chain complexes.

---

mitochondrion, where it is subsequently condensed with coenzyme-A (see Figure 3). The formed acetyl-CoA is degraded to acetate by an acetate:succinate CoA transferase, producing ATP in this reaction (Van Hellemond *et al.*, 1998). In the procyclic form, all of the TCA cycle enzymes are expressed, suggesting a fully functional and active TCA Cycle. However, different experiments conducted by several research groups indicate the contrary. Studies of an aconitase knockout cell line revealed that depletion of this enzyme, which catalyzes the isomerisation of citrate into isocitrate, presents no lethal growth phenotype in the procyclic form (van Weelden *et al.*, 2003).

In fact, the aconitase knockout cell line produces the same metabolic end products as the wild type cell line. Further, carbons derived from glucose do not enter the TCA cycle, and low-carbohydrate conditions do not result in a shift of the fermentative process towards a complete oxidation of the intermediates to CO_2 (van Weelden *et al.*, 2005b; Lamour *et al.*, 2005). Finally, in absence of both glucose and

glycerol, proline is consumed 2-fold the "normal" rate with CO_2 production altered accordingly, but succinate excretion does not change, which implies a recycling of carbons into biosynthetic pathways (van Weelden *et al.*, 2005b).

The following important question arises: if the TCA cycle does not function as a cycle for energy production, why are all of its enzymes then expressed in the procyclic form of the parasite? The simple answer seems to be that different parts of the TCA cycle are required for the function of other metabolic pathways. For example, the succinate/succinyl Co-A cycle, which is responsible for ATP generation via the conversion of succinate to acetate (Figure 3), involves part of the TCA cycle (Van Hellemond *et al.*, 1998; Besteiro *et al.*, 2005; Van Hellemond *et al.*, 2005). Also the production of succinate from malate, and the concomitant reoxidation of the formed NADH via NADH:fumarate reductase, requires some of the TCA cycle enzymes (Figure 3). Furthermore, the mitochondrial degradation of proline and glutamate to succinate, involves several TCA cycle enzymes, i.e. α-ketoglutarate dehydrogenase and succinyl CoA synthetase (van Weelden *et al.*, 2005b; Van Hellemond *et al.*, 2005; Besteiro *et al.*, 2005). It has been further proposed that the TCA cycle intermediary product acetyl Co-A functions as a regeneration intermediary, that might exit the mitochondrion most likely as either citrate or malate, again requiring some part of the TCA cycle (Van Hellemond *et al.*, 2005). Finally, part of the TCA cycle is also required for gluconeogenesis in procyclic form *T. brucei*, especially when the parasite is cultured in the absence of glucose (van Weelden *et al.*, 2005b; Van Hellemond *et al.*, 2005).

4. Oxidative phosphorylation versus substrate-level phosphorylation

Procyclic form trypanosomes cultured in presence of glucose and amino acids have been described previously to depend on oxidative phosphorylation for the generation of ATP. Oxidative phosphorylation requires the presence of an active electron transport chain for the maintenance of a proton motive force, which in turn allows the F_1/F_0- ATP synthase (complex V) to perform oxidative phosphorylation. This process seems however to be incomplete in procyclic form trypanosomes, which would account for the excretion of succinate by these parasites (Tielens and Van Hellemond, 1998).

The origin of the excreted succinate was cause of controversy amongst researchers for many years (Turrens, 1999; Tielens and Van Hellemond, 1999). The main site of

succinate production was initially thought to be mitochondrial, through the activity of succinyl-CoA synthetase and a NADH-dependent fumarate reductase (Tielens and Van Hellemond, 1998; Turrens, 1989). With the discovery of glycosomal fumarate reductase activity in procyclic form trypanosomes, additional experiments were done which demonstrated that the bulk (approximately 80%) of excreted succinate was produced in the glycosomes, whereas the remaining succinate resulted from mitochondrial fumarate reductase activity (Coustou *et al.*, 2005; Besteiro *et al.*, 2002). The succinate produced in the glycosomes originated from the oxidation of glycolytic phosphoenolpyruvate (PEP), which had been re-imported into the organelle (Figure 3). PEP is subsequently converted into malate by the combined action of phospho*enol*pyruvate carboxy kinase (PEPCK) and malate dehydrogenase (MDH), with concomitant regeneration of NAD and the production of ATP.

Later, after further studies of the mitochondrial NADH-FRD, additional aspects of the intermediary metabolism of *T. brucei* were elucidated. Using labelled D-[1-^{13}C] glucose and RNA interference-mediated depletion of the glycosomal NADH-FRD, labelled succinate could be detected in the culture medium. This result indicated transfer of carbons from the glycosome into the mitochondrion, most probably through malate, which in turn would be converted into succinate by the mitochondrial fumarase and NADH-FRD. The formation of succinate in the mitochondrion is essential for the maintenance of the redox balance in this organelle (Coustou *et al.*, 2005). Another role for the succinate produced in the mitochondrion would be the production of acetate through ASCT. This acetate is mainly produced in the mitochondrion and has recently been described as an important precursor for lipid biosynthesis in *T. brucei* (Rivière *et al.*, 2009).

The production of succinate as one of the main metabolic end products led to a further evaluation of the importance of oxidative phosphorylation for the energy metabolism of procyclic form *T. brucei*. It was initially thought that the F_1/F_0- ATP synthase (complex V) was mainly responsible for the production of ATP in procyclic form *T. brucei*. However this assumption was rejected after inhibition studies revealed that F_1/F_0- ATP synthase activity is not always essential for trypanosome survival: procyclic form trypanosomes grown in the presence of glucose did not show any growth defects in the presence of oligomycin, even at 10-fold higher concentrations then normally would be required for the maximum inhibition of F_1/F_0-ATP synthase (Coustou *et al.*, 2003). However, when comparing glucose-grown procyclic form *T. brucei* with glucose-depleted ones, the difference in sensitivity to

oligomycin proved to be 1000-fold. This remarkable difference in oligomycin sensitivity led to the hypothesis that oxidative phosphorylation is only important for ATP production in the absence of glucose (Coustou *et al.*, 2003; Lamour *et al.*, 2005; Verner *et al.*, 2010). This hypothesis was later confirmed by experiments showing that the addition of oligomycin to procyclic form *T. brucei* grown in culture media without glucose, indeed resulted in growth arrest and cell death (Lamour *et al.*, 2005; Besteiro *et al.*, 2005).

Depletion (RNA interference) of the F_1/F_0- ATP synthase in bloodstream form *T. brucei* was found to be lethal, suggesting an important role of the F_1/F_0- ATP synthase in this life cycle stage of the parasite (Schnaufer *et al.*, 2005). Bloodstream forms depend mainly on glycolysis for energy generation and are not depending on OXPHOS for energy production. It was therefore proposed that the F_1/F_0- ATP synthase might be involved in other (than ATP production) roles in bloodstream form *T. brucei.*

If the ATP production in glucose-grown procyclic-form *T. brucei* does not primarily depend on oxidative phosphorylation, which metabolic pathway is then the main source of ATP? This question was answered by the RNAi-directed depletion of pyruvate kinase (PYK), which was found to be lethal for glucose-grown procyclic form *T. brucei*. Pyruvate kinase catalyzes the cytosolic conversion of PEP into pyruvate, with the concomitant production of ATP via substrate-level phosphorylation (Figure 3). The cytosol as main ATP production site of glucose-grown procyclic-form *T. brucei* is further in agreement with previous oligomycin inhibition studies of the F_1/F_0- ATP synthase (Coustou *et al.*, 2003). Also other experiments reinforced the hypothesis that substrate-level phosphorylation is the main route for ATP production in these parasites. For example, ATP production could be measured when isolated procyclic form mitochondria were incubated with ADP and different substrates, i.e. succinate, α-ketoglutarate, and glycerol-3-phosphate, respectively (Allemann and Schneider, 2000). However, repeating the experiment with isolated mitochondria from a α-ketoglutarate dehydrogenase (KDH) depleted RNAi cell line, resulted in complete ablation of α-ketoglutarate-dependent ATP production (Figure 3). Moreover, when doing similar ATP-production experiments with mitochondria isolated from a succinyl CoA synthetase (SCoAS) RNAi cell line, not only no ATP was produced when using α-ketoglutarate as a substrate, but the SCoAS depletion also appeared to be lethal (Bochud-Allemann

and Schneider, 2002). Both KDH and SCoAS are apparently responsible for the mitochondrial ATP production via substrate-level phosphorylation (Figure 3) (Bochud-Allemann and Schneider, 2002; Van Hellemond *et al.*, 1998). Next to KDH and SCoAS, also acetate:succinate CoA transferase (ASCT) activity was shown to make a significant contribution to mitochondrial ATP production by substrate-level phosphorylation (Figure 3). All together, these findings suggest a preference of *T. brucei* for the substrate-level phosphorylation of succinate rather than its oxidative phosphorylation.

ASCT activity results further in the formation of acetate, which next to succinate is the second main end product excreted in the culture medium of procyclic form *T. brucei* (Coustou *et al.*, 2005; Van Hellemond *et al.*, 1998). Acetate excretion has also been observed in bacteria. Excretion of this metabolic intermediate occurs only when the TCA cycle is not operating as a cycle or when the carbon overflow exceeds the cellular capacity to metabolize it completely. Once the bacterial culture exits the log-phase and nutrients become depleted, scavenging of carbon sources takes place and the "acetate switch" is turned on. This "acetate switch" allows the bacterial cell to shift from a log-phase type of growth to a lag-phase type of growth during which acetate is re-assimilated (Wolfe, 2005). A similar feature has also been observed in trypanosomes: acetate that has been produced in the mitochondrion by ASCT is further transported into the cytosol where it is subsequently converted into acetyl-CoA by acetyl-CoA synthetase (AceCS). Acetyl-CoA can be used again for the de-novo biosynthesis of lipids. RNAi of AceCS in procyclic form *T. brucei* proved to be lethal for the parasite, indicating that mitochondrial acetate production and its transport into the cytosol is essential for parasite survival (Rivière *et al.*, 2009).

5. Gluconeogenesis in *Trypanosoma brucei*

Many authors have proposed gluconeogenesis as a means for the procyclic form of *T. brucei* to use amino acids for the *de novo* synthesis of hexoses in glucose-depleted conditions (Hannaert *et al.*, 2003a; Ginger *et al.*, 2010; Coustou *et al.*, 2008). For gluconeogenesis to occur, two key metabolic steps must take place: 1) the conversion of pyruvate into PEP (in cytosol) and 2) the conversion of fructose-1,6 biphosphate into fructose-6-phosphate (in glycosomes). The first step requires a pyruvate carboxylase, an enzyme that has not been found in *T. brucei*, for the production of oxaloacetate, which would be subsequently converted into phosphoenolpyruvate by the activity of a phospho*enol*pyruvate carboxykinase

(PEPCK) (Voet and Voet, 1995). However, malate has been proposed as the substrate of a cytosolic malate dehydrogenase for the production of oxaloacetate in cytosol (Coustou *et al.*, 2008; Vernal *et al.*, 2001; Aranda *et al.*, 2006); and PEPCK, would subsequently convert oxaloacetate into PEP (Hunt and Kohler, 1995; Coustou *et al.*, 2008). Alternatively, malate can act as the substrate of the malic enzyme for the production of pyruvate in cytosol (Coustou *et al.*, 2008). The second step is catalyzed by the activity of fructose-1,6 biphosphatase. This last enzyme has been found in the genome of *T. brucei, T. cruzi* and *Leishmania*, and its sequence displays a PTS-1 targeting signal, which would localize it inside the glycosomes (Berriman *et al.*, 2005; Opperdoes and Szikora, 2006). In *Leishmania major*, elimination of fructose-1,6 biphosphatase renders amastigotes incapable of proliferating inside macrophages, an environment where glucose is not readily available (Naderer *et al.*, 2006). The probability of gluconeogenesis in *T. brucei* was brought to attention when RNAi on the malic enzyme resulted lethal for the procyclic form of the parasite in absence of glucose (Coustou *et al.*, 2008). Inhibition of PEPCK and mitochondrial succinate dehydrogenase, or F_1/F_0-ATP synthase also resulted detrimental for cell survival under glucose-depleted conditions (Ebikeme *et al.*, 2010). The aforementioned evidence implies that both PEPCK and malic enzyme are used by procyclic form *T. brucei* under glucose-depleted conditions (Coustou *et al.*, 2008). Fructose-1,6 biphosphatase activity has not been detected in bloodstream or procyclic forms of *T. brucei* cultured in presence of glucose (Hannaert *et al.*, 2003a).

6. The Mitochondrial Carrier Family

The overview of intermediates transport across organelles in *T. brucei* suggests the need for a regulated transport system for the metabolism to function. Malate translocation from glycosome to mitochondrion; the transfer of acetate from mitochondrion to cytosol for the synthesis of acetyl CoA; proline catabolism; substrate-level phosphorylation for ATP production inside the mitochondrion, are examples of pathways that require intermediates to be transported between cellular compartments. This intermediates traffic between cellular compartments has been ill defined in most metabolic studies in *Trypanosoma brucei*.

The mitochondrial inner membrane of *Trypanosoma brucei* is thought to be impermeable for several metabolites (Schneider *et al.*, 2007), implying the presence of specific membrane-bound transporters. Such transporters are essential for the

maintenance of the mitochondrial and cellular redox balance, and most of the above described mitochondrial pathways in *T. brucei* require the transport of metabolites between the mitochondrion and other cellular compartments, i.e. the glycosomes and the cytosol. Until recently, the only information available about *T. brucei* mitochondrial metabolite transporters was what could be deduced from metabolic studies (van Weelden *et al.*, 2005a; Schneider *et al.*, 2007). In 2006, the molecular and functional characterisation of MCP6 was reported - the first mitochondrial metabolite transporter identified for trypanosomes and a novel member of the mitochondrial carrier family (Colasante *et al.*, 2006a). More recently, 26 different *T. brucei* genes were identified with significant sequence similarity to metabolite transporters of the Mitochondrial Carrier Family (Colasante *et al.*, 2006b; Colasante *et al.*, 2009).

The Mitochondrial Carrier Family (MCF) consists of a number of structurally and functionally related group of membrane proteins that are involved in the transport of metabolites across the inner mitochondrial membrane (Aquila et al., 1987; Palmieri and Klingenberg, 2004; Millar and Heazlewood, 2003). These proteins have been widely described in yeast, fungi, plants and several mammalian systems, including humans. The MCF proteins (Figure 4) exhibit several conserved features such as: 1) their length in 300-450 amino acids; 2) they exhibit the conserved amino acid repeat $Px(D/E)x_2(K/R)x(K/R)x_{20-30}(D/E)Gx_{4-5}(W/F/Y)(K/R)G$ (with x representing any aminoacid); 3) they possess a tripartite structure, consisting of three homologous sequence repeats of about 100 amino acid residues each, folded into two trans membrane helices and linked by a short helix on the matrix side; 4) they present basic pI that ranges between 9-10; 5) they are believed to operate as homodimers; and 6) their N- and C-terminals ends are oriented towards the mitochondrial inter membrane space (Bogner et al., 1986; Aquila et al., 1987; Walker and Runswick, 1993; Kunji, 2004; Palmieri and Klingenberg, 2004; Colasante et al., 2009; Saraste and Walker, 1982; Millar and Heazlewood, 2003).

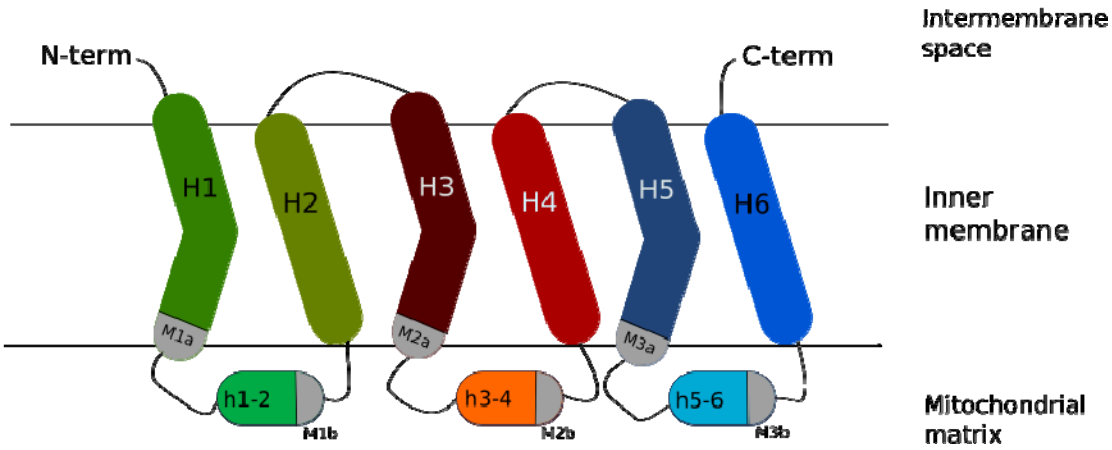

Figure 4. Schematic model for transmembrane domains structure in MCF proteins. Trans-membrane helices are denoted in uppercase (H). Conserved motif starts at the end of each odd-numbered trans-membrane helix and finishes 20-30 residues after the amphipathic helices that intercalate between trans-membrane helices (h1-2, h3-4, h4-5).

MCF proteins have been classified into 6 functional groups, according to the substrate they translocate: i.e. nucleotides, phosphate, carboxylic acids, amino acids, protons and iron (Palmieri, 2004; Palmieri *et al.*, 2006; Kunji and Robinson, 2006; Colasante *et al.*, 2009). It was initially believed that mitochondrial metabolite transport occurred through counter-exchange, as no net accumulation was observed, and therefore osmolarity was maintained in the organelle (Klingenberg, 1976). With the accumulation of data from the analysis of many MCF proteins in different species, it was noted that they are able to function through different mechanisms like uniport, symport, and antiport, and in an electron neutral, proton-compensated or electrophoretic way (Palmieri et al., 2000).

7. The ADP/ATP carrier and its discovery

About 50 years ago it was assumed that ATP was produced during oxidative phosphorylation in mitochondria and was subsequently transported by the ATP synthase across the mitochondrial membrane. Therefore it was also unclear how this organelle obtained its endogenous ADP pool, as no exchange had been described for such process. Mitochondrial metabolism accounts for a great deal of energy production for the cell, as the final steps of carbohydrates oxidation take place in this compartment for the ultimate production of ATP. This energy-rich molecule must be carried towards other cell compartments, as it is not membrane-permeable. It was not until 1968 that the actual counter-exchange between cytosolic

ADP and mitochondrial ATP was described, and the ADP/ATP carrier was discovered (Klingenberg, 1976; Klingenberg, 2008).

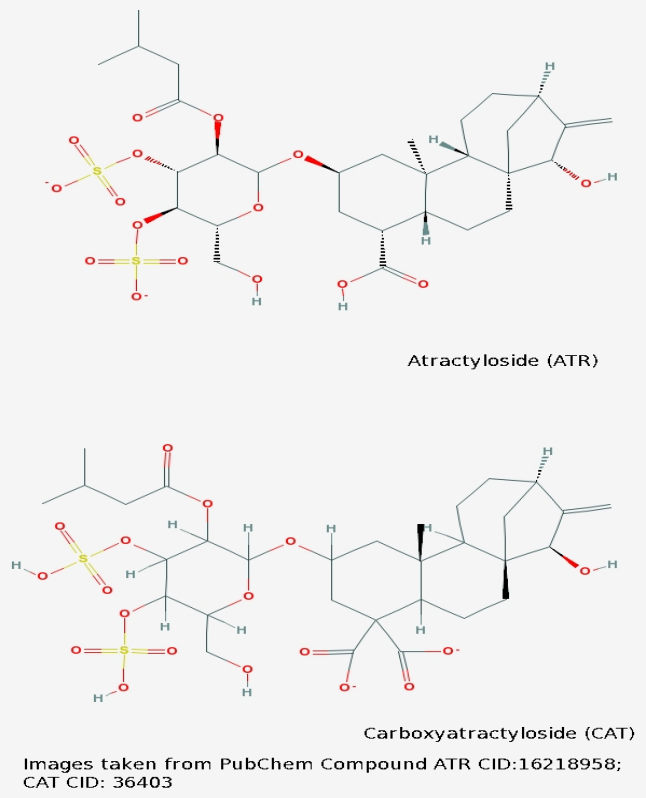

Figure 5. Chemical structures of atractyloside and carboxyatractyloside. Data taken from PubChem Compound.

This mitochondrial ADP/ATP exchange activity was proposed to be a strict 1:1 counter-exchange of ADP for ATP (that virtually excluded AMP transport), is determined by the membrane potential, and involves substantial conformational changes via a “ping-pong”-type mechanism also called Single-Binding Centre-Gated Pore (SBCGP) mechanism (Pfaff and Klingenberg, 1968; Krämer and Klingenberg, 1977; Krämer and Klingenberg, 1982). This mechanism was defined by studying the binding of the ATP/ADP carrier to its best-known inhibitors (Figure 5): i.e. atractylate and bongkrekic acid (Bruni *et al.*, 1964a; Bruni *et al.*, 1964b; Henderson and Lardy, 1970). Atractylate (ATR) binds to the intermembrane-facing side of the carrier, whereas bongkrekic acid (BKA) binds to the matrix-facing side (Figure 6). This way the ATP/ADP carrier could be fixed in one of two possible states: with ATR binding to the intermembrane side, the carrier is locked in its “c” state (c for cytosolic), whereas with BKA binding to the mitochondrial matrix side, the carrier is locked in its “m” state (m for mitochondrial). These transition states were referred to as “ground states” and proved to be the same sites to which the substrates would bind (Klingenberg, 2008; Klingenberg *et al.*, 1995). The binding sites of the inhibitors and

their mechanisms were a discussion point for many years, as other research groups had different points of view on the subject.

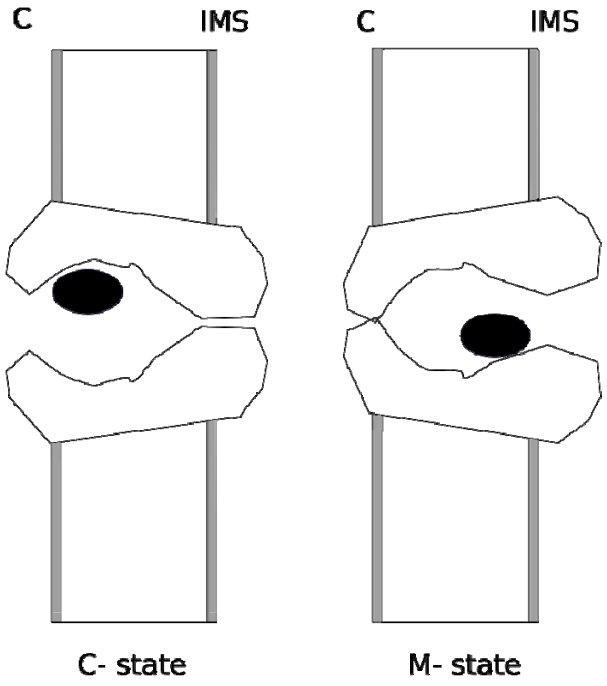

Figure 6. The Single-Binding Center-Gated Pore Mechanism (SBCGP) as proposed by Klingenberg. The substrates bind sequentially to the same site in a "ping-pong" type of mechanism.

Atractyloside is a glucoside naturally occurring in nature, and is produced by a toxic thistle called gummiferin (*Atractylis gummifera*) (Bruni *et al.*, 1964a). Another compound found in the same plant, i.e. carboxyatractyloside (CAT), also acted as an inhibitor of the carrier, but with a higher binding affinity (Danieli *et al.*, 1972; Luciani *et al.*, 1971). A third compound found in the bacteria *Burkholderia gladioli* proved to have similar inhibitory properties. This compound, i.e. bongkrekic acid, is a tri-carboxylic acid that inhibits the ADP/ATP carrier in a different manner as ATR (Henderson and Lardy, 1970). ATR was found to inhibit the carrier in a quasi-competitive manner to ADP. This is in contrast to CAT, which acts as an uncompetitive inhibitor to ADP (Vignais *et al.*, 1966). BKA presented a slightly more complicated mode of action. It inhibited ADP-binding in a quasi-competitive manner, but unlike ATR, this inhibition was time, temperature and pH dependent. This observation led to the conclusion that BKA had to diffuse across the membrane in order to bind to its site of action (Klingenberg and Buchholz, 1973). It was further noted that BKA increased both the binding and the apparent affinity for ADP to a Kd

10 times smaller than without any inhibitor present (Weidemann *et al.*, 1970). The addition of BKA after ADP increased the binding of the latter, but not when added before ADP. These results are all in agreement with the binding of BKA to the mitochondrial side of the AAC, resulting in the locking of the ADP-side on the mitochondrial intermembrane space side (Klingenberg and Buchholz, 1973).

The binding of BKA to the ATP/ADP carrier was proposed to work in one of two possible models. The first model, also called “single site reorientation mechanism” (synonymously used as SBCGP mechanism), suggested that the BKA and ADP binding sites are the same and that BKA is capable of displacing the latter from its site upon addition. In this model, BKA binds exclusively from the inside of the membrane (Klingenberg and Buchholz, 1973). The second model suggested the presence of an alternative or allosteric site for the binding of BKA (different from that of ADP), which forms a ternary complex of AAC-ADP-BKA and increases the binding affinity of the natural substrate (Lauquin and Vignais, 1976; Weidemann *et al.*, 1970). Although this “dual site allosteric mechanism” seemed to be the most plausible in terms of binding affinity of ADP in the presence of BKA, Klingenberg argued that this system was flawed based on two key observations. First, the allosteric mechanism seemed to be true only in the presence of high concentrations of ADP (50μM). When concentrations 10 times lower were used, the majority of sites re-oriented only with BKA, “locking” the carrier in “m state” on the outer side and making the site inaccessible for ADP. Second, double labelling experiments with ^{3}H (for the endogenous nucleotide pool) and ^{14}C (for the outer ADP pool) showed that internal nucleotides remained attached to the carrier in the presence of BKA, in which most of the binding sites are oriented towards the “m state” on the outer side of the membrane (Klingenberg, 2008). Other groups argued that real initial velocities were not taken into account by the “ping-pong” mechanism proposed by Klingenberg, as well as the energized state of the mitochondrion, which changes the K_m and V_{max} for both ATP and ADP. These data further suggested the formation of a ternary complex, i.e. two adenylate molecules bound to the homodimer of the ATP/ADP carrier (Duyckaerts *et al.*, 1980; Barbour and Chan, 1981).

Studies using combinations of inhibitors showed that the addition of BKA prior to ^{35}S-CAT inhibits partially the binding of the latter, meanwhile displacing ^{35}S-ATR uncompetitively when added after (Klingenberg *et al*., 1971). In the case of both CAT and BKA being mixed with mitochondria at the same time, CAT was not

removed, even though BKA remained attached to its site, which is in accordance with the model that establishes different binding sites for each of these inhibitors (Block *et al*., 1980). Contraries argued that this was due to unspecific uptake of BKA in mitochondria by attesting that when ^{35}-S CAT was bound, ^{3}H-BKA could not bind to its site. This would agree with the mutual displacement model and the ADP-binding dependence of these compounds in the SBCGP mechanism (Klingenberg, 2008).

The latest mathematical model for ATP/ADP exchange takes into account several structural and kinetic properties of the transporter, as well as the effect of the membrane potential and the pH of the surrounding environment where the carrier is embedded (Metelkin *et al.*, 2006). This model is based on a homodimeric structure of the ADP/ATP carrier and takes into account the possible anisotropy of the carrier binding sites by making allowances for differences in binding of the different adenylates (Brandolin *et al.*, 1980). The model suggests further that: (1) the binding of ADP and ATP is independent of each other, although it supports the 1:1 stoichiometry of the reaction as proposed by Kramer and Klingenberg (1982); (2) the pH influences the exchange rate of the carrier (Klingenberg and Rottenberg, 1977); and (3) under uncoupled conditions, ADP leaves the mitochondria due to its dependence on membrane potential (Metelkin *et al.*, 2006).

8. The ADP/ATP carrier mode of transport

Early studies of the ADP/ATP carrier revealed that ADP/ATP transport across the inner mitochondrial membrane is electrogenic in nature (Klingenberg and Rottenberg, 1977; Wulf *et al.*, 1978; LaNoue *et al.*, 1978). Electrogenic transport refers to the transport of one or two ions coupled by a symport or antiport, involving the movement of net charge at molecular level (Nicholls and Ferguson, 2002).

The distinction between net charge movement at a molecular level and the overall neutrality of charge of total ion movement must be made based on the physical properties of the membrane, i.e. their low electrical capacitance. The separation of very small quantities of charge across a membrane cannot take place without the building of a large membrane potential (ψ). Charge balances across the mitochondrial inner membrane have classically been studied with the aid of ionophores, antibiotics or synthetic molecules that are capable of functioning as mobile ion carriers. Examples of these molecules are valinomycin, nigericin, gramidicin and FCCP. Their use depends on the study performed, whether charge,

protons or both are needed to observe ion flux across membranes. Valinomycin is an uncharged ionophore that catalyzes the uniport of Cs^+, Rb^+, K^+ or $NH4^+$. It complexes with an ion and diffuses across the membrane, after which the ion is released, therefore carrying the charge across membrane. Nigericin is an example of a proton carrier, due to the fact that it looses a proton when it binds a cation. The formed complex is then able to diffuse across the mitochondrial membrane, with no net charge change in the process. FCCP, on the other hand, acts as a protonophore or uncoupler, and its net transport involves both protons and charges. FCCP crosses the membrane in its protonated form, after which the H^+ is released and the protonated acid of the uncoupler is reacquired (Nicholls and Ferguson, 2002).

The electrical nature of the ADP/ATP transport catalyzed by AAC was studied with the aid of ionophores. ADP/ATP transport implies the transport of an H^+ across the membrane in order to counterbalance the net charge change involved in the ATP^{4-} /ADP^{3-} counter-exchange across the mitochondrial inner membrane. When mitochondrial preparations were studied in the presence of valinomycin and in a K^+-free medium, ATP entered mitochondria with a H^+ and left it with a K^+. When the experiment was performed in presence of 150mM KCl, ATP entered with a K^+ and left it with a H^+. Similarly, when using FCCP, the H^+/ATP ratio was approximately 1, in either K^+-free or 150mM KCl buffer. These results were in accordance with an electrogenic transport for ATP, where H^+ transport would not necessarily be linked to the ATP/ADP carrier itself (i.e. co-transported) but it would be required for organelle electroneutrality (LaNoue *et al.*, 1978; Wulf *et al.*, 1978; Nicholls and Ferguson, 2002).

9. Structure-function relationship of the ADP/ATP carrier

9.1. The role of Cardiolipin

The interaction of the ADP/ATP carrier with other mitochondrial membrane proteins has been described to be strongly related to the complex structure it forms with cardiolipin (Claypool *et al.*, 2008; Claypool, 2009; Zhang *et al.*, 2002; Mileykovskaya and Dowhan, 2009). Cardiolipin (CL) is a widely distributed phospholipid, found in virtually all organisms. In eukaryotic cells, it is predominantly found in the mitochondrion. Cardiolipin bears an unusual structure (Figure 7), with 2 glycerol chains attached to 2 acyl chains each (Schlame, 2008).

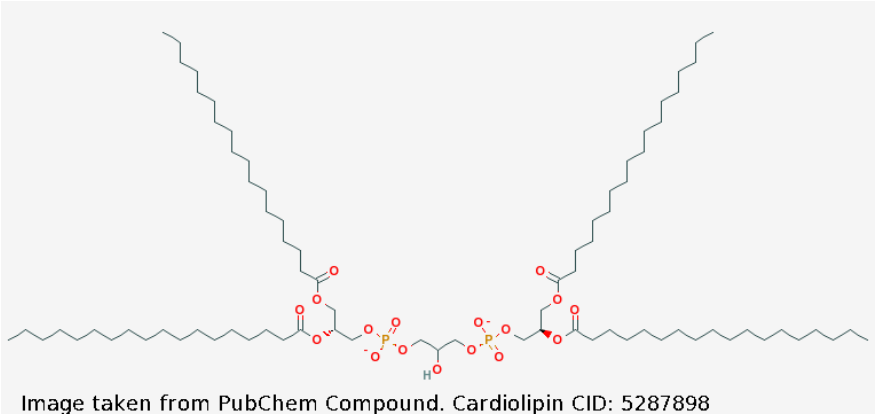

Figure 7. Schematic representation of the cardiolipin structure: the two phosphatidyl moieties are linked via a glycerol to four acyl-chains.

The interaction of cardiolipin with the ADP/ATP carrier was first described by Klingenberg (Riccio *et al.*, 1975b). He and his co-workers acknowledged the fact that once the carrier was “solubilised” with certain detergents, especially anionic detergents like SDS or DOC, it would loose its active conformation in an irreversible way. Other groups also noticed this when trying to reconstitute the ADP/ATP carrier for transport assays. ^{31}P NMR and electron spin resonance studies revealed the presence of 6 cardiolipin molecules per molecule of solubilised carrier (3 per monomer), and that their excision with phospholipase A (PLA) would render the transporter inactive (Beyer and Klingenberg, 1985; Drees and Beyer, 1988; Nury *et al.*, 2005). ^{31}P NMR indicated further the presence of other phospholipids, i.e. phosphatidylcholine (PC), phosphatidyl-ethanolamine (PE), phosphatidylinositol (PI) and phosphatidic acid (PA), in solubilised and purified ADP/ATP carrier preparations (Hoffmann *et al.*, 1994; Epand *et al.*, 2009). All of the studies propose that the interaction of the carrier with CL is rather strong.

To achieve an optimally functioning ADP/ATP carrier for *in vitro* reconstitution studies, different acid phospholipids were tested. Both phosphatidic acid (PA) and phosphatidylserine (PS) were tested along with CL, with the latter being the most efficient of all for the reconstitution of ADP/ATP carrier activity. Upon addition of CL to liposomes, it was noted that CL significantly increased the transport activity of the ADP/ATP carrier and that an optimum was reached in the process (Heimpel *et al.*, 2001). It was further noted that the natural ADP/ATP carrier from beef heart mitochondria required less cardiolipin for optimal transport activity than the recombinant carrier from *Neurospora crassa,* which was overexpressed in *E. coli*.

The recombinant *Neurospora crassa* ADP/ATP carrier isolated from *E. coli* contains lower CL levels, which would explain the observed difference in CL requirement. Crystallographic studies of the ADP/ATP carrier from beef heart mitochondria confirmed further the presence of 3 CL molecules per protein monomer and a strong interaction between the helices and the monomers as well, which would contribute to the stable structure of the dimer (Beyer and Klingenberg, 1985; Nury *et al.*, 2005). Knockout studies of cardiolipin synthase in yeast revealed that the resulting knockout strain *cdr1* was temperature-sensitive and had an impaired growth phenotype on non-fermentable sources (Jiang *et al.*, 2000). Nevertheless, the amount of ADP/ATP carrier per weight of mitochondria did not differ from that observed for the WT. When isolated and reconstituted into liposomes, no ADP/ATP exchange activity was found without the addition of 8% cardiolipin, and even then the transport activity never reached the same level as that of the WT. These experiments confirmed that CL is crucial for the maintenance of transport activity of the ADP/ATP carrier (Heimpel *et al.*, 2001; Klingenberg, 2009).

The precise sites for CL attachment were determined by electron spin resonance studies (Drees and Beyer, 1988). These studies revealed that negatively charged groups from the lipid molecules (head groups) do interact with positively charged amino acids on the protein surface. These observations were corroborated by partial crystallographic studies performed on the bovine heart muscle AAC, showing that the amino acids which interact with CL indeed have a polar character (Nury *et al.*, 2005).

Further proof was provided when analyzing the *S. cerevisiae* AAC (C73S) mutant. This strain is capable of growth on glycerol, but the isolated mutant ADP/ATP carrier failed to show any transport activity when reconstituted into liposomes (Hoffmann *et al.*, 1994). Upon the addition of cardiolipin, activation of transport activity was observed. Specific chemical modifications on the structure of cardiolipin revealed further that not only the negative charges are necessary for the molecule to activate the *S. cerevisiae* AAC, but that removal of the CL acyl-chains resulted in significant loss (approximately 90%) of transport activity (Hoffmann *et al.*, 1994). It was assumed that the ability of the *S. cerevisiae* AAC (C73S) mutant to grow on glycerol was because the C73 residue did not interfere with the ability of the carrier to be expressed or translocated into the mitochondrial membrane. Once embedded in the membrane, the carrier is in close proximity to CL and correspondingly active.

However, after solubilisation of the AAC, CL was easily lost, resulting in inactivation of the AAC carrier.

9.2. ADP/ATP carrier assembly: monomers or dimers?

The notion of an oligomeric state of the ADP/ATP carrier dates its origin to the inhibition studies performed with ATR, CAT and BKA. Evidence for a dimeric form of the protein was found both in mitochondria and in reconstituted proteoliposomes. Sucrose gradients and gel filtration experiments revealed that ^{35}S-CAT formed a complex with protein-detergent (TX-100) micelles in an estequiometric balance, implying a dimeric association of the ADP/ATP carrier (Riccio *et al.*, 1975a; Hackenberg and Klingenberg, 1980). Later, a chimeric tandem-repeated homodimeric ADP/ATP carrier was expressed in an AAC-depleted strain of *S. cerevisiae*. This chimeric ADP/ATP carrier managed to rescue the growth phenotype of this strain by allowing it to grow to WT levels in medium containing the non-fermentable carbon source glycerol. Additionally, active OXPHOS could be measured in the presence of glycerol (Hatanaka *et al.*, 1999). Also other studies supported the idea that the ADP/ATP carrier is only active as a homodimer, with some of them even proposing an important role of CL in the interaction of the two ADP/ATP carrier monomers (Krämer and Klingenberg, 1980; Hackenberg and Klingenberg, 1980; Beyer and Klingenberg, 1985; Epand *et al.*, 2009).

The previously explained SBCGP mechanism is based on the assumption that the carrier works as a homodimer. However, recent studies have challenged this view. Projected electron density maps of two-dimensional AAC3 crystals from *S. cerevisiae*, revealed that the carriers do not form a 12-helix bundle, as it would be expected from a homodimer structure consisting of two 6-helices monomers (Kunji and Harding, 2003). Furthermore, co-expression studies were performed using two different copies of the AAC: one copy which is sensitive to chemical inhibition (WT AAC2) and a second copy (mutated AAC2), which is not sensitive to chemical inhibition. The chemical-insensitive (mutated) AAC2 version was achieved by substituting all 4 cysteines for alanines: these cysteines have previously been proposed to be important for dimerization of the ADP/ATP carrier. Both the WT AAC2 and it mutated copy version were co-expressed in the *S. cerevisiae* KO (Δ*aac2*Δ*cdr1*) strain DNY1, which lacks both functional AAC1 and AAC2. Liposomes were prepared and fused with mitochondrial membranes to perform transport assays in the presence of MTSES, a sulfhydryl reagent. The results revealed that the co-expression of both sensitive and insensitive AAC did not hamper the overall

ADP/ATP exchange activity of the carrier, leading to the conclusion that the carrier works in its monomeric form instead of being associated in dimers (Bamber *et al.*, 2007a). Similar results were obtained by co-expressing differentially tagged carriers and attempting to purify them by affinity chromatography (Bamber *et al.*, 2007b).

The use of a cysteine-less mutant in the above-described experiments is however debatable. Several studies revealed that these cysteines, especially C73 as studied in the above-mentioned C73S mutant of *S. cerevisiae* AAC2, are important in the maintenance of a stable carrier structure, including that of the homodimer, therefore weakening the monomer hypothesis (Claypool, 2009). It is evident that the homo- or dimeric structure of the AAC is still a matter of debate.

10. The ADP/ATP carrier and Oxidative Phosphorylation

As stated earlier, the ADP/ATP carrier catalysis the exchange of cytosolic ADP for mitochondrial ATP. Its connection to oxidative phosphorylation (OXPHOS) places it as the last member of this machinery. The importance of the ADP/ATP carrier in OXPHOS was first observed in a natural respiration-deficient yeast mutant called *pet9*, which is an AAC2 (R96H) mutant (Adrian *et al.*, 1986; Lawson *et al.*, 1990). Although AAC2 is the main ADP/ATP carrier expressed in WT *Saccharomyces cerevisiae*, a KO strain for both AAC 1 and 2 was constructed. The resulting *S. cerevisiae* strain DNY1 was unable to grow on the non-fermentable carbon source glycerol, indicating a reduced OXPHOS capacity. Mutated ADP/ATP carriers were expressed from plasmids, and mutagenesis was performed on amino acids residues that had aroused interest in all the ADP/ATP carriers studied at the time: i.e. the R triads found in the RRRMMM motif, and the 4 positively charged amino acids K38, R96, R204, and R294, which are 100% conserved in all the carriers studied to date (Nelson *et al.*, 1993). Mutations of the individual arginine residues rendered the mutant strains unable to grow on glycerol. Furthermore, their OXPHOS activities were 40 times less that of the yeast containing the WT AAC, suggesting an important role of the ADP/ATP carrier in oxidative phosphorylation (Müller *et al.*, 1996). Reconstitution of the mutated AACs into liposomes and subsequent transport assays confirmed that these AACs were indeed affected in their ADP/ATP exchange activity (Heidkamper *et al.*, 1996).

11. Function of the ADP/ATP carrier in the mitochondrial respiratome

Early mitochondrial respiration studies stated that the components of the respiratory chain, particularly the soluble ones, i.e. cytochrome c and ubiquinone, behaved in

mammalian mitochondrial preparations as a “pool” (Kroger and Klingenberg, 1973; Gupte and Hackenbrock, 1988b; Gupte and Hackenbrock, 1988a). It was postulated that the two smallest components of the respiratory chain acted as mobile electron carriers between diffusible respiratory complexes, which is also described as the “random-collision model” (Chazotte and Hackenbrock, 1988).

With new insights in the respiration process, a different model was proposed. Inhibition studies in yeast revealed that titration of NADH-dehydrogenase and cytochrome c oxidoreductase with antimycin, did not result in a sigmoid-type inhibition curve, as would have been expected if mobile “pools” would exist. The observed inhibition was independent of the substrate used for the respiration experiments, suggesting that both cytochrome c and ubiquinone in yeast were not available in freely diffusible pools under physiological conditions. These experiments suggested further that the respiratory chain works as a single large complex unit, a so-called substrate-channelling complex that improves the rate of respiration (Boumans *et al.*, 1998). The stoichiometric associations of the respiratory chain complexes I-IV in bovine heart mitochondria was assessed with the aid of 2D BN/SDS-PAGE and enzyme assays (Schägger and Pfeiffer, 2001). The obtained results confirmed the existence of supercomplexes, also called “respirasomes”. Additional studies revealed further that the CoQ mobile pool is in equilibrium with protein-bound CoQ (Genova *et al.*, 2008). This equilibrium was found to be dependent on metabolic conditions that could shift the electron transfer mode between substrate-channelling and random diffusion (Genova *et al.*, 2008; Piccoli *et al.*, 2006).

Recent lipid-protein interactions studies strengthened the supercomplex/respirasome model. Especially the observed strong interaction of cardiolipin with several members of the respiratory chain resulted in additional structural evidence for this model (Claypool *et al.*, 2008; Mileykovskaya and Dowhan, 2009). In cardiolipin-defective yeasts, the structural integrity of the supercomplexes is lost. Also the behaviour of the cytochrome c pool was found to be impaired. These observations are consistent with the lack of a substrate-channelling structure in cardiolipin-defective yeasts (Pfeiffer *et al.*, 2003; Zhang *et al.*, 2005). In mammalian cells, Barth syndrome is a condition caused by a mutation of the TAZ gene, which is responsible for the remodelling of the cardiolipin fatty acid composition. Lymphoblasts from Barth syndrome patients have been found to display reduced supercomplex organization, particularly of the I_1III_2 supercomplex,

as well as a lack of inclusion of complex IV in the main structure (McKenzie *et al.*, 2006).

The respiratory chain complex formation does not necessarily include the AAC as a main component. However, recent 2D BN/SDS-PAGE analysis of Δ*aac2*, Δ*cdr1* and Δ*aac2*Δ*cdr1* yeast KO strains indicated that the ADP/ATP carrier indeed structurally interacts with the respirasome (Claypool *et al.*, 2008). In WT yeast, a clear structural relationship was found between AAC2 and the III_2IV complex. In the Δ*aac2* mutant, however, an increased complex III_2IV/ III_2IV_2 ratio was found when compared to the WT. This ratio increased even further in the Δ*aac2*Δ*cdr1* double mutant. As expected, the complex IV activity decreased accordingly in the different AAC KO strains (Claypool *et al.*, 2008), suggesting an important role of the AAC in respirasome activity. Physical association of AAC2 with the cytochrome c reductase (cytochrome bc1)/cytochrome c oxidase (COX) supercomplex was recently demonstrated for yeast (Dienhart and Stuart, 2008).

12. Other roles besides energy production: The Mitochondrial Permeability Transition Pore

The mitochondrial inner membrane forms, under certain conditions, a large nonspecific pore called the Mitochondrial Permeability Transition Pore (MPTP). Formation of the MPTP is initiated by Ca^{2+}, and is inhibited by cyclosporine A and the withdrawal of Ca^{2+} (Haworth and Hunter, 1979; Hunter and Haworth, 1979; Crompton and Costi, 1988; Zoratti and Szabò, 1995). The MPTP has been very well studied, particularly in mammalian heart mitochondria where its role in ischemia reperfusion damage and apoptosis is striking (Crompton, 1999). The Voltage Gated Anion Channel (VDAC) in the outer mitochondrial membrane, cyclophilin D (CyP-D) in the mitochondrial matrix, and the ANT (the mammalian version of the AAC) in the inner mitochondrial membrane, represent the core complex of the MPTP (Figure 8) (Halestrap and Brenner, 2003; Zoratti and Szabò, 1995; Brustovetsky *et al.*, 2002; Crompton *et al.*, 1988; Broekemeier *et al.*, 1989). The proposed function of this core complex is to establish contact points between the inner and outer mitochondrial membranes (Ohlendieck *et al.*, 1986; Moynagh, 1995). Also other proteins (see Figure 8) can be associated with this complex, like for example hexokinase (HK), glycerol kinase (GK), and the mitochondrial benzodiazepin receptor (mBr).

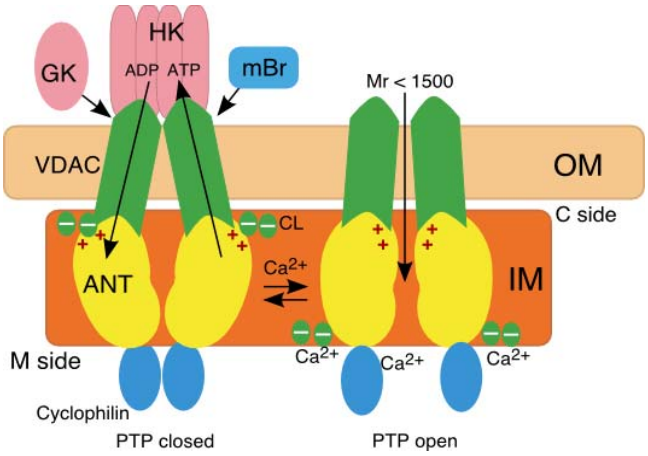

Figure 8. Model of the mitochondrial permeability transition pore. Hexokinase (HK), glycerol kinase (GK) and the mitochondrial benzodiazepin (mBr) receptor bind to the VDAC-ANT-CyP-D complex in the contact sites of mitochondria. Ca^{2+} can interact with CL bound to the ANT. Image taken from Vyssokikh and Brdiczka (2003).

Klingenberg observed that the ADP/ATP carrier could open reversibly as an specific channel in the presence of elevated levels of Ca^{2+} (Brustovetsky and Klingenberg, 1996). This change in transport function is mainly driven by Ca^{2+}, which binds to ANT-associated CL. As mentioned before, CL plays a key role in ADP/ATP carrier function. Moreover, in absence of adenylates, AAC inhibitors would cause an efflux of K^+ (Panov *et al.*, 1980). Channel opening could be reversed by the addition of ADP and BKA, but not by CAT (Brustovetsky and Klingenberg, 1996). Both CAT and ATR induced opening of the channel, implicating that the carrier must be locked in the c-state in order to aid in the mitochondrial permeability pore (Halestrap and Brenner, 2003; Crompton, 1999). Klingenbergs studies were performed with purified AAC, which omitted the possibility of cyclophilin D in the preparations; therefore cyclosporine A did not inhibit the channel activity. Similar Ca^{2+}-dependent channel activity was also observed by other groups using AAC-containing liposomes filled with different substrates (Rück *et al.*, 1998; Brustovetsky *et al.*, 2002).

Mitochondrial permeability transition (MPT) has been described as a mitochondrial dysfunction arising from Ca^{2+} overload (Crompton, 1999). Ca^{2+} enters the mitochondrion via a Ca^{2+}-uniporter and exits by counter exchange with Na^+, through the Na^+/Ca^{2+}-antiporter. The in general slow cycling of these ions is driven by the membrane potential (Crompton and Heid, 1978). Ca^{2+} has been shown previously to have regulatory roles in the activity of different mitochondrial enzymes such as pyruvate dehydrogenase, α-ketoglutarate dehydrogenase and isocitrate

dehydrogenase (McCormack *et al.*, 1990). When Ca^{2+} accumulates inside the mitochondrion under pathological conditions, cell damage is not triggered until the mitochondrial adenylate ratio collapses, leading to: (1) opening of the MPTP, (2) the efflux of Ca^{2+} from the mitochondrion, and (3) subsequent loss of the mitochondrial membrane potential.

The presence of ANT in the MPTP complex suggested a role of this carrier in MPT. Recent studies performed with ΔANT1/ΔANT2 KO mice revealed however that MPT still could take place in the absence of these carriers, leading to the initial conclusion that both ANT1 and ANT2 are not essential for MPT (Kokoszka *et al.*, 2004). This conclusion was contradicted by other observations showing that the MPTP in the ΔANT1/ΔANT2 KO mice was less sensitive to Ca^{2+}, and was not regulated by either ADP or ATP (Kokoszka *et al.*, 2004). This suggests that ANT is involved in MPT, and the earlier contradiction results were explained with the hypothesis that maybe another MCF protein could have taken on part of the role of ANT in the ΔANT1/ΔANT2 KO mice (Halestrap, 2004; Palmieri, 2004). This MCF protein has not been identified yet, and the exact role of ANT in MPT remains still elusive.

13. Aims of the PhD project

The putative transport function of a particular MCF protein can be predicted from its amino acid sequence by (1) determining its sequence similarity to functionally characterised MCF proteins of other eukaryotes, (2) determining its phylogenetic relationship to other known MCF proteins, and (3) the presence of specific “contact points”, i.e. meaning particular conserved amino acids, in the MCF protein sequence which are involved in the binding of specific substrates (Section 5 of the Introduction). However, it has been demonstrated that it is not possible to reliably predict substrate specificity from the deduced amino acid sequences alone. Mitochondrial carrier family proteins were further shown to be highly divergent. Therefore, the most important tools for functional characterisation of MCF proteins are still metabolic studies of knockout cell lines and the in vitro reconstitution in liposomes followed by metabolite transport assays.

The ADP/ATP carrier plays a key role in the energy metabolism of virtually all mitochondriate eukaryotes, and as is evident from this Introduction, it represents the best-characterized MCF protein to date. A similar important role is also anticipated for any ADP/ATP carrier found in *Trypanosoma brucei*. Major aims of this Ph.D.

project were (A) the identification of putative *T. brucei* nucleotide carriers, i.e. ADP/ATP and GDP/GTP carriers, and (B) the determination of their physiological roles in trypanosomes.

The objectives to be achieved were:

- Identify ADP/ATP and GDP/GTP-exchanging MCF proteins in *T. brucei*, and subsequently analyse their sequences by molecular and phylogenetic tools.
- Determine the expression of identified ADP/ATP and GDP/GTP carriers at the RNA and protein level, and in different life cycle stages of *T. brucei*.
- Determine the subcellular localization of the identified ADP/ATP and GDP/GTP carriers in different life cycle stages of *T. brucei*.
- Generate stable knockout cell lines for the identified putative ADP/ATP and GDP/GTP carriers in procyclic form *T. brucei*, and determine the physiological consequences of the gene knockouts.
- Express the putative ADP/ATP and GDP/GTP carriers in different heterologous systems, followed by solubilization and purification of these MCF proteins for their subsequent reconstitution in liposomes.
- Determine the substrate specificity of the putative ADP/ATP and GDP/GTP carriers and their kinetic parameters.

14. References

Acosta, H., Dubourdieu, M., Quinones, W., Caceres, A., Bringaud, F. & Concepcion, J. L. 2004. Pyruvate phosphate dikinase and pyrophosphate metabolism in the glycosome of Trypanosoma cruzi epimastigotes. *Comp Biochem Physiol B Biochem Mol Biol,* 138**,** 347-56.

Acosta-Serrano, A., Cole, R., Mehlert, A., Lee, M., Ferguson, M. & Englund, P. 1999. The Procyclin Repertoire of Trypanosoma brucei Identification and Structural Characterizationof the Glu-Pro-Rich Polypeptides. *J Biol Chem,* 274**,** 29763-29771.

Adams, E. R., Hamilton, P. B. & Gibson, W. C. 2010. African trypanosomes: celebrating diversity. *Trends Parasitol,* 26**,** 324-8.

Adrian, G. S., McCammon, M. T., Montgomery, D. L. & Douglas, M. G. 1986. Sequences required for delivery and localization of the ADP/ATP translocator to the mitochondrial inner membrane. *Mol Cell Biol,* 6**,** 626-34.

Alarcon, C. M., Son, H. J., Hall, T. & Donelson, J. E. 1994. A monocistronic transcript for a trypanosome variant surface glycoprotein. *Mol Cell Biol,* 14**,** 5579-91.

Allemann, N. & Schneider, A. 2000. ATP production in isolated mitochondria of procyclic Trypanosoma brucei. *Mol Biochem Parasitol,* 111**,** 87-94.

Amin, D. N., Masocha, W., Ngan'dwe, K., Rottenberg, M. & Kristensson, K. 2008. Suramin and minocycline treatment of experimental African trypanososmiasis at an early stage of parasite brain invasion. *Acta Trop,* 106**,** 72-4.

Antonenkov, V. D. 1989. Dehydrogenases of the pentose phosphate pathway in rat liver peroxisomes. *Eur J Biochem,* 183**,** 75-82.

Aquila, H., Link, T. A. & Klingenberg, M. 1987. Solute carriers involved in energy transfer of mitochondria form a homologous protein family. *FEBS Lett,* 212**,** 1-9.

Aranda, A., Maugeri, D., Uttaro, A. D., Opperdoes, F., Cazzulo, J. J. & Nowicki, C. 2006. The malate dehydrogenase isoforms from Trypanosoma brucei:

subcellular localization and differential expression in bloodstream and procyclic forms. *Int J Parasitol,* 36**,** 295-307.

Bacchi, C. J. 2009. Chemotherapy of human african trypanosomiasis. *Interdiscip Perspect Infect Dis,* 2009**,** 195040.

Bacchi, C. J., Garofalo, J., Mockenhaupt, D., McCann, P. P., Diekema, K. A., Pegg, A. E., Nathan, H. C., Mullaney, E. A., Chunosoff, L., Sjoerdsma, A. & Hutner, S. H. 1983. In vivo effects of alpha-DL-difluoromethylornithine on the metabolism and morphology of Trypanosoma brucei brucei. *Mol Biochem Parasitol,* 7**,** 209-25.

Balmer, O., Beadell, J. S., Gibson, W. & Caccone, A. 2011. Phylogeography and taxonomy of Trypanosoma brucei. *PLoS Negl Trop Dis,* 5**,** e961.

Bamber, L., Harding, M., Monné, M., Slotboom, D.-J. & Kunji, E. R. S. 2007a. The yeast mitochondrial ADP/ATP carrier functions as a monomer in mitochondrial membranes. *Proc Natl Acad Sci USA,* 104**,** 10830-4.

Bamber, L., Slotboom, D.-J. & Kunji, E. R. S. 2007b. Yeast mitochondrial ADP/ATP carriers are monomeric in detergents as demonstrated by differential affinity purification. *J Mol Biol,* 371**,** 388-95.

Barbour, R. L. & Chan, S. H. 1981. Characterization of the kinetics and mechanism of the mitochondrial ADP-atp carrier. *J Biol Chem,* 256**,** 1940-8.

Barrett, M. P., Boykin, D. W., Brun, R. & Tidwell, R. R. 2007. Human African trypanosomiasis: pharmacological re-engagement with a neglected disease. *Br J Pharmacol,* 152**,** 1155-71.

Barrett, M. P., Zhang, Z. Q., Denise, H., Giroud, C. & Baltz, T. 1995. A diamidine-resistant Trypanosoma equiperdum clone contains a P2 purine transporter with reduced substrate affinity. *Mol Biochem Parasitol,* 73**,** 223-9.

Barry, J. D. & McCulloch, R. 2001. Antigenic variation in trypanosomes: enhanced phenotypic variation in a eukaryotic parasite. *Adv Parasitol,* 49**,** 1-70.

Benaim, G., Lopez-Estrano, C., Docampo, R. & Moreno, S. N. 1993. A calmodulin-stimulated Ca2+ pump in plasma-membrane vesicles from Trypanosoma brucei; selective inhibition by pentamidine. *Biochem J,* 296 (Pt 3)**,** 759-63.

Berriman, M., Ghedin, E., Hertz-Fowler, C., Blandin, G., Renauld, H., Bartholomeu, D. C., Lennard, N. J., Caler, E., Hamlin, N. E., Haas, B., Bohme, U., Hannick, L., Aslett, M. A., Shallom, J., Marcello, L., Hou, L., Wickstead, B., Alsmark, U. C., Arrowsmith, C., Atkin, R. J., Barron, A. J., Bringaud, F., Brooks, K., Carrington, M., Cherevach, I., Chillingworth, T. J., Churcher, C., Clark, L. N., Corton, C. H., Cronin, A., Davies, R. M., Doggett, J., Djikeng, A., Feldblyum, T., Field, M. C., Fraser, A., Goodhead, I., Hance, Z., Harper, D., Harris, B. R., Hauser, H., Hostetler, J., Ivens, A., Jagels, K., Johnson, D., Johnson, J., Jones, K., Kerhornou, A. X., Koo, H., Larke, N., Landfear, S., Larkin, C., Leech, V., Line, A., Lord, A., Macleod, A., Mooney, P. J., Moule, S., Martin, D. M., Morgan, G. W., Mungall, K., Norbertczak, H., Ormond, D., Pai, G., Peacock, C. S., Peterson, J., Quail, M. A., Rabbinowitsch, E., Rajandream, M. A., Reitter, C., Salzberg, S. L., Sanders, M., Schobel, S., Sharp, S., Simmonds, M., Simpson, A. J., Tallon, L., Turner, C. M., Tait, A., Tivey, A. R., Van Aken, S., Walker, D., Wanless, D., Wang, S., White, B., White, O., Whitehead, S., Woodward, J., Wortman, J., Adams, M. D., Embley, T. M., Gull, K., Ullu, E., Barry, J. D., Fairlamb, A. H., Opperdoes, F., Barrell, B. G., Donelson, J. E., Hall, N., Fraser, C. M., et al. 2005. The genome of the African trypanosome Trypanosoma brucei. *Science,* 309**,** 416-22.

Besteiro, S., Barrett, M. P., Riviere, L. & Bringaud, F. 2005. Energy generation in insect stages of Trypanosoma brucei: metabolism in flux. *Trends Parasitol,* 21**,** 185-91.

Besteiro, S., Biran, M., Biteau, N., Coustou, V., Baltz, T., Canioni, P. & Bringaud, F. 2002. Succinate secreted by Trypanosoma brucei is produced by a novel and unique glycosomal enzyme, NADH-dependent fumarate reductase. *J Biol Chem,* 277**,** 38001-12.

Beyer, K. & Klingenberg, M. 1985. ADP/ATP carrier protein from beef heart mitochondria has high amounts of tightly bound cardiolipin, as revealed by 31P nuclear magnetic resonance. *Biochemistry,* 24**,** 3821-6.

Bitonti, A. J., Bacchi, C. J., McCann, P. P. & Sjoerdsma, A. 1986. Uptake of alpha-difluoromethylornithine by Trypanosoma brucei brucei. *Biochem Pharmacol,* 35**,** 351-4.

Bochud-Allemann, N. & Schneider, A. 2002. Mitochondrial substrate level phosphorylation is essential for growth of procyclic Trypanosoma brucei. *J Biol Chem,* 277**,** 32849-54.

Bogner, W., Aquila, H. & Klingenberg, M. 1986. The transmembrane arrangement of the ADP/ATP carrier as elucidated by the lysine reagent pyridoxal 5-phosphate. *Eur J Biochem,* 161**,** 611-20.

Boumans, H., Grivell, L. A. & Berden, J. A. 1998. The respiratory chain in yeast behaves as a single functional unit. *J Biol Chem,* 273**,** 4872-7.

Brandolin, G., Doussiere, J., Gulik, A., Gulik-Krzywicki, T., Lauquin, G. J. & Vignais, P. V. 1980. Kinetic, binding and ultrastructural properties of the beef heart adenine nucleotide carrier protein after incorporation into phospholipid vesicles. *Biochim Biophys Acta,* 592**,** 592-614.

Bridges, D. J., Gould, M. K., Nerima, B., Maser, P., Burchmore, R. J. & de Koning, H. P. 2007. Loss of the high-affinity pentamidine transporter is responsible for high levels of cross-resistance between arsenical and diamidine drugs in African trypanosomes. *Mol Pharmacol,* 71**,** 1098-108.

Broekemeier, K. M., Dempsey, M. E. & Pfeiffer, D. R. 1989. Cyclosporin A is a potent inhibitor of the inner membrane permeability transition in liver mitochondria. *J Biol Chem,* 264**,** 7826-30.

Brown, R. C., Evans, D. A. & Vickerman, K. 1973. Changes in oxidative metabolism and ultrastructure accompanying differentiation of the mitochondrion in Trypanosoma brucei. *Int J Parasitol,* 3**,** 691-704.

Brown, S. D., Huang, J. & Van der Ploeg, L. H. 1992. The promoter for the procyclic acidic repetitive protein (PARP) genes of Trypanosoma brucei shares features with RNA polymerase I promoters. *Mol Cell Biol,* 12**,** 2644-52.

Bruni, A., Luciani, S. & Contessa, A. R. 1964a. Inhibition by Atractyloside of the Binding of Adenine-Nucleotides to Rat-Liver Mitochondria. *Nature,* 201**,** 1219-20.

Bruni, A., Luciani, S., Contessa, A. R. & Azzone, G. F. 1964b. Effects of Atractyloside and Oligomycin on Energy-Transfer Reactions. *Biochim Biophys Acta,* 82**,** 630-2.

Brustovetsky, N. & Klingenberg, M. 1996. Mitochondrial ADP/ATP carrier can be reversibly converted into a large channel by Ca2+. *Biochemistry,* 35**,** 8483-8.

Brustovetsky, N., Tropschug, M., Heimpel, S., Heidkämper, D. & Klingenberg, M. 2002. A large Ca2+-dependent channel formed by recombinant ADP/ATP carrier from Neurospora crassa resembles the mitochondrial permeability transition pore. *Biochemistry,* 41**,** 11804-11.

Byers, T. L., Bush, T. L., McCann, P. P. & Bitonti, A. J. 1991. Antitrypanosomal effects of polyamine biosynthesis inhibitors correlate with increases in Trypanosoma brucei brucei S-adenosyl-L-methionine. *Biochem J,* 274 (Pt 2)**,** 527-33.

Caceres, A. J., Portillo, R., Acosta, H., Rosales, D., Quinones, W., Avilan, L., Salazar, L., Dubourdieu, M., Michels, P. A. & Concepcion, J. L. 2003. Molecular and biochemical characterization of hexokinase from Trypanosoma cruzi. *Mol Biochem Parasitol,* 126**,** 251-62.

Campbell, D. A., Thomas, S. & Sturm, N. R. 2003. Transcription in kinetoplastid protozoa: why be normal? *Microbes Infect,* 5**,** 1231-40.

Carter, N. S. & Fairlamb, A. H. 1993. Arsenical-resistant trypanosomes lack an unusual adenosine transporter. *Nature,* 361**,** 173-6.

Cazzulo, J. J. 1992. Aerobic fermentation of glucose by trypanosomatids. *FASEB J,* 6**,** 3153-61.

Chazotte, B. & Hackenbrock, C. R. 1988. The multicollisional, obstructed, long-range diffusional nature of mitochondrial electron transport. *J Biol Chem,* 263**,** 14359-67.

Claypool, S. M. 2009. Cardiolipin, a critical determinant of mitochondrial carrier protein assembly and function. *BBA - Biomembranes***,** 1-10.

Claypool, S. M., Oktay, Y., Boontheung, P., Loo, J. A. & Koehler, C. M. 2008. Cardiolipin defines the interactome of the major ADP/ATP carrier protein of the mitochondrial inner membrane. *J Cell Biol,* 182**,** 937-50.

Clayton, J. 2010. Chagas disease: pushing through the pipeline. *Nature,* 465**,** S12-S15 %U http://dx.doi.org/10.1038/nature09224.

Colasante, C., Alibu, V. P., Kirchberger, S., Tjaden, J., Clayton, C. & Voncken, F. 2006a. Characterization and developmentally regulated localization of the mitochondrial carrier protein homologue MCP6 from Trypanosoma brucei. *Eukaryot Cell,* 5**,** 1194-205.

Colasante, C., Ellis, M., Ruppert, T. & Voncken, F. 2006b. Comparative proteomics of glycosomes from bloodstream form and procyclic culture form Trypanosoma brucei brucei. *Proteomics,* 6**,** 3275-3293.

Colasante, C., Peña Diaz, P., Clayton, C. & Voncken, F. 2009. Mitochondrial carrier family inventory of Trypanosoma brucei brucei: Identification, expression and subcellular localisation. *Mol Biochem Parasitol,* 167**,** 104-17.

Concepcion, J. L., Gonzalez-Pacanowska, D. & Urbina, J. A. 1998. 3-Hydroxy-3-methyl-glutaryl-CoA reductase in Trypanosoma (Schizotrypanum) cruzi: subcellular localization and kinetic properties. *Arch Biochem Biophys,* 352**,** 114-20.

Coppens, I., Opperdoes, F. R., Courtoy, P. J. & Baudhuin, P. 1987. Receptor-mediated endocytosis in the bloodstream form of Trypanosoma brucei. *J Protozool,* 34**,** 465-73.

Coustou, V., Besteiro, S., Biran, M., Diolez, P., Bouchaud, V., Voisin, P., Michels, P. A., Canioni, P., Baltz, T. & Bringaud, F. 2003. ATP generation in the Trypanosoma brucei procyclic form: cytosolic substrate level is essential, but not oxidative phosphorylation. *J Biol Chem,* 278**,** 49625-35.

Coustou, V., Besteiro, S., Rivière, L., Biran, M., Biteau, N., Franconi, J.-M., Boshart, M., Baltz, T. & Bringaud, F. 2005. A mitochondrial NADH-dependent fumarate reductase involved in the production of succinate excreted by procyclic Trypanosoma brucei. *J Biol Chem,* 280**,** 16559-70.

Coustou, V., Biran, M., Breton, M., Guegan, F., Riviere, L., Plazolles, N., Nolan, D., Barrett, M. P., Franconi, J. M. & Bringaud, F. 2008. Glucose-induced remodeling of intermediary and energy metabolism in procyclic Trypanosoma brucei. *J Biol Chem,* 283**,** 16342-54.

Crompton, M. 1999. The mitochondrial permeability transition pore and its role in cell death. *Biochem. J.,* 341**,** 233-249.

Crompton, M. & Costi, A. 1988. Kinetic evidence for a heart mitochondrial pore activated by Ca2+, inorganic phosphate and oxidative stress. A potential mechanism for mitochondrial dysfunction during cellular Ca2+ overload. *Eur J Biochem,* 178**,** 489-501.

Crompton, M., Ellinger, H. & Costi, A. 1988. Inhibition by cyclosporin A of a Ca2+-dependent pore in heart mitochondria activated by inorganic phosphate and oxidative stress. *Biochem J,* 255**,** 357-60.

Crompton, M. & Heid, I. 1978. The cycling of calcium, sodium, and protons across the inner membrane of cardiac mitochondria. *Eur J Biochem,* 91**,** 599-608.

Czichos, J., Nonnengaesser, C. & Overath, P. 1986. Trypanosoma brucei: cis-aconitate and temperature reduction as triggers of synchronous transformation of bloodstream to procyclic trypomastigotes in vitro. *Exp Parasitol,* 62**,** 283-91.

Danieli, B., Bombardelli, E., Bonati, A. & Gabetta, B. 1972. Structure of the diterpenoid carboxyatractyloside. *Phytochemistry,* 11**,** 3501-3504.

de Hoop, M. J. & Geert, A. 1992. Import of proteins into peroxisomes and other microbodies. *Biochem J,* 286 (Pt 3)**,** 657-69.

de Koning, H. P. 2001a. Transporters in African trypanosomes: role in drug action and resistance. *Int J Parasitol,* 31**,** 512-22.

de Koning, H. P. 2001b. Uptake of pentamidine in Trypanosoma brucei brucei is mediated by three distinct transporters: implications for cross-resistance with arsenicals. *Mol Pharmacol,* 59**,** 586-92.

Dean, S., Marchetti, R., Kirk, K. & Matthews, K. R. 2009. A surface transporter family conveys the trypanosome differentiation signal. *Nature,* 459**,** 213-7.

Dienhart, M. K. & Stuart, R. A. 2008. The yeast Aac2 protein exists in physical association with the cytochrome bc1-COX supercomplex and the TIM23 machinery. *Mol Biol Cell,* 19**,** 3934-43.

Docampo, R., de Souza, W., Miranda, K., Rohloff, P. & Moreno, S. N. 2005. Acidocalcisomes - conserved from bacteria to man. *Nat Rev Microbiol,* 3**,** 251-61.

Dovey, H. F., Parsons, M. & Wang, C. C. 1988. Biogenesis of glycosomes of Trypanosoma brucei: an in vitro model of 3-phosphoglycerate kinase import. *Proc Natl Acad Sci USA,* 85**,** 2598-602.

Drees, M. & Beyer, K. 1988. Interaction of phospholipids with the detergent-solubilized ADP/ATP carrier protein as studied by spin-label electron spin resonance. *Biochemistry,* 27**,** 8584-91.

Duffieux, F., Van Roy, J., Michels, P. A. & Opperdoes, F. R. 2000. Molecular characterization of the first two enzymes of the pentose-phosphate pathway of Trypanosoma brucei. Glucose-6-phosphate dehydrogenase and 6-phosphogluconolactonase. *J Biol Chem,* 275**,** 27559-65.

Duyckaerts, C., Sluse-Goffart, C. M., Fux, J. P., Sluse, F. E. & Liebecq, C. 1980. Kinetic mechanism of the exchanges catalysed by the adenine-nucleotide carrier. *Eur J Biochem,* 106**,** 1-6.

Ebikeme, C., Hubert, J., Biran, M., Gouspillou, G., Morand, P., Plazolles, N., Guegan, F., Diolez, P., Franconi, J.-M., Portais, J.-C. & Bringaud, F. 2010. Ablation of succinate production from glucose metabolism in the procyclic trypanosomes induces metabolic switches to the glycerol 3-phosphate/dihydroxyacetone phosphate shuttle and to proline metabolism. *J Biol Chem,* 285**,** 32312-24.

El Rayah, I. E., Kaminsky, R., Schmid, C. & El Malik, K. H. 1999. Drug resistance in Sudanese Trypanosoma evansi. *Vet Parasitol,* 80**,** 281-7.

Epand, R. M., Epand, R. F., Berno, B., Pelosi, L. & Brandolin, G. 2009. Association of phosphatidic acid with the bovine mitochondrial ADP/ATP carrier. *Biochemistry,* 48**,** 12358-64.

Fairlamb, A. H., Blackburn, P., Ulrich, P., Chait, B. T. & Cerami, A. 1985. Trypanothione: a novel bis(glutathionyl)spermidine cofactor for glutathione reductase in trypanosomatids. *Science,* 227**,** 1485-7.

Fairlamb, A. H., Henderson, G. B. & Cerami, A. 1989. Trypanothione is the primary target for arsenical drugs against African trypanosomes. *Proc Natl Acad Sci U S A,* 86**,** 2607-11.

Fenn, K. & Matthews, K. R. 2007. The cell biology of Trypanosoma brucei differentiation. *Curr Opin Microbiol,* 10**,** 539-46.

Ferella, M., Li, Z. H., Andersson, B. & Docampo, R. 2008. Farnesyl diphosphate synthase localizes to the cytoplasm of Trypanosoma cruzi and T. brucei. *Exp Parasitol,* 119**,** 308-12.

Ferguson, M. A. 1997. The surface glycoconjugates of trypanosomatid parasites. *Philos Trans R Soc Lond B Biol Sci,* 352**,** 1295-302.

Field, M. C., Menon, A. K. & Cross, G. A. 1991. A glycosylphosphatidylinositol protein anchor from procyclic stage Trypanosoma brucei: lipid structure and biosynthesis. *EMBO J,* 10**,** 2731-9.

Frearson, J. A., Brand, S., Mcelroy, S. P., Cleghorn, L. A. T., Smid, O., Stojanovski, L., Price, H. P., Guther, M. L. S., Torrie, L. S., Robinson, D. A., Hallyburton, I., Mpamhanga, C. P., Brannigan, J. A., Wilkinson, A. J., Hodgkinson, M., Hui, R., Qiu, W., Raimi, O. G., van Aalten, D. M. F., Brenk, R., Gilbert, I. H., Read, K. D., Fairlamb, A. H., Ferguson, M. A. J., Smith, D. F. & Wyatt, P. G. 2010. N-myristoyltransferase inhibitors as new leads to treat sleeping sickness. *Nature,* 464**,** 728-32.

Gao, G., Nara, T., Nakajima-Shimada, J. & Aoki, T. 1999. Novel organization and sequences of five genes encoding all six enzymes for de novo pyrimidine biosynthesis in Trypanosoma cruzi. *J Mol Biol,* 285**,** 149-61.

Genova, M. L., Baracca, A., Biondi, A., Casalena, G., Faccioli, M., Falasca, A. I., Formiggini, G., Sgarbi, G., Solaini, G. & Lenaz, G. 2008. Is supercomplex organization of the respiratory chain required for optimal electron transfer activity? *Biochim Biophys Acta,* 1777**,** 740-6.

Gibson, W. 2003. Species concepts for trypanosomes: from morphological to molecular definitions? *Kinetoplastid Biol Dis,* 2**,** 10.

Gibson, W. & Bailey, M. 2003. The development of Trypanosoma brucei within the tsetse fly midgut observed using green fluorescent trypanosomes. *Kinetoplastid Biol Dis,* 2**,** 1.

Gilinger, G. & Bellofatto, V. 2001. Trypanosome spliced leader RNA genes contain the first identified RNA polymerase II gene promoter in these organisms. *Nucleic Acids Res,* 29**,** 1556-64.

Ginger, M. L., McFadden, G. I. & Michels, P. A. 2010. Rewiring and regulation of cross-compartmentalized metabolism in protists. *Philos Trans R Soc Lond B Biol Sci,* 365**,** 831-45.

Guler, J. L., Kriegova, E., Smith, T. K., Lukes, J. & Englund, P. T. 2008. Mitochondrial fatty acid synthesis is required for normal mitochondrial morphology and function in Trypanosoma brucei. *Mol Microbiol,* 67**,** 1125-42.

Gupte, S. S. & Hackenbrock, C. R. 1988a. Multidimensional diffusion modes and collision frequencies of cytochrome c with its redox partners. *J Biol Chem,* 263**,** 5241-7.

Gupte, S. S. & Hackenbrock, C. R. 1988b. The role of cytochrome c diffusion in mitochondrial electron transport. *J Biol Chem,* 263**,** 5248-53.

Hackenberg, H. & Klingenberg, M. 1980. Molecular weight and hydrodynamic parameters of the adenosine 5'-diphosphate--adenosine 5'-triphosphate carrier in Triton X-100. *Biochemistry,* 19**,** 548-55.

Haegele, K. D., Alken, R. G., Grove, J., Schechter, P. J. & Koch-Weser, J. 1981. Kinetics of alpha-difluoromethylornithine: an irreversible inhibitor of ornithine decarboxylase. *Clin Pharmacol Ther,* 30**,** 210-7.

Halestrap, A. P. 2004. Mitochondrial permeability: dual role for the ADP/ATP translocator? *Nature,* 430**,** 1 p following 983.

Halestrap, A. P. & Brenner, C. 2003. The adenine nucleotide translocase: a central component of the mitochondrial permeability transition pore and key player in cell death. *Curr Med Chem,* 10**,** 1507-25.

Hall, B. S., Bot, C. & Wilkinson, S. R. 2011. Nifurtimox activation by trypanosomal type I nitroreductases generates cytotoxic nitrile metabolites. *J Biol Chem,* 286**,** 13088-95.

Hamilton, P. B., Stevens, J. R., Gaunt, M. W., Gidley, J. & Gibson, W. C. 2004. Trypanosomes are monophyletic: evidence from genes for glyceraldehyde

phosphate dehydrogenase and small subunit ribosomal RNA. *Int J Parasitol,* 34**,** 1393-404.

Hammond, D., Aman, R. & Wang, C. 1985. The role of compartmentation and glycerol kinase in the synthesis of ATP within the glycosome of Trypanosoma brucei. *J Biol Chem,* 260**,** 15646-15654.

Hanau, S., Rippa, M., Bertelli, M., Dallocchio, F. & Barrett, M. P. 1996. 6-Phosphogluconate dehydrogenase from Trypanosoma brucei. Kinetic analysis and inhibition by trypanocidal drugs. *Eur J Biochem,* 240**,** 592-9.

Hannaert, V., Bringaud, F., Opperdoes, F. R. & Michels, P. A. 2003a. Evolution of energy metabolism and its compartmentation in Kinetoplastida. *Kinetoplastid Biol Dis,* 2**,** 11.

Hannaert, V., Saavedra, E., Duffieux, F., Szikora, J.-P., Rigden, D. J., Michels, P. A. M. & Opperdoes, F. R. 2003b. Plant-like traits associated with metabolism of Trypanosoma parasites. *Proc Natl Acad Sci USA,* 100**,** 1067-71.

Hart, D. T., Baudhuin, P., Opperdoes, F. R. & de Duve, C. 1987. Biogenesis of the glycosome in Trypanosoma brucei: the synthesis, translocation and turnover of glycosomal polypeptides. *EMBO J,* 6**,** 1403-11.

Hatanaka, T., Hashimoto, M., Majima, E., Shinohara, Y. & Terada, H. 1999. Functional expression of the tandem-repeated homodimer of the mitochondrial ADP/ATP carrier in Saccharomyces cerevisiae. *Biochem Biophys Res Commun,* 262**,** 726-30.

Haworth, R. A. & Hunter, D. R. 1979. The Ca2+-induced membrane transition in mitochondria. II. Nature of the Ca2+ trigger site. *Arch Biochem Biophys,* 195**,** 460-7.

Heidkamper, D., Muller, V., Nelson, D. R. & Klingenberg, M. 1996. Probing the role of positive residues in the ADP/ATP carrier from yeast. The effect of six arginine mutations on transport and the four ATP versus ADP exchange modes. *Biochemistry,* 35**,** 16144-52.

Heimpel, S., Basset, G., Odoy, S. & Klingenberg, M. 2001. Expression of the mitochondrial ADP/ATP carrier in Escherichia coli. Renaturation,

reconstitution, and the effect of mutations on 10 positive residues. *J Biol Chem,* 276**,** 11499-506.

Heise, N. & Opperdoes, F. R. 1999. Purification, localisation and characterisation of glucose-6-phosphate dehydrogenase of Trypanosoma brucei. *Mol Biochem Parasitol,* 99**,** 21-32.

Heise, N. & Opperdoes, F. R. 2000. Localisation of a 3-hydroxy-3-methylglutaryl-coenzyme A reductase in the mitochondrial matrix of Trypanosoma brucei procyclics. *Z Naturforsch C,* 55**,** 473-7.

Henderson, P. J. & Lardy, H. A. 1970. Bongkrekic acid. An inhibitor of the adenine nucleotide translocase of mitochondria. *J Biol Chem,* 245**,** 1319-26.

Hill, J. E., Scott, D. A., Luo, S. & Docampo, R. 2000. Cloning and functional expression of a gene encoding a vacuolar-type proton-translocating pyrophosphatase from Trypanosoma cruzi. *Biochem J,* 351**,** 281-8.

Hillebrand, H., Schmidt, A. & Krauth-Siegel, R. L. 2003. A second class of peroxidases linked to the trypanothione metabolism. *J Biol Chem,* 278**,** 6809-15.

Hoare, C. 1972. *The Trypanosomes of Mammals,* Oxford, Blackwell Scientific Publications.

Hoffmann, B., Stöckl, A., Schlame, M., Beyer, K. & Klingenberg, M. 1994. The reconstituted ADP/ATP carrier activity has an absolute requirement for cardiolipin as shown in cysteine mutants. *J Biol Chem,* 269**,** 1940-4.

Hotz, H. R., Hartmann, C., Huober, K., Hug, M. & Clayton, C. 1997. Mechanisms of developmental regulation in Trypanosoma brucei: a polypyrimidine tract in the 3'-untranslated region of a surface protein mRNA affects RNA abundance and translation. *Nucleic Acids Res,* 25**,** 3017-26.

Hudock, M. P., Sanz-Rodríguez, C. E., Song, Y., Chan, J. M. W., Zhang, Y., Odeh, S., Kosztowski, T., Leon-Rossell, A., Concepción, J. L., Yardley, V., Croft, S. L., Urbina, J. A. & Oldfield, E. 2006. Inhibition of Trypanosoma cruzi hexokinase by bisphosphonates. *J Med Chem,* 49**,** 215-23.

Hunt, M. & Kohler, P. 1995. Purification and characterization of phospho enol pyruvate carboxykinase from Trypanosoma brucei. *Biochim Biophys Acta,* 1249**,** 15-22.

Hunter, D. R. & Haworth, R. A. 1979. The Ca2+-induced membrane transition in mitochondria. III. Transitional Ca2+ release. *Arch Biochem Biophys,* 195**,** 468-77.

Iten, M., Mett, H., Evans, A., Enyaru, J. C., Brun, R. & Kaminsky, R. 1997. Alterations in ornithine decarboxylase characteristics account for tolerance of Trypanosoma brucei rhodesiense to D,L-alpha-difluoromethylornithine. *Antimicrob Agents Chemother,* 41**,** 1922-5.

Janz, L. & Clayton, C. 1994. The PARP and rRNA promoters of Trypanosoma brucei are composed of dissimilar sequence elements that are functionally interchangeable. *Mol Cell Biol,* 14**,** 5804-11.

Jeganathan, S., Sanderson, L., Dogruel, M., Rodgers, J., Croft, S. & Thomas, S. A. 2011. The distribution of nifurtimox across the healthy and trypanosome-infected murine blood-brain and blood-cerebrospinal fluid barriers. *J Pharmacol Exp Ther,* 336**,** 506-15.

Jiang, F., Ryan, M. T., Schlame, M., Zhao, M., Gu, Z., Klingenberg, M., Pfanner, N. & Greenberg, M. L. 2000. Absence of cardiolipin in the crd1 null mutant results in decreased mitochondrial membrane potential and reduced mitochondrial function. *J Biol Chem,* 275**,** 22387-94.

Kennedy, P. G. E. 2004. Human African trypanosomiasis of the CNS: current issues and challenges. *J Clin Invest,* 113**,** 496-504.

Klingbeil, M., Drew, M., Liu, Y., Morris, J., Motyk, S., Saxowsky, T., Wang, Z. & Englund, P. 2001. Unlocking the secrets of trypanosome kinetoplast DNA network replication. *Protist,* 152**,** 255-262.

Klingenberg, M. 1976. The ADP-ATP Carrier in Mitochondrial Membranes. *Membranes and Transport,* 3**,** 383-438.

Klingenberg, M. 2008. The ADP and ATP transport in mitochondria and its carrier. *BBA-Biomembranes,* 1778**,** 1978-2021.

Klingenberg, M. 2009. Cardiolipin and Mitochondrial Carriers. *BBA - Biomembranes*, 1-38.

Klingenberg, M. & Buchholz, M. 1973. On the mechanism of bongkrekate effect on the mitochondrial adenine-nucleotide carrier as studied through the binding of ADP. *Eur J Biochem,* 38, 346-58.

Klingenberg, M. & Rottenberg, H. 1977. Relation between the gradient of the ATP/ADP ratio and the membrane potential across the mitochondrial membrane. *Eur J Biochem,* 73, 125-30.

Klingenberg, M., Winkler, E. & Huang, S. 1995. ADP/ATP carrier and uncoupling protein. *Methods Enzymol,* 260, 369-89.

Kohl, L., Drmota, T., Thi, C. D., Callens, M., Van Beeumen, J., Opperdoes, F. R. & Michels, P. A. 1996. Cloning and characterization of the NAD-linked glycerol-3-phosphate dehydrogenases of Trypanosoma brucei brucei and Leishmania mexicana mexicana and expression of the trypanosome enzyme in Escherichia coli. *Mol Biochem Parasitol,* 76, 159-73.

Kokoszka, J. E., Waymire, K. G., Levy, S. E., Sligh, J. E., Cai, J., Jones, D. P., MacGregor, G. R. & Wallace, D. C. 2004. The ADP/ATP translocator is not essential for the mitochondrial permeability transition pore. *Nature,* 427, 461-5.

Krämer, R. & Klingenberg, M. 1977. Reconstitution of adenine nucleotide transport with purified ADP, ATP-carrier protein. *FEBS Lett,* 82, 363-7.

Krämer, R. & Klingenberg, M. 1980. Enhancement of reconstituted ADP,ATP exchange activity by phosphatidylethanolamine and by anionic phospholipids. *FEBS Lett,* 119, 257-60.

Krämer, R. & Klingenberg, M. 1982. Electrophoretic control of reconstituted adenine nucleotide translocation. *Biochemistry,* 21, 1082-9.

Kroger, A. & Klingenberg, M. 1973. Further evidence for the pool function of ubiquinone as derived from the inhibition of the electron transport by antimycin. *Eur J Biochem,* 39, 313-23.

Kunji, E. 2004. The role and structure of mitochondrial carriers. *FEBS Lett,* 564**,** 239-244.

Kunji, E. R. S. & Harding, M. 2003. Projection structure of the atractyloside-inhibited mitochondrial ADP/ATP carrier of Saccharomyces cerevisiae. *J Biol Chem,* 278**,** 36985-8.

Kunji, E. R. S. & Robinson, A. J. 2006. The conserved substrate binding site of mitochondrial carriers. *BBA - Bioenergetics,* 1757**,** 1237-1248.

Lamour, N., Rivière, L., Coustou, V., Coombs, G. H., Barrett, M. P. & Bringaud, F. 2005. Proline Metabolism in Procyclic Trypanosoma brucei Is Down-regulated in the Presence of Glucose. *J Biol Chem,* 280**,** 11902-11910.

LaNoue, K., Mizani, S. & Klingenberg, M. 1978. Electrical imbalance of adenine nucleotide transport across the mitochondrial membrane. *J Biol Chem,* 253**,** 191-198.

Lanteri, C. A., Stewart, M. L., Brock, J. M., Alibu, V. P., Meshnick, S. R., Tidwell, R. R. & Barrett, M. P. 2006. Roles for the Trypanosoma brucei P2 transporter in DB75 uptake and resistance. *Mol Pharmacol,* 70**,** 1585-92.

Lanteri, C. A., Tidwell, R. R. & Meshnick, S. R. 2008. The mitochondrion is a site of trypanocidal action of the aromatic diamidine DB75 in bloodstream forms of Trypanosoma brucei. *Antimicrob Agents Chemother,* 52**,** 875-82.

Lauquin, G. J. & Vignais, P. V. 1976. Interaction of (3H) bongkrekic acid with the mitochondrial adenine nucleotide translocator. *Biochemistry,* 15**,** 2316-22.

Lawson, J., Gawaz, M., Klingenberg, M. & Douglas, M. 1990. Structure-function studies of adenine nucleotide transport in mitochondria. I. Construction and genetic analysis of yeast mutants encoding the ADP/ATP carrier protein of mitochondria. *J Biol Chem,* 265**,** 14195-14201.

Liu, B., Liu, Y., Motyka, S. A., Agbo, E. E. C. & Englund, P. T. 2005. Fellowship of the rings: the replication of kinetoplast DNA. *Trends Parasitol,* 21**,** 363-9.

Luciani, S., Martini, N. & Santi, R. 1971. Effects of carboxyatractyloside a structural analogue of atractyloside on mitochondrial oxidative phosphorylation. *Life Sci II,* 10**,** 961-8.

Lux, H., Heise, N., Klenner, T., Hart, D. & Opperdoes, F. R. 2000. Ether--lipid (alkyl-phospholipid) metabolism and the mechanism of action of ether--lipid analogues in Leishmania. *Mol Biochem Parasitol,* 111**,** 1-14.

Marché, S., Michels, P. A. & Opperdoes, F. R. 2000. Comparative study of Leishmania mexicana and Trypanosoma brucei NAD-dependent glycerol-3-phosphate dehydrogenase. *Mol Biochem Parasitol,* 106**,** 83-91.

Martínez-Calvillo, S., Vizuet-de-Rueda, J. C., Florencio-Martínez, L. E., Manning-Cela, R. G. & Figueroa-Angulo, E. E. 2010. Gene expression in trypanosomatid parasites. *J Biomed Biotechnol,* 2010**,** 525241.

Martinez-Calvillo, S., Yan, S., Nguyen, D., Fox, M., Stuart, K. & Myler, P. J. 2003. Transcription of Leishmania major Friedlin chromosome 1 initiates in both directions within a single region. *Mol Cell,* 11**,** 1291-9.

Mathis, A. M., Bridges, A. S., Ismail, M. A., Kumar, A., Francesconi, I., Anbazhagan, M., Hu, Q., Tanious, F. A., Wenzler, T., Saulter, J., Wilson, W. D., Brun, R., Boykin, D. W., Tidwell, R. R. & Hall, J. E. 2007. Diphenyl furans and aza analogs: effects of structural modification on in vitro activity, DNA binding, and accumulation and distribution in trypanosomes. *Antimicrob Agents Chemother,* 51**,** 2801-10.

Mathis, A. M., Holman, J. L., Sturk, L. M., Ismail, M. A., Boykin, D. W., Tidwell, R. R. & Hall, J. E. 2006. Accumulation and intracellular distribution of antitrypanosomal diamidine compounds DB75 and DB820 in African trypanosomes. *Antimicrob Agents Chemother,* 50**,** 2185-91.

Matthews, K., Ellis, J. & Paterou, A. 2004. Molecular regulation of the life cycle of African trypanosomes. *Trends Parasitol,* 20**,** 40-47.

Matthews, K. R. 2005. The developmental cell biology of Trypanosoma brucei. *J Cell Sci,* 118**,** 283-90.

McCormack, J. G., Halestrap, A. P. & Denton, R. M. 1990. Role of calcium ions in regulation of mammalian intramitochondrial metabolism. *Physiol Rev,* 70**,** 391-425.

McCulloch, R. 2004. Antigenic variation in African trypanosomes: monitoring progress. *Trends Parasitol,* 20**,** 117-21.

McKenzie, M., Lazarou, M., Thorburn, D. R. & Ryan, M. T. 2006. Mitochondrial respiratory chain supercomplexes are destabilized in Barth Syndrome patients. *J Mol Biol,* 361**,** 462-9.

Metelkin, E., Goryanin, I. & Demin, O. 2006. Mathematical modeling of mitochondrial adenine nucleotide translocase. *Biophys J,* 90**,** 423-32.

Michels, P. A. & Opperdoes, F. R. 1991. The evolutionary origin of glycosomes. *Parasitol Today (Regul Ed),* 7**,** 105-9.

Michels, P. A. M., Bringaud, F., Herman, M. & Hannaert, V. 2006. Metabolic functions of glycosomes in trypanosomatids. *Biochim Biophys Acta,* 1763**,** 1463-77.

Miezan, T. W., Bronner, U., Doua, F., Cattand, P. & Rombo, L. 1994. Long-term exposure of Trypanosoma brucei gambiense to pentamidine in vitro. *Trans R Soc Trop Med Hyg,* 88**,** 332-3.

Mileykovskaya, E. & Dowhan, W. 2009. Cardiolipin membrane domains in prokaryotes and eukaryotes. *Biochim Biophys Acta,* 1788**,** 2084-91.

Millar, A. H. & Heazlewood, J. L. 2003. Genomic and proteomic analysis of mitochondrial carrier proteins in Arabidopsis. *Plant Physiol,* 131**,** 443-53.

Montalvetti, A., Rohloff, P. & Docampo, R. 2004. A functional aquaporin co-localizes with the vacuolar proton pyrophosphatase to acidocalcisomes and the contractile vacuole complex of Trypanosoma cruzi. *J Biol Chem,* 279**,** 38673-82.

Moreno, S. N. & Docampo, R. 2009. The role of acidocalcisomes in parasitic protists. *J Eukaryot Microbiol,* 56**,** 208-13.

Moynagh, P. N. 1995. Contact sites and transport in mitochondria. *Essays Biochem,* 30**,** 1-14.

Muller, S., Liebau, E., Walter, R. D. & Krauth-Siegel, R. L. 2003. Thiol-based redox metabolism of protozoan parasites. *Trends Parasitol,* 19**,** 320-8.

Müller, V., Basset, G., Nelson, D. R. & Klingenberg, M. 1996. Probing the role of positive residues in the ADP/ATP carrier from yeast. The effect of six

arginine mutations of oxidative phosphorylation and AAC expression. *Biochemistry,* 35**,** 16132-43.

Naderer, T., Ellis, M. A., Sernee, M. F., De Souza, D. P., Curtis, J., Handman, E. & McConville, M. J. 2006. Virulence of Leishmania major in macrophages and mice requires the gluconeogenic enzyme fructose-1,6-bisphosphatase. *Proc Natl Acad Sci U S A,* 103**,** 5502-7.

Nara, T., Hshimoto, T. & Aoki, T. 2000. Evolutionary implications of the mosaic pyrimidine-biosynthetic pathway in eukaryotes. *Gene,* 257**,** 209-22.

Nelson, D. R., Lawson, J. E., Klingenberg, M. & Douglas, M. G. 1993. Site-directed mutagenesis of the yeast mitochondrial ADP/ATP translocator. Six arginines and one lysine are essential. *J Mol Biol,* 230**,** 1159-70.

Nicholls, D. G. & Ferguson, S. J. 2002. *Bioenergetics 3*, Academic Press.

Nury, H., Dahout-Gonzalez, C., Trézéguet, V., Lauquin, G., Brandolin, G. & Pebay-Peyroula, E. 2005. Structural basis for lipid-mediated interactions between mitochondrial ADP/ATP carrier monomers. *FEBS Lett,* 579**,** 6031-6.

Ohlendieck, K., Riesinger, I., Adams, V., Krause, J. & Brdiczka, D. 1986. Enrichment and biochemical characterization of boundary membrane contact sites from rat-liver mitochondria. *Biochim Biophys Acta,* 860**,** 672-89.

Oldfield, E. 2010. Targeting isoprenoid biosynthesis for drug discovery: bench to bedside. *Acc Chem Res,* 43**,** 1216-26.

Opperdoes, F. R. 1984. Localization of the initial steps in alkoxyphospholipid biosynthesis in glycosomes (microbodies) of Trypanosoma brucei. *FEBS Lett,* 169**,** 35-9.

Opperdoes, F. R. & Borst, P. 1977. Localization of nine glycolytic enzymes in a microbody-like organelle in Trypanosoma brucei: the glycosome. *FEBS Lett,* 80**,** 360-4.

Opperdoes, F. R. & Michels, P. A. M. 2007. Horizontal gene transfer in trypanosomatids. *Trends Parasitol,* 23**,** 470-6.

Opperdoes, F. R. & Szikora, J. P. 2006. In silico prediction of the glycosomal enzymes of Leishmania major and trypanosomes. *Mol Biochem Parasitol,* 147**,** 193-206.

Osorio, A. L., Madruga, C. R., Desquesnes, M., Soares, C. O., Ribeiro, L. R. & Costa, S. C. 2008. Trypanosoma (Duttonella) vivax: its biology, epidemiology, pathogenesis, and introduction in the New World--a review. *Mem Inst Oswaldo Cruz,* 103**,** 1-13.

Overath, P., Czichos, J. & Haas, C. 1986. The effect of citrate/cis-aconitate on oxidative metabolism during transformation of Trypanosoma brucei. *Eur J Biochem,* 160**,** 175-82.

Palmieri, F. 2004. The mitochondrial transporter family (SLC25): physiological and pathological implications. *Pflugers Arch,* 447**,** 689-709.

Palmieri, F., Agrimi, G., Blanco, E., Castegna, A., Di Noia, M. A., Iacobazzi, V., Lasorsa, F. M., Marobbio, C. M. T., Palmieri, L., Scarcia, P., Todisco, S., Vozza, A. & Walker, J. 2006. Identification of mitochondrial carriers in Saccharomyces cerevisiae by transport assay of reconstituted recombinant proteins. *Biochim Biophys Acta,* 1757**,** 1249-62.

Palmieri, F. & Klingenberg, M. 2004. Mitochondrial Metabolite Transporter Family. *Encyclopedia of Biological Chemistry,* 2**,** 725-732.

Palmieri, L., Runswick, M. J., Fiermonte, G., Walker, J. E. & Palmieri, F. 2000. Yeast Mitochondrial Carriers: Bacterial Expression, Biochemical Identification and Metabolic Significance. *J Bioenerg Biomembr,* 32**,** 67-77.

Paniz-Mondolfi, A. E., Perez-Alvarez, A. M., Lanza, G., Marquez, E. & Concepcion, J. L. 2009. Amiodarone and itraconazole: a rational therapeutic approach for the treatment of chronic Chagas' disease. *Chemotherapy,* 55**,** 228-33.

Panov, A., Filippova, S. & Lyakhovich, V. 1980. Adenine nucleotide translocase as a site of regulation by ADP of the rat liver mitochondria permeability to H+ and K+ ions. *Arch Biochem Biophys,* 199**,** 420-6.

Parsons, M., Nelson, R. G., Watkins, K. P. & Agabian, N. 1984. Trypanosome mRNAs share a common 5' spliced leader sequence. *Cell,* 38**,** 309-16.

Pena-Diaz, J., Montalvetti, A., Flores, C. L., Constan, A., Hurtado-Guerrero, R., De Souza, W., Gancedo, C., Ruiz-Perez, L. M. & Gonzalez-Pacanowska, D. 2004. Mitochondrial localization of the mevalonate pathway enzyme 3-Hydroxy-3-methyl-glutaryl-CoA reductase in the Trypanosomatidae. *Mol Biol Cell,* 15**,** 1356-63.

Pepin, J. & Mpia, B. 2006. Randomized controlled trial of three regimens of melarsoprol in the treatment of Trypanosoma brucei gambiense trypanosomiasis. *Trans R Soc Trop Med Hyg,* 100**,** 437-41.

Pfaff, E. & Klingenberg, M. 1968. Adenine nucleotide translocation of mitochondria. 1. Specificity and control. *Eur J Biochem,* 6**,** 66-79.

Pfeiffer, K., Gohil, V., Stuart, R. A., Hunte, C., Brandt, U., Greenberg, M. L. & Schägger, H. 2003. Cardiolipin stabilizes respiratory chain supercomplexes. *J Biol Chem,* 278**,** 52873-80.

Phillips, M. A. & Wang, C. C. 1987. A Trypanosoma brucei mutant resistant to alpha-difluoromethylornithine. *Mol Biochem Parasitol,* 22**,** 9-17.

Piccoli, C., Scrima, R., Boffoli, D. & Capitanio, N. 2006. Control by cytochrome c oxidase of the cellular oxidative phosphorylation system depends on the mitochondrial energy state. *Biochem J,* 396**,** 573-83.

Priotto, G., Kasparian, S., Mutombo, W., Ngouama, D., Ghorashian, S., Arnold, U., Ghabri, S., Baudin, E., Buard, V., Kazadi-Kyanza, S., Ilunga, M., Mutangala, W., Pohlig, G., Schmid, C., Karunakara, U., Torreele, E. & Kande, V. 2009. Nifurtimox-eflornithine combination therapy for second-stage African Trypanosoma brucei gambiense trypanosomiasis: a multicentre, randomised, phase III, non-inferiority trial. *Lancet,* 374**,** 56-64.

Quiñones, W., Peña, P., Domingo-Sananes, M., Cáceres, A., Michels, P. A. M., Avilan, L. & Concepción, J. L. 2007. Leishmania mexicana: molecular cloning and characterization of enolase. *Exp Parasitol,* 116**,** 241-51.

Reuner, B., Vassella, E., Yutzy, B. & Boshart, M. 1997. Cell density triggers slender to stumpy differentiation of Trypanosoma brucei bloodstream forms in culture. *Mol Biochem Parasitol,* 90**,** 269-80.

Riccio, P., Aquila, H. & Klingenberg, M. 1975a. Purification of the carboxy-atractylate binding protein from mitochondria. *FEBS Lett,* 56**,** 133-8.

Riccio, P., Aquila, H. & Klingenberg, M. 1975b. Solubilization of the carboxy-atractylate binding protein from mitochondria. *FEBS Lett,* 56**,** 192-32.

Rivière, L., Moreau, P., Allmann, S., Hahn, M., Biran, M., Plazolles, N., Franconi, J.-M., Boshart, M. & Bringaud, F. 2009. Acetate produced in the mitochondrion is the essential precursor for lipid biosynthesis in procyclic trypanosomes. *Proc Natl Acad Sci USA,* 106**,** 12694-9.

Rodgers, J. 2009. Human African trypanosomiasis, chemotherapy and CNS disease. *J Neuroimmunol,* 211**,** 16-22.

Roditi, I. & Clayton, C. 1999. An unambiguous nomenclature for the major surface glycoproteins of the procyclic form of Trypanosoma brucei. *Mol Biochem Parasitol,* 103**,** 99-100.

Roditi, I. & Lehane, M. J. 2008. Interactions between trypanosomes and tsetse flies. *Curr Opin Microbiol,* 11**,** 345-51.

Rohloff, P., Montalvetti, A. & Docampo, R. 2004. Acidocalcisomes and the contractile vacuole complex are involved in osmoregulation in Trypanosoma cruzi. *J Biol Chem,* 279**,** 52270-81.

Ruan, J. P., Arhin, G. K., Ullu, E. & Tschudi, C. 2004. Functional characterization of a Trypanosoma brucei TATA-binding protein-related factor points to a universal regulator of transcription in trypanosomes. *Mol Cell Biol,* 24**,** 9610-8.

Rück, A., Dolder, M., Wallimann, T. & Brdiczka, D. 1998. Reconstituted adenine nucleotide translocase forms a channel for small molecules comparable to the mitochondrial permeability transition pore. *FEBS Lett,* 426**,** 97-101.

Rudenko, G., Chung, H. M., Pham, V. P. & Van der Ploeg, L. H. 1991. RNA polymerase I can mediate expression of CAT and neo protein-coding genes in Trypanosoma brucei. *EMBO J,* 10**,** 3387-97.

Sanderson, L., Dogruel, M., Rodgers, J., De Koning, H. P. & Thomas, S. A. 2009. Pentamidine movement across the murine blood-brain and blood-

cerebrospinal fluid barriers: effect of trypanosome infection, combination therapy, P-glycoprotein, and multidrug resistance-associated protein. *J Pharmacol Exp Ther,* 329**,** 967-77.

Sanz-Rodríguez, C. E., Concepción, J. L., Pekerar, S., Oldfield, E. & Urbina, J. A. 2007. Bisphosphonates as inhibitors of Trypanosoma cruzi hexokinase: kinetic and metabolic studies. *J Biol Chem,* 282**,** 12377-87.

Saraste, M. & Walker, J. E. 1982. Internal sequence repeats and the path of polypeptide in mitochondrial ADP/ATP translocase. *FEBS letters,* 144**,** 250-4.

Schägger, H. & Pfeiffer, K. 2001. The ratio of oxidative phosphorylation complexes I-V in bovine heart mitochondria and the composition of respiratory chain supercomplexes. *J Biol Chem,* 276**,** 37861-7.

Schlame, M. 2008. Cardiolipin synthesis for the assembly of bacterial and mitochondrial membranes. *J Lipid Res,* 49**,** 1607-20.

Schnaufer, A., Clark-Walker, G. D., Steinberg, A. G. & Stuart, K. 2005. The F1-ATP synthase complex in bloodstream stage trypanosomes has an unusual and essential function. *EMBO J,* 24**,** 4029-40.

Schneider, A., Bouzaidi-Tiali, N., Chanez, A. L. & Bulliard, L. 2007. ATP production in isolated mitochondria of procyclic Trypanosoma brucei. *Methods Mol Biol,* 372**,** 379-87.

Scott, A. G., Tait, A. & Turner, C. M. 1997. Trypanosoma brucei: lack of cross-resistance to melarsoprol in vitro by cymelarsan-resistant parasites. *Exp Parasitol,* 86**,** 181-90.

Scott, D. A., De Souza, W., Benchimol, M., Zhong, L., Lu, H. G., Moreno, S. N. & Docampo, R. 1998. Presence of a plant-like proton-pumping pyrophosphatase in acidocalcisomes of Trypanosoma cruzi. *J Biol Chem,* 273**,** 22151-8.

Sharma, R., Gluenz, E., Peacock, L., Gibson, W., Gull, K. & Carrington, M. 2009. The heart of darkness: growth and form of Trypanosoma brucei in the tsetse fly. *Trends Parasitol,* 25**,** 517-24.

Sharma, R., Peacock, L., Gluenz, E., Gull, K., Gibson, W. & Carrington, M. 2008. Asymmetric cell division as a route to reduction in cell length and change in cell morphology in trypanosomes. *Protist,* 159**,** 137-51.

Simarro, P. P., Jannin, J. & Cattand, P. 2008. Eliminating human African trypanosomiasis: where do we stand and what comes next? *PLoS Med,* 5**,** e55.

Simpson, A. G. B., Stevens, J. R. & Lukes, J. 2006. The evolution and diversity of kinetoplastid flagellates. *Trends Parasitol,* 22**,** 168-74.

Simpson, L. 1986. Kinetoplast DNA in trypanosomid flagellates. *Int Rev Cytol,* 99**,** 119-79.

Stephens, J. L., Lee, S. H., Paul, K. S. & Englund, P. T. 2007. Mitochondrial fatty acid synthesis in Trypanosoma brucei. *J Biol Chem,* 282**,** 4427-36.

Steverding, D. 2008. The history of African trypanosomiasis. *Parasit Vectors,* 1**,** 3.

Steverding, D. 2010. The development of drugs for treatment of sleeping sickness: a historical review. *Parasit Vectors,* 3**,** 15.

Stuart, K. & Panigrahi, A. K. 2002. RNA editing: complexity and complications. *Mol Microbiol,* 45**,** 591-6.

Tetley, L. & Vickerman, K. 1985. Differentiation in Trypanosoma brucei: host-parasite cell junctions and their persistence during acquisition of the variable antigen coat. *J Cell Sci,* 74**,** 1-19.

Tielens, A. G. & Van Hellemond, J. J. 1998. Differences in energy metabolism between trypanosomatidae. *Parasitol Today (Regul Ed),* 14**,** 265-72.

Tielens, A. G. & Van Hellemond, J. J. 1999. Reply. *Parasitol Today,* 15**,** 347-8.

Torreele, E., Bourdin Trunz, B., Tweats, D., Kaiser, M., Brun, R., Mazue, G., Bray, M. A. & Pecoul, B. 2010. Fexinidazole--a new oral nitroimidazole drug candidate entering clinical development for the treatment of sleeping sickness. *PLoS Negl Trop Dis,* 4**,** e923.

Turrens, J. 1999. More differences in energy metabolism between Trypanosomatidae. *Parasitol Today (Regul Ed),* 15**,** 346-8.

Turrens, J. F. 1989. The role of succinate in the respiratory chain of Trypanosoma brucei procyclic trypomastigotes. *Biochem J,* 259**,** 363-8.

Tyler, K. M., Higgs, P. G., Matthews, K. R. & Gull, K. 2001. Limitation of Trypanosoma brucei parasitaemia results from density-dependent parasite differentiation and parasite killing by the host immune response. *Proc Biol Sci,* 268**,** 2235-43.

Urbina, J. A. 2009. Ergosterol biosynthesis and drug development for Chagas disease. *Mem Inst Oswaldo Cruz,* 104 Suppl 1**,** 311-8.

Urbina, J. A. 2010. Specific chemotherapy of Chagas disease: relevance, current limitations and new approaches. *Acta Trop,* 115**,** 55-68.

Urbina, J. A., Concepcion, J. L., Caldera, A., Payares, G., Sanoja, C., Otomo, T. & Hiyoshi, H. 2004. In vitro and in vivo activities of E5700 and ER-119884, two novel orally active squalene synthase inhibitors, against Trypanosoma cruzi. *Antimicrob Agents Chemother,* 48**,** 2379-87.

Urbina, J. A., Concepcion, J. L., Rangel, S., Visbal, G. & Lira, R. 2002. Squalene synthase as a chemotherapeutic target in Trypanosoma cruzi and Leishmania mexicana. *Mol Biochem Parasitol,* 125**,** 35-45.

Urbina, J. A., Moreno, B., Vierkotter, S., Oldfield, E., Payares, G., Sanoja, C., Bailey, B. N., Yan, W., Scott, D. A., Moreno, S. N. & Docampo, R. 1999. Trypanosoma cruzi contains major pyrophosphate stores, and its growth in vitro and in vivo is blocked by pyrophosphate analogs. *J Biol Chem,* 274**,** 33609-15.

Urwyler, S., Studer, E., Renggli, C. K. & Roditi, I. 2007. A family of stage-specific alanine-rich proteins on the surface of epimastigote forms of Trypanosoma brucei. *Mol Microbiol,* 63**,** 218-28.

Van Hellemond, J., Opperdoes, F. & Tielens, A. 1998. Trypanosomatidae produce acetate via a mitochondrial acetate: succinate CoA transferase. *Proc Natl Acad Sci USA,* 95**,** 3036-3041.

Van Hellemond, J., Opperdoes, F. & Tielens, A. 2005. The extraordinary mitochondrion and unusual citric acid cycle in Trypanosoma brucei. *Biochemical Society Transactions,* 33**,** 967.

van Hellemond, J. J. & Tielens, A. G. M. 2006. Adaptations in the lipid metabolism of the protozoan parasite Trypanosoma brucei. *FEBS Lett,* 580**,** 5552-8.

Van Schaftingen, E., Opperdoes, F. R. & Hers, H.-G. 1987. Effects of various metabolic conditions and of the trivalent arsenical melarsen oxide on the intracellular levels of fructose 2,6-bisphosphate and of glycolytic intermediates in Trypanosoma brucei. *Eur J Biochem,* 166**,** 653-61.

van Weelden, S. W., van Hellemond, J. J., Opperdoes, F. R. & Tielens, A. G. 2005a. New functions for parts of the Krebs cycle in procyclic Trypanosoma brucei, a cycle not operating as a cycle. *J Biol Chem,* 280**,** 12451-60.

van Weelden, S. W. H., Fast, B., Vogt, A., van der Meer, P., Saas, J., van Hellemond, J. J., Tielens, A. G. M. & Boshart, M. 2003. Procyclic Trypanosoma brucei do not use Krebs cycle activity for energy generation. *J Biol Chem,* 278**,** 12854-63.

van Weelden, S. W. H., van Hellemond, J. J., Opperdoes, F. R. & Tielens, A. G. M. 2005b. New functions for parts of the Krebs cycle in procyclic Trypanosoma brucei, a cycle not operating as a cycle. *J Biol Chem,* 280**,** 12451-60.

Vanhamme, L., Pays, A., Tebabi, P., Alexandre, S. & Pays, E. 1995. Specific binding of proteins to the noncoding strand of a crucial element of the variant surface glycoprotein, procyclin, and ribosomal promoters of trypanosoma brucei. *Mol Cell Biol,* 15**,** 5598-606.

Vanhamme, L. & Pays, E. 1995. Control of gene expression in trypanosomes. *Microbiol Rev,* 59**,** 223-40.

Vansterkenburg, E. L., Coppens, I., Wilting, J., Bos, O. J., Fischer, M. J., Janssen, L. H. & Opperdoes, F. R. 1993. The uptake of the trypanocidal drug suramin in combination with low-density lipoproteins by Trypanosoma brucei and its possible mode of action. *Acta Trop,* 54**,** 237-50.

Vassella, E., Reuner, B., Yutzy, B. & Boshart, M. 1997. Differentiation of African trypanosomes is controlled by a density sensing mechanism which signals cell cycle arrest via the cAMP pathway. *J Cell Sci,* 110 (Pt 21)**,** 2661-71.

Vercesi, A. E. & Docampo, R. 1996. Sodium-proton exchange stimulates Ca2+ release from acidocalcisomes of Trypanosoma brucei. *Biochem J,* 315 (Pt 1)**,** 265-70.

Vercesi, A. E., Moreno, S. N. & Docampo, R. 1994. Ca2+/H+ exchange in acidic vacuoles of Trypanosoma brucei. *Biochem J,* 304 (Pt 1)**,** 227-33.

Vernal, J., Munoz-Jordan, J., Muller, M., Cazzulo, J. J. & Nowicki, C. 2001. Sequencing and heterologous expression of a cytosolic-type malate dehydrogenase of Trypanosoma brucei. *Mol Biochem Parasitol,* 117**,** 217-21.

Verner, Z., Cermáková, P., Skodová, I., Kriegová, E., Horváth, A. & Lukeš, J. 2010. Complex I (NADH:ubiquinone oxidoreductase) is active in but non-essential for procyclic Trypanosoma brucei. *Mol Biochem Parasitol*.

Vertommen, D., Van Roy, J., Szikora, J. P., Rider, M. H., Michels, P. A. & Opperdoes, F. R. 2008. Differential expression of glycosomal and mitochondrial proteins in the two major life-cycle stages of Trypanosoma brucei. *Mol Biochem Parasitol,* 158**,** 189-201.

Vickerman, K. 1985. Developmental cycles and biology of pathogenic trypanosomes. *Br Med Bull,* 41**,** 105-14.

Vickerman, K. & Coombs, G. H. 1999. Protozoan paradigms for cell biology. *J Cell Sci,* 112**,** 2797-2798.

Vickerman, K., Tetley, L., Hendry, K. A. & Turner, C. M. 1988. Biology of African trypanosomes in the tsetse fly. *Biol Cell,* 64**,** 109-19.

Vignais, P. V., Duee, E. D., Vignais, P. M. & Huet, J. 1966. Effects of atractyligenin and its structural analogues on oxidative phosphorylation and on the translocation of adenine nucleotides in mitochondria. *Biochim Biophys Acta,* 118**,** 465-83.

Vincent, I. M., Creek, D., Watson, D. G., Kamleh, M. A., Woods, D. J., Wong, P. E., Burchmore, R. J. & Barrett, M. P. 2010. A molecular mechanism for eflornithine resistance in African trypanosomes. *PLoS Pathog,* 6**,** e1001204.

Voet, D. & Voet, J. G. 1995. *Biochemistry*, John Wiley & Sons, Inc.

Voogd, T. E., Vansterkenburg, E. L., Wilting, J. & Janssen, L. H. 1993. Recent research on the biological activity of suramin. *Pharmacol Rev,* 45**,** 177-203.

Vyssokikh, M. Y. & Brdiczka, D. 2003. The function of complexes between the outer mitochondrial membrane pore (VDAC) and the adenine nucleotide translocase in regulation of energy metabolism and apoptosis. *Acta Biochim Pol,* 50**,** 389-404.

Walder, J. A., Eder, P. S., Engman, D. M., Brentano, S. T., Walder, R. Y., Knutzon, D. S., Dorfman, D. M. & Donelson, J. E. 1986. The 35-nucleotide spliced leader sequence is common to all trypanosome messenger RNA's. *Science,* 233**,** 569-71.

Walker, J. & Runswick, M. 1993. The mitochondrial transport protein superfamily. *J Bioenerg Biomembr,* 25**,** 435-446.

Weidemann, M. J., Erdelt, H. & Klingenberg, M. 1970. Effect of bongkrekic acid on the adenine nucleotide carrier in mitochondria: tightening of adenine nucleotide binding and differentiation between inner and outer sites. *Biochem Biophys Res Commun,* 39**,** 363-70.

Wenzler, T., Boykin, D. W., Ismail, M. A., Hall, J. E., Tidwell, R. R. & Brun, R. 2009. New treatment option for second-stage African sleeping sickness: in vitro and in vivo efficacy of aza analogs of DB289. *Antimicrob Agents Chemother,* 53**,** 4185-92.

WHO. 2010. *WHO | African trypanosomiasis (sleeping sickness) http://www.who.int/mediacentre/factsheets/fs259/en* [Online]. [Accessed December 2010].

Wiemer, E. A., L, I. J., van Roy, J., Wanders, R. J. & Opperdoes, F. R. 1996. Identification of 2-enoyl coenzyme A hydratase and NADP(+)-dependent 3-hydroxyacyl-CoA dehydrogenase activity in glycosomes of procyclic Trypanosoma brucei. *Mol Biochem Parasitol,* 82**,** 107-11.

Wilkinson, S., Meyer, D., Taylor, M., Bromley, E., Miles, M. & Kelly, J. 2002. The Trypanosoma cruzi enzyme TcGPXI is a glycosomal peroxidase and can be linked to trypanothione reduction by glutathione or tryparedoxin. *J Biol Chem,* 277**,** 17062-17071.

Wilson, W. D., Tanious, F. A., Mathis, A., Tevis, D., Hall, J. E. & Boykin, D. W. 2008. Antiparasitic compounds that target DNA. *Biochimie,* 90**,** 999-1014.

Wolfe, A. J. 2005. The acetate switch. *Microbiol Mol Biol Rev,* 69**,** 12-50.

Wulf, R., Kaltstein, A. & Klingenberg, M. 1978. H+ and cation movements associated with ADP, ATP transport in mitochondria. *Eur J Biochem,* 82**,** 585-92.

Zhang, M., Mileykovskaya, E. & Dowhan, W. 2002. Gluing the respiratory chain together. Cardiolipin is required for supercomplex formation in the inner mitochondrial membrane. *J Biol Chem,* 277**,** 43553-6.

Zhang, M., Mileykovskaya, E. & Dowhan, W. 2005. Cardiolipin is essential for organization of complexes III and IV into a supercomplex in intact yeast mitochondria. *J Biol Chem,* 280**,** 29403-8.

Zomer, A. W., Michels, P. A. & Opperdoes, F. R. 1999. Molecular characterisation of Trypanosoma brucei alkyl dihydroxyacetone-phosphate synthase. *Mol Biochem Parasitol,* 104**,** 55-66.

Zoratti, M. & Szabò, I. 1995. The mitochondrial permeability transition. *Biochim Biophys Acta,* 1241**,** 139-76.

Chapter II.
Materials and Methods

Table of Contents

Chapter II. Materials and Methods

Part I. Biological material and cell culture conditions

Procyclic form *Trypanosoma brucei* PCF449 strain was used as parental cell line for the subsequent production of knockout and expression cell lines, and it is regarded as "wild type" cell line (WT) in this work. PCF449 originated from the 927 *T. brucei* procyclic form cell line, by stable transfection with the pHD449 construct (BLE resistance), bearing the tetracycline repressor (Biebinger *et al*., 1997) for controlled tet-inducible expression. PCF449 was cultured in MEM-Pros media (Overath *et al*., 1986), supplemented with 10% (v/v) heat-inactivated foetal calf serum (FCS) and 7.5mg/L hemin. Bloodstream form 449 (BSF449) was cultured in HMI-9 media (Hirumi and Hirumi, 1989), supplemented with 10% (v/v) heat-inactivated FCS. The formulations for the media are shown in the Appendix.

Part II. Sequence alignment and phylogenetic analysis

II.1. Identification of putative MCF protein-encoding genes

T. b. brucei open reading frames (ORFs) encoding putative MCF proteins were identified through reciprocal database searches using the program BLASTP (v2.2.9: http://www.ncbi.nlm.nih.gov/blast) and the kinetoplastid genome databases available for *T. b. brucei*, *T. cruzi*, and *Leishmania major* (http://www.genedb.org). The amino acid sequences of previously identified and functionally characterised MCF proteins from higher eukaryotes (http://www.ncbi.nlm.nih.gov) were used as queries (Millar and Heazlewood, 2003; Picault *et al.*, 2004; Palmieri *et al.*, 2006; Wohlrab, 2006).

II.2. Sequence analysis and phylogenetic reconstruction

All sequences used for sequence alignment and phylogenetic reconstruction were retrieved through NCBI (http://www.ncbi.nlm.nih.gov/).

Sequences were aligned with ClustalW2 (http://www.ebi.ac.uk/Tools/clustalw2/index.html) (Thompson *et al*., 1994) and the results were edited by hand using Se-Al v2.0a11 (http://tree.bio.ed.ac.uk/software/seal/), an alignment editor and/or ClustalX-2.0.12 (http://www.clustal.org/) (Larkin *et al*., 2007). The pair-wise distances, neighbour-joining trees and consensus trees were obtained using the phylogeny platform programs (Protdist, Neighbour-Joining and Consense) from Mobyle@Pasteur

(http://mobyle.pasteur.fr/cgi-bin/portal.py) (Néron *et al*., 2009). Consensus trees were edited using SplitsTree4 v.4.11.3 (Huson and Bryant, 2006). Only bootstraps values above 50% are shown. All software used for these analyses are freeware.

The phylogenetic tree based on human MCP sequences was constructed using the PHYLIP program package v3.6a of J. Felsenstein (http://evolution.genetics.washington.edu). Pair-wise sequence distance matrices were calculated using the program PROTDIST (Dayhoff and Orcutt, 1979). Unrooted phylogenetic trees were constructed from distance matrices using the Neighbour-Joining method of Saitou (Saitou and Nei, 1987). The final phylogenetic tree was drawn with SplitsTree v4.8 (Huson, 1998). The statistical relevance of the resulting phylogenetic tree was assessed with the SEQBOOT program of the PHYLIP programme package by bootstrap re-sampling analysis generating 1000 reiterated data sets. The resulting bootstrap values, expressed as percentage, were added manually to each node. Only bootstrap values above 55% are shown.

The GeneDB (http://www.genedb.org) accession numbers for the putative *T. b. brucei* MCF protein-encoding genes are listed in Table 1, Chapter II. The Genbank (gb), EMBL (emb) and Swissprotein (sp) accession numbers for the human MCF (SLC25A) genes are: SLC25A1, gb|AAH04980; SLC25A2, gb|AAO31753; SLC25A3, gb|AAH00998; SLC25A4, gb|AAA51736; SLC25A5, gb|AAA51737; SLC25A6, gb|AAG01998; SLC25A7, gb|AAA85271; SLC25A8, gb|AAC51336; SLC25A9, gb|AAC51367; SLC25A10, gb|AAH07355; SLC25A11, gb|AAC28637; SLC25A12, gb|AAH16932; SLC25A13, gb|AAH06566; SLC25A14, gb|AAG29584; SLC25A15, emb|CAC83972; SLC25A16, sp|P16260; SLC25A17, emb|CAA73367; SLC25A18, gb|AAG22855; SLC25A19, gb|AAH01075; SLC25A20, gb|AAV38345; SLC25A21, emb|CAC27562; SLC25A22, gb|AAH19033; SLC25A24, gb|AAH14519; SLC25A25, gb|AAH89448; SLC25A26, gb|EAW65451; SLC25A27, gb|AAD16995; SLC25A29, gb|EAW81695; SLC25A30, gb|AAI32740; SLC25A31, gb|AAH22032; SLC25A32, gb|AAH21893; SLC25A33, gb|AAH04991; SLC25A34, gb|AAH27998; SLC25A35, gb|AAI01330; SLC25A36, gb|EAW79012; SLC25A37, gb|AAI32800; SLC25A38, gb|AAH13194; SLC25A39, gb|AAH01398; SLC25A40, gb|AAH27322; SLC25A42, gb|AAH45598; SLC25A43, gb|AAH19584; SLC25A44, gb|AAH08843; SLC25A45, gb|EAW74380; SLC25A46, gb|AAH17169.

GeneBank (gb), EMBL (emb) and SwissProtein (sp) accession numbers used in **MCP5** analysis: *Trypanosoma brucei* MCP5 gb|AAC23561; *Trypanosoma cruzi* gb|EAN90413.1; *Leishmania major* emb|CAJ07106.1; *Leishmania amazonensis* gb|AAO32064.1; *Neurospora crassa* emb|CAE75740.1; *Schizosaccharomyces pombe* emb|CAA19176.1; *Saccharomyces cerevisiae* sp|P18239.2; *Pichia jadinii* emb|CAB88028.1; *Arabidopsis thaliana* gb|BAH19937.1*; Zea mays* gb|*ACG24998.1*; *Sorghum bicolour* gb|*EER89687.1*; *Solanum lycopersicum* gb|AAB49700.1; *Solanum tuberosum* sp|P25083.1; *Drosophila melanogaster* gb|AAB23114.1; *Anopheles gambiae* sp|Q27238.2; *Aedes aegypti* gb|EAT43748.1; *Marsupenaeus japonicus* gb|ABN04118.1; *Bombyx mori* gb|AAO32817.1; *Harpegnathos saltator* gb|EFN81827.1; *Ictalurus punctatus* gb|ADO29492.1; *Schistosoma japonicum* emb|CAX71878.1; *Xenopus laevis* gb|*AAH43821.1; Danio rerio* gb|*AAI54239.1*; *Rana rugosa* dbj|BAA36513.1; *Bos taurus* gb|DAA13433.1; *Ovis aries* gb|ACC93604.1; *Callithrix jacchus* XP_002763405.1; *Mus musculus* gb|AAF64471.1; *Homo sapiens* ANT SCL25A4 sp|P12235.4.

Accession numbers used in **MCP15** sequence and phylogenetic analysis:
Trypanosoma brucei MCP15 gb|AAZ12901.1; *Trypanosoma cruzi* mitochondrial carrier protein (putative) gb|EAN87637.1; *Leishmania infantum* ADP/ATP carrier-like protein emb|CAM65622.1; *Leishmania major* ADP/ATP carrier-like protein emb|CAJ07014.1; *Leishmania braziliensis* ADP/ATP carrier-like protein emb|CAM41671.1; *Ajellomyces dermatitidis* gb|EEQ78320.1; *Tetrahymena thermophila* ADP/ATP carrier protein 1 gb|EEQ78320.1; *Arthroderma gypseum* gb|EFQ98049.1; *Zygosaccharomyces rouxii* emb|CAR29621.1; *Neocallimastix frontalis* hydrogenosomal ATP/ADP carrier gb|AAN04660.1; *Drosophila melanogaster* ANT2A gb|AAF47956.1; *Drosophila melanogaster* ANT2B gb|AAO41648.1; *Schizosaccharomyces japoni*cus Anc1 gb|EEB06978.1; *Toxoplasma gondii* gb|EEB04619.1; *Bos taurus* 25 member 6 sp|P32007.3; *Ovis aries* SLC25A6 gb|ACC93605.1; *Lepeophtheirus salmonis* ADP/ATP carrier protein 3 gb|ACO12488.1; *Homo sapiens* SLC25A5 gb|AAH68199.1; *Saccharomyces cerevisiae* Aac3p tpg|DAA07205.1; *Arabidopsis thaliana* AAC3 NP_194568.1.

Accession numbers used in **MCP16** sequence and phylogenetic analysis:
Oikopleura dioica emb|CBY13776.1; *Neocallimastix frontalis* gb|AAN04660.1; *Drosophila melanogaster* stress-sensitive B, isoform A NP_511109.1; *Drosophila melanogaster* stress-sensitive B, isoform B NP_727450.1; *Drosophila melanogaster* stress-sensitive B, isoform C NP_727448.1; *Drosophila melanogaster* stress-

sensitive B, isoform D NP_727449.1; *Callithrix jacchus* ADP/ATP translocase 4 XP_002745417.1; *Rana rugosa* dbj|BAA36507.1; *Xenopus tropicalis* SLC25A5 emb|CAJ82932.1; *Bos taurus* 25 member 31 sp|Q2YDD9.1; *Ixodes scapularis* gb|EEC13826.1; *Talaromyces stipitatus* gb|EED20116.1; *Trypanosoma cruzi* ADP/ATP carrier putative 1 gb|EAN90730.1; *Trypanosoma cruzi* ADP/ATP translocase putative 2 gb|EAN90731.1; *Leishmania infantum* ADP/ATP mitochondrial carrier-like emb|CAM66663.1; *Leishmania major* ADP/ATP mitochondrial carrier-like emb|CAJ03149.1; *Leishmania braziliensis* ADP/ATP mitochondrial carrier-like emb|CAM37567.1; *Neurospora crassa* gb|EAA33965.1; *Candida dubliniensis* emb|CAX41441.1; *Leishmania major* 1 emb|CAJ07106.1; *Tetrahymena thermophila* ADP/ATP carrier protein 1 gb|EAR94678.1; *Lepeophtheirus salmonis* ADP/ATP carrier protein 3 gb|ACO12488.1; *Schistosoma japonicum* emb|CAX78321.1; *Arabidopsis thaliana* ADP/ATP translocase-like gb|AAM65037.1

Accession numbers used in **MCP13** sequence and phylogenetic analysis (all sequences putative GDP/GTP carriers, except for *Saccharomyces cerevisiae* Ggcp1): *Pichia pastoris* XP_002492471.1; *Saccharomyces cerevisiae* tpg|DAA11666.1; *Talaromyces stipitatus* XP_002484981.1; *Pyrenophora tritici-repentis* XP_001934060.1; *Penicillium marneffei* XP_002149192.1; *Schizosaccharomyces japonicus* XP_002172029.1; *Leishmania infantum* XP_001462754.1; *Leishmania braziliensis* XP_001561578.1; *Leishmania major* XP_822265.1; *Trypanosoma cruzi* XP_810620.1; *Trypanosoma brucei* MCP13 XP_951572.1.

II.3. Homology-based modelling

The 3D structures of the *T. b. brucei* MCF proteins were predicted by homology-based modelling using the previously determined crystal structure-based 3D models of the bovine mitochondrial ADP/ATP carrier for threading. Protein Data Bank (PDB) accession numbers of these models are *1okc* (Pebay-Peyroula *et al.*, 2003) and *2c3e* (Nury *et al.*, 2005). The programs used for modelling were SWISS-MODEL (Schwede *et al.*, 2003; Arnold *et al.*, 2006) and CPHmodels 2.0 available at the CPHmodels-2.0 Server (www.cbs.dtu.dk/services/CPHmodels) using standard parameter settings. The obtained 3D structure models were viewed and edited using PyMOL (W.L. DeLano, The PyMOL Molecular Graphics System (2002), accessible at http://www.pymol.org).

Part III. Knockout and expression constructs cloning in trypanosomes

III.1. Design of gene knockout constructs

Open reading frames in *T. brucei* procyclic form 449 (PCF449) were replaced by homologous recombination using antibiotic resistance cassettes. The replacement constructs consist of a backbone of pBlueScript SK II, modified to bear a specific antibiotic resistance cassette that will be expressed once inserted in the genome. The recombination event will make use of selected target 5' and 3' untranslated regions (UTR) to recombine in the sequence of interest. Two antibiotic resistance cassettes are required to "knockout" a single *T. brucei* gene, due to diploidy of this parasite (Neomycin (NEO) and Blasticidin (BLA) resistance cassettes were used for the construction of the knockout (Voncken *et al*., 2003). MCP5, MCP13, MCP15 and MCP16 UTR sequences were chosen from GeneDB, using IDs Tb10.61.1810, Tb927.2.2970, Tb927.8.1310, Tb927.7.3940, respectively. Oligos were designed (refer to Appendix for a full list of oligos) to specifically amplify UTRs target sequences by PCR. The PCR products were cloned into pGEM-T-easy vector (Promega®) and subcloned into the different NEO and BLA replacement constructs. 5' UTRs were cloned using SacI/SpeI restriction sites, whereas BamHI/ApaI restriction sites were used for the 3'UTR. The final constructs were linearized by digestion with SacI/ApaI restriction enzymes, and used for transfection of PCF449 *Trypanosoma brucei* strain.

III.2. Expression of myc-tagged MCPs in procyclic form *Trypanosoma brucei*

The complete ORFs of the identified MCF protein encoding genes were amplified from genomic DNA of *T. b. brucei* strain Lister 427 by PCR, using sense and antisense oligonucleotide primers containing unique restriction enzyme sites (e.g. *Bam*HI, *Hind*III, and *Hpa*I) for subsequent cloning into the different *T. b. brucei* expression vectors. The PCR products were initially cloned into the pGEM-T Easy TA cloning vector (Invitrogen) and their DNA sequences determined (Eurofins Medigenomix, Martinsried, Germany). Using the added unique restriction sites, the MCF genes were subsequently cloned into the *T. b. brucei* expression vectors pHD1700 and pHD1701 (Colasante *et al.*, 2006). Tetracycline-inducible expression from these vectors results in the expression of a double (2x) Myc-tagged recombinant protein: for pHD1700 a carboxy-terminal 2xMyc-tag is added to the expressed protein, whereas for pHD1701 an amino-terminal 2xMyc-tag is added.

The constructs were transfected into procyclic-form *T. b. brucei* 449 for further immunolocalisation studies. *T. b. brucei* procyclic cell lines expressing recombinant GIM5 (glycosomal membrane protein (Lorenz *et al.*, 1998) or chloramphenicol acetyl transferase (cytosolic localisation (Colasante *et al.*, 2007) using the expression vectors pHD1700 and pHD1701, were used as controls to show that subcellular protein targeting is not affected by the vectors used (results not shown).

MCP5, 13, 15 and 16 open reading frames (ORFs) were cloned into the pHD1700 and 1701 vectors for inducible expression in *Trypanosoma brucei* PCF449, using HindIII and BamHI restriction sites (Colasante *et al.*, 2006; Colasante *et al.*, 2009). Protein expression from pHD1700 and pHD1701 vectors results in the addition of a myc tag at the n-terminus of the protein. The constructs further contain a Hygromycin resistance cassette and a tetracycline-inducible promoter (Colasante *et al.*, 2006; Colasante *et al.*, 2009). The constructs were linearized by NotI digestion prior to transfection.

III.3. Trypanosome transfection and selection of clones

$2x10^7$ cells of procyclic form *T. brucei* were used for each transfection. Parasites were centrifuged at 2000x*g* for 10 minutes at room temperature and washed twice with cold Zimmerman's Post Fusion Medium (ZPFM 132mM NaCl, 8mM KCl, 8mM Na_2HPO_4, 1.5mM K_2HPO_4, 1.5mM magnesium acetate, 90mM calcium diacetate, pH 7.0 (Clayton *et al.*, 1990)). Cells were resuspended in 0.5mL of ZPFM and placed in electroporation cuvettes (4mm) altogether with the DNA to be transfected (10μg, NotI digested). Parasites were electroporated 3 times at 1500V, and incubated overnight in MEM-Pros medium at 28°C without selective antibiotic for recovery. After recovery, cells were plated in 24-well culture plates using serial dilutions in MEM-Pros medium (Beverley and Clayton, 1993). Serial dilutions were performed in titer plates as follows: 0, 1:10, 1:30, 1:60. Depending on the antibiotic resistance cassette, clones were selected with 15μg/mL G418 (NEO), 50μg/mL Blasticidin (BLA), 50 μg/mL Hygromycin (HYG), or 10 μg/mL Puromycin (PUR) for 10-14 days, at 28°C.

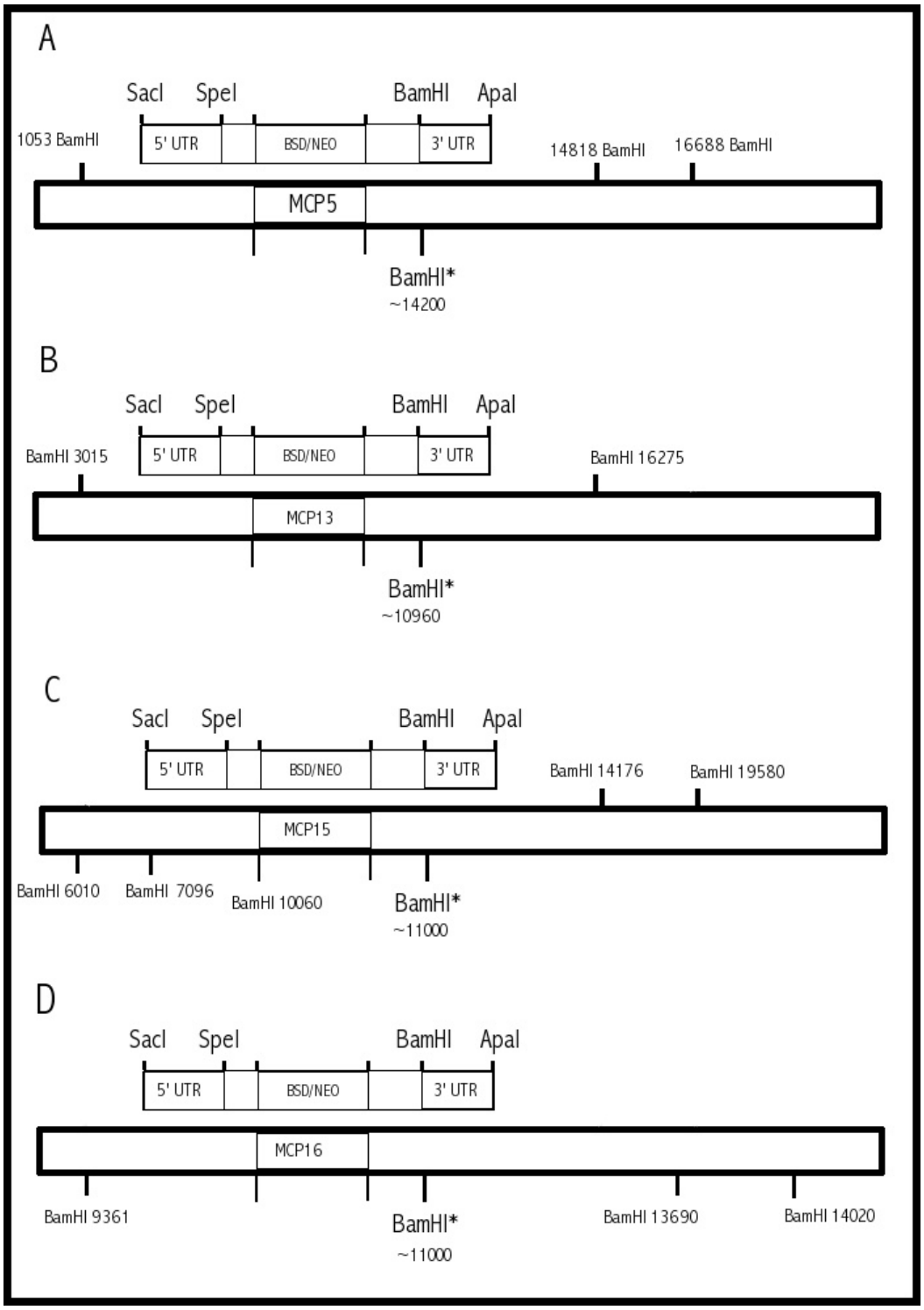

Figure 1. Schematic representation of the KO strategy of MCPs in PCF449 *Trypanosoma brucei*. The insertion of the resistance cassette by homologous recombination adds a restriction site (BamHI* site) that produces a band shift through Southern blotting. All values in the chart are relative.

Part IV. Assessment of KO approach: PCR and Southern blot analysis

IV.1. PCR for KO assessment

PCR was used to assess the proper insertion of the KO constructs in the loci of interest. For that purpose, an oligo was designed upstream of the 5' UTR target sequence used for the KO. PCR was performed using this oligo as a forward primer and the reverse primer from the NEO or BLA cassette.

IV.2. Genomic DNA isolation

Genomic DNA (gDNA) was isolated from logarithmic phase procyclic form *Trypanosoma brucei* cultures. $5x10^7$ cells were centrifuged at 2000*xg* for 10 minutes at room temperature, washed twice with PBS and finally obtained in a pellet after centrifugation. The pellet was resuspended in 0.5 mL gDNA lysis buffer (10 mM Tris-HCl, pH 8.0, 200mM NaCl, 5mM EDTA, 0.2% (w/v) SDS) and was incubated with 2U RNase and 1U Proteinase K for 30 minutes. Protein was subsequently "salted out" of the preparation with 250mL ice-cold 5M NaCl and the sample was centrifuged at 20000*xg* for 15 minutes at room temperature. The supernatant was placed in a fresh 1.5mL tube, mixed with 700mL pure isopropanol and incubated on ice for 10 minutes. The gDNA (pellet) was obtained after centrifugation at 20000*xg* for 10 minutes, washed twice with 70% ethanol and allowed to air dry. The final pellet was resuspended in 10mM Tris-HCl, pH 8.0. The concentration of gDNA was measured spectrophotometrically in an Eppendorf BioPhotometer.

IV.3. Southern blotting

Southern blotting was performed essentially as described in Sambrook *et al*. (1989) with slight modifications. DNA Electrophoresis was carried out in an agarose gel system (0.8% (w/v) agarose in 1X TAE buffer). For each sample 10μg of genomic DNA was used digested with BamHI. The agarose gel was run in 1X TAE buffer at 15 V constant overnight. Before capillary blotting, the agarose gel was processed as follows: 1) Depurination with 250mM HCl for 10 minutes at room temperature with gentle agitation; 2) denaturation (1.5M NaCl, 0.5M NaOH) for 25 minutes at room temperature with gentle agitation and; 3) neutralisation (1.5M NaCl, 0.5M Tris-HCl, pH 7.5) for 30 minutes at room temperature with gentle agitation. Capillary blotting unto Hybond-N+ (Amersham™, GE Healthcare) was set up by placing the membrane in contact with the gel, topped by 2 consecutive Whatman paper sheets

and paper towels. Transfer was allowed to take place overnight at room temperature. The membrane was placed in a UV cross-linking chamber at 0.120 J/cm^2.

IV.4. Northern blotting

RNA from 2x10^8 *T. brucei* cells was isolated using the Qiagen® RNEasy® Mini kit. The RNA concentration was assessed through spectrophotometry. Northern blotting was performed as described by Sambrook *et al.* (1989) with slight modifications. The RNA gel contained 0.9% (w/v) agarose, 20mM MOPS, pH 7.0, 2.2M formaldehyde. The RNA was mixed with the sample preparation solution (2μL 10X MOPS (200mM MOPS, 80mM Na-Acetate, 10mM EDTA), 3.5μL formaldehyde, 10μL formamide, 1μL EtBr (1mg/mL stock), 1μL RNA loading dye) and heated at 65°C for 15 minutes. 5μL RNA molecular weight standard ladder (Invitrogen™) was treated the same way as the sample. The gels were ran overnight in 20mM MOPS, 8mM Na-Acetate, 1mM EDTA (1X MOPS) at 20V. The next day the gel was blotted by capillarity to a Nylon membrane in presence of 10X SSC (0.15M Na_2Citrate, 1.5M NaCl) overnight. The membrane was submitted to UV-crosslinking at 0.120 J/cm^2 after overnight blotting. Afterwards, it was pre-hybridized and hybridized under the same conditions as the Southern blot, at 65°C. The probe was also prepared the same way, using ORF as template.

IV.5. Probe preparation

The hot probe was prepared by PCR, by incorporation of labelled $^{[32P]}$-dCTP (PerkinElmer, Inc.) into the PCR product. For Southern blot analysis 3'UTRs were used as probes. The PCR mix was prepared as follows: 20mM Tris-HCl pH 8.3, 20mM KCl, 5mM $(NH_4)_2SO_4$ (TrueStart™ PCR buffer, Fermentas); 1.5mM $MgCl_2$; 0.5μM Fw primer; 0.5μM Rev primer; 0.1mM dATP; 0.1mM dGTP; 0.1mM dTTP; 0.05μg DNA template, 1U TrueStart™ Hot Start DNA *Taq* polymerase (Fermentas). Pre and hybridization steps took place in a 65°C hybridization oven. 10mL of hybridization solution (5X SSC: 0.075M Na_2Citrate, 0.075M NaCl, 5X Denhardt's, 0.5% (w/v) SDS, 100μg of denatured salmon sperm DNA) was used for every blot. Pre-hybridization was performed for at least 30 minutes before adding the probe. The probe was denatured at 95°C for 10 minutes and snapped cool on ice before overnight hybridization with the blot. The next day, the blots were washed 3 times as follows: 2X SSC, 0.1% (w/v) SDS for 10 minutes at 60°C; 1X SSC, 0.1% (w/v) SDS

at 60°C for 15 minutes; and 0.1X SSC 0.1% (w/v) SDS at room temperature for 10 minutes. The blots were exposed to X-ray film at -80°C in an autoradiography cassette.

Part V. Expression of MCPs in heterologous systems

V.1. Expression of his-tagged MCPs into different strains of *Escherichia coli*

Open reading frames (ORFs) of MCP5, 13, 15 and 16 were amplified by PCR and cloned into the pGEM T-easy vector (Promega®), according to manufacturer's instructions. The ORFs were subcloned into different expression vectors: pTrcHis A & C (Invitrogen), pET16b (Novagen), pac28 (Kholod and Mustelin, 2001) and pIvex2.4 (Roche) (refer Appendix for restriction sites and oligos information).

The constructs were transformed into *E. coli* BL21(DE3), Codon Usage, Rossetta2(DE3)pLysS, Tuner(DE3)pLysS and Rossetta_gami2(DE3)pLysS strains for inducible expression with IPTG. Rossetta® and Tuner® strains were obtained from Novagen (Novy *et al*., 2001). Single colonies were inoculated into LB media with 100μg/mL ampicillin (for pTrcHis A&C, pET16b and pIvex2.4 vectors), 30μg/mL Kanamycin (with pac28 vector) and additional 25μg/mL Chloramphenicol when using Codon Usage, Rossetta2(DE3)pLysS, Tuner(DE3)pLysS strains and Rossetta_gami2(DE3)pLysS strains. Precultures were grown overnight at 37°C at 250 r.p.m. Precultures were used in a 1/20 dilution in LB media and further grown at 37°C at 250 r.p.m. Once the cultures O.D. reached 0.48-0.5, they were induced with 1mM IPTG. Induction was allowed for 4-6 hours and 1mL aliquots of culture were taken every hour for growth curve purposes.

V.1.1 Auto-induction in *Escherichia coli*

The auto-induction approach (Studier, 2005) was used to express MCP5, 13 and 16 in Rossetta2(DE3)pLysS strain of *Escherichia coli*. 5mL of LB in presence of 25μg/mL Chloramphenicol, were inoculated in the morning of day 1 using single colonies freshly obtained from agar plates. Depending on the construct transformed in the host strain, 100μg/mL ampicillin and/or 30μg/mL kanamycin were added to the cultures. Culture was allowed to grow at 37°C at 250 r.p.m. 8-10 hours later, a similar LB pre-culture (5mL) was set up using 1:100 dilution from the previous culture and was allowed to grow overnight. On day 2 the procedure was repeated:

1:100 dilution of the overnight culture in 5mL LB. 8-10 hours later, 10mL of MDG medium (25mM Na_2HPO_4, 25mM KH_2PO_4, 50mM NH_4Cl, 5mM Na_2SO_4, 2mM Mg_2SO_4, 0.5% (w/v) Glucose, 0.25% (w/v) Aspartate) were inoculated with a 1:50 dilution of the morning culture. The MDG culture was grown in strong shaking overnight at 37°C. Autoinduction was set up the next morning using a 1:100 dilution of the overnight culture on ZYM-5052 medium (1% (w/v) Tryptone, 0.5% (w/v) Yeast extract, 0.05% (w/v) Glucose, 0.2% (w/v) Lactose, 0.5% (v/v) Glycerol, 2mM $MgSO_4$, 25mM Na_2HPO_4, 25mM KH_2PO_4, 50mM NH_4Cl, 5mM Na_2SO_4) and was allowed to grow in constant shaking at 28°C for 26 hours.

V.2. MCPs heterologous expression in insect cells. Baculovirus expression system.

The system BAC-to-BAC from Invitrogen® was used for expression in insects cells (Invitrogen, 2009). All procedures were performed according to the manufacturer's user manual. The method involves the cloning of the gene of interest in an expression vector (pFastBac HT) with a n-terminal his-tag sequence; the construct is then transformed into an *E. coli* DH10Bac strain bearing a bacmid in which the expression vector will recombine and disrupt a lacZ gene inserted as a marker. Subsequently the positive bacmid is isolated for its further transfection into the Sf21 cell line (insect cell) to produce viral particles and to express the protein.

The pFastBAC HTA, B or C constructs were transformed into DH10Bac using a modified transformation procedure with a recuperation time of 5 hours before plating on LB plates containing ampicillin, gentamicin, tetracycline, IPTG and Xgal. Positive big, white colonies were screened after 48 hours at 37°C incubation. The colonies were further subcultured and grown in LB media for midiprep isolation of the bacmid.

The purified bacmid (1µg) was transfected into Sf21 cells using Cellfectin® reagent on 6-wells plates. The transfected cells produced viral particles after 4-7 days; this first viral stock called P1 was the medium harvested after centrifugation of the infected cells. This stock could be amplified for maximum viral number (P2) by re-infection in Sf21 cells. Expression assays were performed using a MOI (multiplicity of infection) of 0.5 and cells were harvested after 72 hours of infection.

Part VI. Protein preparation, detergent solubilization and reconstitution into liposomes

E. coli cultures were centrifuged at 3000xg to separate cells from the medium. The pellet was resuspended in 5mL buffer K (50mM Potassium phosphate, pH 7.5; 0.1%TX-100) or buffer T (50mM Tris-HCl, pH 7.5, 50mM KCl, 0.1% (v/v) TX-100) with 2 mg lysozyme and incubated on ice for 2 hours. 2-5 U DNAse was added to clear the lysate and was incubated for 1 hour on ice. The lysate was passed through a French Press 2 times and centrifuged at 5000*xg* for 15 minutes at 4°C. The supernatant was used for protein purification.

VI.1. Protein solubilization under denaturing conditions using guanidinuim chloride

Protein sample was equilibrated to 6M Guanidinium Chloride (GC) by incubation on ice for 1 hour, followed by centrifugation at 16000*xg* for 10 minutes. The supernatant was dialized overnight against 5M urea, in order to eliminate the guanidinium salt. The same sample was further dialyzed with buffer T (50mM Tris-HCl, pH 7.5, 50mM KCl, 0.1% (v/v) TX-100) and centrifuged at 16000*xg* for 10 minutes, separating this fraction into supernatant and pellet.

VI.2. Protein solubilization using sarkosyl

In order to solubilize the protein with sarkosyl, a modification of the protocol used by Fiermonte *et al*. (1993) was performed. After separating soluble fraction from pellet, most of the protein was found in the latter. This fraction was dissolved in 1.5% (w/v) sarkosyl in buffer K (50mM potassium phosphate, pH 7.5; 0.1% (v/v) TX-100) and incubated overnight at 4°C in gentle agitation. Sample was centrifuged at 15000*xg* for 15 minutes and supernatant was separated from pellet. The supernatant fraction was used for TALON® purification.

VI.3. Protein preparation from insect cells cultures

Cultures of 35mL with a density a 1-1.5x10^6 cell/mL were used for each protein purification step. The cells were centrifuged at 700*xg* and washed once with PBS. The cell pellet was resuspended in 5mL lysis buffer (50mM NaPi pH 7.8, 10mM β-mercaptoethanol, 10% (v/v) glycerol) and passed through a One-Shot® machine at 0.7kpsi. The lysate was centrifuged at 700*xg* for 10 minutes at 4°C to separate cell

rest and nuclear fractions. The supernatant was further spun down at 8000*xg* for 10 minutes at 4°C to further separate the mitochondrial fraction (pellet with the expressed protein of interest). This mitochondrial fraction was further solubilised with 0.3% (w/v) sarkosyl in buffer 1 (50mM Tris-HCl, pH 7.6, 50mM KCl, 2% (w/v) TX-100) for no longer than 5 minutes, to further centrifuge at 20000*xg* for 10 minutes at 4°C. The supernatant was used immediately for purification.

VI.4. Protein purification

VI.4.1 Protein purification from *E. coli* through TALON® chromatography

The solubilised protein sample was loaded into a column (3 x 0.5cm) with 1mL of TALON® (Clontech Laboratories, Inc.) resin equilibrated with buffer K (50mM Potassium phosphate, pH 7.5; 0.1% (w/v) TX-100), with or without sarkosyl, depending on the treatment the protein had received for solubilisation. The unbound protein fraction was collected and beads were washed twice with 2 ml of buffer K. The protein was eluted with 2mL of buffer K, 200mM imidazole.

VI.4.2 Protein purification from *E. coli* and insect cells using Ni-NTA chromatography

500uL Ni-NTA (Qiagen) beads were equilibrated with buffer TK (50mM Tris-HCl, pH 7.6, 50mM KCl, 2% (w/v) TX-100). The sarkosyl-solubilised lysate was mixed with the beads and the purification was performed through batch method with centrifugation steps of 700*xg* at 4C. The unbound protein fraction was collected and 3 washes were performed with buffer TK and one last wash with buffer TK, 10mM imidazole. The protein was eluted with 500μL buffer TK, 150mM imidazole.

VI.5. MCPs reconstitution into liposomes for activity assays

Various conditions were tested for the reconstitution of the carriers into liposomes. The main protocol is presented here and the combinations/changes of the mainstream protocol will be extended in Chapter VI.

VI.5.1 Liposomes preparation

VI.5.1.1 Extrusion method

Egg yolk phosphatidylcholine (PC) was dissolved in water to a concentration of 0.9mg/mL. An extrusion syringe ensemble (Avanti Polar Lipids, Inc) consisting of a mini-extruder and two Hamilton® syringes was set up to prepared the liposomes. The phospholipid solution was loaded into one of the syringes and passed through the extruder 11 times from one syringe to the other. The membrane inside the extruder was 100nm pore size. The liposomes clarified by the end of the procedure.

VI.5.1.2 Sonication method

Egg yolk phosphatidylcholine (PC) was dissolved in water to a concentration of 0.9mg/mL. The mix was sonicated using on ice for 10 minutes, at 50% output. The liposomes clarified by the end of the procedure.

VI.5.2 Reconstitution

VI.5.2.1 Palmieri's method

5-10 μg of purified protein was mixed with 1.3% (v/v) TX-114, 0.1mg/mL extruded phospholipids, 50mM ADP, 400μg cardiolipin and 10mM MOPS, pH 7.0 in a final volume of 700μL. The proteoliposomes were formed and filled with ADP by passing the mix 24 times through an Amberlite XAD-2 column (3cm X 0.5cm) equilibrated with 0.9mg/mL egg yolk phospholipids (not extruded), 0.5μg/μL cardiolipin, 50mM ADP, 10mM MOPS, pH 7.0. In order to eliminate the ADP outside the liposomes, the sample was passed through a Dowex AG1-X8 column (3cm X 0.5cm) equilibrated with 10mM MOPS, pH 7.0, 30mM sucrose and eluted with 1mL of the same buffer.

VI.5.2.2 Klingenberg's method

The liposomes were solubilized with $C_{10}E_5$ in a PC/detergent ratio of 1.4 (Heimpel *et al*., 2001) and subsequently mixed with the purified protein in a PC/protein ratio of 200. Cardiolipin was added to the mixture in a range of concentrations, from 1 to 12% (w/w) (mg cardiolipin/mg PC). The buffer of choice (Pipes, Tris-HCl, K-Pi), H_2O, salts (KCl, NaCl or Na_2SO_4) and ADP (20mM final concentration) were subsequently mixed with the PC/detergent/protein solution to a volume of 0.7mL. For the formation of the proteoliposomes, the sample was passed through a Bio-beads column (10 x 0.3cm) equilibrated with the 10mM buffer of choice, 20mM ADP

and 0.4mg/mL cardiolipin (Klingenberg *et al.*, 1995; Krämer and Heberger, 1986). The proteoliposomes were eluted from the column with 1mL 10mM buffer pH 7.0, 30mM salt or 50mM sucrose (when testing absence of salts).

External ADP was eliminated from the proteoliposomes by passage through a Sephadex G-75 column (30 x 0.3cm) equilibrated with 10mM buffer pH 7.0, 30mM salt or 50mM sucrose (when testing absence of salts). The proteoliposomes were eluted with 2mL of the same buffer.

VI.5.3 Transport assay with reconstituted liposomes

VI.5.3.1 Palmieri's method

The transport assay was started by adding 5mM ATP to the proteoliposomes in a mix of cold and ^{3}H-labelled ATP (PerkinElmer). The reaction was performed in time points of 0, 1, 2 and 5 minutes. The reactions were stopped at each time point with 30mM pyridoxal 5' phosphate (Sigma-Aldrich®) and 10mM bathophenanthroline (Sigma-Aldrich®). The mix was subsequently loaded into a Dowex AG1-X8 column (3cm X 0.5cm) equilibrated with 10mM MOPS, pH 7.0, 30mM sucrose, to eliminate non-specific radioactivity from the proteoliposomes. The proteoliposomes were eluted with 1mL of 10mM MOPS, pH 7.0, 30mM sucrose, and were placed in scintillation vials with 10mL of EcoScint RX for counting of ^{3}H.

VI.5.3.2 Alternative method

The transport assay was performed by adding ATP to the proteoliposomes, in a mix of cold and hot ATP (^{3}H-labelled) in a range from 1mM to 20mM ATP. 1ml of proteoliposomes was used for the assay, from which aliquots were taken at time intervals that ranged from 15 seconds to 2 minutes. Samples were quickly mixed with 1μg BKA and 2μg CAT; immediately loaded into a Sephadex G-75 column (30 x 0.3cm) equilibrated with 10mM buffer, pH 7.0, 30mM salt or 50mM sucrose; and eluted with 2mL of the same buffer. The eluated proteoliposomes were mixed with 10mL EcoScint RX (National Diagnostics, Inc) in a scintillation vial and counted for ^{3}H.

VI.6. Transport assays in *Escherichia coli*

The transport assays with whole *E. coli* cells were performed according to Tjaden *et al*. (1998) with slight modifications. The assay was performed after bacterial expression of MCP5 by auto-induction. The cells were centrifuged at 3000*xg* for 10 minutes to eliminate media and washed with buffer A (20mM Tris-HCl, pH 7.2; 225mM sucrose; 20mM KCl; 10 mM KH_2PO4; 1mM $MgSO_4$) to be finally resuspended in the same buffer to a 1:2 relation of the original culture.

For each time point of the assay 100μL cells were mixed with 2.5μL ^{3}H ATP and "cold" ATP (0 - 10mM) and buffer A to a final volume of 200μL. The reactions were incubated at 30°C, for time intervals from 15 seconds to 2 minutes and were rapidly placed on nitrocellulose filters in a vacuum filter. The filters were washed quickly with excess of buffer A and placed in scintillation vials containing 10mL of EcoScint RX (National Diagnostics, Inc) for scintillation counting.

Part VII. Visualization methods

VII.1. Antibody production

For the identification of MCP5, two peptide antibodies were produced. The amino acid sequences for the two peptides used for immunisation are derived from the respective N-terminal (N-term) and C-terminal (C-term) ends of MCP5. Peptide synthesis and the immunisation of rabbits were performed by EZBiolab (USA). The synthesized peptides ' DKKREPAPKLGFLEE ' (amino acids 3-17 of MCP5 for the N-term peptide antibody) and ' VDALKPIYVEWRRSN ' (amino acids 293-307 of MCP5 for the C-term peptide antibody) were coupled to keyhole limpet hemocyanin (KLH) and used for the immunization of two rabbits per peptide. Immunisation was initiated by injection of 1.0 mg of the KLH-coupled peptides emulsified in complete Freund's adjuvant, after collection of 2 ml pre-immune serum for each rabbit. The first injection was followed by 3 subsequent boosts in weeks 2, 4 and 7, respectively, with 0.5 mg of KLH-coupled peptides emulsified in incomplete Freund's adjuvant. The final antisera were collected in week 9, after determination of the MCP5 antibody titers for the different raised MCP5 peptide-antisera: i.e. 1:1,536,000 for the N-term MCP5 antisera and 1:1,192,000 for the C-term MCP5 antisera (determined by EZBiolab, USA).

Whole lysates of *T. brucei* procyclic form were used in order to test the antibodies by Western blot. Serial dilutions of the antibodies were prepared in order to detect the proteins, in the following range: 1:10000, 1:8000, 1:5000, 1:2500, 1:1000, 1:500 and 1:100. Western blots using pre-immune sera were performed as controls.

VII.2. Immunofluorescence microscopy of *Trypanosoma brucei* MCPs

Immunofluorescence was performed as described by Voncken *et al*. (2003). Procyclic *T. brucei* cells were centrifuged at 2000*xg* for 10 minutes, resuspended in 5mL MEM-Pros media with MitoTracker® stain (1:10000 dilution) and incubated at 28°C for 20 minutes. The cells were washed twice with fresh MEM-Pros medium, and resuspended in 1mL of MEM-Pros media for subsequent incubation at 28°C for 30 minutes. After elimination of the medium, the cells were diluted in 0.4% (w/v) formaldehyde in PBS for fixing. Incubation took place for 18 minutes without shaking, after which the cells were washed 3 times with PBS and finally resuspended in PBS. The cells in PBS were transferred to each square of chamber glass slide, and allowed to settle and attach to the poly-lysine coat for 30 minutes at room temperature. The slides were further incubated with 0.2% (v/v) TX-100 in PBS for 20 minutes before washing 3 times with excess of PBS. The blocking was performed with 0.5% (w/v) gelatin in PBS for 30 minutes. Afterwards, the primary antibody was added (1:100 dilution) in PBS/gelatin and incubated for 60 minutes before washing 3 times with excess of PBS. Further blocking was performed with 150-200μL of PBS/gelatin in each chamber for 5 minutes. The slides were then incubated with secondary antibody (1:500 dilution) in PBS/gelatin for 60 minutes in the dark. Excess antibody was washed 2 times with PBS. DAPI staining (100ng/mL) was performed in PBS/gelatin by incubation for 15 minutes before washing 2 times with excess of PBS. Slides were allowed to air-dry, before adding 10μL of embedding solution (90% (v/v) glycerol/PBS) to seal each chamber with a cover slide.

When MitoTracker® was not used as mitochondrial marker, rabbit anti-LPDH (dihydroxylipoamide dehydrogenase) was used as a mitochondrial marker of *T. b. brucei* (Schoneck *et al.*, 1997). Cells were examined using a Leica DM RXA digital deconvolution microscope, and images were recorded with a digital charge-coupled-device camera (Hamamatsu).

VII.3. SDS-PAGE and Western Blotting

SDS-PAGE was performed following the Laemmli method (Laemmli, 1970). Samples were prepared in Laemmli buffer (0.0625M Tris-HCl pH 6.8, 0.1% (v/v) β-mercaptoethanol, 0.1% (w/v) EDTA, 0.1% (v/v) glycerol) and heated at 95°C for 5 minutes. Denaturing 12% polyacrylamide gels (0.375M Tris-HCl pH 8.0, 0.1% (w/v) SDS, 0.1% (w/v) APS for the Running gel; and 0.125 M Tris-HCl pH 6.8, 0.1% (w/v) SDS, 0.1% (w/v) APS, 4% polyacrylamide, for the Stacking gel) were used to run samples. Gels were ran at 20mA/gel until front reached the end of the gel.

For Western blotting, samples were separated by SDS-PAGE and transferred to nitrocellulose or PVDF membranes at 100 V for 45 minutes in buffer 48 mM Tris, 39 mM Glycine, 20% (v/v) methanol, pH 8.3. Membranes were blocked with Tris-buffered saline (TBS) buffer, containing 5% (w/v) skimmed dry milk, 0.1% (v/v) Tween 20, in agitation at room temperature for 1 hour. Subsequently, membranes were incubated with primary antibody (see Table 1) in TBS buffer, 5% (w/v) skimmed dry milk, 0.1% (v/v) Tween 20, for 1 hour at room temperature. Antibody was washed 3X with excess TBS buffer, for 10 minutes each wash. Secondary antibody incubation and washes were performed in similar condition to the primary antibody. Protein detection was performed using ECL detection kit (Amersham™, GE Healthcare) for further film exposure.

Antibody	Manufacturer	Type	Made in	Target	Dilution	Technique
Anti-c-myc	Roche	Monoclonal (clone 9E10)	Mouse	c-myc-tag sequence	1:2000	WB, IFA
Anti-nterm	EZBiolab	Polyclonal (peptide antibody)	Rabbit	MCP5 n-terminus	1:1000	WB, IFA
Anti-cterm	EZBiolab	Polyclonal (peptide antibody)	Rabbit	MCP5 c-terminus	1:1000	WB, IFA
Anti-aldolase	C.Clayton's lab	Polyclonal	Rabbit	Aldolase	1:10,000	WB, IFA
Anti-Rabbit IgG HRP-linked	Amersham	Polyclonal	Donkey	Rabbit IgG	1:1000	WB
Anti-Mouse IgG HRP-linked	Amersham	Polyclonal	Sheep	Mouse IgG	1:1000	WB
Anti-Mouse	Molecular	Polyclonal	Goat	Mouse	1:500	IFA

IgG-Cy3 Alexa Fluor® 488	Probes			IgG		
Anti-Rabbit IgG-Cy3 Alexa Fluor® 488	Molecular Probes	Polyclonal	Goat	Rabbit IgG	1:500	IFA
ANT (H-188)	Santa Cruz Biotechnology, Inc.	Polyclonal	Rabbit	Amino acids 45-233 of human ANT1	1:2000	WB

Table 1. Antibodies used for the detection of proteins in Western blot (WB) and Immunofluorescence microscopy (IFA) experiments.

Part VIII. Phenotype assessment methods

VIII.1. Growth curves in MEM-Pros (NMP), MEM-Pros in glucose-depleted FCS (GDMP) and MEM-Pros glucose supplemented (MPglu).

MEM-Pros medium (Appendix) was used for all the cell culture of trypanosomes. The media was completed by the addition of 10% (v/v) heat-inactivated foetal calf serum (FCS), 7.5mg/L hemin and 5000U Penicillin/Streptomycin. Three versions of MEM-Pros were used for growth curve purposes. NMP stands for Normal MEM-Pros; GDMP (Glucose Depleted MEM-Pros) was prepared by incubating the FCS with glucose oxidase and catalase prior to completing the media. MPglu was prepared by addition of 5mM glucose.

The growth curves were set up with $5x10^5$ cells/mL of both *Δmcp5/MCP5-nmyc*^{ti} and PCF449 *Trypanosoma brucei*. The *Δmcp5/MCP5-nmyc*^{ti} cell line was tested both uninduced and induced with tetracycline. Cells were counted everyday (24, 48, 72 and 96 hours) and culture aliquots were taken for RNA isolation, metabolite measurements and Western blot analysis.

For metabolite measurements, 1mL of culture was precipitated with 100μL 35% (v/v) perchloric acid and incubated on ice for 10 minutes. The sample was further neutralized with 150μL 0.2M MOPS/5M KOH and centrifuged at 20000*xg* for 10 minutes to eliminate the precipitated protein. The deproteinized samples were stored at -80°C for further analysis. Proline, glucose, acetate and succinate were measured in these samples.

For western blot analysis, $2x10^5$ cells/μL were used as dilution factor in Laemmli buffer.

Carbon sources consumption and metabolites production data was normalized into [metabolite] and/or [carbon source]/10^6 cells in culture. Each set of normalized data was submitted to One-way ANOVA (Analysis of Variance) test (Currell and Dowman, 2005). Where significant differences were observed ($p<0.05$), the Holm-Sidak method for control group (pair-wise) was used to determine significance between KOs and PCF449 profiles (control). The statistical analysis was performed using SigmaPlot 11 © 2008, Systat Software, Inc.

VIII.2. Determination of carbon sources consumption

VIII.2.1 Proline

20μL of sample was mixed with 100mL 3% sulfosalicylic acid, 200μL acetic acid, 200μl proline reagent (25mg/mL ninhydrine, 60% acetic acid, 2.4M phosphoric acid) and 80μL H_2O and incubated at 100°C for 1 hour. Sample was mixed with 500μL toluene and vortexed to extract the upper organic phase with the proline. Top phase was separated and further diluted in toluene for O.D. measuring at 520nm.

VIII.2.2 Glucose

Reaction mixes were prepared in 1mL final volume of 25mM Tris-HCl pH 7.5, 2mM $MgSO_4$, 5mM ATP, 0.72mM $NADP^+$, 1U glucose-6-phosphate dehydrogenase (G6PDH), 1U hexokinase (HK), using 50mL sample. O.D. at 340nm was measured before and after addition of HK for measurement of NADPH (6220 M^{-1} molar extinction coefficient) as presented in the following equation: (Boehringer-Mannheim, 1973).

$$\text{Glucose} + \text{ATP} \xrightarrow{\text{HK}} \text{G-6-P} + \text{ADP} \xrightarrow{\text{G6PDH}} \text{6-phosphonoglucolactone} + \text{NADPH} \qquad \text{eq.1}$$

VIII.3. Determination of metabolites excretion

VIII.3.1 Succinate

Succinate was measured using a Succinic Acid assay kit from Megazyme®. Reaction mixes were performed as described by manufacturer's kit instruction. O.D. was measured at 340nm to assess the disappearance of NADH, as presented in the following equation:

$$\text{Succinate} + \text{ATP} + \text{CoA} \xrightarrow{\text{SCS}} \text{succinyl-CoA} + \text{ADP} + \text{Pi}$$

$$\text{ADP} + \text{PEP} \xrightarrow{\text{PK}} \text{ATP} + \text{pyruvate}$$

$$\text{Pyruvate} + \text{NADH} + \text{H}^+ \xrightarrow{\text{L-LDH}} \text{L-lactate} + \text{NAD}^+ \qquad \text{eq. 2}$$

VIII.3.2 Acetate

Acetate was measured using an Acetic Acid assay kit from Megazyme®. Reaction mixes were performed as described by manufacturer's kit instruction. O.D. was measured at 340nm to assess the disappearance of NADH, as presented in the following equation:

$$\text{Acetic acid} + \text{ATP} \xrightarrow{\text{AK}} \text{acetyl-phosphate} + \text{ADP}$$

$$\text{Acetyl-phosphate} + \text{CoA} \xrightarrow{\text{PTA}} \text{acetyl CoA} + \text{Pi}$$

$$\text{ADP} + \text{PEP} \xrightarrow{\text{PK}} \text{pyruvate} + \text{ATP}$$

$$\text{Pyruvate} + \text{NADH} \xrightarrow{\text{D-LDH}} \text{NAD}^+ + \text{D-Lactic acid} \qquad \text{eq. 3}$$

VIII.4. Mitochondrial ATP production assay

The mitochondrial ATP assay was performed according to Schneider *et al*. (Schneider *et al*., 2007) with modifications. Cells (trypanosomes) were obtained from a 72-hours grown culture and washed with SoTE buffer (20mM Tris-HCl pH 7.5, 2mM EDTA, 0.6M Sorbitol), to be further resuspended in SoTE at a concentration of $1x10^8$ cells/mL. Permeabilization of whole cells was performed with 0.008% (w/v) digitonin, allowing the detergent to permeabilize the cells for 5 minutes at room temperature, followed by immediate centrifugation at 8000*xg* for 5 minutes at 4°C. The supernatant was eliminated and pellet was washed twice with SoTE.

The final pellet (mitochondrial fraction) was resuspended in 0.750mL AAB (ATP Assay Buffer; 20mM Tris-HCl pH 7.4, 15mM KH_2PO_4, 0.6M Sorbitol, 5mM $MgSO_4$) per every $1x10^8$ cells initially used.

100μL of mitochondria were used for the assay. The mitochondrial ATP production was started by addition of 67μM ADP and 5 mM substrate. The different substrates tested were: succinate, α-ketoglutarate and glycerol-3-phosphate. The presence of different inhibitors was tested in the ATP production assay: antimycin (25mg/mL), FCCP (5mM), malonate (10mM), rotenone (15mM) and carboxyatractyloside (CAT) (4μg/mL). All inhibitors were purchased from Sigma-Aldrich®. The samples to be tested with inhibitors where incubated with the drug 10 minutes prior to starting the reaction with ADP and substrate. Once started, the reaction was allowed to take place for 30 minutes at room temperature.

The reaction was stopped by addition of 5μL 35% (v/v) perchloric acid and incubating for 5 minutes on ice. The precipitated protein was eliminated from the sample by centrifugation 15000*xg* for 5 minutes at 4°C. The supernatant was placed in a fresh eppendorf tube and neutralized with 20μL of 1M Tris/1M KOH solution.

Luciferase activity was measured in the sample using ATP Bioluminescence Assay Kit CLS II (Roche®). For the assay, 5μL of sample were mixed with 45 μL AAB and 50μL of luciferase reagent and placed in luminometer for RLU (Relative Light Units) measurement.

Part IX. References

Arnold, K., Bordoli, L., Kopp, J. & Schwede, T. 2006. The SWISS-MODEL workspace: a web-based environment for protein structure homology modelling. *Bioinformatics,* 22**,** 195-201.

Beverley, S. M. & Clayton, C. E. 1993. Transfection of Leishmania and Trypanosoma brucei by electroporation. *Methods Mol Biol,* 21**,** 333-48.

Biebinger, S., Elizabeth Wirtz, L., Lorenz, P. & Clayton, C. 1997. Vectors for inducible expression of toxic gene products in bloodstream and procyclic Trypanosoma brucei. *Mol Biochem Parasitol,* 85**,** 99-112.

Boehringer-Mannheim 1973. *Biochemica information*, Boeringher Mannheim GmbH.

Clayton, C. E., Fueri, J. P., Itzhaki, J. E., Bellofatto, V., Sherman, D. R., Wisdom, G. S., Vijayasarathy, S. & Mowatt, M. R. 1990. Transcription of the procyclic acidic repetitive protein genes of Trypanosoma brucei. *Mol Cell Biol,* 10**,** 3036-47.

Colasante, C., Alibu, V. P., Kirchberger, S., Tjaden, J., Clayton, C. & Voncken, F. 2006. Characterization and developmentally regulated localization of the mitochondrial carrier protein homologue MCP6 from Trypanosoma brucei. *Eukaryot Cell,* 5**,** 1194-205.

Colasante, C., Peña Diaz, P., Clayton, C. & Voncken, F. 2009. Mitochondrial carrier family inventory of Trypanosoma brucei brucei: Identification, expression and subcellular localisation. *Mol Biochem Parasitol,* 167**,** 104-17.

Colasante, C., Robles, A., Li, C. H., Schwede, A., Benz, C., Voncken, F., Guilbride, D. L. & Clayton, C. 2007. Regulated expression of glycosomal phosphoglycerate kinase in Trypanosoma brucei. *Mol Biochem Parasitol,* 151**,** 193-204.

Currell, G. & Dowman, A. 2005. *Essential Mathematics and Statistics for Science*, John Wiley & Sons, Ltd.

Dayhoff, M. O. & Orcutt, B. C. 1979. Methods for identifying proteins by using partial sequences. *Proc Natl Acad Sci U S A,* 76**,** 2170-4.

Fiermonte, G., Walker, J. E. & Palmieri, F. 1993. Abundant bacterial expression and reconstitution of an intrinsic membrane-transport protein from bovine mitochondria. *Biochem J,* 294 (Pt 1)**,** 293-9.

Heimpel, S., Basset, G., Odoy, S. & Klingenberg, M. 2001. Expression of the mitochondrial ADP/ATP carrier in Escherichia coli. Renaturation, reconstitution, and the effect of mutations on 10 positive residues. *J Biol Chem,* 276**,** 11499-506.

Hirumi, H. & Hirumi, K. 1989. Continuous cultivation of Trypanosoma brucei blood stream forms in a medium containing a low concentration of serum protein without feeder cell layers. *J Parasitol,* 75**,** 985-9.

Huson, D. H. 1998. SplitsTree: analyzing and visualizing evolutionary data. *Bioinformatics,* 14**,** 68-73.

Huson, D. H. & Bryant, D. 2006. Application of Phylogenetic Networks in Evolutionary Studies *Mol Biol Evol,* 23**,** 254-267.

Invitrogen 2009. Bac-to-Bac Baculovirus Expression System. User Manual. *An efficient site-specific transposition system to generate baculovirus for high level expression of recombinant proteins.* Invitrogen.

Kholod, N. & Mustelin, T. 2001. Novel Vectors for Co-Expression of Two proteins in E. coli. *BioTechniques,* 31**,** 322-328.

Klingenberg, M., Winkler, E. & Huang, S. 1995. ADP/ATP carrier and uncoupling protein. *Methods Enzymol,* 260**,** 369-89.

Krämer, R. & Heberger, C. 1986. Functional reconstitution of carrier proteins by removal of detergent with a hydrophobic ion exchange column. *Biochim Biophys Acta,* 863**,** 289-96.

Laemmli, U. K. 1970. Cleavage of structural proteins during the assembly of the head of bacteriophage T4. *Nature,* 227**,** 680-5.

Larkin, M. A., Blackshields, G., Brown, N. P., Chenna, R., McGettigan, P. A., McWilliam, H., Valentin, F., Wallace, I. M., Wilm, A., Lopez, R., Thompson, J. D., Gibson, T. J. & Higgins, D. G. 2007. Clustal W and Clustal X version 2.0. *Bioinformatics,* 23**,** 2947-48.

Lorenz, P., Maier, A., Erdmann, R., Baumgart, E. & Clayton, C. 1998. Elongation and clustering of glycosomes in *Trypanosoma brucei* overexpressing the glycosomal Pex11p. *EMBO J.,* 17**,** 3542-3555.

Millar, A. H. & Heazlewood, J. L. 2003. Genomic and proteomic analysis of mitochondrial carrier proteins in Arabidopsis. *Plant Physiol,* 131**,** 443-53.

Néron, B., Ménager, H., Maufrais, C., Joly, N., Maupetit, J., Letort, S., Carrere, S., Tuffery, P. & Letondal, C. 2009. Mobyle: a new full web bioinformatics framework. *Bioinformatics Advance Access* 25**,** 3005-11.

Novy, R., Drott, D., Yaeger, K. & Mierendorf, R. 2001. Overcoming the codon bias of E. coli for enhanced protein expression. *inNovations. Newsletter of Novagen, Inc,* 12**,** 1-3.

Nury, H., Dahout-Gonzalez, C., Trezeguet, V., Lauquin, G., Brandolin, G. & Pebay-Peyroula, E. 2005. Structural basis for lipid-mediated interactions between mitochondrial ADP/ATP carrier monomers. *FEBS Lett,* 579**,** 6031-6.

Overath, P., Czichos, J. & Haas, C. 1986. The effect of citrate/cis-aconitate on oxidative metabolism during transformation of Trypanosoma brucei. *Eur J Biochem,* 160**,** 175-82.

Palmieri, F., Agrimi, G., Blanco, E., Castegna, A., Di Noia, M. A., Iacobazzi, V., Lasorsa, F. M., Marobbio, C. M., Palmieri, L., Scarcia, P., Todisco, S., Vozza, A. & Walker, J. 2006. Identification of mitochondrial carriers in Saccharomyces cerevisiae by transport assay of reconstituted recombinant proteins. *Biochim Biophys Acta,* 1757**,** 1249-62.

Pebay-Peyroula, E., Dahout-Gonzalez, C., Kahn, R., Trezeguet, V., Lauquin, G. J. & Brandolin, G. 2003. Structure of mitochondrial ADP/ATP carrier in complex with carboxyatractyloside. *Nature,* 426**,** 39-44.

Picault, N., Hodges, M., Palmieri, L. & Palmieri, F. 2004. The growing family of mitochondrial carriers in Arabidopsis. *Trends Plant Sci,* 9**,** 138-46.

Saitou, N. & Nei, M. 1987. The neighbor-joining method: a new method for reconstructing phylogenetic trees. *Mol Biol Evol,* 4**,** 406-25.

Sambrook, J., Fritsch, E. F. & Maniatis, T. 1989. *Molecular Cloning: A Laboratory Manual,* United States of America, Cold Spring Harbor Laboratory Press.

Schneider, A., Bouzaidi-Tiali, N., Chanez, A. L. & Bulliard, L. 2007. ATP production in isolated mitochondria of procyclic Trypanosoma brucei. *Methods Mol Biol,* 372**,** 379-87.

Schoneck, R., Billaut-Mulot, O., Numrich, P., Ouaissi, M. A. & Krauth-Siegel, R. L. 1997. Cloning, sequencing and functional expression of dihydrolipoamide dehydrogenase from the human pathogen Trypanosoma cruzi. *Eur J Biochem,* 243**,** 739-47.

Schwede, T., Kopp, J., Guex, N. & Peitsch, M. C. 2003. SWISS-MODEL: An automated protein homology-modeling server. *Nucleic Acids Res,* 31**,** 3381-5.

Studier, F. W. 2005. Protein production by auto-induction in high-density shaking cultures. *Protein Expres Purif,* 41.

Thompson, J., Higgins, D. & Gibson, T. 1994. CLUSTAL W: improving the sensitivity of progressive multiple sequence alignment through sequence weighting, position-specific gap penalties and weight matrix choice. *Nucleic Acids Res,* 22**,** 4673-80.

Tjaden, J., Schwöppe, C., Möhlmann, T., Quick, P. W. & Neuhaus, H. E. 1998. Expression of a plastidic ATP/ADP transporter gene in Escherichia coli leads to a functional adenine nucleotide transport system in the bacterial cytoplasmic membrane. *J Biol Chem,* 273**,** 9630-6.

Voncken, F., van Hellemond, J. J., Pfisterer, I., Maier, A., Hillmer, S. & Clayton, C. 2003. Depletion of GIM5 causes cellular fragility, a decreased glycosome number, and reduced levels of ether-linked phospholipids in trypanosomes. *J Biol Chem,* 278**,** 35299-310.

Wohlrab, H. 2006. The human mitochondrial transport/carrier protein family. Nonsynonymous single nucleotide polymorphisms (nsSNPs) and mutations that lead to human diseases. *Biochim Biophys Acta,* 1757**,** 1263-70.

Chapter III.

Mitochondrial Carrier Family inventory of *Trypanosoma brucei brucei*: identification, expression and subcellular localization.

The contents of this chapter have been published.

Claudia Colasante, P. Pena-Diaz, Christine Clayton and Frank Voncken.

Molecular & Biochemical Parasitology. 167 (2009) 104-117.

Table of Contents

Chapter III. Mitochondrial Carrier Family inventory of *Trypanosoma brucei brucei*: identification, expression and subcellular localization.

1. Introduction

Like mitochondria from higher eukaryotes, the mitochondria of *Trypanosoma brucei* are thought to be impermeable to several metabolites (Schneider *et al.*, 2007), implying the presence of specific membrane-bound transporters. Such transporters are required for the maintenance of the cellular redox balance, and most of the known or postulated *T. brucei* mitochondrial pathways require the transport of metabolites between the mitochondria and other cellular compartments, i.e. the glycosome and the cytosol. The only information available about *T. brucei* mitochondrial metabolite transporters is what can be deduced from metabolic studies (van Weelden *et al.*, 2005; Schneider *et al.*, 2007). Recently, the molecular and functional characterisation of MCP6 was reported - the first mitochondrial metabolite transporter identified for trypanosomes and a novel member of the mitochondrial carrier family (Colasante *et al.*, 2006).

The mitochondrial carrier family (MCF) is defined as a large and diverse group of structurally related proteins that are located in the mitochondrial inner membrane and mediate the transport of a wide range of metabolic intermediates (see Chapter 1). Conserved sequence features of MCF proteins can be used to identify proteins of unknown function as members of the mitochondrial carrier family (Millar and Heazlewood, 2003; Picault *et al.*, 2004; Palmieri *et al.*, 2006; Wohlrab, 2006). All MCF proteins exhibit a canonical sequence structure consisting of three tandem repeats of about 100 amino acids, containing each two transmembrane (TM) alpha-helices connected by a hydrophilic loop and a conserved signature sequence motif (Saraste and Walker, 1982; Aquila *et al.*, 1987). Using the conserved sequence features of MCF proteins, the genome of *Saccharomyces cerevisiae* was predicted to encode 34 MCF proteins (Palmieri *et al.*, 2006), whereas the *Dictyostelium discoideum* (Satre *et al.*, 2007), *Arabidopsis thaliana* (Millar and Heazlewood, 2003; Picault *et al.*, 2004) and human (Wohlrab, 2006) genomes were predicted to encode 31, 58 and 67 MCF proteins respectively. So far, the functional characterization of MCF proteins, by metabolic studies of knockout and mutant cell lines or by in vitro reconstitution in liposomes and transport assays (Palmieri *et al.*, 2006), has been exclusively done for those identified in multicellular eukaryotes and yeast

(Opisthokonta). Virtually nothing is however known about MCF proteins from organisms in other eukaryotic branches. Functional and structural knowledge of mitochondrial carrier proteins derived from widely divergent organisms such as trypanosomes, and their comparison across evolution, may give valuable insights into conserved amino acid residues and sequence motifs important for the structure and transport function of MCF proteins. Furthermore, the identification and functional characterisation of *T. b. brucei* transporters involved in the shuttling of metabolites between the mitochondria, glycosomes and cytosol is of key importance for full understanding of the remarkable compartmentalisation of the energy metabolism in these parasites.

Analysis of the genome databases (http://www.genedb.org) from *T. b. brucei* strain TREU92 (Berriman *et al.*, 2005), *Trypanosoma cruzi* strain CL Brener (El-Sayed *et al.*, 2005) and *Leishmania major* strain Friedlin (Ivens *et al.*, 2005), allowed the identification of different genes encoding putative MCF proteins with significant homology to known mitochondrial carrier proteins from higher eukaryotes. In this chapter, the molecular analysis of MCF protein-coding genes from *T. b. brucei* is described. Their putative transport function is predicted by sequence analysis, phylogenetic reconstruction and homology-based modelling. We further analysed the expression of the different MCF genes at the mRNA level in both bloodstream-form and procyclic-form *T. brucei*, and confirmed the mitochondrial localization of the encoded MCF proteins in procyclic-form *T. b. brucei* by immunofluorescence microscopy.

2. Results

2.1. Identification of putative *T. b. brucei* mitochondrial carrier family proteins

Amino acid sequences of previously identified and functionally characterized mitochondrial carrier family (MCF) proteins from other eukaryotes were used as BLASTP queries to identify putative MCF protein-coding genes in the genome sequence database of *Trypanosoma brucei brucei* strain TREU927 (http://www.geneDB.com). In total 26 genes coding for 24 different *T. b. brucei* MCF proteins (TbMCP1-24) could be identified and are listed in Table 1.

TbMCP	GeneDB ID	kDa	pI	Human homologue	Id/Sim (%)	Yeast homologue	Id/Sim (%)	Transport function supported by		
								Similarity (BLASTP)	Phylogenetic Reconstruction	Conserved signature and CP residues (see Fig. 3)
1	Tb09.211.3200	35.7	9.63	SLC25A17 (PMP34)	28/49	P40556 (YIA6)	25/45	ATP (human)	ATP (SLC25A17: PMP34)	Unclear, conserved 'W' at pos. 3 M2a
2	Tb11.01.5960	38.0	9.65	SLC25A32 (MFT)	25/43	P40464 (FLX1)	26/45	Folate (human) FAD (yeast)	ATP (SLC25A17: PMP34)	unclear conserved 'W' at pos. 3 M2a
3	Tb09.211.2370	33.2	9.11	?	-	?	-	-	no clustering w. spec. SLC25A	-
4	Tb10.70.2290	78.0	9.49	SLC25A16 (GDC)	42/59	P38702 (LEU5)	32/52	CoA (human/yeast)	CoA	CoA
5a **b** **c**	Tb10.61.1810 Tb10.61.1820 Tb10.61.1830	34.1	9.72	SLC25A4 (AAC1)	53/69	P18239 (ANT2)	64/78	ADP/ATP (human/yeast)	ADP/ATP	ADP/ATP, conserved 'RRRMMM' in M3a
6	Tb927.4.1660	42.2	9.30	SLC25A25 (APC)	30/48	P18239 (ANT2)	30/47	ATP-Mg/Pi (human) ATP/ADP (yeast)	ATP-Mg/Pi	ATP-Mg/Pi, conserved 'A' at pos. 3 in M3a
7	Tb10.61.0610	35.9	9.79	SLC25A19 (TPC)	26/45	Q12251 (unknown)	25/44	thiamine pyrophosphate (human)	thiamine pyrophosphate	thiamine pyrophosphate
8	Tb10.406.0470	42.4	9.20	SLC25A3 (PTP)	42/58	P40035 (PIC2)	40/58	phosphate (human/yeast)	phosphate	Phosphate, conserved 'V' at pos. 6 in M3a
9	Tb11.02.2960	29.9	9.47	SLC25A45 (CAC)	33/53	Q12289 (CRC1)	34/50	carnitine/acylcarnitine (human/yeast)	ornithine	carnitine/acylcarnitine
10	Tb11.03.0870	34.0	8.85	SLC25A15 (ORNT)	31/48	Q12375 (ORT1)	31/52	ornithine (human/yeast)	carnitine/acylcarnitine	ornithine
11	Tb09.211.1750	34.3	9.29	SLC25A3 (PTP)	53/66	P40035 (PIC2)	42/61	phosphate (human/yeast)	phosphate	Phosphate, conserved 'V' at pos. 6 in M3a
12	Tb10.389.0690	33.1	9.88	SLC25A11 (OGC1)	28/46	Q06142 (DIC1)	22/41	2-oxoglutarate/dicarboxylate (human/yeast)	2-oxoglutarate/dicarboxylate	2-oxoglutarate/dicarboxylate
13	Tb927.2.2970	34.0	9.74	?	-	P38988 (YHM1)	46/66	GDP/GDP (yeast)	no homologue found in human	-
14	Tb10.389.0340	37.4	9.93	SLC25A44 (unknown)	23/39	?	-	Function SLC25A44 unknown	groups with SLC25A44	-
15	Tb927.8.1310	36.9	8.32	SLC25A5 (AAC2)	30/45	P18239 (ANT2)	27/47	ATP/ADP (human/yeast)	ATP/ADP	ADP/ATP: CP II, III partial 'RRRMM' motif (M3a)
16	Tb927.7.3940	36.3	8.72	SLC25A31 (AAC4)	23/40	P18239 (ANT2)	24/39	ATP/ADP (human/yeast)	branches close to thiamine pyrophosphate	unclear
17	Tb927.3.2980	31.1	8.50	SLC25A37 (MFRN)	31/48	P10566 (MRS3)	31/48	iron (human/yeast)	iron	iron conserved 'S' at pos. 9 in M2b

18	Tb927.8.3330	37.7	10.26	?	-	?	-	-	no clustering w. spec. SLC25A	-
19	Tb927.8.4440	40.3	7.56	SLC25A44 (unknown)	24/41	?	-	Function SLC25A44 unknown	groups with SLC25A44	-
20	Tb10.61.2510	33.0	9.94	SLC25A26 (SAMC)	36/50	P38921 (PET8)	32/46	S-adenosylmethionine (human/yeast)	S-adenosylmethionine	CPI, III
21	Tb11.01.5040	35.1	9.74	SLC25A29 (CACL)	28/42	?	-	carnitine/acylcarnitine-like (human)	branches close to carnitine/acylcarnitine	carnitine/acylcarnitine
22	Tb11.01.5950	38.7	9.54	SLC25A32 (MFT)	28/46	P40464 (FLX1)	28/47	Folate (human) FAD (yeast)	ATP (SLC25A17: PMP34)	unclear conserved 'W' at pos. 3 M2a
23	Tb927.5.1550	34.1	9.61	SLC25A36 (PNC)	27/45	EDN64801 (RIM2)	29/49	pyrimidine nucleotide (human/yeast)	pyrimidine nucleotide or FAD	unclear 'F' at pos. 3 M2a
24	Tb927.8.5810	32.9	8.49	SLC25A29 (CACL)	36/52	Q12375 (ORT1)	32/55	carnitine/acylcarnitine-like (human) ornithine (yeast)	carnitine/acylcarnitine	ornithine

Table 1. MCF protein inventory of *Trypanosoma brucei brucei. T. b. brucei* MCF protein (TbMCP) sequences were retrieved from www.genedb.org, and human (SLC25A) and *Saccharomyces cerevisiae* MCF protein sequences from www.ncbi.nlm.nih.gov. Abbreviations: kDa, kilodalton; pI, isoelectric point; Id, identity; Sim, similarity; CP, contact point; w. spec., with specific; ?, no specific homologue found.

Reciprocal database searches and sequence analysis confirmed that the identified *T. b. brucei* proteins are indeed members of the mitochondrial carrier family: all TbMCPs show significant amino acid similarity (39%-78%) to known human (SLC25A) and *S. cerevisiae* MCF proteins, all contain six transmembrane (TM) helices, and all consist of three semi-conserved protein domains of about 100 amino acids, each of which harbours a canonical MCF signature sequence motif (Millar and Heazlewood, 2003; Picault *et al.*, 2004; Palmieri *et al.*, 2006; Wohlrab, 2006). The calculated isolelectric points (IP) of the identified TbMCPs are basic with an average of about 9.3 (Table 1), which is characteristic for MCF proteins (Millar and Heazlewood, 2003; Picault *et al.*, 2004; Palmieri *et al.*, 2006; Wohlrab, 2006). The only deviation is found for TbMCP19, which has a significant lower predicted IP of about 7.6 (Table 1). The calculated molecular weights (MW) of virtually all identified TbMCP proteins vary between 30 and 42 kDa (Table 1), which is within the size range of MCF proteins from other eukaryotes (Millar and Heazlewood, 2003; Picault *et al.*, 2004; Palmieri *et al.*, 2006; Wohlrab, 2006). The only exception here is TbMCP4, for which a calculated MW of about 78 kDa is predicted (Table 1).

The TbMCPs are nearly all encoded by single copy genes. The exception is TbMCP5, for which 3 identical neighbouring gene copies, Tb10.61.1810 (*TbMCP5A*), Tb10.61.1820 (*TbMCP5B*), and Tb10.61.1830 (*TbMCP5C*), exist in the *T. b. brucei* genome (Table 1). The distribution of the TbMCP-coding genes is about proportional to the sizes of the 11 megabase-sized chromosomes (Melville *et al.*, 2000): most of the genes are situated on the largest chromosomes, 8-11, whereas medium-sized chromosomes 2-5 and 7 each contain only one *TbMCP* gene, and no TbMCP-coding gene was found on the smallest chromosomes, 1 and 6. No evidence was found for clustering of TbMCP-coding genes on the *T. b. brucei* genome, except for the above-mentioned *TbMCP5A-C* genes.

For all 24 TbMCPs, highly conserved orthologous genes could be identified in the genome databases (http://www.genedb.org) of the two related Kinetoplastids, *Trypanosoma cruzi* strain CL Brener and *Leishmania major* strain Friedlin (see Table 2). In the *T. cruzi* genome, two copies were found for most *MCP* genes. This is expected, since the *T. cruzi* strain CL Brener strain is known to be a hybrid, with many genes being present as two allelic versions in the genome database (El-Sayed *et al.*, 2005; Arner *et al.*, 2007). In the *Leishmania major* genome, most of the orthologous MCF protein-coding genes are present as 1-3 copies; exceptionally, *LmMCP12* is present as 8 identical and in tandem arranged copies (Table 2).

TbMCP	*T. b. brucei*	*T. cruzi*	Exp	*L. major*	Exp
1	Tb09.211.3200	Tc00.1047053510663.64 Tc00.1047053510737.30	1.8e-71 2.9e-71	LmjF35.3330	1.3e-67
2	Tb11.01.5960	Tc00.1047053511725.134 Tc00.1047053511725.140	4.5e-82 3.2e-56	LmjF32.1110 LmjF32.1120	6.5e-50 5.3e-48
3	Tb09.211.2370	Tc00.1047053508461.284	1.7e-96	LmjF35.3990 LmjF35.3330	3.1e-27 2.1e-21
4	Tb10.70.2290	Tc00.1047053508659.18 Tc00.1047053510291.14	2.7e-219 7.1e-219	LmjF36.0510	4.1e-167
5a,b,c	Tb10.61.1810/20/30	Tc00.1047053506211.160 Tc00.1047053511289.70	4.8e-149 2.1e-148	LmjF19.0200 LmjF19.0210	5.4e-133 5.4e-133
6	Tb927.4.1660	Tc00.1047053504057.140	1.1e-135	LmjF34.3060	1.1e-86
7	Tb10.61.0610	Tc00.1047053511365.80	8.0e-124	LmjF19.1110	1.0e-99
8	Tb10.406.0470	Tc00.1047053509551.30	6.4e-51	LmjF35.4430 LmjF35.4420 LmjF05.0290	1.8e-47 5.4e-46 9.0e-45
9	Tb11.02.2960	Tc00.1047053504131.190 Tc00.1047053504125.50	3.3e-102 4.2e-102	LmjF16.0200 LmjF25.0210	2.5e-32 9.7e-24
10	Tb11.03.0870	Tc00.1047053504109.70	1.1e-117	LmjF25.0210	2.8e-97
11	Tb09.211.1750	Tc00.1047053509551.30	4.2e-150	LmjF35.4430 LmjF35.4420	9.0e-140 1.2e-135
12	Tb10.389.0690	Tc00.1047053503939.20 Tc00.1047053509805.190	3.7e-103 7.7e-103	LmjF18.1260 LmjF18.1265 LmjF18.1270 LmjF18.1275 LmjF18.1280 LmjF18.1285 LmjF18.1290 LmjF18.1300	4.8e-86 1.7e-83 4.4e-83 4.4e-83 4.4e-83 4.4e-83 4.4e-83 3.9e-84
13	Tb927.2.2970	Tc00.1047053508737.150 Tc00.1047053509127.50	4.8e-94 1.3e-93	LmjF02.0670	4.8e-86
14	Tb10.389.0340	Tc00.1047053506359.70 Tc00.1047053503521.39	3.3e-95 1.1e-94	LmjF18.1000	5.1e-76
15	Tb927.8.1310	Tc00.1047053510835.24 Tc00.1047053506401.304	6.1e-78 1.0e-77	LmjF07.0530	1.0e-77
16	Tb927.7.3940	Tc00.1047053511249.10	5.5e-93	LmjF14.0990	2.9e-63
17	Tb927.3.2980	Tc00.1047053508153.630 Tc00.1047053510315.20	7.4e-89 1.5e-88	LmjF29.2780	1.7e-74
18	Tb927.8.3330	Tc00.1047053509769.90	5.3e-79	LmjF23.1370	5.9e-67
19	Tb927.8.4440	Tc00.1047053508989.20 Tc00.1047053509569.110	1.4e-124 3.8e-124	LmjF10.1020	7.3e-90
20	Tb10.61.2510	Tc00.1047053511283.124 Tc00.1047053506525.130	1.9e-58 1.7e-57	LmjF32.0110	1.0e-37
21	Tb11.01.5040	Tc00.1047053510359.69 Tc00.1047053506755.74	1.3e-82 1.3e-82	LmjF09.1270	7.7e-63
22	Tb11.01.5950	Tc00.1047053511725.140 Tc00.1047053511725.134	5.6e-84 4.8e-62	LmjF32.1110 LmjF32.1120	1.4e-70 1.2e-62
23	Tb927.5.1550	Tc00.1047053506739.80 Tc00.1047053510819.100	1.6e-102 4.2e-102	LmjF15.0120	6.9e-94
24	Tb927.8.5810	Tc00.1047053510603.90 Tc00.1047053509109.114	8.9e-109 6.3e-108	LmjF16.0200	1.5e-82

Table 2. Orthologous TbMCP genes in *T. cruzi* and *L. major*. *T. cruzi* and *Leishmania* protein sequences were retrieved from www.genedb.org. Abbreviation: Exp, expectation (probability)

2.2. BLASTP analysis and phylogenetic reconstruction

The putative transport function of the identified TbMCPs was predicted by using different approaches. Reciprocal BLASTP database searches and phylogenetic reconstruction were used to determine the similarity of the identified TbMCPs to functionally characterised MCF proteins from other eukaryotes. Substrate specificities have been determined for the majority of human (SLC25A) and *S. cerevisiae* MCF proteins, either by *in vitro* proteoliposome-based transport assays using purified MCF proteins, or by genetic and physiological experiments pointing to a particular subset of substrates (Palmieri, 2004; Palmieri *et al.*, 2006; Wohlrab, 2006). Based on the type of transported substrate, MCF proteins can generally be divided into 6 functional groups: nucleotide, inorganic phosphate (Pi), carboxylic acid, amino acid, proton, and iron carriers (Kunji and Robinson, 2006; Palmieri, 2004; Palmieri *et al.*, 2006; Wohlrab, 2006). Highly similar MCF proteins were found to transport identical or similar substrates (Millar and Heazlewood, 2003; Picault *et al.*, 2004; Palmieri *et al.*, 2006; Wohlrab, 2006).

BLASTP database searches using the identified TbMCPs as queries resulted in the retrieval of homologous MCF proteins for all TbMCPs with significant E-value scores ranging between e^{-23} and e^{-114} (not shown). Table 1 shows the similarities found between the TbMCP queries and the retrieved human (SLC25A) or *S. cerevisiae* MCF protein sequence top hits. Of the 24 identified TbMCPs, 20 were found to show significant amino acid sequence similarity to specific human and *S. cerevisiae* MCF proteins. Eleven of these sequences (Table 1) were found to be of the nucleotide transport type; the most conserved members were TbMCP5A-C, showing 78% amino acid similarity to the *S. cerevisiae* ADP/ATP carrier ANT2 and 69% similarity to the human ADP/ATP carrier SLC25A4 (AAC1). Five TbMCPs could be assigned to the amino acid transport group, including one S-adenosylmethionine carrier (TbMCP20) and four putative carriers for carnitine/acylcarnitine or ornithine-like substrates (TbMCPs 9, 10, 21 and 24). In addition, TbMCP8 and TbMCP11 belong to the inorganic phosphate transport group, both showing 58%-66% sequence similarity (Table 1) to inorganic phosphate carriers from *S. cerevisiae* (PIC2) and human (PTP).

TbMCP12 could be assigned to the carboxylate transport group, with 41%-46%; sequence similarity (Table 1) to *S. cerevisiae* and human oxoglutarate and dicarboxylate carriers. Finally, TbMCP17 could be assigned to the iron transport group, having 48% sequence similarity (Table 1) to iron carriers from yeast (MRS3) and humans (MFRN). For the remaining 4 TbMCPs, no specific transport function could be predicted. TbMCPs 14 and 19 showed substantial similarity to the human MCF protein homologue SLC25A44 (without known transport function), and TbMCPs 3 and 18 could not be assigned to any particular group because they had similar, low scores for various MCF proteins from different groups (Table 1).

The BLASTP-predicted functions of the 24 TbMCPs were next assessed by phylogenetic reconstruction. The resulting neighbor-joining (NJ) tree is shown in figure 1 and includes, in addition to the TbMCPs, 43 different human (SLC25A) MCF protein sequences. For the largest MCF transport group, i.e. the nucleotide carriers, at least 6 different subgroups (Figure 1, marked solid green) can be distinguished: in each subgroup, one or more SLC25A proteins were shown previously to transport a specific nucleotide or nucleotide-related substrate (Palmieri *et al.*, 2006; Wohlrab, 2006). TbMCP5 and TbMCP15 cluster specifically with the human ADP/ATP carriers SLC25A4 (AAC1) and SLC25A5 (AAC2), which is in agreement with their BLASTP-predicted transport function (Table 1). Concurrence of BLASTP-based function prediction and phylogenetic clustering was also observed for other TbMCPs, including TbMCP1 (SLC25A17: ATP carrier), TbMCP4 (SLC25A16: Coenzyme A carrier), TbMCP6 (SLC25A25: ATP-Mg/Pi carrier), TbMCP7 (SLC25A19: thiamine pyrophosphate carrier), and TbMCP23 (SLC25A36: pyrimidine nucleotide carrier) (Table 1). The functional predictions for TbMCP2 and TbMCP22 are contradictory and change depending on the database and method used (see Table1). For example, BLASTP analysis suggests that, when using the human MCF proteins for comparison, TbMCP2 and TbMCP22 are rather similar to the folate carrier SLC25A32, whereas BLASTP searches against yeast MCF proteins suggests that they are more similar to the flavin (FAD) carrier FLX1. Phylogenetic reconstruction, meanwhile, suggests that both TbMCPs are more related to the ATP carrier SLC25A17 (PMP34) then to the folate carrier SLC25A32 (Fig. 1). In summary, the rather strong divergence of the TbMCP2 and TbMCP22 sequences prohibits similarity-based functional assignment.

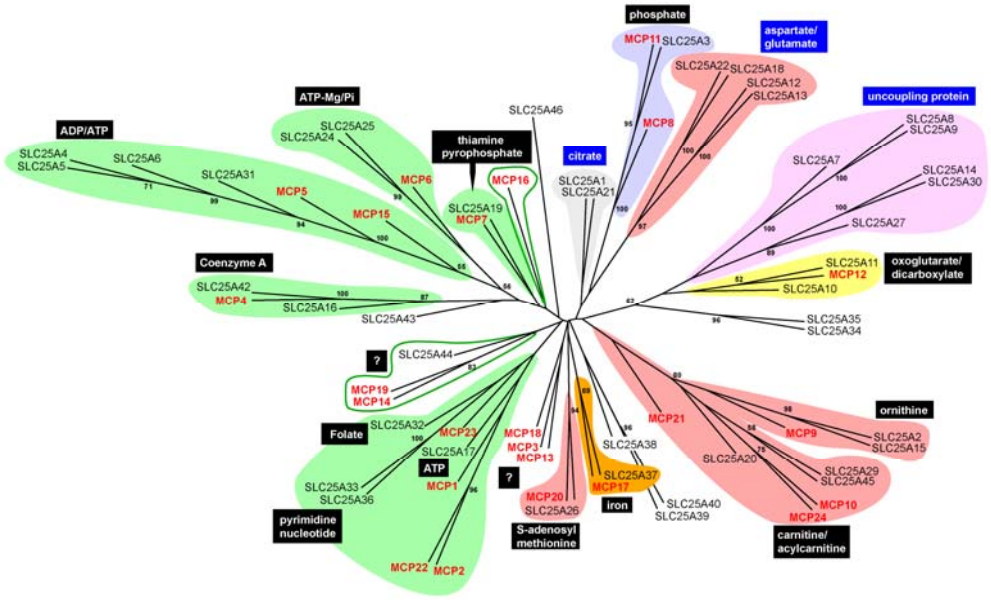

Fig. 1. Neighbour-joining tree showing the evolutionary relationship between TbMCPs and 43 human (SLC25A) MCF proteins. Bootstrap values above 50% are indicated at the relevant nodes. Coloured balloons are used to mark the major functional MCF subgroups: green, nucleotide carriers; pink, amino acid carriers; blue, inorganic phosphate carriers; yellow, dicarboxylate/oxoglutarate carriers; and orange, iron carriers. Blue text boxes represent MCF subgroups for which no *T. b. brucei* homologues could be identified. Question marks indicate TbMCPs for which no transport function could be predicted.

The phylogenetic analysis divided the amino acid carriers into 4 different subgroups (Figure 1, marked pink). Two of these, the carnitine/acylcarnitine carriers and ornithine carriers, are evolutionary very closely related, whereas the S-adenosylmethionine and the glutamate/aspartate carriers are more divergent (Fig. 1). The Neighbour-Joining tree grouped TbMCP10 and TbMCP24 with the acylcarnitine/carnitine carrier SLC25A45, whereas TbMCP9 grouped with the ornithine carrier SLC25A15 (Fig. 1). This result is in contradiction with the BLASTP results, which suggested the reverse assignment (see Table 1). This contradiction is most probably caused by the recent branching and close evolutionary relationship of the carnitine/acylcarnitine and ornithine carrier subgroups (Fig. 1), which in combination with the divergence of the *T. b. brucei* sequences could prohibit the assignment of a specific carnitine/acylcarnitine or ornithine transport function. The

putative amino acid carrier TbMCP20 groups confidently with the human S-adenosyl methionine carrier SLC25A26, in agreement with its BLASTP-predicted transport function (Fig.1, Table 1). Branching of TbMCP21 close but prior to the carnitine/acylcarnitine transporter subgroup (Fig. 1) and its sequence similarity to the human carnitine/acylcarnitine-like carrier SLC25A29 (Table 1) suggests that this MCF protein may transport a carnitine-related substrate.

In agreement with the BLASTP results, TbMCP8 and TbMCP11 grouped with the inorganic phosphate transporter SLC25A3, TbMCP12 with the oxoglutarate (SLC25A10) and dicarboxylate carriers (SLC25A11), and TbMCP17 with the iron transporter SLC25A37 (Fig. 1). TbMCP14 and TbMCP19 clustered with SLC25A44, a human MCF protein without known function, while TbMCP16 branched closely to the thiamine pyrophosphate transporter subgroup. Clustering of TbMCPs 14, 16 and 19 within the nucleotide carrier part of the phylogenetic tree (Fig. 1) suggests that these MCF proteins are most probably involved in the transport of nucleotides or nucleotide-related substrates.

2.3. Homology-based modelling of TbMCPs

The molecular structure of the *Bos taurus* mitochondrial ADP/ATP carrier was recently resolved by x-ray crystallography (Pebay-Peyroula *et al.*, 2003; Nury *et al.*, 2006). The crystallographic model can be used to predict a three-dimensional structure for other similar MCF proteins, as has been done previously for the yeast mitochondrial citrate transport protein (Walters and Kaplan, 2004) and MCF proteins of the slime mould *Dictyostelium discoideum* (Satre *et al.*, 2007). We used a similar homology-modelling approach for the 24 TbMCPs. As shown in Figure 2, a satisfactory modelling of the backbone structure could be obtained for 19 of them, confirming the remarkable structural conservation of MCF proteins (Pebay-Peyroula *et al.*, 2003; Nury *et al.*, 2006). The modelled MCP protein structures all display the typical barrel-shaped structure, as observed previously for the bovine mitochondrial ADP/ATP carrier (Pebay-Peyroula *et al.*, 2003; Nury *et al.*, 2006). Nevertheless, many structural differences could be

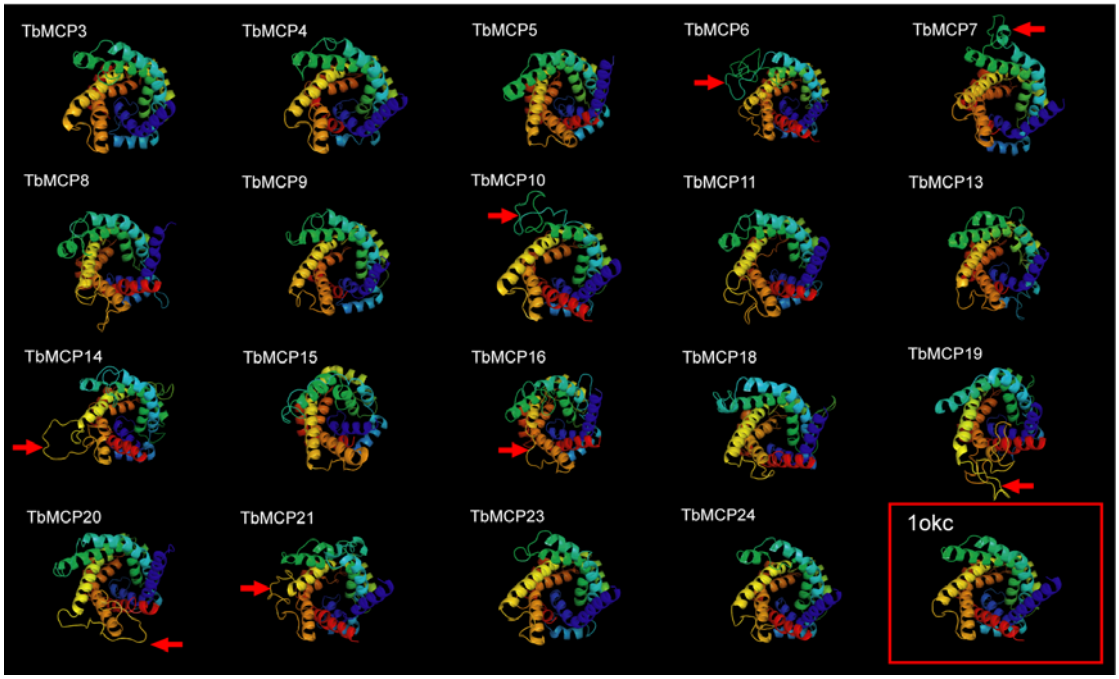

Fig. 2. Top view of 3D protein structures obtained after homology-based modelling of TbMCPs. The models all display the conserved barrel-shaped structure of MCF members. TbMCPs were modelled using SWISS-MODEL and CPHmodels, and the 3D-structures *1okc* and *2c3e* for threading. The obtained 3D-structures were viewed and edited with PyMOL. The modelled 3D protein structure (*1okc*) of the bovine mitochondrial ADP/ATP carrier (Nury *et al.*, 2006; Pebay-Peyroula *et al.*, 2003) is shown for comparison. Red arrows point to structural deviations such as unstructured loops.

observed, including unstructured loops or beta sheet regions (see Fig. 2). For the TbMCPs 1, 2, 12, 17 and 22, no homology-based structure models could be predicted, presumably because these MCF sequences are too dissimilar to that of the *Bos taurus* mitochondrial ADP/ATP carrier.

2.4. Conservation of MCF signature sequences

A hallmark of MCF proteins is the canonical signature sequence $Px(D/E)x_2(K/R)x(K/R)x_{20\text{-}30}(D/E)Gx_{4\text{-}5}(W/F/Y)(K/R)G$ (x = any amino acid residue) found in each of the three semi-conserved repetitive protein domains (Saraste and Walker, 1982; Aquila *et al.*, 1987). Protein structure studies suggested that the

signature sequence contributes to the typical barrel shape of mitochondrial carrier proteins (Pebay-Peyroula *et al.*, 2003; Nury *et al.*, 2006). The first part of the motif, 'Px(D/E)x_2(K/R)x(K/R)', is located at the carboxy-terminal ends of the odd-numbered TM helices H1, H3 and H5, whereas the second part, '(D/E)G$x_{4\text{-}5}$(W/F/Y)(K/R)G', is located 20-30 amino acids downstream, after the amphipathic helices h1-2, h3-4, and h5-6 (see Fig. 3).

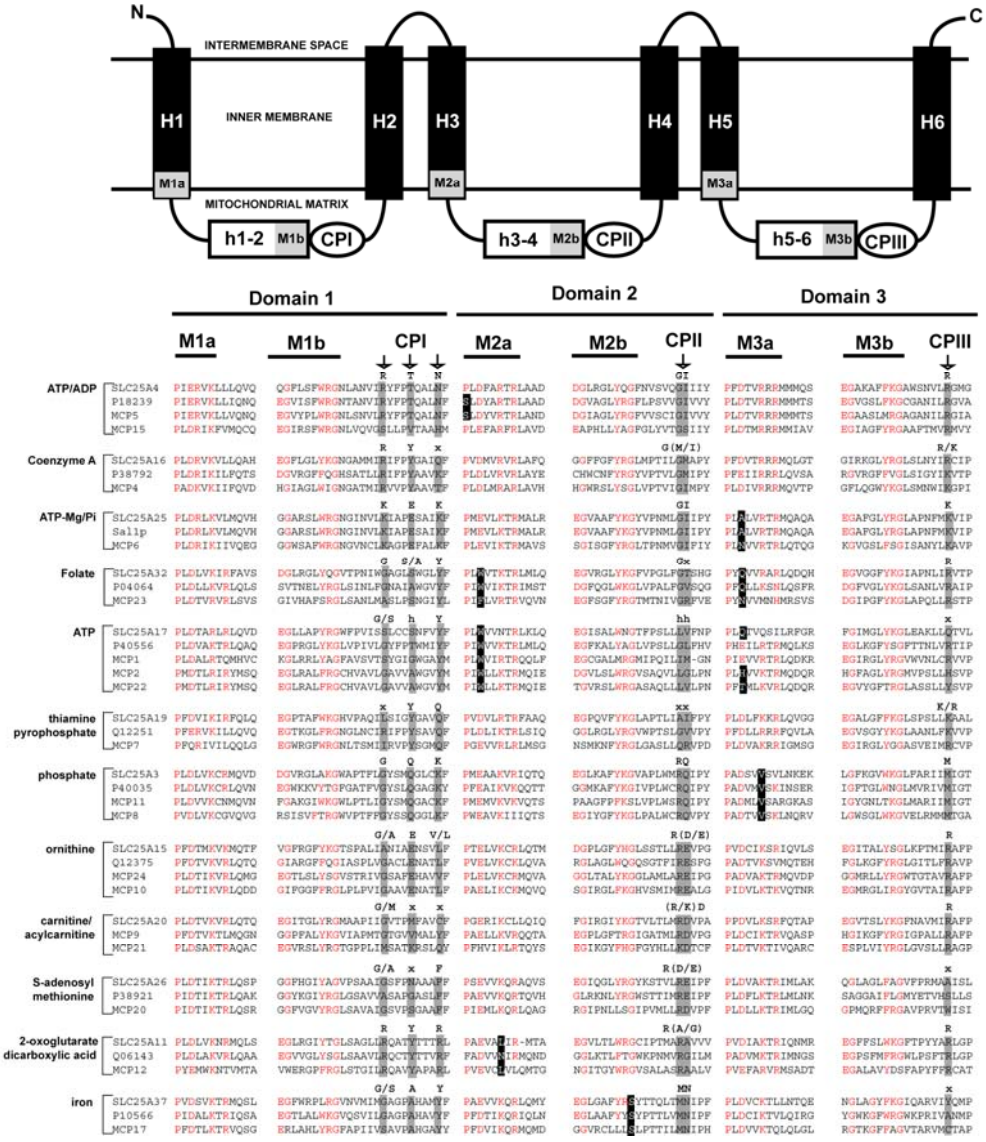

Fig. 3. Schematic representation of the conserved tripartite MCF protein structure. The six transmembrane helices are labelled H1-6, whereas the hydrophilic loops, connecting the 2 transmembrane domains found in each repeat (repeat 1-3), are labelled h1-2, h3-4 and h5-6, respectively. The first part of the canonical signature sequence motif, Px(D/E)xx(K/R)x(K/R), located at the end of the odd-numbered transmembrane helices, is labelled M1a, M2a, and M3a. The second part of the canonical signature sequence motif, (D/E)Gx_n(K/R)G, located at the end of each

hydrophilic loop, is labelled M1b, M2b, and M3b. Substrate contact points are located downstream of the second part of the signature sequence and are labelled CPI, CPII and CPIII. TbMCPs (this paper) and related MCF protein sequences from human (SLC25A) and *S. cerevisiae* were aligned using ClustalW, and the alignment was manually edited using Se-Al v2.0a11. For each of the different functional transporter subgroups only those parts of the alignments containing the conserved signature sequences (identical signature sequence residues are marked red) and the amino acid residues present in each of the contact points (boxed grey) are shown. Signature sequence residues deviating from the canonical signature sequence, but found in all members of a specific carrier subgroup, are boxed black. Putative substrates for each of the carrier subgroups are indicated.

The conservation of signature sequences of TbMCPs was analysed using human (SLC25A) and *S. cerevisiae* MCF homologues for comparison (Fig. 3). The first part of the signature sequence (Fig. 3: motifs M1a, M2a, and M3a) is highly conserved in virtually all TbMCPs, although some remarkable differences - substitutions and rearrangements - were observed. These differences were either unique for specific TbMCPs, or conserved in all MCF sequences within a specific transporter subgroup (Fig. 3). For example, in virtually all MCF proteins a highly conserved proline is found at the start of the signature sequence motifs M1a, M2a, and M3a. This amino acid causes a flexible kink in the protein backbone shortly before the even-numbered TM helices H2, H4 and H6 (Fig. 3) and has been proposed to enable the transition between an ‘open’ and ‘closed’ pore-like state of MCF proteins (Johnston *et al.*, 2008). The proline residue is conserved in all TbMCP signature sequences except for TbMCP5A-C, where it has been substituted by a serine in motif M2a (Fig. 3). This substitution is however not restricted to TbMCP5, since a similar substitution has been reported for several other ADP/ATP carriers, including *S. cerevisiae* ANT2 (P18239, Fig 3) (Nury *et al.*, 2006; Yohannan *et al.*, 2004).

Another characteristic amino acid found in the first part of the signature sequences of virtually all MCF proteins is the acidic amino acid residue, either an aspartic acid or glutamic acid, located at position 3 of the motifs M1a, M2a, and M3a (Fig. 3). In some MCF proteins, however, this acidic residue has been substituted by a non-similar amino acid, in one or even more signature sequences of the same MCF protein. In case of ATP-Mg/Pi, FAD or ATP carriers, the substitution is conserved amongst all members of the respective carrier subgroups (Fig. 3). For example, the

M2a motifs of both the FAD and ATP carriers invariably contain a non-polar aromatic amino acid (either tryptophan or phenylalanine) at position 3, whereas in the M3a motifs of the ATP-Mg/Pi transporters this aromatic amino acid has been replaced by a non-conserved neutral amino acid (Fig. 3). Similar amino acid substitutions were also found for TbMCPs 1, 2, 6, and 22; they support the BLASTP- and phylogeny-based assignment of these TbMCPs to their respective carrier subgroups.

Also other canonical signature sequence amino acids were found to be substituted in a carrier-subgroup-dependent manner. Virtually all MCF proteins contain a positively charged amino acid, either a lysine or an arginine, at position 6 of the M1a, M2a and M3a motifs (see Fig. 3). The phosphate carrier subgroup is an exception: they have a conserved non-polar valine instead. The characteristic valine is indeed found in the M3a motifs of TbMCP8 and TbMCP11, supporting the assignment of these MCF proteins to the phosphate carriers (Fig. 3).

Another deviation from the canonical MCF signature sequence is found in the first part of the M1a motifs of all sequence members of the ATP/ADP, Coenzyme A and ATP-Mg/Pi carrier subgroups (Fig. 3). Whereas most other MCF proteins contain a conserved lysine or arginine at position 6 of the M1a motif, in these subgroups it is found at position 4 instead, adjacent to the conserved acidic amino acid residue (aspartic acid or glutamic acid) located in position 3. A similar spatial rearrangement, i.e. from 'Px(D/E)x_2(K/R)x(K/R)' to 'Px(D/E)(K/R)x(K/R)', is found in TbMCPs 4, 5, 6 and 15, supporting their assignment to these carrier subgroups (Fig. 3).

In contrast to the first part of the sequence signature, the second part of the signature sequence, '(D/E)Gx_{4-5}(W/F/Y)(K/R)G', is less conserved (Fig. 3: M1b, M2b, and M3b). The first two amino acids of the motif, i.e. '(D/E)G', are not well conserved and the number of amino acids (x) between the '(D/E)G' and the '(W/F/Y)(K/R)G' part of the motif also varies. The final glycine of the motif, which allows flexibility of the loop that links the two helices (Nury *et al.*, 2006), is however highly conserved, as is the aromatic residue at position 7 (Fig. 3).

2.5. Conservation of proposed substrate contact points

Sequence analysis revealed the presence of several conserved residues downstream of the canonical signature sequences (see Fig. 3). Structural studies of the bovine ATP/ADP carrier showed that some of these amino acids are located in the substrate-binding pocket, and they were proposed to play a key role in the recognition of, and discrimination between, different substrate classes (Kunji and Robinson, 2006; Robinson and Kunji, 2006). In total, 3 different substrate-contact points were proposed, called CPI, CPII and CPIII, with the first amino acid of each substrate-contact point located six amino acids downstream of the conserved glycine residue that marks the end of each signature sequence motif (Fig. 3) (Kunji and Robinson, 2006; Robinson and Kunji, 2006). These substrate-contact points were reported to be conserved in MCF proteins from different eukaryotes transporting similar substrates (Kunji and Robinson, 2006; Robinson and Kunji, 2006). Contact point II in particular was proposed to play an important role in substrate discrimination: it is defined by a conserved amino acid (AA) pair for each substrate type: i.e. 'G(IVLM)' for nucleotide carriers, '(R/K)Q' for phosphate carriers, 'R(QHNT)' for dicarboxylic acid carriers, 'R(D/E)' for amino acid carriers, and 'MN' for iron carriers (Kunji and Robinson, 2006; Robinson and Kunji, 2006).

In the majority of TbMCPs, the conserved amino acid pair at CPII agrees with the transport function predicted by BLASTP and phylogeny (Fig. 3, Table 1). For example, the putative phosphate carriers TbMCPs 8 and 11 contain the expected 'RQ' pair at CPII, while the putative iron carrier TbMCP17 contains the expected 'MN' pair. Also, the predicted *T. b. brucei* amino acid carriers, TbMCPs 9, 10, 20, 21 and 24, contain the expected 'R(D/E)' pair at CPII (Fig. 3). Comparison of CPII AA pairs for the putative *T. b. brucei* nucleotide carriers revealed that only the ADP/ATP carriers TbMCPs 5 and 15, the ATP-Mg/Pi carrier TbMCP6, and the Coenzyme A carrier TbMCP4 contain the expected 'G(I/M)' sequence (Fig. 3). For the other nucleotide carriers (the putative *T. b. brucei* folate (TbMCP23), ATP (TbMCP1, 2, 22), and thiamine pyrophosphate (TbMCP7) carriers), the CPII AA pair is less conserved (Fig. 3). A similar deviation of the CPII rule is observed for the putative carboxylate carrier TbMCP12, which contains a conserved 'R' at the first position of CPII, while the second amino acid residue is highly variable, as has been observed previously for other carboxylate carriers (Kunji and Robinson, 2006; Satre *et al.*, 2007).

2.6. Remarkable features of the kinetoplastid mitochondrial carrier family inventory

Analysis of the *T. b. brucei*, *T. cruzi* and *Leishmania* mitochondrial carrier family inventories revealed some remarkable deviations in comparison with those previously reported for other eukaryotes (Millar and Heazlewood, 2003; Picault *et al.*, 2004; Palmieri *et al.*, 2006; Wohlrab, 2006). Most notable is the lack of sequences similar to the uncoupling protein (UCP), an essential MCF protein member found in virtually all eukaryotes (Echtay *et al.*, 2002; Palmieri, 2004). Extensive sequence analysis of the different kinetoplastid genome databases by a variety of database analysis programs, and using a large number of different UCP sequences from a wide range of eukaryotes as query, failed to identify any possible trypanosome or *Leishmania* UCP (Table 1, Fig. 1). Thorough analysis of the kinetoplastid genome databases failed further to identify two other MCF members, i.e. the citrate (tricarboxylate) carrier and the glutamate/aspartate carrier (Table 1, Fig. 1). Genes encoding these prototypical MCF proteins have been identified previously for all other, eukaryotes studied so far (Millar and Heazlewood, 2003; Picault *et al.*, 2004; Palmieri *et al.*, 2006; Wohlrab, 2006).

Another observation is that virtually all identified TbMCPs obey the expected size rule of about 300-400 amino acids (Table 1). None of the identified TbMCPs contains an N-terminal extension with EF hand calcium-binding motifs or sequence repeats. These features have been reported previously for a large number of MCF proteins from other eukaryotes (Millar and Heazlewood, 2003; Picault *et al.*, 2004; Palmieri *et al.*, 2006; Wohlrab, 2006). The only deviation from the canonical MCF protein length is found for TbMCP4, which has a calculated MW of about 78 kDa, approximately twice the size of an average MCF protein (Table 1). TbMCP4 contains 12 TM domains and 6 signature sequence motifs, double the number expected for a standard MCF member (not shown). BLASTP analysis showed that the first part (residues 100-400) of TbMCP4 shows significant sequence similarity (59%) to GDC, the Grave's disease carrier from mammals (Fiermonte *et al.*, 1992) and its *Saccharomyces cerevisiae* homologue Leu5p (Prohl *et al.*, 2001); in contrast, the second part of TbMCP4 was not clearly homologous to a particular human or yeast MCF protein. The MCP4 proteins from *T. cruzi* and *L. major* had the same structure as TbMCP4 (Table 2), ruling out a sequence assembly mistake. The only other eukaryotic organism with an MCF protein of this type (large, without EF-hand calcium-binding motifs or substantial sequence repeats) is *Ostreococcus tauri*,

a unicellular alga and the smallest free-living mitochondriate eukaryote known so far (Derelle *et al.*, 2006). BLASTP analysis of the *Ostreococcus tauri* genome database with TbMCP4 revealed the 676-AA protein CAL55012, which has 47-51% similarity to the *T. brucei, T. cruzi* and *L. major* MCP4s.

2.7. Subcellular localisation of TbMCPs

The majority of MCF proteins characterised so far are in the mitochondrion, with the exception of a few which were found to be associated with the membranes of other intracellular compartments like peroxisomes (Nakagawa *et al.*, 2000; van Roermund *et al.*, 2001; Palmieri *et al.*, 2001). We have previously shown that myc-tagged TbMCP6 has a dual subcellular localisation depending on the life-cycle stage of *T. b. brucei*: in procyclic-form trypanosomes it is predominantly found in the mitochondria, whereas in bloodstream-form trypanosomes it is mainly localised in the glycosomes (Colasante *et al.*, 2006). To determine the subcellular localisation of the remaining TbMCPs, we expressed, in procyclic-form trypanosomes, recombinant versions carrying either a carboxy- or amino-terminal 2xmyc-tag. Expression of the myc-tagged TbMCPs was confirmed by western blot analysis (not shown) and the subcellular localisation determined by immunofluorescence microscopy (Fig. 4). 18 of the 24 identified TbMCPs could be expressed; and all were found in the mitochondria, co-localising with the mitochondrial marker protein dihydroxylipoamide dehydrogenase (Fig. 4). For TbMCPs 1, 9, 18, 20, 21 and 24, either no viable clones could be obtained after multiple transfection attempts, or, if a viable clone was obtained, no expression of the tagged protein was detected (not shown). In case these TbMCPs could only be expressed in bloodstream forms, we repeated the experiments in that stage, but again either no viable clones could be obtained or no expression of the recombinant 2xMyc-tagged protein was found (not shown).

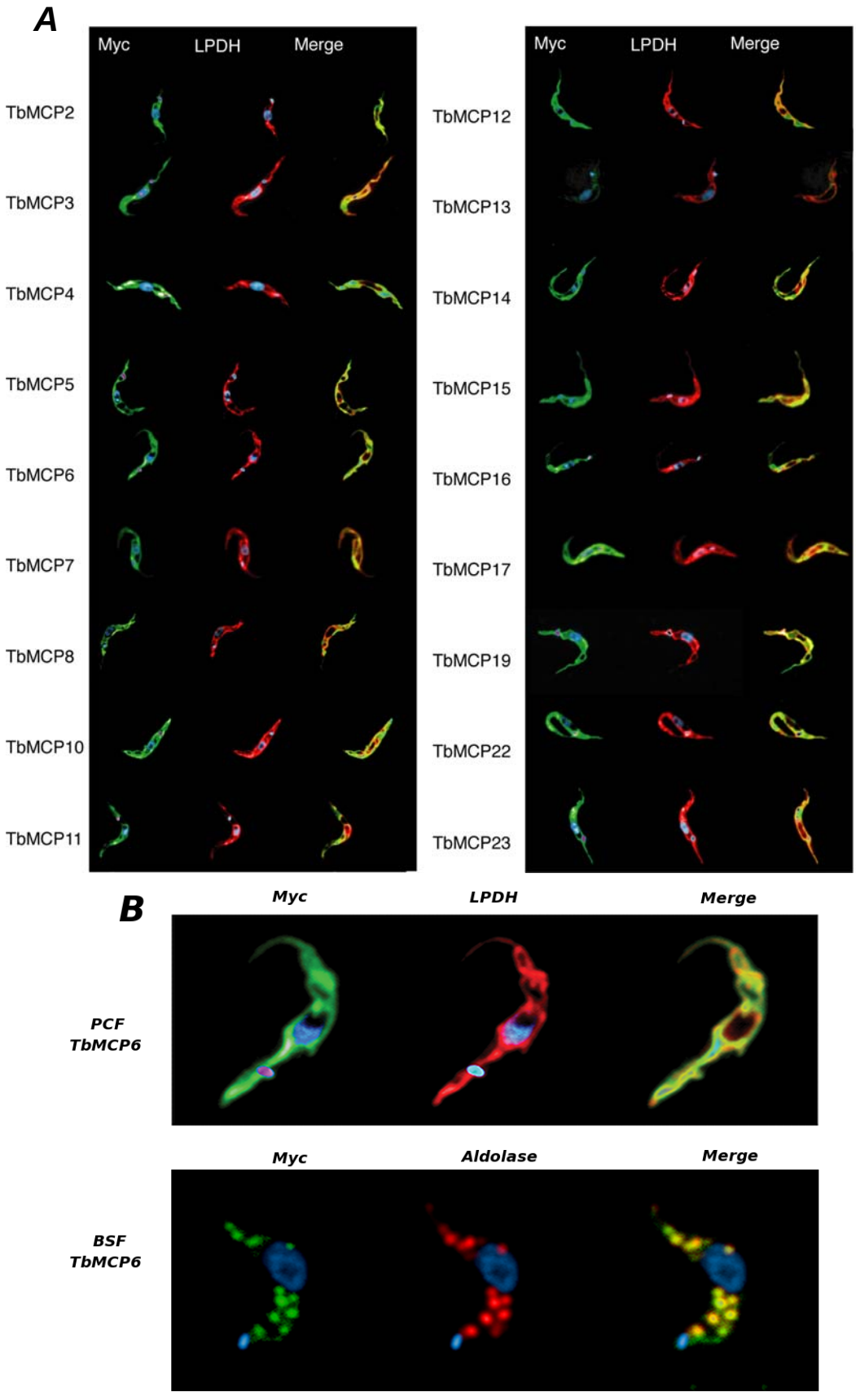
A
Myc
LPDH
Merge
TbMCP2
TbMCP3
TbMCP4
TbMCP5
TbMCP6
TbMCP7
TbMCP8
TbMCP10
TbMCP11
TbMCP12
TbMCP13
TbMCP14
TbMCP15
TbMCP16
TbMCP17
TbMCP19
TbMCP22
TbMCP23
B
Myc
LPDH
Merge
PCF
TbMCP6
Myc
Aldolase
Merge
BSF
TbMCP6

Fig. 4. Immunofluorescence microscopy of procyclic-form *T. b. brucei* cell lines expressing myc-tagged TbMCPs (green) (A). The mitochondria were stained red with an antibody directed against the *T. b. brucei* mitochondrial marker protein lipoamid-dehydrogenase (LPDH), while nucleus and kinetoplast DNA were stained blue with DAPI. Overlays (merge) are shown to visualize the overlap (co-localisation) in the staining patterns. B) Upper panel: Myc-tagged TbMCP6 in procyclic-form *T.b. brucei*, showing mitochondrial localization as shown by merge with the mitochondrial marker LPDH (red). Lower panel: Myc-tagged TbMCP6 in bloodstream-form *T.b. brucei* showing glycosomal localization, confirmed by the merge with aldolase signal (red). Note the difference in staining pattern, which demonstrates mitochondrial localization for all the carriers shown in A.

TbMCP	GeneDB ID	P/B
1	Tb09.211.3200	0.98
2	Tb11.01.5960	0.94
3	Tb09.211.2370	1.02
4	Tb10.70.2290	0.92
5a,b,c	Tb10.61.1810/20/30	1.72
6	Tb927.4.1660	1.04
7	Tb10.61.0610	1.41
8	Tb10.406.0470	ND
9	Tb11.02.2960	1.00
10	Tb11.03.0870	1.48
11	Tb09.211.1750	***2.78***
12	Tb10.389.0690	***2.69***
13	Tb927.2.2970	0.98
14	Tb10.389.0340	0.96
15	Tb927.8.1310	1.22
16	Tb927.7.3940	1.62
17	Tb927.3.2980	ND
18	Tb927.8.3330	0.97
19	Tb927.8.4440	0.74
20	Tb10.61.2510	1.60
21	Tb11.01.5040	0.87
22	Tb11.01.5950	0.93
23	Tb927.5.1550	1.22
24	Tb927.8.5810	1.49
SRP	Tb11.02.3070	**1.00**

Table 3. Quantitative comparison of TbMCP mRNA levels in procyclic-form and bloodstream-form *Trypanosoma brucei brucei*. Signal recognition particle (SRP) (Michaeli et al., 1992) mRNA-levels were used as internal standard (procyclic-form/bloodstream-form mRNA ratio set to 1.00). Abbreviations: P, procyclic-form; B, bloodstream-form; P/B, procyclic-form/bloodstream-form mRNA level ratio; ND, not detectable.

2.8. Expression of TbMCP mRNAs

It has been shown previously that many proteins are differentially expressed (developmentally regulated) at the mRNA level in the two main replicating life cycle stages of *T. b. brucei*, i.e. the bloodstream-form and the procyclic-form (Brems *et al.*, 2005). Northern blot analysis was used to assess whether a similar differential expression is also found for the TbMCPs. For 22 of the *TbMCP* genes we detected

a single mRNA band of the expected size for both bloodstream-form and procyclic-form *T. b. brucei* (not shown). No signal could be detected for TbMCP8 (inorganic phosphate carrier) and TbMCP17 (iron carrier), in either bloodstream-form or procyclic-form *T. b. brucei*, indicating that mRNAs from these genes are absent or present at levels below the detection limit of the used method. Quantitation (Table 3) revealed that only TbMCP11 (inorganic phosphate carrier) and TbMCP12 (oxoglutarate or dicarboxylate carrier) are differently expressed at the mRNA level, with roughly 2-fold more mRNA in procyclic-form than in bloodstream-form *T. b. brucei* (Fig. 5). The up-regulation of both TbMCP11 and TbMCP12 expression in procyclic-form *T. b. brucei* was also seen in a comparative transcriptome analysis of bloodstream-form and procyclic-form *T. b. brucei* TREU 927 (Brems *et al.*, 2005).

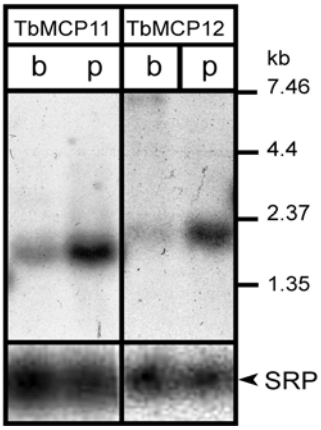

Fig. 5. Northern blot analysis of *TbMCP11* and *TbMCP12* showing differential expression in bloodstream-form and procyclic-form *T. b. brucei*. 20 µg total RNA isolated from bloodstream-form (b) and procyclic-form (p) was loaded per lane. The complete open reading frames of *TbMCP11* and *TbMCP12* were used as hybridization probes. The *T. b. brucei* signal recognition particle (*SRP*) RNA was used as a loading control (Michaeli *et al.*, 1992).

3. Discussion

Putative carrier functions were predicted for 20 of the 24 identified TbMCPs by using a combination of methods: reciprocal BLASTP analysis (Table 1), phylogenetic reconstruction (Fig. 1), and analyses of conserved function-related amino acid residues in signature sequences motifs and proposed substrate contact points (Fig. 3). The expression of TbMCPs in bloodstream-form and procyclic-form *T. b. brucei* was confirmed by the presence of detectable mRNA levels in both life-cycle stages

(Table 3), and their mitochondrial localisation was confirmed by immunofluorescence microscopy (Fig. 4). Using the information obtained, a basic mitochondrial map can be drawn showing the predicted MCF protein transport activities, in relation to a subset of *T. b. brucei* mitochondrial pathways that require metabolite exchange across the mitochondrial inner membrane (Fig. 6). In procyclic-form *T. b. brucei* mitochondria the Krebs cycle is not involved in cellular energy (ATP) generation, although a complete set of Krebs cycle enzymes and a functional respiratory chain are present (van Hellemond *et al.*, 2005). Instead, procyclic-form trypanosomes gain most of their ATP by substrate-level phosphorylation during the mitochondrial degradation of amino acids, particularly proline (Bringaud *et al.*, 2006; Bochud-Allemann and Schneider, 2002). The ATP generated has to be exported from the mitochondrion to supply cytosolic energy-consuming biosynthetic pathways. The best-studied and most conserved member of the mitochondrial carrier family is the ADP/ATP carrier, which plays a vital role in the maintenance of the mitochondrial ADP/ATP ratio (Aquila *et al.*, 1987; Klingenberg, 2008). ATP generated in the mitochondrial matrix is exported via this carrier to the cytosol in exchange for ADP, which serves as a substrate for further mitochondrial phosphorylation reactions. Up to 4 different ADP/ATP carriers have been found in eukaryotes examined so far; each plays a somewhat different role in the cellular energy metabolism (Klingenberg, 2008). *T. b. brucei* also has multiple putative ADP/ATP carriers, TbMCP5A-C and TbMCP15, most similar to human AAC1 and AAC2, respectively (Table 1). Whether TbMCP16 functions as a third type of ADP/ATP carrier is unclear at this point, as its predicted ADP/ATP transport function is supported by BLASTP analysis, but not phylogenetic reconstruction (Table 1, Fig. 1).

Mitochondrial ATP synthesis from ADP and inorganic phosphate (Pi) requires the replenishment of Pi in the mitochondrial matrix. The *T. b. brucei* MCF protein inventory shows four TbMCPs that could function in this way (Table 1). The first two, TbMCPs 8 and 11, are highly similar to known inorganic phosphate carriers from human (PTP) and yeast (PIC2), which were previously shown to co-transport Pi and protons into the mitochondrial matrix (Palmieri, 2004). The two other putative candidates for mitochondrial Pi import are TbMCP6 and TbMCP12 (Table 1, Fig. 6).

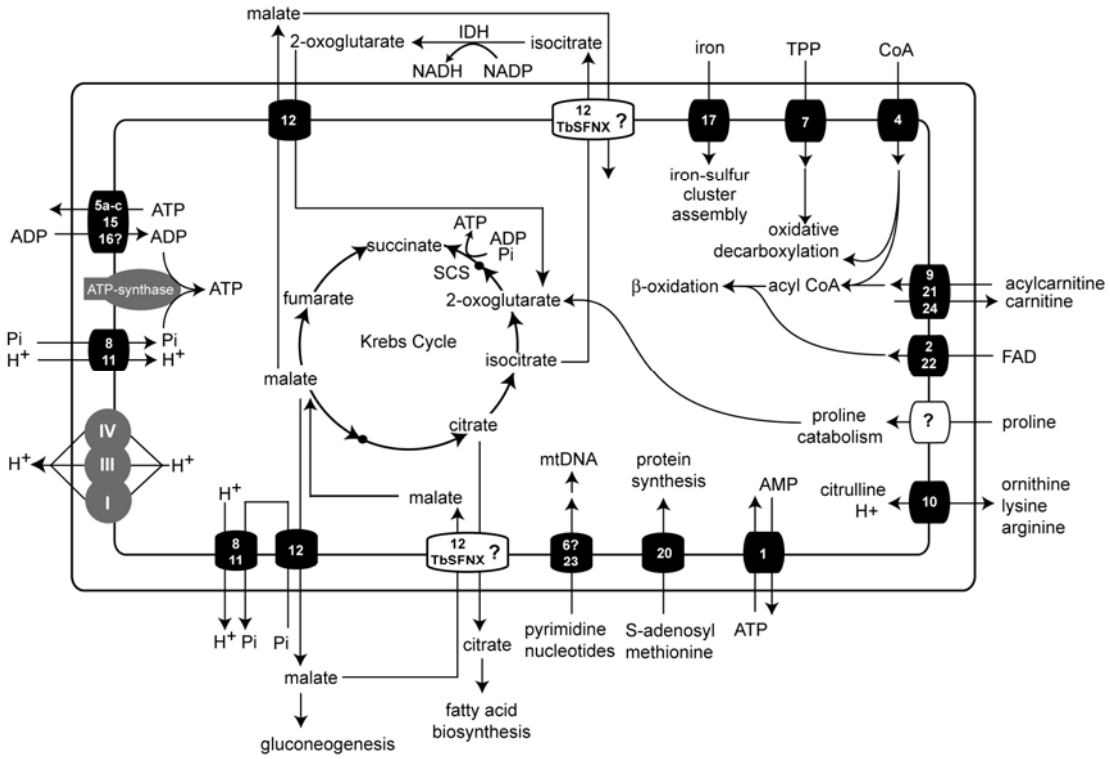

Fig. 6. Schematic representation of predicted TbMCP transport functions in the procyclic-form *T. b. brucei* mitochondrion. Not all relevant mitochondrial metabolic pathways are shown. TbMCPs are represented by black boxes. Respiratory chain complexes are boxed grey. Abbreviations: I/III/IV, complex I/III/IV of the respiratory chain; Pi, inorganic phosphate; mtDNA, mitochondrial DNA; IDH, NADP-dependent isocitrate dehydrogenase; SCS, succinyl-CoA synthetase; ?, transporter unknown.

The closest human homologue of TbMCP6, the ATP-Mg/Pi carrier APC, was previously shown to function in the mitochondrial import of Pi in exchange for ATP-Mg generated in the mitochondrion (Fiermonte *et al.*, 2004). However, transport assays with functionally reconstituted recombinant TbMCP6 failed to reveal any ATP-Mg/Pi carrier function (Colasante *et al.*, 2006). Moreover, depletion of TbMCP6 in procyclic-form *T. b. brucei* inhibited trypanosome growth and replication of the mitochondrial (kinetoplast) DNA, suggesting a possible role of TbMCP6 in mitochondrial nucleotide import (Colasante *et al.*, 2006).

Malate is an important metabolic intermediate in the energy metabolism of procyclic-form *T. b. brucei* (van Weelden *et al.*, 2005; Bringaud *et al.*, 2006). Metabolic studies suggested that malate has to be exported from the mitochondrion for gluconeogenesis purposes or that cytosolic malate, generated in the glysocomes,

has to be imported into the mitochondrion for its subsequent oxidation to succinate (van Weelden *et al.*, 2005; Bringaud *et al.*, 2006). In human cells and yeast, two different MCF proteins were experimentally shown to be involved in malate exchange across the mitochondrial inner membrane: the oxoglutarate carrier, which predominantly exchanges malate for 2-oxoglutarate, and the dicarboxylate carrier, which exchanges malate for an inorganic compound such as inorganic phosphate or sulfates (Palmieri, 2004). Only TbMCP12 grouped with oxoglutarate and dicarboxylate carriers from humans and yeast (Table 1), suggesting a putative role for TbMCP12 in mitochondrial malate/2-oxoglutarate exchange and maybe also in malate/Pi exchange (Fig. 6).

The oxoglutarate carrier has further been proposed to be involved in the maintenance of the cellular redox balance by transferring redox equivalents across the mitochondrial inner membrane as part of the isocitrate/oxoglutarate shuttle (Palmieri, 2004). This shuttle plays an important role in the provision of cytosolic NADPH for biosynthetic purposes, and requires, in addition to the oxoglutarate carrier, the presence of a NADP-dependent cytosolic isocitrate dehydrogenase and a citrate carrier (see Fig. 6). The citrate or tricarboxlate carrier is involved in the exchange of a tricarboxylate (citrate or isocitrate) against either another tricarboxylate, or a dicarboxylate (malate), or phospohoenolpyruvate (Palmieri, 2004). Extensive database searches failed to reveal a tricarboxylate carrier in any of the kinetoplastid genomes analysed. This is unexpected since procyclic-form trypanosomes previously were proposed to be dependent on the export of mitochondrial citrate for cytosolic fatty acid biosynthesis (van Hellemond *et al.*, 2005). It is therefore possible that another TbMCP is capable of transporting tricarboxylates. Recently, a novel di-tricarboxylate carrier protein (DTC), has been reported for *Arabidopsis thaliana* (Picault *et al.*, 2002). DTC showed significant sequence similarity to both di- and tricarboxylate carriers and was shown to be able to transport both di- and tricarboxylates. BLASTP searches using the *A. thaliana* DTC sequence as query against the *T. b. brucei* genome database retrieved TbMCP12 as top hit (48% similarity). Since this is the only putative carboxylate carrier predicted, it is possible that it can transport tricarboxylates. Alternatively, the kinetoplastid mitochondrion may contain another, non-MCF tricarboxylate transporter. The function could be fulfilled by homologues of sideroflexin1 (SFNX1), a mitochondrial membrane protein that previously has been shown to transport citrate (Azzi *et al.*, 1993; Fleming *et al.*, 2000). BLASTP analysis revealed the presence of a SFNX1 homologue in the *T. b. brucei* genome database (not shown).

Another important metabolic function of the mitochondrion is the catabolism of fatty acids via the mitochondrial beta-oxidation pathway. For that purpose, long chain fatty acids have to be imported into the mitochondrion (Kerner and Hoppel, 2000). Prior to mitochondrial import, an acyl-CoA thioester is formed through the activation of the fatty acid by cytosolic coenzyme A (CoA). Next, the acyl-group of this CoA-ester is transferred to carnitine and the resulting acylcarnitine transported across the mitochondrial inner membrane via the acylcarnitine/carnitine carrier in exchange with carnitine (Kerner and Hoppel, 2000; Palmieri, 2004). In the mitochondrial matrix, the acyl group is finally transferred to CoA, and the acyl-CoA formed is degraded via the β-oxidation pathway to short chain fatty acids or acetyl-CoA units. The *T. b. brucei* MCF protein inventory showed three putative acylcarnitine/carnitine carriers, TbMCPs 9, 24 and 21, according to BLASTP similarity searches (Table 1). However, phylogenetic reconstruction suggested that TbMCP9 is evolutionary more related to the human ornithine carrier SLC25A15 then to the human acylcarnitine/carnitine carrier SLC25A5 (Fig. 1). The ornithine carrier plays a central role in the urea cycle, connecting the cytosolic and mitochondrial part of this nitrogen (urea) disposal pathway. Metabolic studies have shown that the ornithine carrier is involved in the exchange of cytosolic ornithine against mitochondrial citrulline, but it can also exchange basic amino acids like lysine or arginine against protons (see (Palmieri, 2004) and references therein). BLASTP similarity searches initially identified TbMCP10 as a putative *T. b. brucei* ornithine carrier (Table 1). Phylogenetic analysis, however, suggested that TbMCP10 is more related to the acylcarnitine/carnitine carriers (Fig. 1). The most probable explanation for this contradiction is that the acylcarnitine/carnitine and ornithine carriers of humans and yeast are evolutionary very closely related, whereas the corresponding TbMCPs are rather divergent, prohibiting a reliable functional assignment by phylogenetic reconstruction.

The *T. b. brucei* mitochondrion contains metabolic pathways requiring specific coenzymes and cofactors. For example, Coenzyme A is needed for the activation of fatty acids in the mitochondrial matrix for β-oxidation (see above) or is used for the preservation of energy in energy-rich compounds like acetyl-CoA and succinyl-CoA and concomitant ATP generation via oxidative decarboxylation and substrate level phosphorylation. The coenzyme thiamine pyrophosphate (TPP) is required for the proper function of several enzymes involved in the oxidative decarboxylation of pyruvate (pyruvate dehydrogenase E1) and alpha-ketoglutarate (alpha-ketoglutarate

dehydrogenase). The cofactor flavin adenine dinucleotide (FAD) fulfills many functions: as a redox carrier in mitochondrial oxidative phosphorylation ($FADH_2$), as a prosthetic group in succinate dehydrogenase and pyruvate dehydrogenase (E3), and as a coenzyme for mitochondrial acyl-CoA dehydrogenase (β-oxidation). All these coenzymes and cofactors have to be imported from the cytosol into the mitochondrion. TbMCPs 2, 4, 7 and 22 are putatively involved in the exchange of mitochondrial coenzymes and cofactors. TbMCP4 and TbMCP7 are highly similar and evolutionary related to the CoA and thiamine pyrophosphate carriers, respectively, suggesting a role of these TbMCPs in mitochondrial coenzyme import (Table 1, Fig. 1). Possible candidates for mitochondrial FAD import are TbMCPs 2 and 22, which are similar to the yeast FAD carrier FLX1 (Table 1, Fig. 1).

In addition to lacking of a prototypical MCF citrate carrier, kinetoplastid genomes seem not to have an identifiable homologue of the uncoupling protein (UCP). UCPs are responsible for the free-fatty-acid-mediated transport of protons across the mitochondrial inner membrane (Echtay *et al.*, 2002; Palmieri, 2004). An influx of protons through UCPs into the mitochondrial matrix dissipates the proton gradient built up by the respiratory chain, and as a result heat is produced. This feature of UCPs was initially thought to be mainly important for non-shivering thermogenesis in newborn, and in cold-acclimated and hibernating, animals (Echtay *et al.*, 2002; Palmieri, 2004). However, UCPs were also found in non-thermogenic tissues of animals (Costford *et al.*, 2007) and more importantly, also in non-mammalian organisms like plants and protozoa (Haferkamp, 2007), suggesting another function for UCPs. More recent experimental evidence suggests that UCPs can modulate the coupling between mitochondrial respiration and ATP synthesis, and are involved in defence against reactive oxygen species (Skulachev, 1996; Sluse and Jarmuszkiewicz, 2002; Sluse *et al.*, 2006): the UCP-mediated influx of protons into the mitochondrion decreases the extent of reduction of the electron carriers, and prevents over-reduction of the respiratory chain; this latter could eventually lead to the formation of reactive oxygen species (ROS) that could damage DNA and proteins in the mitochondrion. The lack of identifiable UCP homologues in the *T. b. brucei*, *T. cruzi* and *Leishmania* genomes, suggests that kinetoplastid parasites must posses an alternative mechanism to avoid the formation of damaging ROS in their mitochondria. Fungi, bacteria, plants and other protozoa contain in addition to UCPs an alternative oxidation system, the alternative oxidase (AOX). This system decreases ROS production by removing the excess of reducing equivalents and transferring them directly to oxygen (Maxwell *et al.*, 1999; Siedow and Umbach,

2000; Jarmuszkiewicz, 2001; Umbach *et al.*, 2005). *T. b. brucei*, *T. cruzi* and *Leishmania* indeed have an AOX, and a role for it in the defence against ROS was proposed (Fang and Beattie, 2003). RNA depletion experiments revealed that AOX is essential for *T. b. brucei* survival (Chaudhuri *et al.*, 2006).

In this chapter an overview is provided of the MCF protein inventory of the early-branching kinetoplastid parasite *T. b. brucei.* Sequence analysis provided insight into the evolution and conservation of these MCF proteins, and resulted in the prediction of putative transport functions for most of the 24 identified TbMCPs. The predicted transport functions will be analysed further by biochemical characterisation including the functional reconstitution of TbMCPs in liposomes and determination of their specific transport function by metabolite transport assays.

4. References

Aquila, H., Link, T. A. & Klingenberg, M. 1987. Solute carriers involved in energy transfer of mitochondria form a homologous protein family. *FEBS Lett,* 212**,** 1-9.

Arner, E., Kindlund, E., Nilsson, D., Farzana, F., Ferella, M., Tammi, M. T. & Andersson, B. 2007. Database of Trypanosoma cruzi repeated genes: 20,000 additional gene variants. *BMC Genomics,* 8**,** 391.

Azzi, A., Glerum, M., Koller, R., Mertens, W. & Spycher, S. 1993. The mitochondrial tricarboxylate carrier. *J Bioenerg Biomembr,* 25**,** 515-24.

Berriman, M., Ghedin, E., Hertz-Fowler, C., Blandin, G., Renauld, H., Bartholomeu, D. C., Lennard, N. J., Caler, E., Hamlin, N. E., Haas, B., Bohme, U., Hannick, L., Aslett, M. A., Shallom, J., Marcello, L., Hou, L., Wickstead, B., Alsmark, U. C., Arrowsmith, C., Atkin, R. J., Barron, A. J., Bringaud, F., Brooks, K., Carrington, M., Cherevach, I., Chillingworth, T. J., Churcher, C., Clark, L. N., Corton, C. H., Cronin, A., Davies, R. M., Doggett, J., Djikeng, A., Feldblyum, T., Field, M. C., Fraser, A., Goodhead, I., Hance, Z., Harper, D., Harris, B. R., Hauser, H., Hostetler, J., Ivens, A., Jagels, K., Johnson, D., Johnson, J., Jones, K., Kerhornou, A. X., Koo, H., Larke, N., Landfear, S., Larkin, C., Leech, V., Line, A., Lord, A., Macleod, A., Mooney, P. J., Moule, S., Martin, D. M., Morgan, G. W., Mungall, K., Norbertczak, H., Ormond, D., Pai, G., Peacock, C. S., Peterson, J., Quail, M. A., Rabbinowitsch, E., Rajandream, M. A., Reitter, C., Salzberg, S. L., Sanders, M., Schobel, S., Sharp, S., Simmonds, M., Simpson, A. J., Tallon, L., Turner, C. M., Tait, A., Tivey, A. R., Van Aken, S., Walker, D., Wanless, D., Wang, S., White, B., White, O., Whitehead, S., Woodward, J., Wortman, J., Adams, M. D., Embley, T. M., Gull, K., Ullu, E., Barry, J. D., Fairlamb, A. H., Opperdoes, F., Barrell, B. G., Donelson, J. E., Hall, N., Fraser, C. M., et al. 2005. The genome of the African trypanosome Trypanosoma brucei. *Science,* 309**,** 416-22.

Bochud-Allemann, N. & Schneider, A. 2002. Mitochondrial substrate level phosphorylation is essential for growth of procyclic Trypanosoma brucei. *J Biol Chem,* 277**,** 32849-54.

Brems, S., Guilbride, D. L., Gundlesdodjir-Planck, D., Busold, C., Luu, V. D., Schanne, M., Hoheisel, J. & Clayton, C. 2005. The transcriptomes of

Trypanosoma brucei Lister 427 and TREU927 bloodstream and procyclic trypomastigotes. *Mol Biochem Parasitol,* 139**,** 163-72.

Bringaud, F., Riviere, L. & Coustou, V. 2006. Energy metabolism of trypanosomatids: adaptation to available carbon sources. *Mol Biochem Parasitol,* 149**,** 1-9.

Chaudhuri, M., Ott, R. D. & Hill, G. C. 2006. Trypanosome alternative oxidase: from molecule to function. *Trends Parasitol,* 22**,** 484-91.

Colasante, C., Alibu, V. P., Kirchberger, S., Tjaden, J., Clayton, C. & Voncken, F. 2006. Characterization and developmentally regulated localization of the mitochondrial carrier protein homologue MCP6 from Trypanosoma brucei. *Eukaryot Cell,* 5**,** 1194-205.

Costford, S., Gowing, A. & Harper, M. E. 2007. Mitochondrial uncoupling as a target in the treatment of obesity. *Curr Opin Clin Nutr Metab Care,* 10**,** 671-8.

Derelle, E., Ferraz, C., Rombauts, S., Rouze, P., Worden, A. Z., Robbens, S., Partensky, F., Degroeve, S., Echeynie, S., Cooke, R., Saeys, Y., Wuyts, J., Jabbari, K., Bowler, C., Panaud, O., Piegu, B., Ball, S. G., Ral, J. P., Bouget, F. Y., Piganeau, G., De Baets, B., Picard, A., Delseny, M., Demaille, J., Van de Peer, Y. & Moreau, H. 2006. Genome analysis of the smallest free-living eukaryote Ostreococcus tauri unveils many unique features. *Proc Natl Acad Sci U S A,* 103**,** 11647-52.

Echtay, K. S., Roussel, D., St-Pierre, J., Jekabsons, M. B., Cadenas, S., Stuart, J. A., Harper, J. A., Roebuck, S. J., Morrison, A., Pickering, S., Clapham, J. C. & Brand, M. D. 2002. Superoxide activates mitochondrial uncoupling proteins. *Nature,* 415**,** 96-9.

El-Sayed, N. M., Myler, P. J., Bartholomeu, D. C., Nilsson, D., Aggarwal, G., Tran, A. N., Ghedin, E., Worthey, E. A., Delcher, A. L., Blandin, G., Westenberger, S. J., Caler, E., Cerqueira, G. C., Branche, C., Haas, B., Anupama, A., Arner, E., Aslund, L., Attipoe, P., Bontempi, E., Bringaud, F., Burton, P., Cadag, E., Campbell, D. A., Carrington, M., Crabtree, J., Darban, H., da Silveira, J. F., de Jong, P., Edwards, K., Englund, P. T., Fazelina, G., Feldblyum, T., Ferella, M., Frasch, A. C., Gull, K., Horn, D., Hou, L., Huang, Y., Kindlund, E., Klingbeil, M., Kluge, S., Koo, H., Lacerda, D., Levin, M. J., Lorenzi, H., Louie, T., Machado, C. R., McCulloch, R., McKenna, A., Mizuno, Y., Mottram, J. C., Nelson, S., Ochaya, S., Osoegawa, K., Pai, G., Parsons, M., Pentony, M., Pettersson, U., Pop, M., Ramirez, J. L., Rinta, J., Robertson, L., Salzberg, S. L., Sanchez, D. O., Seyler, A., Sharma, R., Shetty, J., Simpson, A. J., Sisk, E., Tammi, M. T., Tarleton, R., Teixeira, S.,

Van Aken, S., Vogt, C., Ward, P. N., Wickstead, B., Wortman, J., White, O., Fraser, C. M., Stuart, K. D. & Andersson, B. 2005. The genome sequence of Trypanosoma cruzi, etiologic agent of Chagas disease. *Science,* 309**,** 409-15.

Fang, J. & Beattie, D. S. 2003. Alternative oxidase present in procyclic Trypanosoma brucei may act to lower the mitochondrial production of superoxide. *Arch Biochem Biophys,* 414**,** 294-302.

Fiermonte, G., De Leonardis, F., Todisco, S., Palmieri, L., Lasorsa, F. M. & Palmieri, F. 2004. Identification of the mitochondrial ATP-Mg/Pi transporter. Bacterial expression, reconstitution, functional characterization, and tissue distribution. *J Biol Chem,* 279**,** 30722-30.

Fiermonte, G., Runswick, M. J., Walker, J. E. & Palmieri, F. 1992. Sequence and pattern of expression of a bovine homologue of a human mitochondrial transport protein associated with Grave's disease. *DNA Seq,* 3**,** 71-8.

Fleming, R. E., Migas, M. C., Holden, C. C., Waheed, A., Britton, R. S., Tomatsu, S., Bacon, B. R. & Sly, W. S. 2000. Transferrin receptor 2: continued expression in mouse liver in the face of iron overload and in hereditary hemochromatosis. *Proc Natl Acad Sci U S A,* 97**,** 2214-9.

Haferkamp, I. 2007. The diverse members of the mitochondrial carrier family in plants. *FEBS Lett,* 581**,** 2375-9.

Ivens, A. C., Peacock, C. S., Worthey, E. A., Murphy, L., Aggarwal, G., Berriman, M., Sisk, E., Rajandream, M. A., Adlem, E., Aert, R., Anupama, A., Apostolou, Z., Attipoe, P., Bason, N., Bauser, C., Beck, A., Beverley, S. M., Bianchettin, G., Borzym, K., Bothe, G., Bruschi, C. V., Collins, M., Cadag, E., Ciarloni, L., Clayton, C., Coulson, R. M., Cronin, A., Cruz, A. K., Davies, R. M., De Gaudenzi, J., Dobson, D. E., Duesterhoeft, A., Fazelina, G., Fosker, N., Frasch, A. C., Fraser, A., Fuchs, M., Gabel, C., Goble, A., Goffeau, A., Harris, D., Hertz-Fowler, C., Hilbert, H., Horn, D., Huang, Y., Klages, S., Knights, A., Kube, M., Larke, N., Litvin, L., Lord, A., Louie, T., Marra, M., Masuy, D., Matthews, K., Michaeli, S., Mottram, J. C., Muller-Auer, S., Munden, H., Nelson, S., Norbertczak, H., Oliver, K., O'Neil, S., Pentony, M., Pohl, T. M., Price, C., Purnelle, B., Quail, M. A., Rabbinowitsch, E., Reinhardt, R., Rieger, M., Rinta, J., Robben, J., Robertson, L., Ruiz, J. C., Rutter, S., Saunders, D., Schafer, M., Schein, J., Schwartz, D. C., Seeger, K., Seyler, A., Sharp, S., Shin, H., Sivam, D., Squares, R., Squares, S., Tosato, V., Vogt, C., Volckaert, G., Wambutt, R., Warren, T., Wedler, H., Woodward, J., Zhou, S., Zimmermann, W., Smith, D. F., Blackwell, J. M.,

Stuart, K. D., Barrell, B., et al. 2005. The genome of the kinetoplastid parasite, Leishmania major. *Science,* 309**,** 436-42.

Jarmuszkiewicz, W. 2001. Uncoupling proteins in mitochondria of plants and some microorganisms. *Acta Biochim Pol,* 48**,** 145-55.

Johnston, J. M., Khalid, S. & Sansom, M. S. 2008. Conformational dynamics of the mitochondrial ADP/ATP carrier: a simulation study. *Mol Membr Biol***,** 1-12.

Kerner, J. & Hoppel, C. 2000. Fatty acid import into mitochondria. *Biochim Biophys Acta,* 1486**,** 1-17.

Klingenberg, M. 2008. The ADP and ATP transport in mitochondria and its carrier. *Biochim Biophys Acta,* 1778**,** 1978-2021.

Kunji, E. R. & Robinson, A. J. 2006. The conserved substrate binding site of mitochondrial carriers. *Biochim Biophys Acta,* 1757**,** 1237-48.

Maxwell, D. P., Wang, Y. & McIntosh, L. 1999. The alternative oxidase lowers mitochondrial reactive oxygen production in plant cells. *Proc Natl Acad Sci U S A,* 96**,** 8271-6.

Melville, S. E., Leech, V., Navarro, M. & Cross, G. A. 2000. The molecular karyotype of the megabase chromosomes of Trypanosoma brucei stock 427. *Mol Biochem Parasitol,* 111**,** 261-73.

Michaeli, S., Podell, D., Agabian, N. & Ullu, E. 1992. The 7SL RNA homologue of Trypanosoma brucei is closely related to mammalian 7SL RNA. *Mol Biochem Parasitol,* 51**,** 55-64.

Millar, A. H. & Heazlewood, J. L. 2003. Genomic and proteomic analysis of mitochondrial carrier proteins in Arabidopsis. *Plant Physiol,* 131**,** 443-53.

Nakagawa, T., Imanaka, T., Morita, M., Ishiguro, K., Yurimoto, H., Yamashita, A., Kato, N. & Sakai, Y. 2000. Peroxisomal membrane protein Pmp47 is essential in the metabolism of middle-chain fatty acid in yeast peroxisomes and Is associated with peroxisome proliferation. *J Biol Chem,* 275**,** 3455-61.

Nury, H., Dahout-Gonzalez, C., Trezeguet, V., Lauquin, G. J., Brandolin, G. & Pebay-Peyroula, E. 2006. Relations between structure and function of the mitochondrial ADP/ATP carrier. *Annu Rev Biochem,* 75**,** 713-41.

Palmieri, F. 2004. The mitochondrial transporter family (SLC25): physiological and pathological implications. *Pflugers Arch,* 447**,** 689-709.

Palmieri, F., Agrimi, G., Blanco, E., Castegna, A., Di Noia, M. A., Iacobazzi, V., Lasorsa, F. M., Marobbio, C. M., Palmieri, L., Scarcia, P., Todisco, S., Vozza, A. & Walker, J. 2006. Identification of mitochondrial carriers in Saccharomyces cerevisiae by transport assay of reconstituted recombinant proteins. *Biochim Biophys Acta,* 1757**,** 1249-62.

Palmieri, L., Rottensteiner, H., Girzalsky, W., Scarcia, P., Palmieri, F. & Erdmann, R. 2001. Identification and functional reconstitution of the yeast peroxisomal adenine nucleotide transporter. *Embo J,* 20**,** 5049-59.

Pebay-Peyroula, E., Dahout-Gonzalez, C., Kahn, R., Trezeguet, V., Lauquin, G. J. & Brandolin, G. 2003. Structure of mitochondrial ADP/ATP carrier in complex with carboxyatractyloside. *Nature,* 426**,** 39-44.

Picault, N., Hodges, M., Palmieri, L. & Palmieri, F. 2004. The growing family of mitochondrial carriers in Arabidopsis. *Trends Plant Sci,* 9**,** 138-46.

Picault, N., Palmieri, L., Pisano, I., Hodges, M. & Palmieri, F. 2002. Identification of a novel transporter for dicarboxylates and tricarboxylates in plant mitochondria: bacterial expression, reconstitution, functional characterization and tissue distribution. *J Biol Chem,* 26**,** 26.

Prohl, C., Pelzer, W., Diekert, K., Kmita, H., Bedekovics, T., Kispal, G. & Lill, R. 2001. The yeast mitochondrial carrier Leu5p and its human homologue Graves' disease protein are required for accumulation of coenzyme A in the matrix. *Mol Cell Biol,* 21**,** 1089-97.

Robinson, A. J. & Kunji, E. R. 2006. Mitochondrial carriers in the cytoplasmic state have a common substrate binding site. *Proc Natl Acad Sci U S A,* 103**,** 2617-22.

Saraste, M. & Walker, J. E. 1982. Internal sequence repeats and the path of polypeptide in mitochondrial ADP/ATP translocase. *FEBS Lett,* 144**,** 250-4.

Satre, M., Mattei, S., Aubry, L., Gaudet, P., Pelosi, L., Brandolin, G. & Klein, G. 2007. Mitochondrial carrier family: repertoire and peculiarities of the cellular slime mould Dictyostelium discoideum. *Biochimie,* 89**,** 1058-69.

Schneider, A., Bouzaidi-Tiali, N., Chanez, A. L. & Bulliard, L. 2007. ATP production in isolated mitochondria of procyclic Trypanosoma brucei. *Methods Mol Biol,* 372**,** 379-87.

Siedow, J. N. & Umbach, A. L. 2000. The mitochondrial cyanide-resistant oxidase: structural conservation amid regulatory diversity. *Biochim Biophys Acta,* 1459**,** 432-9.

Skulachev, V. P. 1996. Role of uncoupled and non-coupled oxidations in maintenance of safely low levels of oxygen and its one-electron reductants. *Q Rev Biophys,* 29**,** 169-202.

Sluse, F. E. & Jarmuszkiewicz, W. 2002. Uncoupling proteins outside the animal and plant kingdoms: functional and evolutionary aspects. *FEBS Lett,* 510**,** 117-20.

Sluse, F. E., Jarmuszkiewicz, W., Navet, R., Douette, P., Mathy, G. & Sluse-Goffart, C. M. 2006. Mitochondrial UCPs: new insights into regulation and impact. *Biochim Biophys Acta,* 1757**,** 480-5.

Umbach, A. L., Fiorani, F. & Siedow, J. N. 2005. Characterization of transformed Arabidopsis with altered alternative oxidase levels and analysis of effects on reactive oxygen species in tissue. *Plant Physiol,* 139**,** 1806-20.

van Hellemond, J. J., Opperdoes, F. R. & Tielens, A. G. 2005. The extraordinary mitochondrion and unusual citric acid cycle in Trypanosoma brucei. *Biochem Soc Trans,* 33**,** 967-71.

van Roermund, C. W., Drissen, R., van Den Berg, M., Ijlst, L., Hettema, E. H., Tabak, H. F., Waterham, H. R. & Wanders, R. J. 2001. Identification of a peroxisomal ATP carrier required for medium-chain fatty acid beta-oxidation and normal peroxisome proliferation in Saccharomyces cerevisiae. *Mol Cell Biol,* 21**,** 4321-9.

van Weelden, S. W., van Hellemond, J. J., Opperdoes, F. R. & Tielens, A. G. 2005. New functions for parts of the Krebs cycle in procyclic Trypanosoma brucei, a cycle not operating as a cycle. *J Biol Chem,* 280**,** 12451-60.

Walters, D. E. & Kaplan, R. S. 2004. Homology-modeled structure of the yeast mitochondrial citrate transport protein. *Biophys J,* 87**,** 907-11.

Wohlrab, H. 2006. The human mitochondrial transport/carrier protein family. Nonsynonymous single nucleotide polymorphisms (nsSNPs) and mutations that lead to human diseases. *Biochim Biophys Acta,* 1757**,** 1263-70.

Yohannan, S., Yang, D., Faham, S., Boulting, G., Whitelegge, J. & Bowie, J. U. 2004. Proline substitutions are not easily accommodated in a membrane protein. *J Mol Biol,* 341**,** 1-6.

Chapter IV.
Identification and Functional Characterization of MCP5

Table of Contents

Chapter IV . Identification and Functional characterization of MCP5

1. Introduction

Reciprocal BLASTP analysis resulted in the identification of 26 *T. brucei* genes, coding for 24 different putative proteins with significant sequence similarities to known MCF proteins from higher eukaryotes (Chapter III). Aim of this chapter is the functional characterisation of MCP5, the most conserved member of the *T. brucei* MCF protein inventory, with 78% amino acid similarity to the *S. cerevisiae* ADP/ATP carrier ANT2 and 69% similarity to the human ADP/ATP carrier SLC25A4 (AAC1). MCP5 is the only *T. brucei* MCF protein that is present in more than one genomic copy, i.e. MCP5A, MCP5B and MCP5C, respectively (Colasante *et al.*, 2009). The in chapter III predicted ADP/ATP exchange function of MCP5 was further assessed at the sequence level by a more in-depth analysis of its specific substrate-binding amino acid residues and the identification of other sequence motifs that are conserved in all functionally characterised ADP/ATP carriers. Also the evolutionary relationship of MCP5 to known ADP/ATP carriers from other eukaryotes was further investigated by phylogenetic reconstruction. The presence of a specific gene in a genome does not automatically implicate that this gene indeed is expressed. Expression of MCP5 was analysed in the two different life-cycle stages of *T. brucei*, i.e. the bloodstream-form and the procyclic-form, at both the RNA (northern blotting) and protein level (western blotting). Majority of the MCF proteins found in other eukaryotes are mitochondrial, although some of them are located in other organelles (Palmieri *et al.*, 2001; Colasante *et al.*, 2006). The subcellular localisation of MCP5 in the different life-cycle stages of *T. brucei* was determined by immunofluorescence microscopy. To assess the physiological role(s) of this putative ADP/ATP carrier in the *T. brucei* energy metabolism, a stable MCP5 knockout cell lines were generated. These cell lines were further analyzed regarding their substrate consumption and metabolic end product formation, and their ability to exchange ATP and ADP at the mitochondrial level.

2. Results and Discussion

2.1. Sequence analysis and phylogenetic reconstruction of *T. brucei* MCP5

Next to the observed sequence similarities to prototypical MCF proteins, MCP5 also contained all of the conserved sequence features characteristic for MCF proteins, including the multiple presence of the conserved signature sequence $Px(D/E)x_2(K/R)x(K/R)x_{20-30}(D/E)Gx_{4-5}(W/F/Y)(K/R)G$ (with x representing any amino

acid; Figures 1 and 2), which is the hallmark of MCF proteins (Aquila *et al.*, 1987; Saraste and Walker, 1982). The first half of this signature sequence can be found at the end of each odd-numbered trans-membrane helix, whereas the second half is located 20-30 amino acid residues downstream of the amphipathic helices that intercalate between trans-membrane helices H1/H2, H3/H4, and H5/H6 (Colasante *et al.*, 2009). Another conserved sequence motif, which is only found in ADP/ATP carriers, is the "RRRMMM" sequence located at the end of the 5th transmembrane domain (Müller *et al.*, 1996; Adrian *et al.*, 1986). The presence of this motif in MCP5 is a strong indication that this MCF protein functions as an ADP/ATP carrier.

Sequence alignment of MCP5 with other known AACs, including those of the related kinetoplastids *T. cruzi* and *Leishmania*, and prototypical MCF protein representatives from other eukaryotic classes, i.e. yeasts, plants, arthropods, fish, amphibians and mammals, revealed significant sequence similarities with values ranging between 64-78% for ADP/ATP carriers from human and yeast (Colasante *et al.*, 2009).

Recent studies proposed a number of conserved amino acid residues in MCF proteins that are essential for the binding of specific substrates. These conserved residues have been called substrate "contact points" accordingly (Colasante *et al.*, 2009). In MCF proteins, three different contact points (I-III) have been predicted from crystallographic and modelling studies of natural and mutant MCF proteins during substrate binding (Robinson and Kunji, 2006).

The first set of amino acids involved in substrate binding, called "contact point I", is found at the end of the first signature sequence, and is represented by an arginine (R), threonine (T) and asparagine (N) residue (Figure 2). Mutation analysis of yeast AAC2 indicated that the conserved amino acid residues in contact point I are essential for transport function. In particular the mutation of the positively charged amino acid residue R96 in yeast AAC2, rendered this ADP/ATP carrier incapable of performing ADP/ATP exchange (Müller *et al.*, 1996). The second set of amino acids involved in substrate binding, called "contact point II", is found at the end of the second signature sequence, and is represented by a glycine (G182 in yeast AAC2) and an isoleucine (I183 in yeast AAC2). These amino acids were previously shown to be required for transport activity in other MCF proteins such as the oxoglutarate carrier (OGC) and the uncoupling protein (UCP), but are also conserved in ADP/ATP carriers (Robinson and Kunji, 2006).

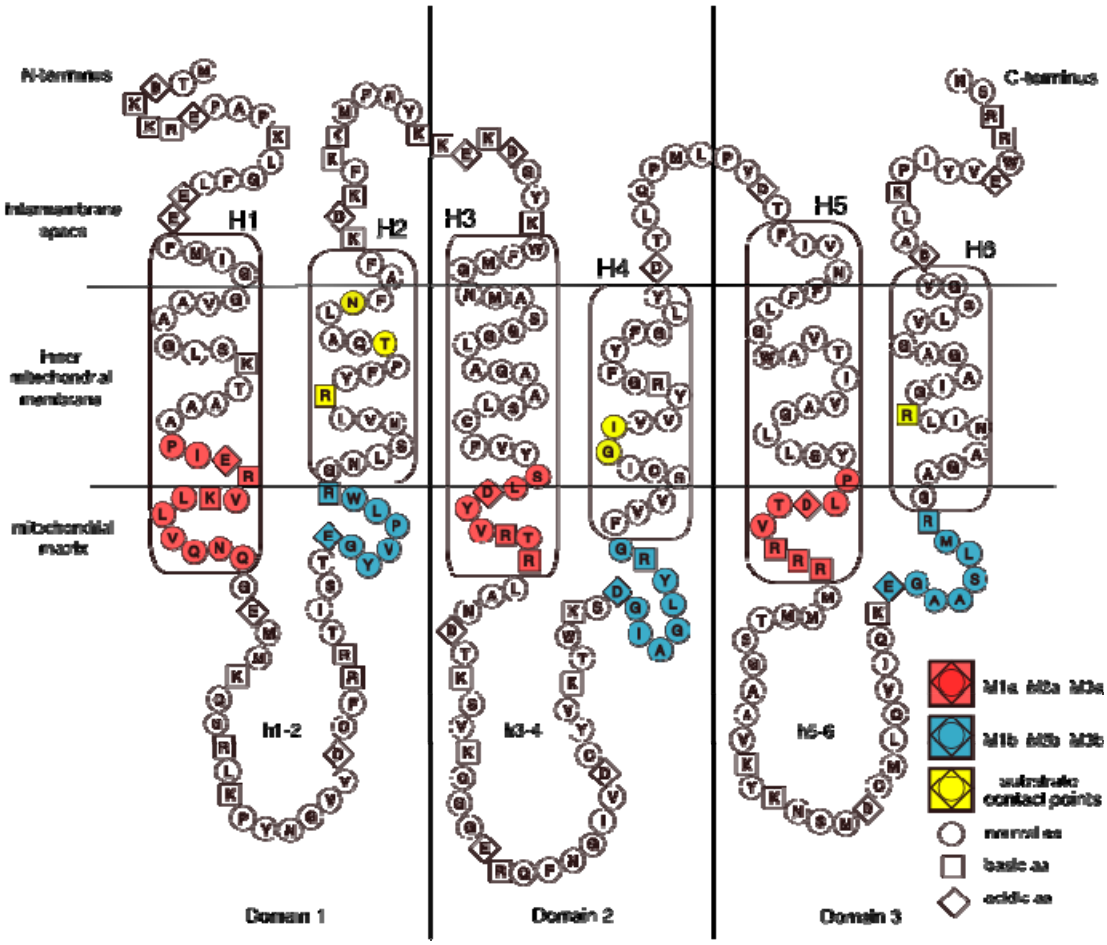

Figure 1. Schematic representation of MCP5 showing the conserved sequence structure of MCF proteins. Transmembrane helices are shown as H1-H6. The first half of the signature sequence, found at the end of the odd numbered transmembrane helices, is indicated with M1a, M2a and M3a, and its amino acid residues are shown red. The second half of the signature sequence, found at the end of the odd numbered transmembrane helices, is indicated with M1b, M2b and M3b, and its amino acid residues are shown in blue. The amphipatic helices, which separate the two halves of each signature sequence, are indicated as h1-2, h3-4, and h5-6, respectively. Contact points are shown in yellow. Both the N- and C-terminal ends of MCP5 are facing the mitochondrial intermembrane space.

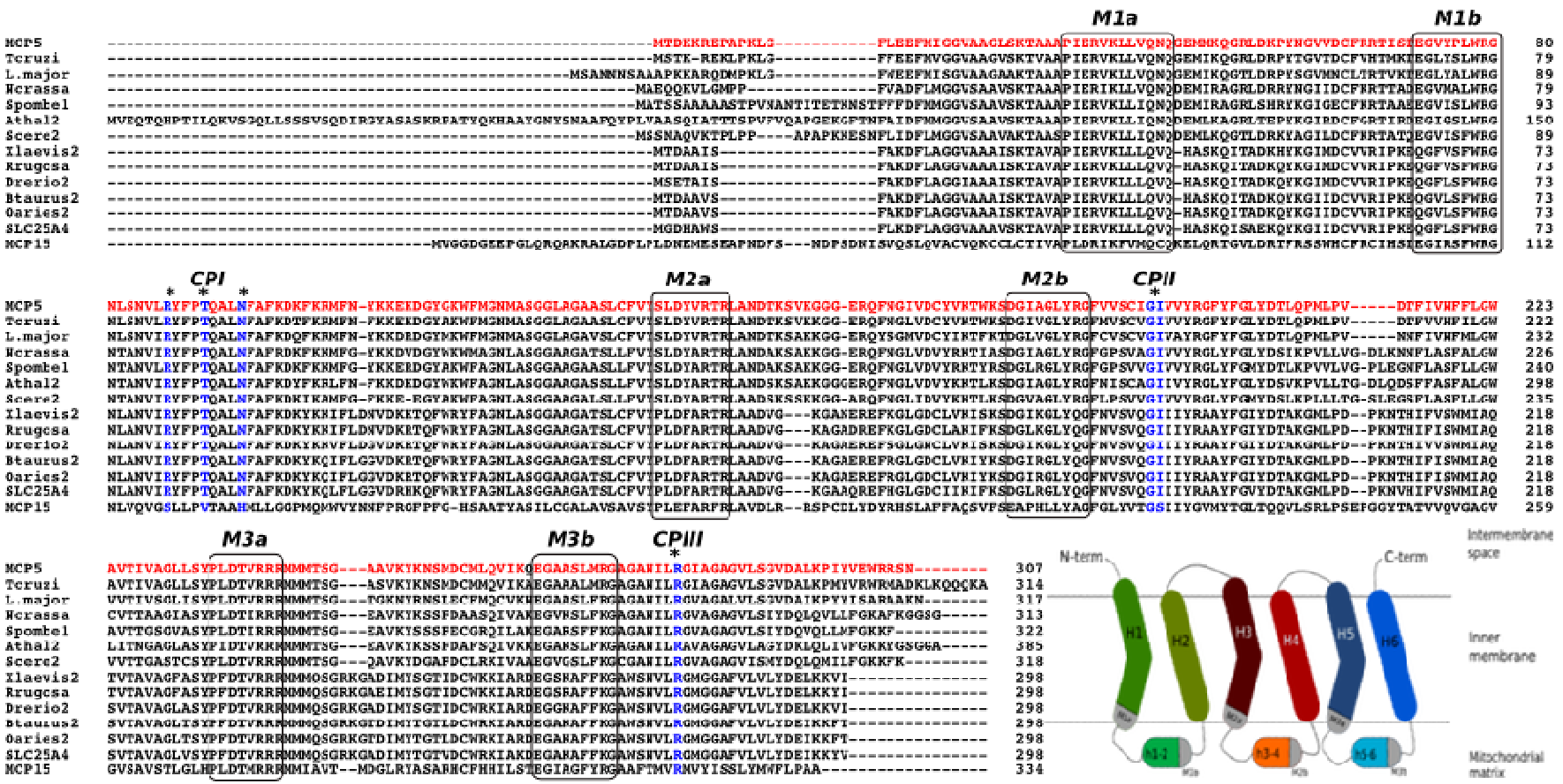

Figure 2. Sequence alignment and conserved MCF sequence features of MCP5 and selected ADP/ATP carriers from other eukaryotes. The different halves of the conserved signature sequences M(1-3)a and M(1-3)b are indicated (in rectangles). The conserved amino acids in contact points I, II and III are shown in blue. Amphipatic helices, are indicated as h1-2, h3-4, and h5-6.

Contact point III is represented by a single conserved amino acid, i.e. an arginine (R), which is conserved in all ADP/ATP carriers. This positively charged amino acid residue has been studied in yeast AAC2 by changing it to an alanine (R294A). This mutation affected the OXPHOS dramatically, and resulted in low ADP/ATP exchange activity as well as a changed exchange mode in the isolated carrier (Müller *et al.*, 1996; Heidkamper *et al.*, 1996). All “contact point” residues required for substrate binding and ADP/ATP exchange are conserved in MCP5, and strengthens the assumption that MCP5 functions as an ADP/ATP carrier.

Phylogenetic reconstruction was used as a complementary approach for the prediction of transport function. Previously published sequence and phylogenetic analyses revealed that the MCP5 sequence is highly similar to and forms a reliable (supported by high bootstrap values) phylogenetic distinct group with the human ADP/ATP carrier SLC25A4 (see Introduction; Colasante *et al.*, 2009). Here we performed a more in-depth phylogenetic analysis by also including ADP/ATP carriers from related kinetoplastids and representative ADP/ATP carrier sequences from other eukaryotes, i.e. those from yeasts, plants, arthropods, fish, and amphibians. The resulting neighbor-joining tree is shown in Figure 3. MCP5 specifically clustered with putative MCF proteins from *Trypanosoma cruzi* and different *Leishmania species*, suggesting a common origin for the kinetoplastid metabolite transporters.

Another interesting observation is the apparent separation of the ADP/ATP carriers in two predominant clades (Figure 3). The first clade includes the AACs from yeast and plants, whereas the second contains all other metazoan AACs. A similar distribution of AACs in at least two distinct clades has previously been published (Löytynoja and Milinkovitch, 2001). The kinetoplastid AACs clustered specifically with AACs found in the first clade, suggesting a common origin with those from yeast and plants. Such phylogenetic relationship, especially with plant sequences, has previously been observed for other *T. brucei* proteins. It has been proposed that kinetoplastids evolved via a temporary symbiotic association with a photosynthetic microorganism, which resulted in the acquisition (horizontal transfer) of several plant-related genes (Michels and Opperdoes, 1991; Hannaert *et al.*, 2003a; Hannaert *et al.*, 2003b).

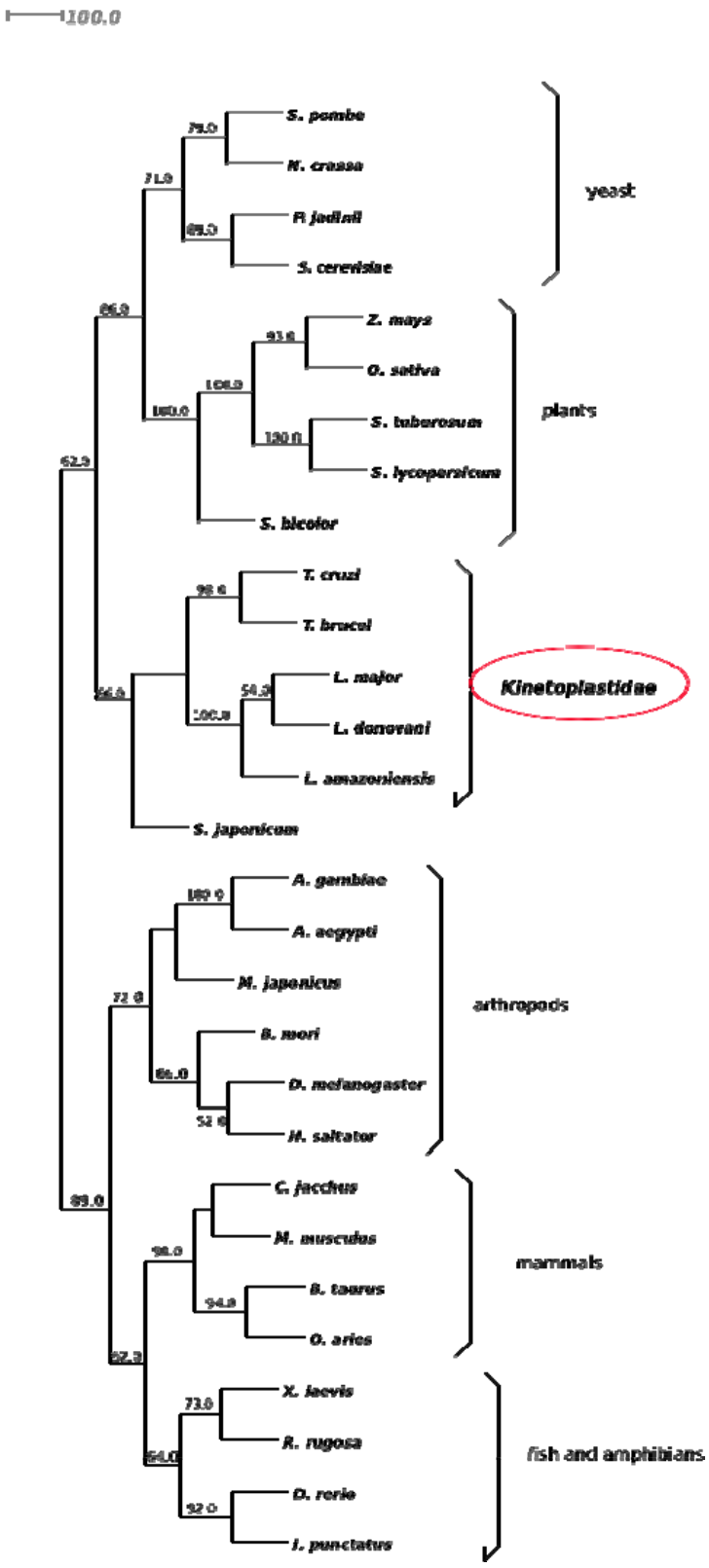

Figure 3. Neighbour-joining consensus tree including MCP5 and representative AAC sequences from yeast, plants, arthropods, mammals, fish and amphibians. Only bootstraps values higher then 50 are shown at each node. This NJ consensus tree was constructed using the Protdist and Neighbour-Joining programs available on Mobyle@Pasteur, and edited using Splitstree4.

MCP5 is the only identified MCF protein that is present in more than one gene copy in the genome of *T. brucei* (Colasante *et al.*, 2009). Genome sequence analysis indicated 3 identical, in tandem-arranged MCP5-encoding genes in the *T. brucei* genome: annotated as MCP5a, 5b and 5c, respectively. Next to MCP5a-c, two other MCF proteins were identified with significant sequence similarity to prototypical ADP/ATP carriers, i.e. MCP15 and MCP16. Their sequence similarities to known AACs are however much lower than those found for MCP5 (Colasante *et al.* 2009). Phylogentic analysis and sequence comparison revealed that MCP5 is more similar to MCP15 than to MCP16 (Colasante *et al.* 2009). The presence of multiple putative AAC-encoding genes in *T. brucei* is not unexpected. Virtually all eukaryotes contain multiple genes coding for ADP/ATP carriers (AACs). For example, the unicellular yeast *S. cerevisiae* genome contains 3 similar (but non-identical) genes coding for different ADP/ATP carrier isoforms, i.e. AAC1, AAC2 and AAC3 (Adrian *et al.*, 1986; Kolarov *et al.*, 1990). Functional studies and mutation analysis revealed that these ADP/ATP carriers play different physiological roles in *S. cerevisiae* (Lawson *et al.*, 1990; Gawaz *et al.*, 1990; Kolarov *et al.*, 1990; Drgon *et al.*, 1991). Also in multicellular eukaryotes, like mammals and humans, multiple non-identical AAC-encoding genes are found whose expression can be tissue-specific and their physiological function is location-dependent (Powell *et al.*, 1989). The divergence of AACs into multiple tissue-dependent isoforms is most probably a direct consequence of the evolution to multicellular life forms (Löytynoja and Milinkovitch, 2001).

2.2. Expression of MCP5 in procyclic form *Trypanosoma brucei*

MCP5 peptide antibodies were raised to facilitate subsequent expression (western blotting) and immunolocalisation studies. The amino acid sequences for the two peptides used for immunisation are derived from the respective N-terminal (N-term) and C-terminal (C-term) ends of MCP5 (Figure 4). Peptide synthesis and the subsequent immunisations in rabbits were performed by EZBiolab (www.ezbiolab.com).

Figure 4. Amino (N)-terminal and carboxy (C)-terminal MCP5 peptide-sequences (boxed red) used for the immunisation of rabbits.

The suitability of the raised polyclonal rabbit antisera was tested on whole lysates of procyclic form *T. brucei* 449 (PCF449). The western blotting results are shown in Figure 5. The antiserum directed against the N-term peptide was found to be very specific and detected only a single protein band with an approximate molecular weight of 32 kDa (Figure 5, lane 1). The observed molecular weight is agreement with the calculated weight of MCP5, i.e. 34 kDa. For the C-term peptide antiserum, a second high molecular weight band was found, which is regarded as a non-specific cross-reaction of this antiserum (Figure 5, lane 2). The obtained results indicated that in particular the N-term peptide antiserum is suitable for the subsequent detection of MCP5. Control experiments with the different pre-immune sera did not show any detectable bands after western blotting (results not shown), emphasising the specificity of the raised antisera.

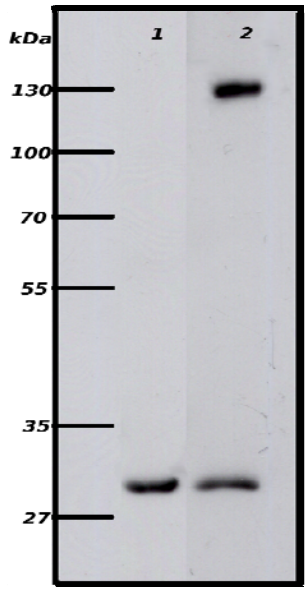

Figure 5. Western blot analysis of *T. brucei* PCF449 using MCP5 N-term (lane 1) and C-term (lane 2) antibodies.

The raised N-term peptide antiserum was subsequently used to determine the MCP5 expression (protein) levels in the two different life cycle stages of the parasite, i.e. PCF449 and bloodstream form (BSF449) *T. brucei*. The western blotting results shown in Figure 6A revealed that MCP5: (1) is also expressed in BSF449, and (2) is about 4 times more abundant in PCF449 then in BSF449.

The expression of MCP5 at the mRNA level was assessed by northern blot analysis. For both PC449 and BS449 *T. brucei*, a single cross-reacting mRNA band was found after hybridisation with the MCP5 DNA probe (Figure 6B).

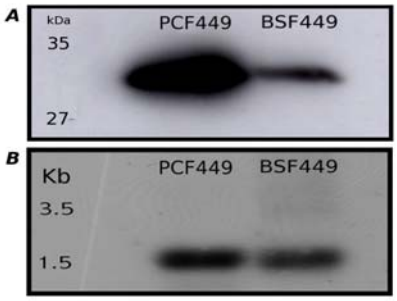

Figure 6. Analysis of MCP5 expression at the protein (A) and mRNA (B) level in PCF449 and BSF449 *T. brucei*. (A) For western blot analysis, $2x10^6$ *T. brucei* cells were loaded per well, and MCP5 was detected with the raised N-term peptide antibody (1:1000 dilution). (B) For northern blot analysis, 10μg of total RNA was loaded per well and hybridised with the full-length MCP5 DNA sequence as probe.

The size of this cross-reacting mRNA is approximately 1.5 kilobases (kb), which is in agreement with (i.e. larger than) the expected minimum MCP5 mRNA size of 0.9 kb plus additional 5' and 3' untranslated (UTR) mRNA regions. Quantification revealed that the MCP5 mRNA is only slightly more abundant, approximately 1.2 times, in PCF449 when compared to BSF449. This is in agreement with previously published MCP5 mRNA quantification data showing similar minor differences in the BSF449 and PCF449 mRNA expression profiles (Chapter 3, Table 3: Colasante *et al.*, 2009).

Comparison of the obtained MCP5 expression data revealed a significant inconsistency between MCP5-expression at the mRNA (1.2 times) level and the expression of this protein at the protein (4 times) level. In contrast to most eukaryotes, trypanosome transcription is polycistronic, with expression control taking place at the posttranscriptional level (Imboden *et al.*, 1987; Ben Amar *et al.*, 1988; Gibson *et al.*, 1988). As a consequence, differences in transcription levels do not necessarily correlate to differences in correspondingly translated protein.

The observed differences in MCP5 expression between BSF449 and PCF449 is further indicative for the substantial differences in mitochondrial ATP production in the two *T. brucei* life cycle stages. In BSF449 *T. brucei*, majority of the ATP is produced via glycolysis, with little or none mitochondrial ATP production, while in the PC449 most of the cellular ATP is produced in the mitochondrion (Tielens and Van

Hellemond, 1998; Hannaert *et al.*, 2003a; Chaudhuri *et al.*, 2006; Michels *et al.*, 2006; Tielens and van Hellemond, 2009). Accordingly, more MCP5 is required in the procyclic-form mitochondrion in order to facility its substantial ADP/ATP exchange, and making mitochondria-produced ATP available to the rest of the cell. Why BSF449 mitochondria do require MCP5 at all, is unclear at this point. One possible explanation could be that the apparent "non-functional" mitochondria in bloodstream-form trypanosomes (see Section 4, Introduction) still require minimal levels of ATP for the maintenance of its proton motive force (pmf), which again is essential for the conservation of the mitochondrial integrity. The most important facilitator of the mitochondrial pmf is the F_0F_1-ATPase found in the mitochondrial inner membrane. RNAi-directed depletion of this F_0F_1-ATPase in BSF449 resulted in cell death (Zíková *et al.*, 2009). This result indicates an important role of the F_0F_1-ATPase in bloodstream-form mitochondria, most probably via the generation of an essential pmf and the concomitant consumption of mitochondrial ATP, which needs to be replenished with cytosolic ATP by an ADP/ATP carrier, here MCP5.

2.3. Subcellular localization of MCP5

Virtually all MCF proteins characterised so far are mitochondrial, although some of them have been discovered in other cellular compartments, which are different from the mitochondrion. For example, Ant1p of yeast has been found exclusively in peroxisomes, although it displays all conserved sequence features of a true "mitochondrial" MCF protein (Palmieri *et al.*, 2001; Lasorsa *et al.*, 2004). Ant1p was found to transport ATP into the peroxisomal matrix in exchange for cytosolic AMP, and is suggested to play a key role in peroxisomal lipid biosynthesis (van Roermund *et al.*, 2001; Palmieri *et al.*, 2001). MCP6, a recently identified putative ATP-Mg^{2+}-Pi carrier of *T. brucei*, showed an even more complex subcellular distribution: in the bloodstream form of *T. brucei* it was found predominantly in the glycosome (i.e. peroxisome), whereas in the procyclic form of the parasite it displayed a predominantly mitochondrial localization (Colasante *et al.*, 2006). It is evident from the above-mentioned examples that the apparent mitochondrial localisation of MCF proteins has to be determined experimentally for each of them.

The subcellular localisation of MCP5 was initially determined by immunofluorescence microscopy in a PCF449 *MCP5-nmyc*^{ti} cell line, which had been obtained after transfection of PCF449 *T. brucei* with the plasmid pHD1701-MCP5. The resulting cell line PCF449 *MCP5-nmyc*^{ti} allows the inducible expression

of a recombinant N-terminal myc-tagged version of MCP5. That this cell line indeed expresses MCP-nmyc in a tetracycline-dependent fashion was confirmed by western blotting (Figure 7). After induction with tetracycline, a cross-reacting (anti-myc antibody) protein band was observed with the expected molecular weight of 36 kDa. Whereas, no expression was observed in the absence of tetracycline, indicating a tight control of the tetracycline inducible promoter.

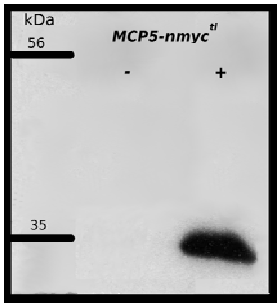

Figure 7. Western blot analysis of the PCF449 *MCP5-nmyc*^{ti} cell line, using a commercial myc-tag antibody (1:1000 dilution). The minus (–) indicates non-induced trypanosome cells, whereas the plus (+) indicates trypanosomes, which have been induced with tetracycline (1μg/ml). 2x10^6 trypanosomes have been loaded per lane.

The immunofluorescence microscopy results for the analysis of the PCF449 *MCP5-nmyc*^{ti} cell line are shown in Figure 8. Labelling of MCP5-nmyc with the myc-antibody revealed a tubular staining pattern, which is typical for mitochondria of *T. brucei*. Co-labelling with MitoTracker, an established marker for mitochondria, revealed a similar staining pattern, which coincides (panel D, Figure 8) with that of the myc-antibody. This result indicates that MCP5 has an exclusive mitochondrial localisation.

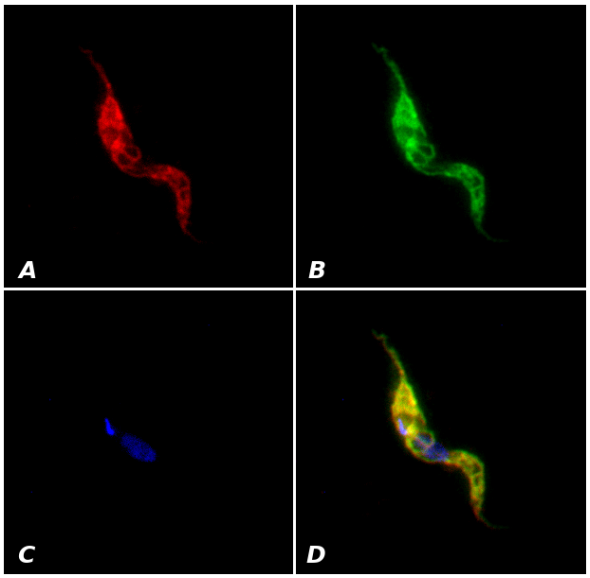

Figure 8. Immunofluorescence microscopy of the PCF449 *MCP5-nmyc*^{ti} cell line. MCP5-nmyc (panel B: green) was detected with a commercially available myc-antibody, where as MitoTracker (panel A: red) was used for the labelling of the mitochondrion. DAPI (panel C: blue) was used for DNA staining. The overlay (panel D: merge) is shown in yellow.

The mitochondrial localisation of MCP5 was further assessed in “wildtype” PCF449, using the raised MCP5 N-term and C-term peptide antibodies. The obtained

immunofluorescence microscopy results are shown in Figure 9. For the C-term peptide antibody, a staining pattern was observed which was more or less similar to the one observed for the *MCP5-nmyc*^{ti} cell line and using the myc-antibody (Figure 8).

However, additional particulate structures were stained by the C-term peptide antibody, next to the expected tubular mitochondria-staining pattern as found for the MitoTracker. This result is not unexpected, since the C-term peptide antibody recognises an additional non-specific protein band during western blotting (Figure 5), explaining the additionally stained particulate structures. For the N-term peptide antibody, a rather distorted staining pattern was found, with no indications of mitochondrial staining (Figure 9).

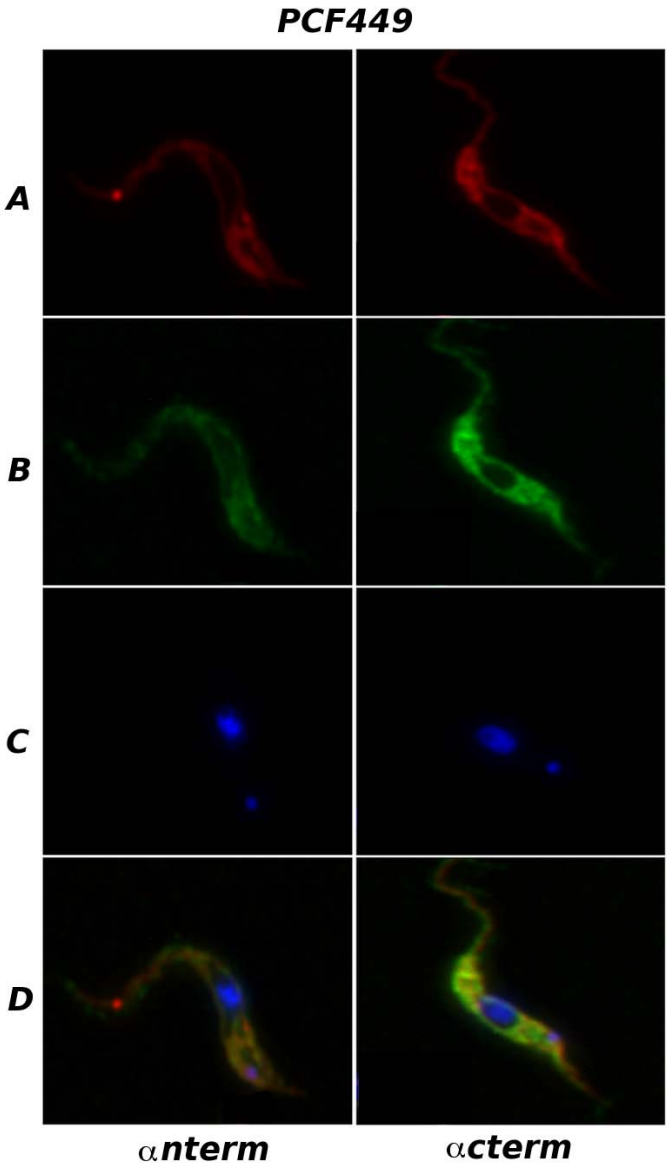

Figure 9. Immunofluorescence microscopy of PCF449, using the raised MCP5 N- and C-term peptide antibodies. N- and C-term peptide antibody staining is shown in

green (panels B), MitoTracker staining is shown in read (panels A), and DNA staining with DAPI is shown in blue (panels C). The overlays of MitoTracker staining pattern with those of the N-term or C-term peptide antibody are shown panel D.

This result can be explained by the structural differences of the MCP5 protein during western blotting and immunofluorescence microscopy. During western blotting, MCP5 is fully denatured and completely accessible to the antibody. This is different for immunofluorescence microscopy, where the protein is more or less in its natural folded conformation. As a consequence, the N-myc epitope could be “hidden”, and not be accessible for the N-term peptide antibody. The presence of an excess of antibody could subsequently result in non-specific reactions with other proteins, explaining the unexpected (distorted) staining pattern observed for the N-term peptide antibody during immunofluorescence microscopy.

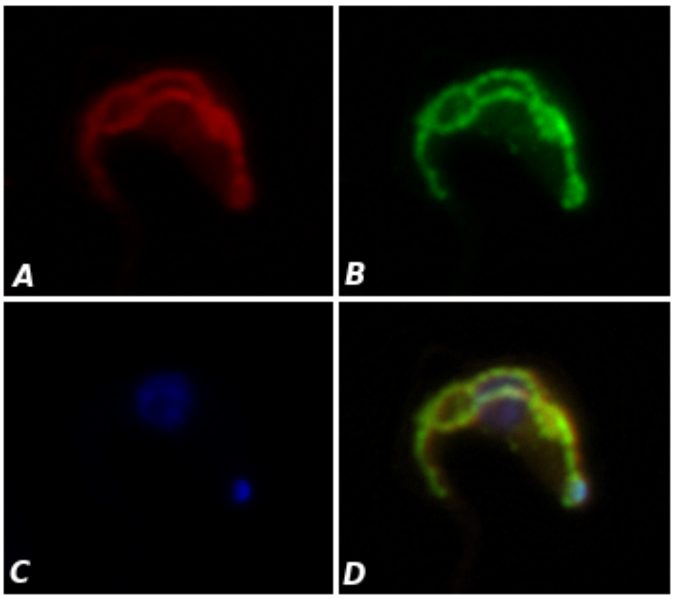

Figure 10. Immunofluorescence microscopy of BSF449 *T. brucei*, using the raised MCP5 C-term peptide antibody. Staining with the MCP5 C-term peptide antibody is shown in green (panel B). MitoTracker (panel A, red) was used for the labelling of the mitochondrion, and DAPI (panel C, blue) was used for DNA staining. The overlay (merge) is shown in yellow.

Western blot analysis revealed earlier that MCP5 is also expressed in the bloodstream-form of *T. brucei* (Figure 6). The subcellular localisation of MCP5 in

BSF449 was determined using the raised MCP5 C-term peptide antibody. The MCP5 N-term peptide antibody was not used since it previously resulted in aberrant staining patterns (Figure 5). The result for the immunofluorescence microscopy with the MCP5 C-term peptide antibody is shown in Figure 10, and revealed that MCP5 is exclusively mitochondrial in bloodstream-form *T. brucei.* In conclusion, MCP5 is mitochondrial in both PCF449 and BSF449 *T. bruce*i.

2.4. Generation of the conditional MCP5 knockout cell line *Δmcp5/MCP5-nmyc*^{ti}

Gene deletion or gene replacement through homologous recombination is an established technique for the functional characterization of proteins in *T. brucei* (Clayton, 1999). The same technique was used here for the deletion (knockout) of the different MCP5-encoding genes in the genome of procyclic-form *T. brucei*. MCP5 is expressed from 3 identical, in tandem organised gene copies on chromosome 10 of *T. brucei*. In order to facilitate a complete aberration of GIM5 expression, all 3 MCP5-encoding genes had to be replaced in a single recombination event. The 5'-UTR and 3'-UTR, required for the homologous recombination event, were chosen upstream of the first MCP5-encoding gene and downstream of the third MCP5-encoding gene, respectively. Initially, it was attempted to generate a conventional double knockout cell line. However, no viable clones could be obtained after many attempts, suggesting that MCP5 is essential for parasite survival. The lack of viable clones when using the conventional double knockout approach has been observed for other essential genes in *T. brucei* (Ajioka and Swindle, 1996; Mottram *et al.*, 1996).

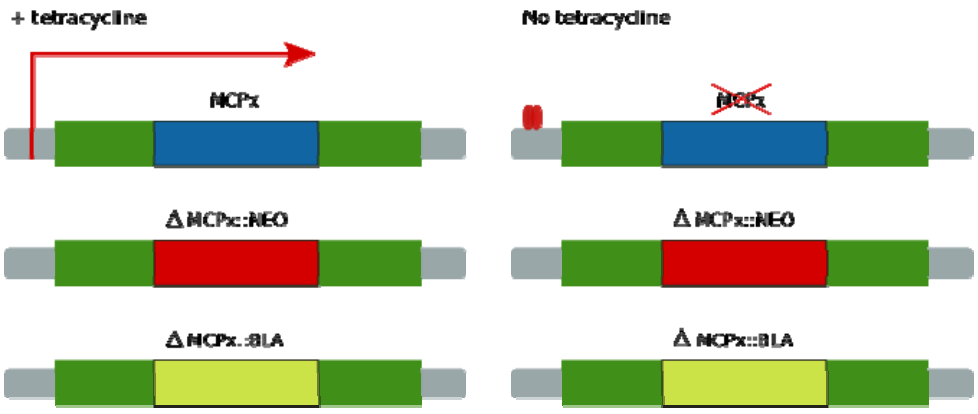

Figure 11. Schematic representation of the conditional double-knockout strategy. An ectopic tetracycline inducible gene copy of the target gene is introduced into the

T. brucei genome. Upon tetracycline addition, expression is induced from the ectopic gene copy. Each allele of the target gene(s) is replaced by different antibiotic resistance cassettes, i.e. for neomycine (NEO) and for blasticidin (BLA), through homologous recombination.

In case of an essential gene a different approach is used: i.e. the generation of a *conditional* double knockout cell line by the introduction of an ectopic tetracycline-inducible copy of the gene in the genome, prior to the elimination of the targeted alleles. This rescue copy of the targeted gene can be turned on or off by the addition or withdrawal of tetracycline (Clayton, 1999). A schematic representation of the conditional double knockout strategy is shown in Figure 11. Trypanosomes are diploid and require two sequential rounds of homologous recombination with different antibiotic selection markers to obtain a complete knockout of a gene (Clayton, 1999).

The above-described PCF449 *MCP5-nmyc*^{ti} cell line was used as a starting point for the generation of the conditional double knockout cell line *Δmcp5/MCP5-nmyc*^{ti}. After the 2 sequential homologous recombination events, using the NEO and BLA knockout plasmids, respectively, three different cell lines (clones) were obtained: i.e. *Δmcp5/MCP5-nmyc*^{ti} 5-1, 5.2 and 5-4. To confirm the proper insertion of the respective antibiotic resistance-cassettes in the intended MCP5 target locus, we analysed these putative *Δmcp5/MCP5-nmyc*^{ti} cell lines by Southern blotting and PCR.

For Southern blot analyses, genomic DNA (gDNA) was isolated from PCF449 and the different *Δmcp5/MCP5-nmyc*^{ti} cell lines, and subsequently digested with the restriction enzyme BamHI. A BamHI restriction site is normally not present in the natural MCP5 triad locus, but a single BamHI restriction site is present in the NEO and BLA antibiotic cassettes used for the gene replacement (Figure 12A). Consequently, successful homologous recombination and gene replacement will introduce an additional BamHI site in the former MCP5 triad loci (Figure 12A, indicated with an asterisk). The introduction of an additional BamHI site into the former MCP5 triad loci will result in specific cross-hybridising gDNA bands of known size (Figure 12A). The results of the Southern blot analyses are shown in Figure 12B.

As expected, a single cross-hybridising band with a size-length of 13.0 kbp was found for the “wildtype” cell line PCF449 (Figure 12B). Also for the putative *⊿mcp5/MCP5-nmyc*^{ti} double knockout cell lines 5-1 and 5-4, a single cross-hybridising band with the expected size-length of 0.6 kbp was found, which indicated a successful MCP5 gene replacement in these cell lines.

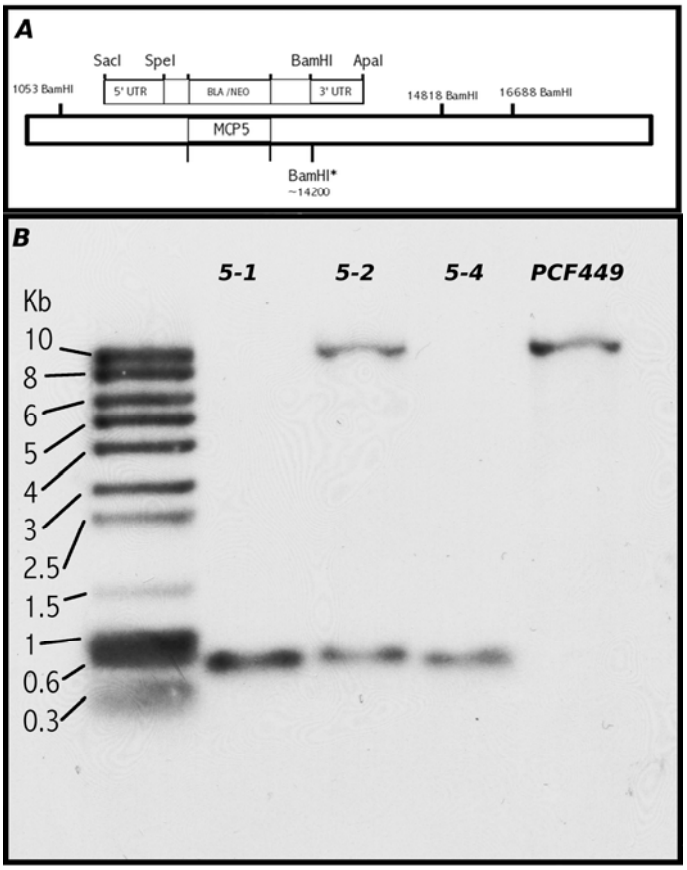

Figure 12. Southern blot analysis of BamHI digested genomic DNA isolated from the putative *⊿mcp5/MCP5-nmyc*^{ti} cell lines (5-1, 5-2, 5-4) and the “wildtype” PCF449 cell line. A schematic representation of the MCP5 target locus indicating the available BamHI restriction sites is shown in (A). The additional BamHI site, which is introduced through replacement with the different antibiotic resistance cassettes, is indicated with an asterisk. All indicated kb values are relative. (B) Southern blotting results for the different *⊿mcp5/MCP5-nmyc*^{ti} cell lines and PCF449. The Southern blot was probed with the 5’-UTR of MCP5.

However, for the putative *⊿mcp5/MCP5-nmyc*^{ti} cell line 5-2 cell line, two cross-hybridising bands were found with size-lengths of 13.0 and 0.6 kbp, respectively (Figure 12B). This hybridisation pattern suggested that the 5-2 cell line most

probably represents a MCP5 half knockout (with only one allelic MCP5 triad replaced), instead of the intended double knockout (with both allelic MCP5 triads replaced).

The successful replacement of all MCP5 gene triads in the genomes of the *Δmcp5/MCP5-nmyc*^{ti} cell lines 5-1 and 5-4 was further confirmed by PCR analysis. For this purpose, a forward primer was designed that specifically binds to a DNA sequence upstream of the intended 5'UTR recombination target region (Figure 13, panel 1). PCR amplification with this primer, in combination with either the NEO or BLA reverse primers, or the control MCP5 5'UTR reverse primer, would result in specific PCR products of a known size. The results of the PCR analysis are shown in Figure 13 (panel 2). The MCP5 5'-UTR control PCRs showed the expected single PCR product in all cell lines. For the *Δmcp5/MCP5-nmyc*^{ti} cell lines 5-1 and 5-4, all of the observed BLA and NEO PCR products were of the expected size: 1,200 bp and 1,500 bp PCR products were found for the respective BLA and NEO reverse primers, in combination with the upstream MCP5 5'UTR forward primer. As expected, the same BLA and NEO PCR products were not found for the wildtype PCF449 cell line, which was used as a control.

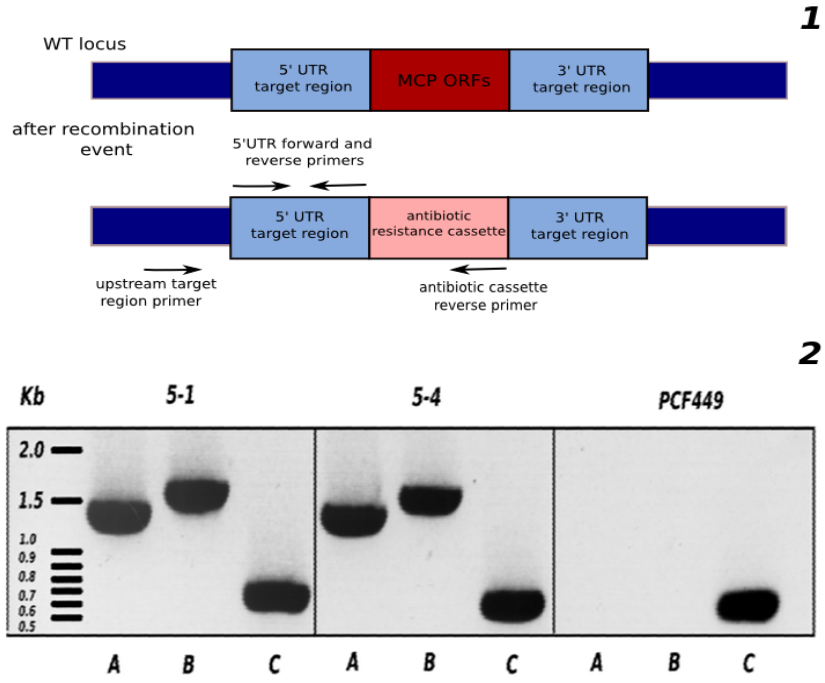

Figure 13. PCR assessment of the putative *Δmcp5/MCP5-nmyc*^{ti} cell lines 5-1 and 5-4. A schematic representation of the PCR strategy is shown in panel (1). The PCR results are shown in panel (2). PCR was performed with the designed forward primer, recognising a sequence upstream of the MCP5 5'-UTR target region used

for homologous recombination, and different reverse primers selective for: (A) the BLA resistance cassette; (B) the NEO resistance cassette; or (C) the 5'UTR of MCP5. Genomic DNA isolated from the *Δmcp5/MCP5-nmyc*^{ti} cell lines 5-1 and 5-4, and the wildtype PCF449 cell line was used as a template for PCR.

The obtained *Δmcp5/MCP5-nmyc*^{ti} cell lines 5-1 and 5-4 were further analysed by western blotting, using the commercial myc-tag antibody and the raised MCP5 N-term and C-term peptide antisera. Purpose of this analysis was to show that the obtained conditional double knockout cell lines (A) indeed lack the natural MCP5, and (B) still express the myc-tagged MCP5 rescue copy in the presence of tetracycline. The results are shown in Figure 14. Western blot analysis with the raised N-term (Figure 14A) or C-term (Figure 14C) peptide antisera confirmed that both the *Δmcp5/MCP5-nmyc*^{ti} cell lines 5-1 and 5-4 (lane 1 and 2, respectively) indeed lack the natural MCP5 protein, whereas in wildtype PCF449 (lane 3) MCP5 still can be detected. The western blotting results confirmed further the presence of recombinant myc-tagged MCP5, with the expected molecular weight of 36 kDa, in both *Δmcp5/MCP5-nmyc*^{ti} cell lines. This recombinant myc-tagged MCP5 was recognised by both the raised N-term or C-term peptide antisera (Figures 14A and 14C, lanes 1 and 2), and the commercial myc-tag antibody (Figures 14B and 14D, lanes 1 and 2).

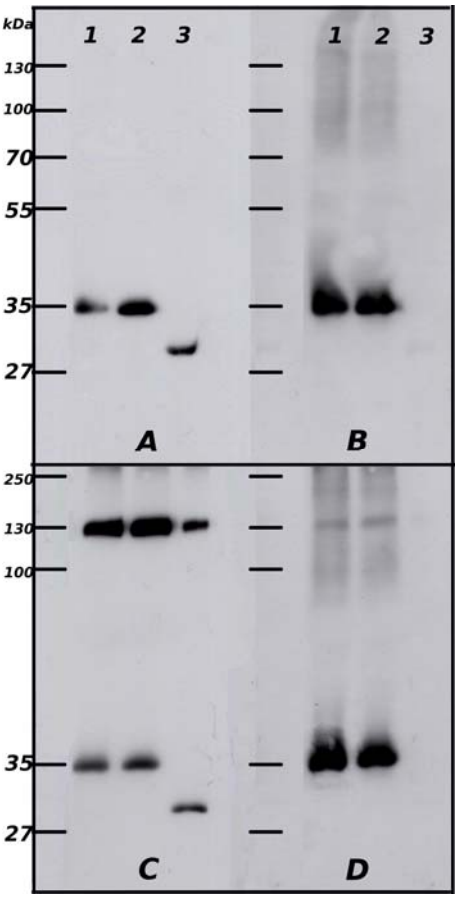

Figure 14. Western blot analysis of the *Δmcp5/MCP5-nmyc*^{ti} cell lines 5-1 (lanes 1) and 5-4 (lanes 2), and PCF449 (lanes 3) *T. brucei.* The raised MCP5 N-term (panel A) and C-term (panel C) peptide antisera, and a commercial myc-tag antibody (panels B and D) were used for analysis. 2x10^6 *T. brucei* cells were loaded per well.

2.5. Functional characterization of the *Δmcp5/MCP5-nmyc*^{ti} cell line: analysis of mitochondrial ATP production.

The ADP/ATP carrier exchanges mitochondrial ATP with cytosolic ADP in a 1:1 ratio (Klingenberg, 2008). If a mitochondrion lacks this exchange, the transport of ATP into the cytosol will be hampered. This principle can be used to study ATP production and the exchange of this molecule in isolated mitochondria. Since the isolation of functional *T. brucei* mitochondria is rather problematic, due to their tubular structure and tight association with the cytoskeleton, an alternative and more reproducible method is used. This alternative method is based on the enrichment of mitochondria by the permeabilization of whole cells with digitonin, followed by extensive washing in order to eliminate the cytosol and other non-mitochondrial organelles, prior to the assays (Schneider *et al*., 2007).

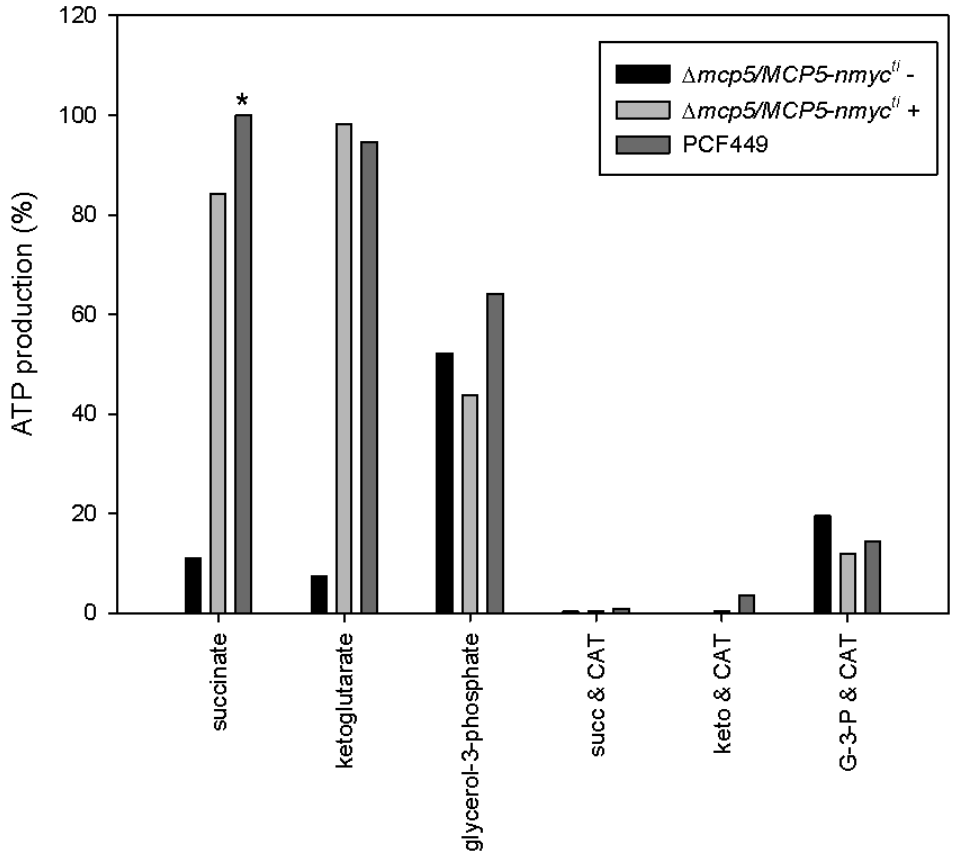

Figure 15. Mitochondrial ATP production in wildtype PCF449, and induced (+) and non-induced (-) *Δmcp5/MCP5-nmyc*^{ti} cell lines, using different metabolic substrates. The different substrates were incubated with mitochondria in absence or presence of the ADP/ATP carrier inhibitor carboxyatractyloside (CAT). ATP production in PCF449 mitochondria with succinate as substrate is set to 100% (indicated with asterisk).

During the assays, different mitochondrial substrates and various inhibitors were added to the enriched *T. brucei* mitochondria together with ADP and Pi, and the production of ATP was measured by using a luciferase-based ATP detection kit (see Materials and Methods for more details). The different substrates and inhibitors used, enable the discrimination between ATP produced during oxidative phosphorylation (OXPHOS) or substrate-level phosphorylation (SUBPHOS) in the mitochondrion of *Trypanosoma brucei* (Schneider *et al*., 2007). The results obtained in various experiments are summarised in the Figures 15 and 16.

Both succinate and ketoglutarate have to be imported into the mitochondrion for subsequent ATP production. This in contrast to glycerol-3-phosphate, which is oxidised on the outside of the mitochondrion and involves the combined action of a glycerol-3-phosphate dehydrogenase in the mitochondrial intermembrane space, a mitochondrial inner membrane bound alternative oxidase, and part of the mitochondrial respiratory chain for ATP production (Figure 25).

Initially, PCF449 mitochondria were tested to demonstrate the functionality of the assay. Addition of the different metabolic substrates to these “wildtype” mitochondria resulted in the concomitant production and export of ATP (Figure 15). Almost similar amounts of ATP were produced on the first two substrates, i.e. succinate and ketoglutarate, whereas significantly less ATP was formed with glycerol-3-phosphate as a substrate: i.e. approximately 65% of the ATP produced with succinate or ketoglutarate. As expected, addition of the specific ADP/ATP carrier inhibitor CAT resulted in a complete ablation of the mitochondrial ATP export, in case of succinate or ketoglutarate as metabolic substrate. Also in case of glycerol-3-phosphate, a significant 85% reduction in ATP production was found after the addition of CAT, in comparison to succinate and ketoglutarate. The observation of some remaining ATP production from glycerol-3-phosphate, even in the presence of CAT, can be explained by de possibility that the mitochondrial preparations still contains some phosphoglycerol kinase (PGK) activity (Allemann and Schneider, 2000). PGK can convert glycerol-3-phosphate into glycerol, with the concomitant production of ATP via substrate-level phosphorylation.

Comparison of the ATP production-values obtained for PCF449 with those obtained from the induced *Δmcp5/MCP5-nmyc*^{ti} cell line revealed that all values were virtually similar (Figure 15). However, for the non-induced *Δmcp5/MCP5-nmyc*^{ti} cell line a more than 90% decrease in ATP production was observed for both succinate and ketoglutarate, when compared to PCF449. For glycerol-3-P, no significant differences were found in ATP production for mitochondria from PCF449 and the induced and non-induced *Δmcp5/MCP5-nmyc*^{ti} cell lines.

From these observations two important conclusions could be drawn. The first conclusion is that MCP5 is responsible for most, i.e. more then 90% of the ADP/ATP exchange in the *T. brucei* mitochondrion. The remaining ADP/ATP exchange activity must also be due to ADP/ATP carrier activity, since addition of CAT to the non-

induced *Δmcp5/MCP5-nmyc*^{ti} mitochondria resulted in a complete ablation of ADP/ATP exchange activity (Figure 15). This residual ADP/ATP exchange activity could be explained by: (A) the presence of residual recombinant MCP5-nmyc in the non-induced *Δmcp5/MCP5-nmyc*^{ti} cell line, with protein levels below the western blotting detection limit (see Figure 17), or (B) the presence of other ADP/ATP carriers in the *T. brucei* mitochondrion, like for example MCP15 or MCP16 (Chapter VI).

The second conclusion that could be drawn from these results is that the recombinant myc-tagged version of MCP5, which has been used as a rescue copy during the knockout procedure, is fully functional in terms of ADP/ATP exchange. The major decrease in ATP production (read ADP/ATP exchange) in the MCP5 knockout mitochondria could be fully reversed to wildtype levels by the induced expression of this recombinant version (Figure 15).

The mitochondrial ATP production was further assessed in the presence of specific metabolic inhibitors: i.e. the electron transport chain inhibitors rotenone (inhibits Complex I), malonate (inhibits Complex II), and antimycin (inhibits Complex III), and the ionophore carbonyl cyanide-p-trifluoromethoxyphenylhydrazone (FCCP). FCCP is in general used to specifically inhibit oxidative phosphorylation-related ATP production, via the dissipation of the mitochondrial proton gradient, which again is required for the production of ATP through the mitochondrial ATP-synthase. ATP that can be formed in the presence of excess FCCP is in general considered to be the result of substrate-level phosphorylation (SUBPHOS). The other mentioned inhibitors allowed the discrimination of the different parts of the electron transport chain that contribute to oxidative phosphorylation (OXPHOS).

The observed ATP production values in “wildtype” PCF449 mitochondria incubated with the different inhibitors (Figure 16) were similar to those previously reported by other research groups (Bochud-Allemann and Schneider, 2002; Allemann and Schneider, 2000), confirming the reproducibility of the used mitochondrial ATP-production assays. Addition of the different electron transport chain inhibitors and the ionophore FCCP resulted in the complete ablation of ATP-production when succinate was used as a metabolic substrate. This was expected since ATP generation via succinate is completely dependent on oxidative phosphorylation (Figure 25).

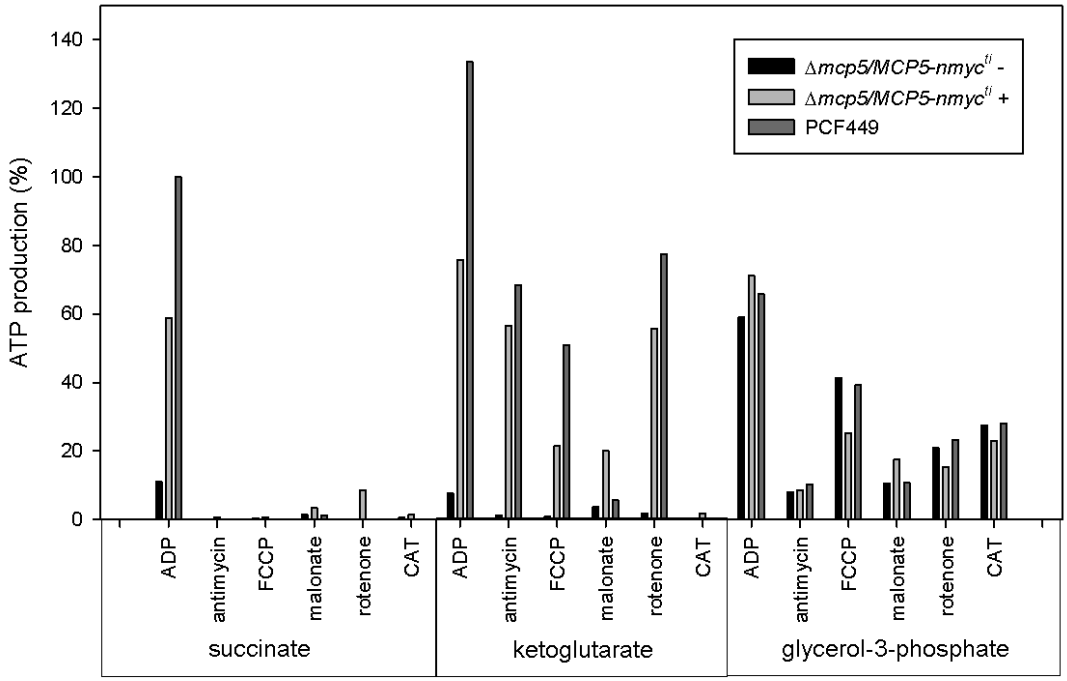

Figure 16. Mitochondrial ATP production in wildtype PCF449, and induced (+) and non-induced (-) *Δmcp5/MCP5-nmyc*^{ti} cell lines, using different metabolic substrates. The different substrates used and ADP/Pi were incubated with mitochondria in absence or presence of various inhibitors, which inhibit different parts of the mitochondrial energy metabolism. ATP production in PCF449 mitochondria with succinate as substrate is set to 100%.

In the case of ketoglutarate, however, different degrees of inhibition were found depending on the inhibitor used. During mitochondrial ketoglutarate catabolism, ATP can be generated by either OXPHOS or SUBPHOS (Chapter 1, Figure 3). Addition of FCCP, which specifically inhibits OXPHOS, resulted in an approximately 60% decrease of ATP-production, and indicated that the remainder of the mitochondrial ATP produced is most probably the result of SUBPHOS. More or less similar decreases in ATP production were also found after addition of the electron transport chain inhibitors antimycin and rotenone (Figure 16). Addition of malonate decreased the mitochondrial ATP production even further. Malonate specifically inhibits Complex II, including its succinate dehydrogenase (SDH) activity. As a consequence, the substrate succinate will accumulate in the mitochondrion. Accumulation of succinate again inhibits the ketoglutarate degradation pathway with less ATP produced via SUBPHOS, which occurs during the conversion of succinyl-

CoA to succinate (Figure 25). This feedback inhibition would be responsible for the observed additional decrease in ATP-production in the presence of malonate, when compared to antimycin and rotenone. A similar decrease in mitochondrial ATP generation was previously observed after RNAi of SDH (Bochud-Allemann and Schneider, 2002) .

When using glycerol-3-phosphate as a metabolic substrate, a 40% reduction in ATP production was observed in the presence of FCCP, reflecting the amount of ATP generated by OXPHOS. In the mitochondrion, glycerol-3-phosphate is converted to dihydroxyacetone phosphate by a FAD-dependent glycerol-3-phosphate dehydrogenase located in the mitochondrial inter membrane space. The resulting electrons are directly transferred to the electron carrier ubiquinone, which subsequently donates them to the alternative oxidase or to complex III in the mitochondrial inner membrane. As a consequence, the electrons will bypass the respiratory Complexes I and II (Kohl *et al*., 1996). As expected, addition of antimycin (Complex III inhibitor) to "wildtype" mitochondria resulted in a significant decrease (>90%) of ATP production when using glycerol-3-phosphate as a substrate (Figure 16). Unexpectedly, also the addition of rotenone (inhibitor of Complex I) and malonate (inhibitor of Complex II) resulted in a significant inhibition of the ATP generation from glycerol-3-phosphate. Rotenone was found previously not to inhibit the glycerol-3-phosphate-based ATP production in *T. brucei* (Alleman & Schneider, 2000).

2.6. Functional characterization of the *Δmcp5/MCP5-nmyc*^{ti} 5-1 cell line: analysis of growth in different culture media.

As indicated in section 2.4, we were unable to generate a conventional (without MCP5 rescue copy) double knockout cell line in PCF449, which suggested that MCP5 is essential for the survival - i.e. growth - of the parasite. Instead, a conditional *Δmcp5/MCP5-nmyc*^{ti} 5-1 cell line was generated, enabling the depletion of a N-myc tagged version of MCP5 after withdrawal of tetracycline. The growth of this cell line was analysed using three different culture media, i.e. normal Mem-Pros (NMP), glucose-depleted Mem-Pros (GDMP), and glucose-supplemented MEM-Pros (MPglu), respectively. NMP, the standard MEM-Pros medium (Overath *et al*., 1986), contains 5 mM proline and approximately 0.2-0.3 mM glucose, which is derived from the glucose present in the added 10% (v/v) foetal calf serum (FCS). The GDMP medium also contains 5mM proline, but has essentially been depleted

for glucose by enzymatic conversion (Chapter II). In contrast, MPglu is similar to NMP medium that has been supplemented with 5 mM glucose.

The simple reason for testing these different culture media is the observed capability of *T. brucei* to produce ATP either in the mitochondrion and/or the cytosol (last part of glycolysis), depending on the available carbon/energy source. For example, the exclusively mitochondrial substrate-level phosphorylation of proline, and the concomitant production of ATP, necessitates a functional ADP/ATP exchanger for the provision of mitochondrial ATP to the rest of the cell. For glucose the situation will be different, since part of the required ATP is generated in the cytosol (Figure 25), an as such is available for the rest of the cell. In the presence of glucose it is expected that *T. brucei* will most probably be less dependent on the mitochondrial provision of ATP, and consequently will be less dependent on the ADP/ATP exchanger for survival.

For growth experiments, *Δmcp5/MCP5-nmyc*^{ti} 5-1 cultures were initiated at the same initial cell density and were grown in the presence (induced: MCP5-nmyc expressed) or absence (non-induced: MCP5-nmyc depleted) of tetracycline. Western blot analysis was used to confirm the depletion of MCP5-nmyc after withdrawal of tetracycline. The “wildtype” PCF449 cell line acted as a reference for the different growth experiments.

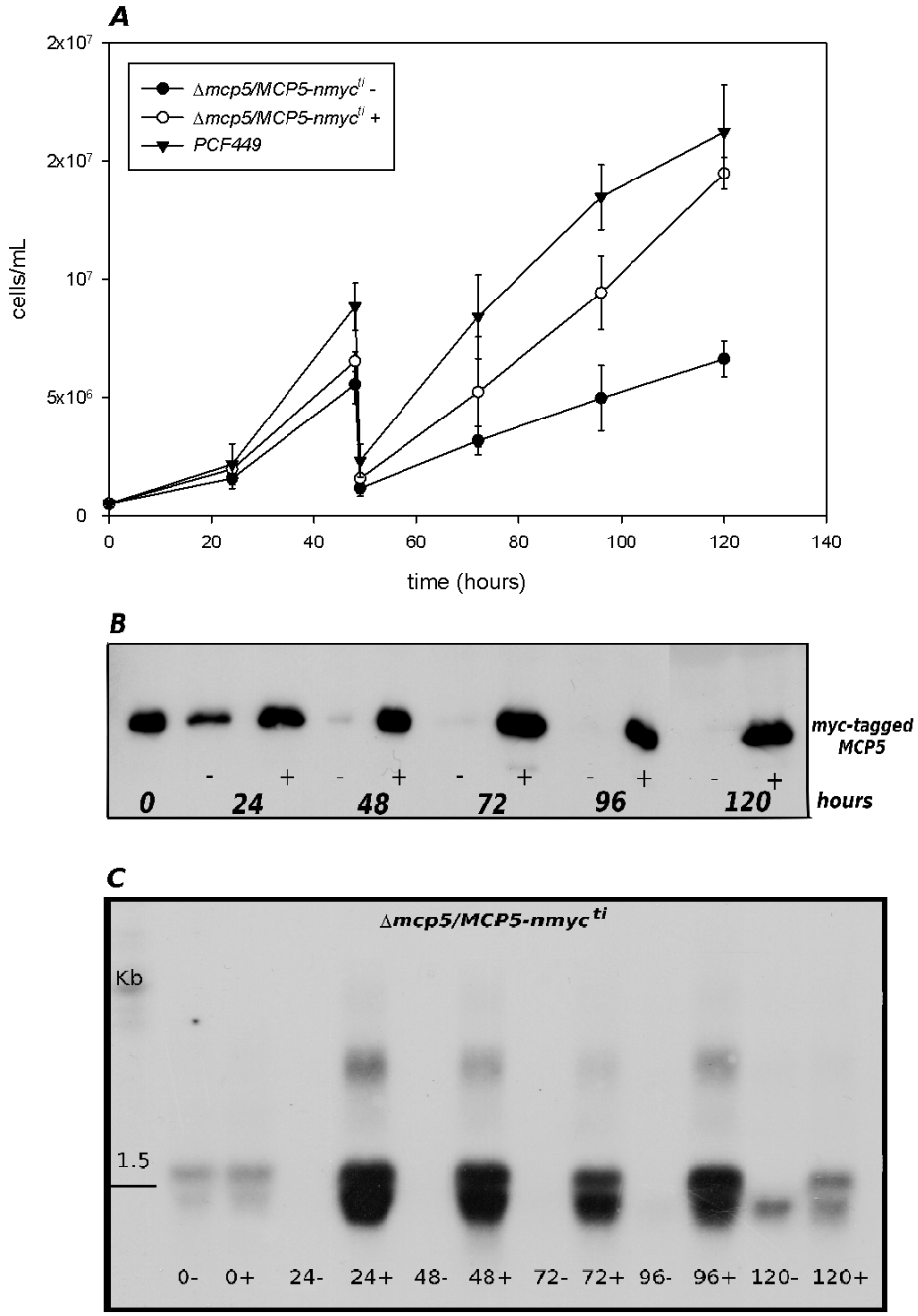

Figure 17. Growth curves for PCF449, and the induced (+) and non-induced (-) *Δmcp5/MCP5-nmyc*^{ti} cell lines in NMP (A). The cultures were subcultured at 48 hours with GDMP at this point of the curve. Panel (B) shows western blotting analysis of culture samples taken every 24 hours from the above-mentioned *Δmcp5/MCP5-nmyc*^{ti} cultures, using the myc-tag antibody. Panel (C) shows northern blot analysis of the same culture samples, with 10 μg of total RNA in each lane and the full length MCP5 DNA sequence was used as a probe for hybridization.

For the first experiment, cultures were initiated on standard NMP medium (containing low concentrations of glucose), with subsequent sub-culturing on GDMP (contains no glucose) after 48 hours. The obtained growth curves are shown in Figure 17A. Culture samples of the induced and non-induced *Δmcp5/MCP5-nmyc*^{ti} cell lines were further analysed for the presence of the myc-tagged MCP5 protein (Figure 17B) and its corresponding messenger mRNA (Figure 17C).

Western blot analysis revealed that the myc-tagged MCP5 protein level in the non-induced *Δmcp5/MCP5-nmyc*^{ti} cell line clearly decreased upon withdrawal of tetracycline at the start of the culture and was completely depleted, i.e. below the western blotting detection limit, after 96 hours of culture (Figure 17B). As expected, the myc-tagged MCP5 protein levels in the induced *Δmcp5/MCP5-nmyc*^{ti} cell line remained constant in the presence tetracycline for the duration (i.e. 120 hours) of the growth experiment.

When comparing the growth curves, a substantial decrease in growth-rate was observed for the non-induced *Δmcp5/MCP5-nmyc*^{ti} 5-1 cell line, when compared to the "wildtype" cell line PCF449 (Figure 17A). This decrease became even more prominent after sub-culturing of these cell lines from standard NMP medium to GDMP medium. These results indicated that the depletion of MCP5 had a substantial negative effect on *T. brucei* growth, especially under glucose-depleted conditions. However the apparent "total" MCP5 depletion (Figure 17B, 96 hours) did not result in cell death, as would have been expected from the previous failed attempts to generate a conventional MCP5 double knockout (i.e. *Δmcp5/Δmcp5*) *T. brucei* cell line. This inconsistency could be explained by the possibility that still some myc-tagged MCP5 protein is present in the non-induced *Δmcp5/MCP5-nmyc*^{ti} 5-1 cells, which is below the detection limit of the used myc-tag antibody during western blot analysis. This explanation is based on the assumption that very low amounts of MCP5 can keep the non-induced *Δmcp5/MCP5-nmyc*^{ti} 5-1 cell line viable. The presence of very low amounts of MCP5 protein in non-induced *Δmcp5/MCP5-nmyc*^{ti} 5-1 cultures 96 hours after tetracycline withdrawal is supported by northern blot analysis, which revealed the presence of low levels of MCP5-encoding mRNAs at that time point (Figure 17C, 96 hours non-induced).

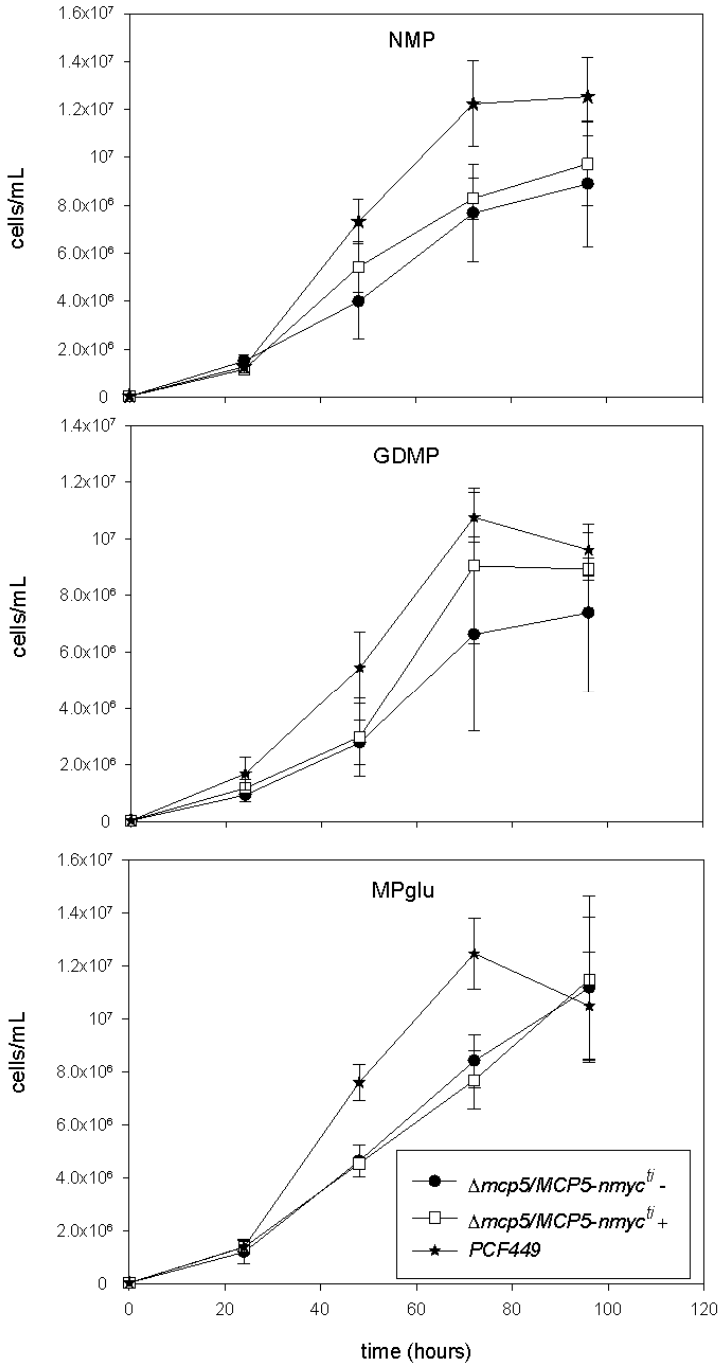

Figure 18. Growth of wildtype PC449 and the induced and non-induced *Δmcp5/MCP5-nmyc*^{ti} cell lines on different culture media, i.e. NMP, GDMP and MPGlu, respectively.

Expression of myc-tagged MCP5 in the induced *Δmcp5/MCP5-nmyc*^{ti} cell line resulted in an only partial restoration of "wildtype" growth (Figure 17A). There are two possible explanations for this unexpected result: (A) the added N-term myc-tag could affect the transport function of MCP5, or (B) the myc-tagged MCP5 version is actually 2-3 fold over-expressed (not shown) when compared to the expression of the native MCP5 in the wildtype, and this abundance of a putative ADP/ATP carrier could negatively affect the function the mitochondrion. Which of these explanations is correct will be further discussed in section 2.9 of this Chapter.

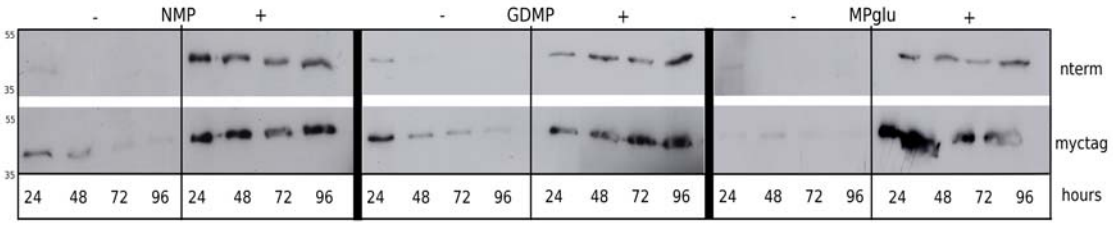

Figure 19. Western blot analysis of tetracycline-induced (+) and non-induced (-) *Δmcp5/MCP5-nmyc*^{ti} cell lines, grown on NMP (normal MEM-Pros), GDMP (glucose-depleted MEM-Pros) and MPglu (glucose-supplemented MEM-Pros), and using the raised N-term and C-term MCP5 peptide antibodies. $2x10^6$ trypanosomes were loaded per well.

When growing trypanosomes in culture, metabolic adaptation(s) might influence the growth rate of the cell line in response to a change in culture conditions. Sub-culturing from NMP to GDMP medium, as has been done for the first experiment (Figure 17A), might introduce such a change in growth rate. To reduce the possible culture medium-induced changes to a minimum, we decided to pre-adapt the induced *Δmcp5/MCP5-nmyc*^{ti} 5-1 and PCF449 cell lines to the different culture media, before performing the growth experiments.

This time, the growth experiment was performed on the 3 different culture media mentioned above. The obtained growth curves are shown in Figure 18, and the corresponding western blots, analysed with both the commercial myc-tag and raised MCP5 N-term peptide antibody, are shown in Figure 19. The western blot results confirmed the depletion of the myc-tagged MCP5 in the non-induced *Δmcp5/MCP5-nmyc*^{ti} cell line (myc-tag panels in Figure 19).

Similar to the first experiment (Figure 17), a distinct difference was observed between the growth of the non-induced *Δmcp5/MCP5-nmyc*^{ti} cell line and the growth of the reference cell line PCF449 (Figure 18). The growth of the non-induced *Δmcp5/MCP5-nmyc*^{ti} cell line was significantly more affected on both the glucose-depleted GDMP medium and low-glucose NMP medium, when compared to its growth on the glucose-rich MPGlu medium. The presence of high glucose concentrations (5mM) in the MPGlu medium apparently compensates partly for the MCP5 knockout-induced growth defect. "Wildtype"-growth was only partial or even not all restored after expression of myc-tagged MCP5 in the induced *Δmcp5/MCP5-nmyc*^{ti} cell line (Figure 18). The same result was found in the previous experiment (Figure 17), and will be further discussed later on in this chapter.

2.7. Functional characterization of the *Δmcp5/MCP5-nmyc*^{ti} 5-1 cell line: analysis of substrate-consumption in different culture media

Analysis of substrate-consumption and end product-formation in the different culture media could give important clues regarding the effect of the MCP5 knockout on the energy metabolism, and the physiological role of MCP5 in *T. brucei*. Both glucose and proline have been described as primarily consumed carbon/energy sources for ATP production in procyclic-form *T. brucei* (Lamour *et al.*, 2005; Coustou *et al.*, 2008). The overall consumption of proline during growth of the different *T. brucei* cell lines in NMP, GDMP and MPglu medium respectively, was analysed. All three used media contain equal amounts of proline (5mM), whereas the initial glucose concentrations are different. The results are shown in Figures 20, 21 and 22 for NMP, GDMP and MPglu medium, respectively. The proline consumption rates (mM proline consumed per 10^6 cells) found for the different cell lines and culture media are shown in Figure 23.

Comparison of the proline consumption by the different cell lines grown in NMP revealed some significant differences (Figures 20 and 23). The final proline concentration found after 96 hours of growth in NMP medium was 3-fold higher in the non-induced *Δmcp5/MCP5-nmyc*^{ti} cell line than for the wildtype cell line PCF449 (Figure 20). When taking into account the reduced growth of the non-induced *Δmcp5/MCP5-nmyc*^{ti} cell line, proline consumption in this cell line had almost halved at 96 hours when compared to PCF449 (Figure 23).

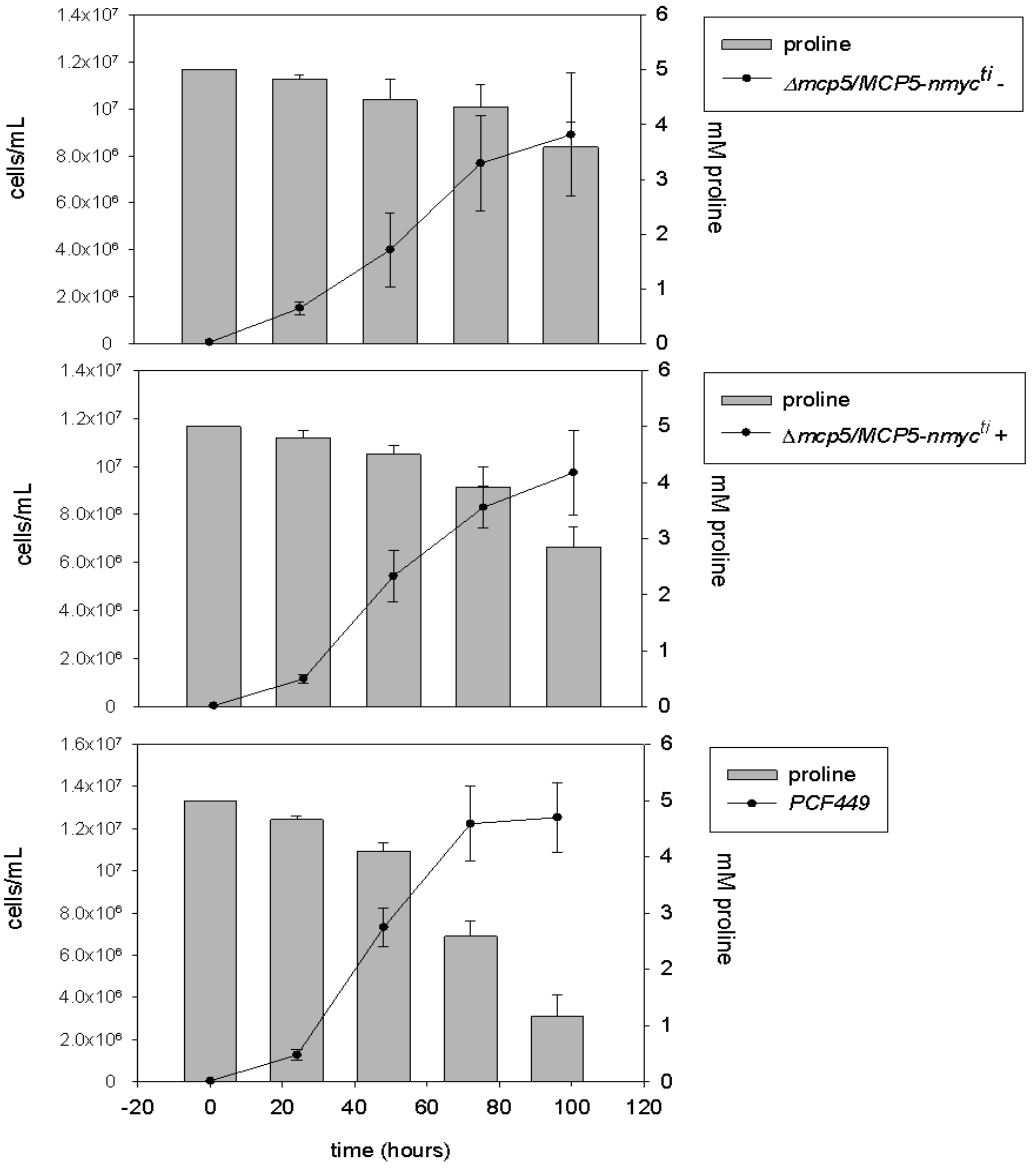

Figure 20. Consumption of proline by non-induced Δ*mcp5/MCP5-nmyc*^{ti} (A), induced Δ*mcp5/MCP5-nmyc*^{ti} (B), and PCF449 (C) cell lines during growth in NMP medium. The corresponding growth curves (●) are shown for comparison.

As expected, proline consumption did somewhat increase in the induced Δ*mcp5/MCP5-nmyc*^{ti} cell line when compared to the same but non-induced cell line (Figures 20 and 23). This result confirmed the previously observed partial restoration of the wildtype proline metabolism. Overall, these results indicated that the knockout of the putative ADP/ATP exchanger MCP5 apparently has a significant effect on the mitochondrial proline metabolism, but apparently does not ablate it completely.

Surprisingly, no significant differences in proline consumption (expressed in mM proline consumed per 10^6 cells) were found when the different cell lines where grown in the essentially glucose-free GDMP medium (Figures 21 and 23). The previously observed differences in growth rates of the different cell lines in GDMP medium (Figure 18) were also found in this experiment (Figure 21).

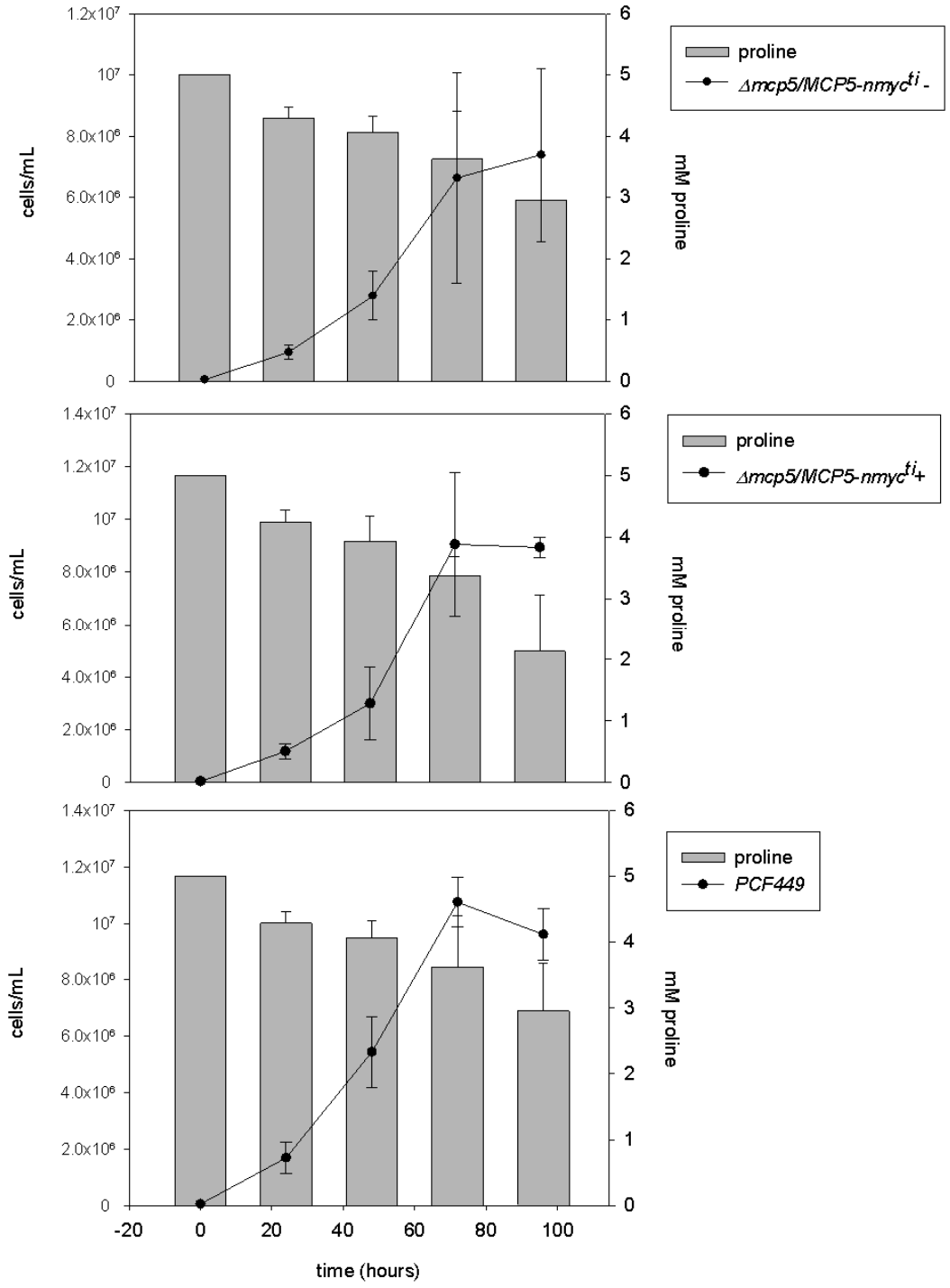

Figure 21. Consumption of proline by non-induced Δ*mcp5/MCP5-nmyc*^{ti} (A), induced Δ*mcp5/MCP5-nmyc*^{ti} (B), and PCF449 (C) cell lines during growth in GDMP medium. The corresponding growth curves (●) are shown for comparison.

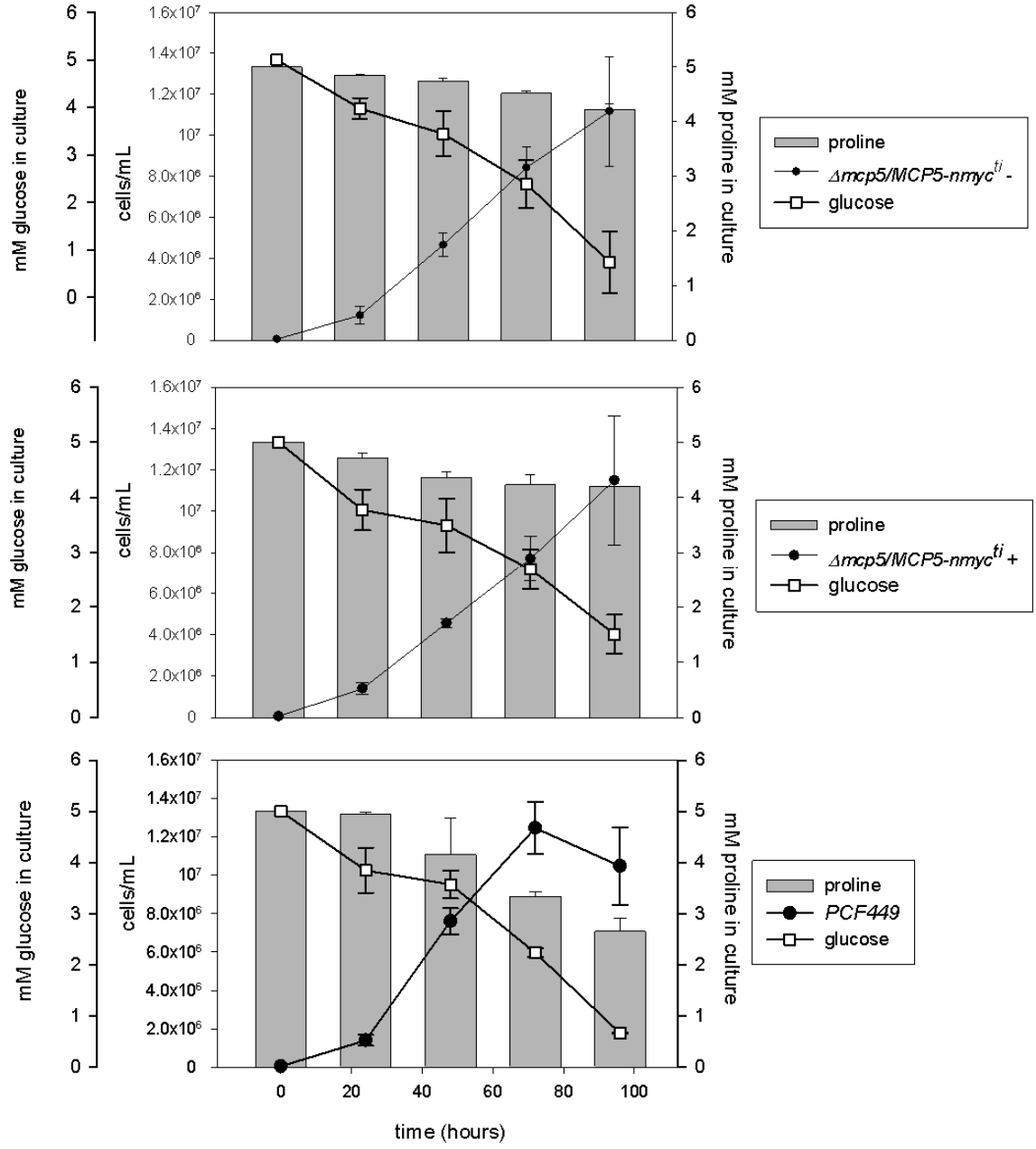

Figure 22. Consumption of proline (grey bars) and glucose (□) by non-induced Δ*mcp5/MCP5-nmyc*^{ti} (A), induced Δ*mcp5/MCP5-nmyc*^{ti} (B), and PCF449 (C) cell lines during growth in MPGlu medium. The corresponding growth curves (●) are shown for comparison.

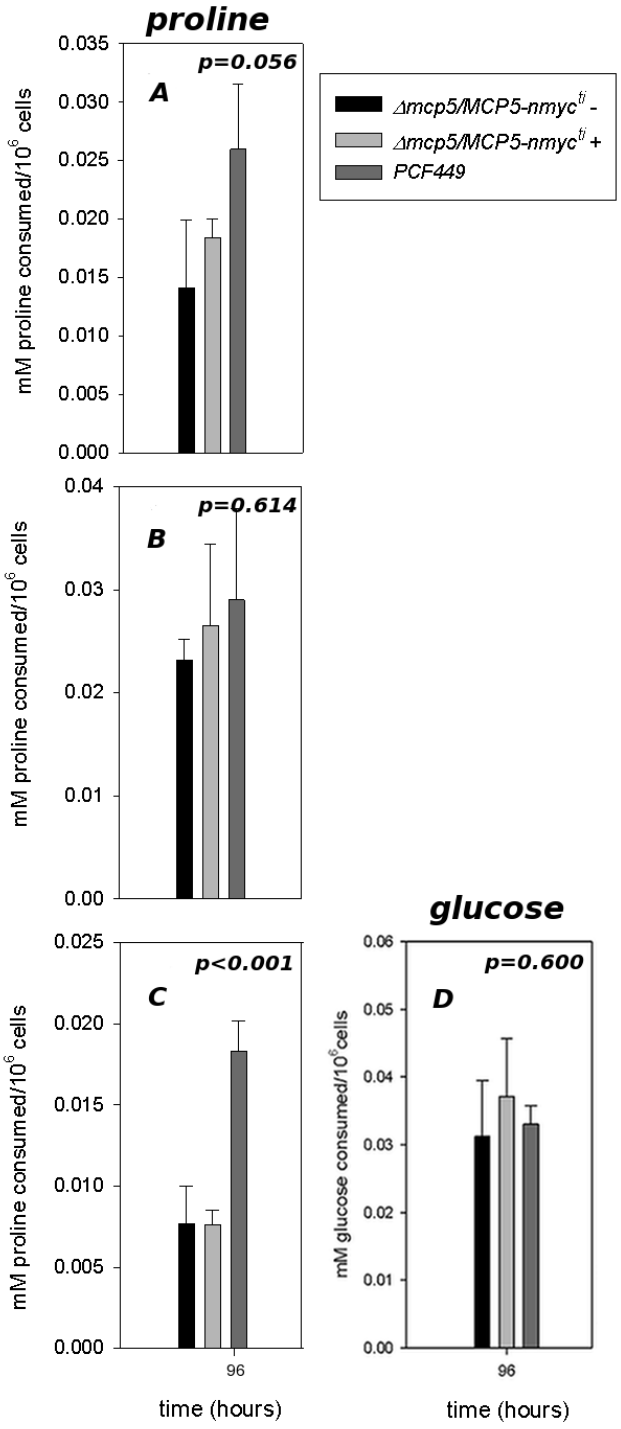

Figure 23. Proline and glucose consumption (mM substrate consumed per 10^6 cells) of the wildtype PCF449, and induced (+) and non-induced (-) *Δmcp5/MCP5-nmyc*^{ti} cell lines, grown in different culture media for 96 hours. Panels A, B and C represent proline consumption rates on NMP, GDMP and MPglu mediums, respectively. Glucose consumption rate in MPglu is shown in panel D. Carbon sources consumption data was normalized into [carbon source]/10^6 cells in culture. Each set of normalized data was submitted to One-way ANOVA. Where significant differences were observed ($p<0.05$), the Holm-Sidak method for control group was used to determine significance between KOs and PCF449 profiles (control).

We finally tested the MPGlu medium, which contained both 5mM proline and 5mM glucose. Comparison of proline consumption by the different cell lines grown in MPGlu revealed some significant differences (Figures 22 and 23). For both the induced and non-induced *Δmcp5/MCP5-nmyc*^{ti} cell lines, the proline consumption per cell was identical, although halved when compared to that of the wildtype PCF449 cell line ($p<0.001$). For glucose consumption, however, no differences could be observed when comparing the different cell lines ($p=0.600$) (Figures 22 and 23). Overall, these results indicated that in particular the mitochondrial proline metabolism is affected.

2.8. Functional characterization of the *Δmcp5/MCP5-nmyc*^{ti} cell line: analysis of end product formation.

The two main metabolic end products of "wildtype" PCF449 are succinate and acetate, which are both excreted into the culture medium. Succinate is the end product of both the glycosomal degradation of glucose and the mitochondrial degradation of proline (Chapter I: Figure 3). This succinate will be further referred to in this Chapter as "total" succinate, since we cannot discriminate between the succinate formed in the glycosome and/or the mitochondrion. Acetate, however, originates from glucose and is only produced in the mitochondrion (Chapter I: Figure 3). The formation of these end products was analysed in the same culture medium samples as used for the above-discussed substrate consumption analyses.

We initially analysed substrate consumption and end product formation in glucose-depleted GDMP medium, which only contained proline as a carbon/energy source. Comparison of the total succinate production by the different cell lines grown in this medium revealed no significant differences between the non-induced *Δmcp5/MCP5-nmyc*^{ti} (MCP5-depleted) cell line and the wildtype PCF449 cell line ($p=0.104$) (Figure 24). On a similar scale, no substantial changes could be observed for the cellular proline consumption ($p=0.614$) (Figure 23) or acetate formation (0.444) (Figure 24), when comparing the same cell lines.

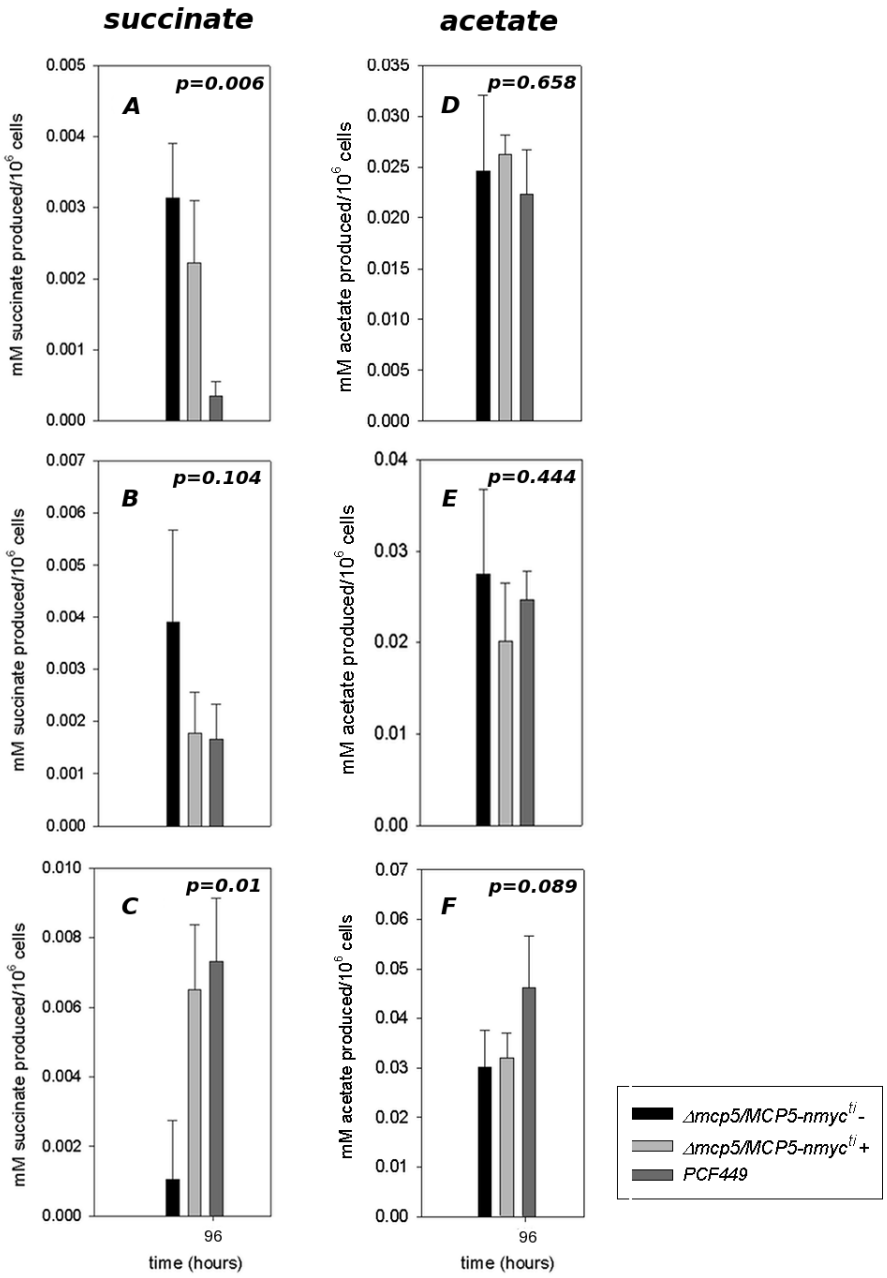

Figure 24. Production of succinate and acetate (mM formed per 10^6 cells) of the wildtype PCF449, and induced (+) and non-induced (-) *Δmcp5/MCP5-nmyc*^{ti} cell lines, grown in different culture media for 96 hours. Succinate production in NMP, GDMP and MPglu medias is shown in panels A, B and C, respectively. Acetate production in the aforementioned medias is shown in panels D, E and F, respectively. Metabolites production data was normalized into [metabolite]/10^6 cells in culture. Each set of normalized data was submitted to One-way ANOVA. Where significant differences were observed ($p<0.05$), the Holm-Sidak method for control group was used to determine significance between KOs and PCF449 profiles (control).

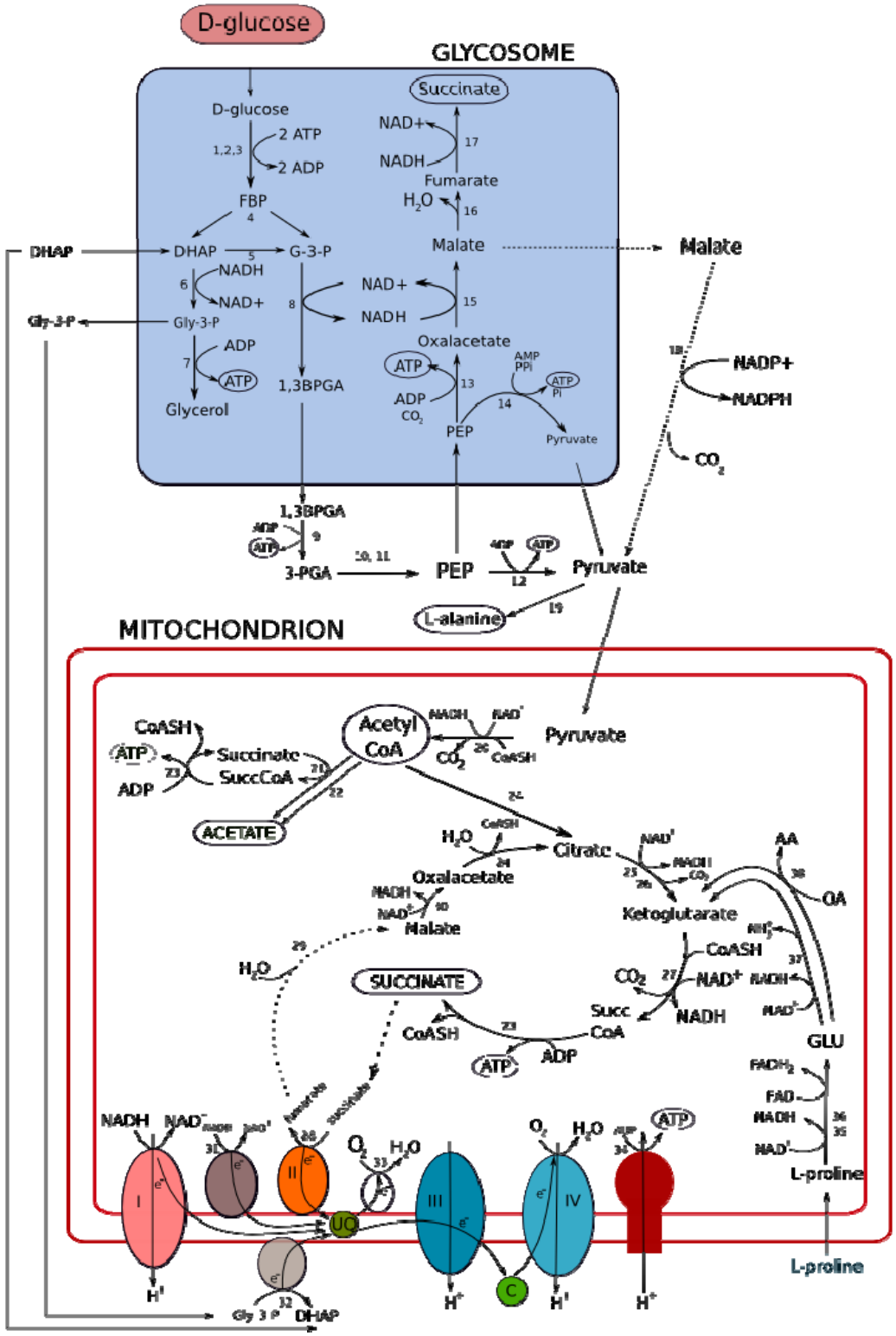

Figure 25. Schematic representation of key energy metabolism pathways from *T. brucei* procyclic form. Acetate, succinate, L-alanine and CO_2 are excreted products. Dashed lines represent steps that are supposed to happen under cultured conditions. Abbreviations: AA: amino acid; OA: 2-oxoacid; FBP: fructose 1,6 bisphosphate; DHAP: dihydroxyacetone phosphate; G-3-P: glycerol-3-phosphate;

1,3BPGA: 1,3 bisphosphoglycerate; 3-PGA: 3-phosphoglycerate; PEP: phospho*enol*pyruvate; PPi, pyrophosphate; Pi: inorganic phosphate; SuccCoA: succinyl CoA; CoASH: Coenzyme A; GLU: glutamate. Enzymes catalyzing reactions: 1, hexokinase; 2, glucose-6-phosphate isomerase; 3, phosphofructokinase; 4, aldolase; 5, triose-phosphate isomerase; 6, glycerol-3-phosphate dehydrogenase; 7, glycerol kinase; 8, glyceraldehyde dehydrogenase; 9, phosphoglycerate kinase; 10, phosphoglycerate mutase; 11, enolase; 12, pyruvate kinase; 13, phospho*enol*pyruvate carboxykinase; 14, pyruvate phosphate dikinase; 15, glycosomal malate dehydrogenase; 16, glycosomal fumarase; 17, NADH-fumarate reductase; 18, malic enzyme; 19, alanine aminotransferase; 20, pyruvate dehydrogenase complex; 21, acetate:succinate CoA transferase; 22, unknown enzyme; 23, succinyl CoA synthetase; 24, citrate synthase; 25, aconitase; 26, isocitrate dehydrogenase; 27, 2-ketoglutarate dehydrogenase complex; 28, succinate dehydrogenase (complex II); 29, mitochondrial fumarase; 30, mitochondrial malate dehydrogenase; 31, rotenone-insensitive NADH dehydrogenase; 32, glycerol-3-phosphate oxidase; 33, alternative oxidase; 34, F_0/F1 ATP synthase; 35, proline dehydrogenase; 36, pyrroline-5-carboxylate dehydrogenase; 37, glutamate dehydrogenase; 38, acetyl-CoA:glycine C-acetyl transferase; I, II, III and IV, respiratory chain complexes.

However, in MPGlu medium, which contained an excess of both glucose and proline, an inversion of the succinate production profile was observed: approximately 7-fold less succinate was produced in non-induced *Δmcp5/MCP5-nmyc*^{ti} cell line compared to the wildtype cell line and the induced *Δmcp5/MCP5-nmyc*^{ti} cell line ($p=0.01$). In contrast to succinate, no substantial changes could be observed for the cellular acetate formation ($p=0.089$) (Figure 24). Proline consumption, however, was found reduced (approximately 60% less) for both the induced and non-induced *Δmcp5/MCP5-nmyc*^{ti} cell lines, in comparison to the wildtype PCF449 cell line ($p<0.01$). The induced *Δmcp5/MCP5-nmyc*^{ti} cell line produced as much succinate in this medium as for the wildtype PCF449 cell line, confirming the complementation of the ADP/ATP exchange activity by expression of N-myc tagged MCP5.

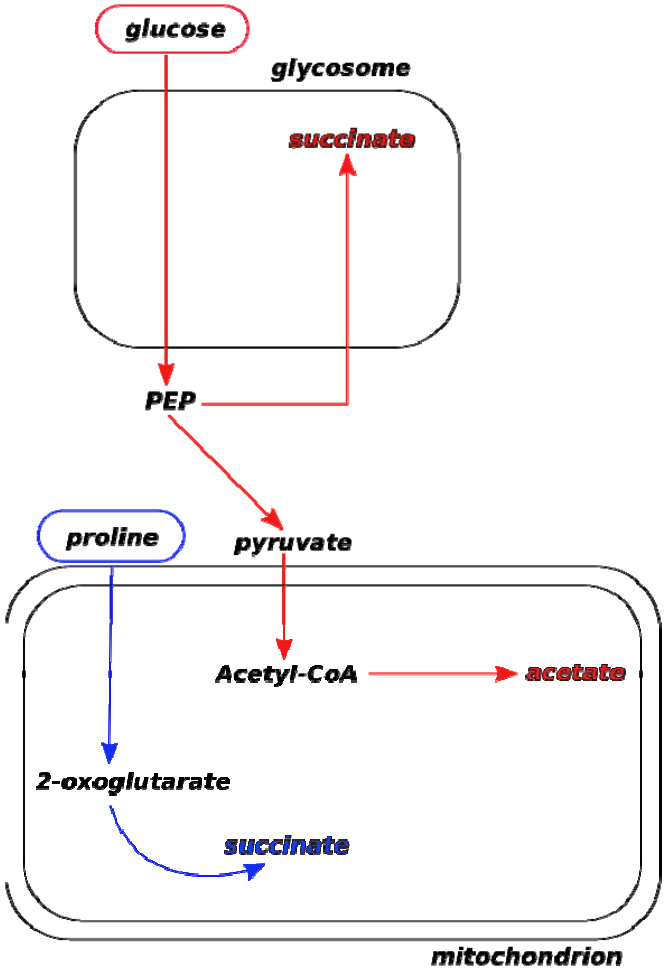

Figure 26. Schematic representation of procyclic from *T. brucei* energy flux depending on the carbon source used for energy production. Pathway shown in blue represents products from the metabolism of proline. Pathway shown in red represents products from glucose metabolism. Final excretion products are shown in the respective colours.

Comparison of the succinate produced by the different cell lines grown in NMP medium, which contained low levels of glucose (0.2-0.3mM) next to an excess of proline (5mM), revealed that in the non-induced *Δmcp5/MCP5-nmyc*^{ti} cell line approximately 6 times more succinate is produced per cell when compared to the wildtype PCF449 cell line (p=0.006). Similar to the observations for the other tested media, also in NMP medium no significant differences were found in cellular acetate production of the wildtype PCF449 cell line and the induced and non-induced *Δmcp5/MCP5-nmyc*^{ti} cell lines (p=0.658) (Figure 24).

It is evident from the results described above, that especially the production of the end-product succinate seems to be affected in the MCP5-depleted *⊿mcp5/MCP5-nmyc*^{ti} cell line. The measured succinate is the sum of the succinate produced in both the mitochondrion and the glycosome (Figure 24, (Besteiro *et al.*, 2002)). Published metabolic studies and gene knockout/depletion experiments with procyclic-form *T. brucei* indicated that the glycosome is the predominant site for succinate production. The main key intermediate in this process is phosphoenolpyruvate (PEP), which is derived from the glycolytic (partly glycosomal) degradation of glucose (Figures 25 and 26). The PEP produced in the cytosol is proposed to re-enter the glycosome, where it plays an important role in the recycling of glycosomal NAD^+ via a NADH-dependent fumarate reductase (Besteiro *et al*., 2002). This process further leads to the concomitant production of glycosomal ATP via a glycosomal phosphoenolpyruvate phosphokinase (PPDK). Re-entry of PEP into the glycosome was shown to be dependent on the activity of a cytosolic pyruvate kinase, which apparently acts as a kind of "switch" between the glycosomal and mitochondrial metabolism (Besteiro *et al*., 2005). The second main site of succinate production is the mitochondrion. This succinate is derived from the mitochondrial oxidation of α-ketoglutarate, which involves several TCA-cycle enzymes (Figure 25). Succinate will subsequently be oxidized by the mitochondrial succinate dehydrogenase (SDH) complex of the respiratory chain (Tielens and Van Hellemond, 1998). Different gene knockout/depletion studies revealed that the depletion of the SDH complex was only lethal for *T. brucei* in the absence glucose. This, and other results, confirmed that in the presence of glucose, majority of the succinate is produced in the glycosome (Besteiro *et al.*, 2002; Coustou *et al.*, 2008; Ebikeme *et al.*, 2010).

For our experiments, it is not possible to discriminate between the different sources of succinate, unless specific NMR-based carbon-labelling experiments would be performed in combination with the generated knockout cell lines (Ebikeme *et al.*, 2010; Besteiro *et al.*, 2002; Coustou *et al.*, 2003; Lamour *et al.*, 2005; Coustou *et al.*, 2008).

Using the above-described model (Figure 25, (Lamour *et al.*, 2005)), hypotheses were made in order to explain some of our observations. The first important observation made was the fact that succinate was still produced in the MCP5-depleted *T. brucei* cell line when grown in glucose-depleted GDMP medium (Figure 24). In this medium, *T. brucei* had to rely completely on proline as the sole source

for its energy metabolism. However for medium containing an excess of glucose, i.e. MPGlu, the results are reversed and revealed a significantly decreased succinate production in the same cell line. This difference in succinate production must be a direct consequence of the MCP5-depletion and is apparently dependent on the presence of glucose.

It is logic to assume that impairment of the major mitochondrial ADP/ATP exchange route, i.e. depletion of MCP5, will lead to a substantial accumulation of ATP in the mitochondrion and concomitant lack of available ADP. As a consequence, all ADP-requiring processes, like for example mitochondrial OXPHOS and SUBPHOS, will eventually become inhibited. Inhibition of OXPHOS will most probably result in a significant accumulation of NADH and the subsequent inhibition of all NAD-requiring processes like the mitochondrial proline degradation pathway. Thinking further along this line, it is anticipated that the succinate production in the mitochondrion will be decreased: remember, mitochondrial succinate production from proline is also dependent on the availability of sufficient ADP and NAD^+. Consequently, for the MCP5-depleted cell line most of the measured succinate has to be derived from the glycosome and its associated cytosolic metabolism, i.e. the formation of the key intermediate PEP and its re-entry into the glycosome.

Inhibition of OXPHOS in the MCP5-depleted cell line has also direct consequences for the glycosomal metabolism. Maintenance of the glycosomal redox balance was previously shown to be essential for trypanosome survival (Ebikeme *et al.*, 2010). Recycling of the glycosomal NADH to NAD^+ is dependent on different NADH-consuming enzyme reactions in the glycosome, and the so-called glycerol-3-phosphate/dihydroxyacetone phosphate (G3P/DHAP) redox shuttle (see Figure 25). This G3P/DHAP redox shuttle was previously shown to be essential for *T. brucei* and involves the combined action of a mitochondrion-associated glycerol-3-phosphate dehydrogenase and either the mitochondrial electron transport chain (OXPHOS) and/or an alternative oxidase (Figure 25). It is conceivable to assume that in the MCP5-depleted cell line the G3P/DHAP redox shuttle will also be inhibited. Consequently, the glycosomal redox balance will be completely dependent on the precise balance of the NADH producing step (i.e. step 8, Figure 25) and the NADH-consuming steps (i.e. step 15 and 16, Figure 25) in the glycosome itself.

In excess glucose, which is most probably used as the main carbon/energy source in MPGlu medium, a significant decrease of succinate production is observed for the

MCP5-depleted cell line. Following the above-described scenario, the production of less succinate in this cell line, in the presence of an excess of glucose, was not unexpected: to maintain the glycosomal redox balance in the MCP5-depleted cell line, less succinate had to be made in this organelle in order to avoid the depletion of NADH. This would further implicate that instead of succinate, malate would be the major intermediate leaving the glycosome. Part of this malate could be further converted to pyruvate by malic enzyme activity in the cytosol. Whether the MCP5-depleted cell line indeed excretes more malate and/or pyruvate into the culture medium has not (yet) been determined.

In case of proline as the sole carbon/energy source (i.e. GDMP medium), a succinate production is still observed in the MCP5-depleted cell line. As assumed above, majority of this succinate will be most probably produced in the glycosome. Consequently, one of the metabolic intermediates formed during the mitochondrial degradation of proline, has to leave the mitochondrion and enter the glycosome for further degradation to succinate. Using the above-described model, it is most likely that this metabolic intermediate is malate (Figure 25, (Lamour *et al.*, 2005)). Malate was previously suggested to act as a metabolic intermediate between glycosomes and mitochondria of *T. brucei* under glucose-depleted conditions (Coustou *et al.*, 2008; Aranda *et al.*, 2006). The substrate proline will initially be converted to ketoglutarate (producing 2 moles NADH per mol of proline), which is subsequently converted to malate by reversal of part of the TCA cycle (costing 2 NADH). In that way the redox balance in mitochondrion would be maintained, i.e. 2 NADH produced versus 2 NADH consumed, for which no functional electron chain is required as is the case for the MCP5-depleted cell line.

Once in the cytosol, malate would be serve as a substrate for two possible enzymatic steps with concomitant production of PEP (Figure 27) (Aranda *et al.*, 2006; Leroux *et al.*, 2011). We propose PEP as a key intermediary based on various assumptions: 1) PEP re-entry in the glycosome would ultimately produce succinate in this organelle, as observed in our results; 2) PEP as a substrate to PEPCK would result in the production of ATP in the glycosome, which is needed for synthesis purposes inside this organelle; and 3) PEP is an important intermediate of gluconeogenesis. Gluconeogenesis was previously proposed to take place in *T. brucei*, although its contribution to the overall metabolic flux has not been measured yet (Coustou *et al.*, 2008; Michels *et al.*, 2006; Hannaert *et al.*, 2003b).

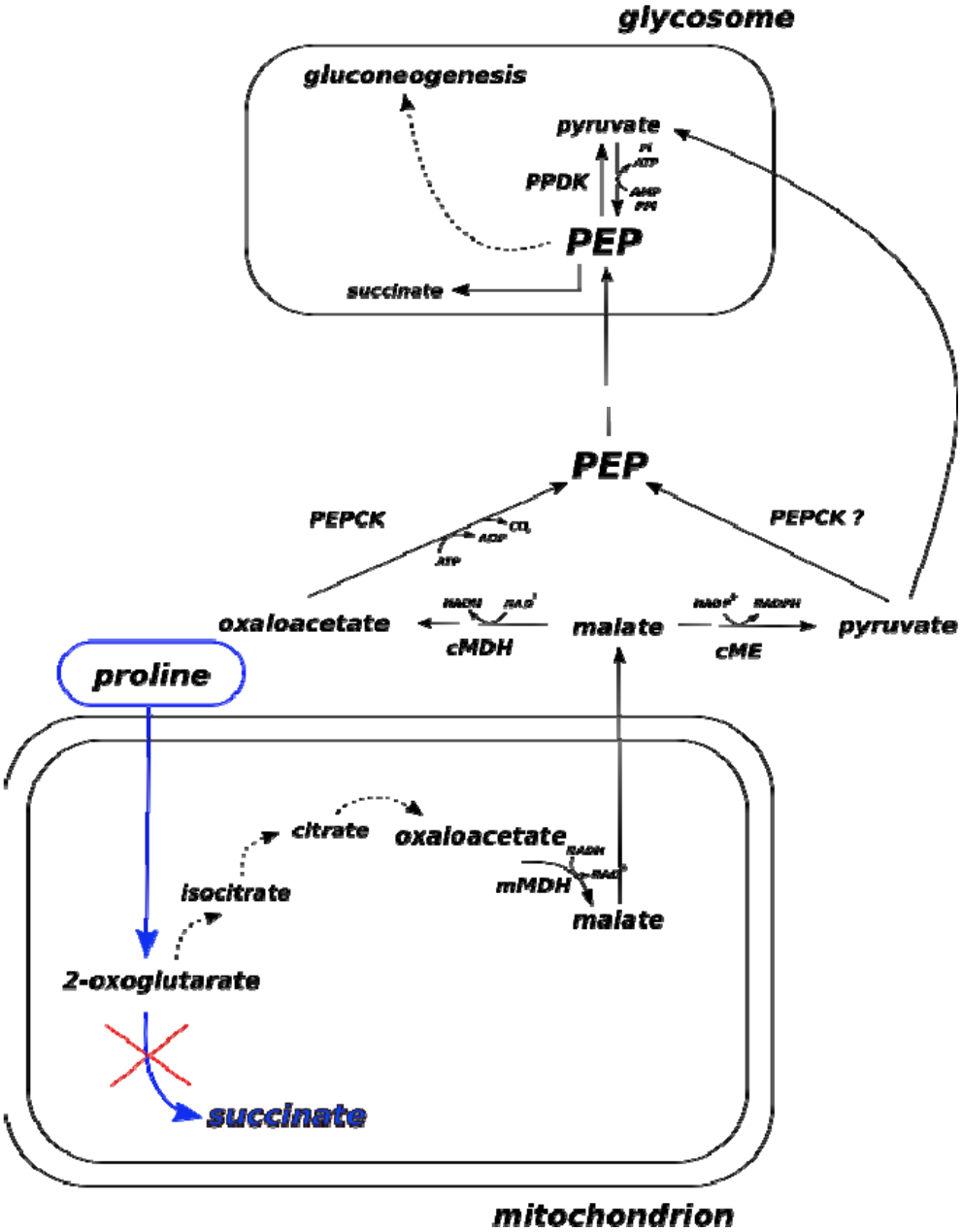

Figure 27. Schematic representation of the *Δmcp5/MCP5-nmyc*^{ti} cell line mitochondrial carbon flux in glucose-depleted conditions. Pathway in blue represents the WT carbon flux in glucose-depleted conditions. Dashed lines represent steps hypothesized to compensate for carbon redirection out of the mitochondrion. Abbreviations: cMDH: cytosolic malate dehydrogenase; mMDH: mitochondrial malate dehydrogenase; cME: cytosolic malic enzyme; PEPCK: phosphoenolpyruvate carboxikinase; PPDK: pyruvate phosphate dikinase; PPi: pyrophosphate; Pi: inorganic phosphate.

Comparison of the acetate values found for the induced and non-induced *Δmcp5/MCP5-nmyc*^{ti} cell lines and the wildtype PCF449 cell line, revealed no

differences in the acetate produced by these cell lines. The main key intermediate in the production of acetate is again PEP (see above and Figures 25 and 26), which is derived from the glycolytic (partly glycosomal) degradation of glucose. PEP is converted to pyruvate by the action of the cytosolic PYK (see Figure 25, step 12). Pyruvate can subsequently enter the mitochondrion, where it is finally converted to acetate with the aid of a mitochondrial acetate:succinate CoA-transferase: this enzyme transfers the energy-rich CoA group from acetyl-CoA to succinate, resulting in the formation of succinyl-CoA and acetate, and the subsequent production of ATP by SUBPHOS (Van Hellemond *et al.*, 1998; Rivière *et al.*, 2004). This mitochondrion-derived acetate was shown recently to be essential for the *de novo* biosynthesis of lipids in *T. brucei*: in that case acetate is transported from the mitochondrion to the cytosol, where it is again converted to acetyl-CoA by a cytosolic acetyl-CoA synthetase and the consumption of cytosolic ATP (Van Hellemond *et al.*, 1998; Rivière *et al.*, 2004; Rivière *et al.*, 2009). The formed acetyl-CoA is subsequently used for the production of phospholipids and neutral lipids in the cytosol.

As discussed above, depletion of MCP5 would have a substantial inhibitory effect on all ADP-requiring mitochondrial metabolic pathways. Correspondingly, an inhibition of the mitochondrial acetate production was expected upon depletion of the mitochondrial ADP/ATP exchanger MCP5. However, this seemed not to be the case: no differences in acetate production were found when comparing the different cell lines. A possible explanation for this unexpected result could be the possible presence of another (non-mitochondrial) acetate-producing pathway in *T. brucei*, which has to be independent of the mitochondrial succinate-producing metabolism. The existence of such an alternative acetate-producing pathway has previously been proposed, although not yet characterised (van Hellemond *et al*., 1998).

2.9. Further discussion of inconsistencies and unexpected results

Comparison of the growth curves (section 2.6), substrate consumption and end-product formation profiles (sections 2.7 and 2.8), and mitochondrial ATP-production (section 2.5) of the different cell lines grown in various culture media, resulted in the discovery of some inconsistencies/unexpected results, which requires further discussion.

The most prominent inconsistency was found with respect to the growth curves and the observed mitochondrial ATP production, which is used as an indicator for ADP/ATP exchange activity. During growth experiments on different culture media (section 2.6, Figures 17 and 18), invariably only a partial complementation was found when comparing the growth of the induced *Δmcp5/MCP5-nmyc*^{ti} cell line (expressing N-myc tagged MCP5) to that of the "wildtype" PCF449. In section 2.6, two possible explanations were given for this unexpected incomplete restoration of "wildtype"-level growth: (A) the added N-term myc-tag could affect the transport function of MCP5, or (B) the myc-tagged MCP5 version is actually over-expressed (2-3 fold) when compared to the expression of the native MCP5 in the wildtype (not shown), which could negatively affect the function of the mitochondrion. The results obtained for the mitochondrial ATP-production experiments in section 2.8 however discredited both explanations: when comparing the mitochondrial ATP-production (i.e. ADP/ATP exchange function) of the induced *Δmcp5/MCP5-nmyc*^{ti} cell line to that of the "wildtype" PCF449 cell line, no differences were found regarding the total ADP/ATP exchange capacity of these mitochondria when using either succinate or ketoglutarate as metabolic substrates. This suggested that the recombinant N-myc tagged MCP5 protein was fully functional, and could restore the observed mitochondrial ATP-production deficit to wildtype levels in the *Δmcp5/MCP5-nmyc*^{ti} cell line upon induction.

However, as discussed in Chapter I, ADP/ATP-carriers do not only exchange mitochondrial ATP for cytosolic ADP, but are also involved in the regulation of other important mitochondrial processes. The involvement of ADP/ATP-carriers in the regulation of mitochondrial metabolism is indicated by the observed interactions of these nucleotide exchangers with important mitochondrial complexes, like for example the mitochondrial permeability transition pore and the various OXPHOS complexes (Chapter I: sections 10, 11 and 12). Protein interaction has been suggested between ADP/ATP-carrier monomers (homodimer conformation: Chapter I, section 9), with other MCF proteins, and with different proteins of the MPTP and OXPHOS complexes (Chapter I, sections 11 and 12). Further, insertion or deletion mutations of either the amino- or carboxy-terminal ends of the ADP/ATP-carrier were recently reported to affect its function (Iwahashi *et al.*, 2008; Clemencon *et al.*, 2008). Its therefore conceivable that an amino- or carboxy-terminal sequence extension of the ADP/ATP-carrier, which is the case for the N-myc tagged MCP5 used in these experiments, could possibly lead to defects in protein interaction, but apparently not in ADP/ADP exchange function.

Another unexpected result was the observation that the MCP5-depleted (non-induced *Δmcp5/MCP5-nmyc*^{ti}) cell line did not grow better in glucose-supplemented MPGlu medium than in glucose-depleted GDMP medium (Figure 18). It was anticipated that the MCP5-depleted cell line, which is hampered in its ability to export ATP from the mitochondrion, would compensate for its cytosolic ATP deficit by a major redirection of its metabolism (in the presence of excess glucose) towards the glucose-dependent glycosomal pathway with concomitant synthesis of cytosolic ATP. Remember, this ATP is normally derived from proline degradation in the mitochondrion (Figure 25). As expected, proline consumption was significantly reduced in the MCP5-depleted cell line to approximately 50% of the wildtype PCF449 levels. However, substrate consumption analysis revealed that glucose was consumed at the same rate in the MCP5-depleted cell line as in the "wildtype" PCF449 cell line. Further, no significant differences in succinate (product of glucose and proline metabolism) or acetate (product of proline metabolism) production were found when comparing the different cell lines grown in MPGlu medium. Depletion of the mitochondrial ADP/ATP carrier MCP5 did apparently not lead to the expected increase in glucose consumption of the MCP5-depleted cell line grown in glucose-supplemented MPGlu medium. The only explanation for this unexpected result would be the occurrence of a complete shift of glucose and proline catabolism to the glycosome and the cytosol, thereby omitting the respective mitochondrial parts of the degradation pathways (Figure 25). This, however, would again require a non-mitochondrial acetate-producing pathway in *T. brucei*, which has to be independent of the mitochondrial succinate-producing metabolism. As discussed previously, such pathway has not yet been characterised in this parasite (Van Hellemond *et al.*, 1998).

The lack of significant difference in the formation of succinate by the uninduced *Δmcp5/MCP5-nmyc*^{ti} when compared to the wildtype is another inconsistency in the present work. Taking into account that the production succinate in the *Δmcp5/MCP5-nmyc*^{ti} cell line when grown in NMP did show a significant difference, this result is somewhat surprising. Although the possibility of experimental error cannot be discarded, the only difference between NMP and GDMP is the very little concentration of glucose found in the FCS of the media. If the adaptation of the KO cell line to the GDMP (where no glucose from FCS can be found) modulates the metabolite excretion pattern in a different way to those cultures in which a very small concentration of glucose can be obtained, remains to be elucidated.

3. Conclusion

Sequence analysis, phylogenetic reconstruction, gene knockout studies and mitochondrial ATP production assays with digitonin-permeabilized *T. brucei* cells indicated that MCP5 functions as a mitochondrial ADP/ATP carrier in this parasite. The observed inability of N-myc tagged MCP5 to complement the growth defect in the MCP5 knockout cell line, indicated that MCP5 is not only essential for the mitochondrial exchange of ADP/ATP, but that this AAC is most probably also involved in the regulation of other essential cellular processes through its interaction with other proteins. It is therefore hypothesized that the knockout of MCP5 might be redirecting carbons out of the mitochondrion in order to compensate for the deficit of the mitochondrial ADP/ATP carrier in *T. brucei* procyclic form.

4. References

Adrian, G. S., McCammon, M. T., Montgomery, D. L. & Douglas, M. G. 1986. Sequences required for delivery and localization of the ADP/ATP translocator to the mitochondrial inner membrane. *Mol Cell Biol,* 6**,** 626-34.

Ajioka, J. & Swindle, J. 1996. The calmodulin-ubiquitin (CUB) genes of Trypanosoma cruzi are essential for parasite viability. *Mol Biochem Parasitol,* 78**,** 217-25.

Allemann, N. & Schneider, A. 2000. ATP production in isolated mitochondria of procyclic Trypanosoma brucei. *Mol Biochem Parasitol,* 111**,** 87-94.

Aquila, H., Link, T. A. & Klingenberg, M. 1987. Solute carriers involved in energy transfer of mitochondria form a homologous protein family. *FEBS Lett,* 212**,** 1-9.

Aranda, A., Maugeri, D., Uttaro, A. D., Opperdoes, F., Cazzulo, J. J. & Nowicki, C. 2006. The malate dehydrogenase isoforms from Trypanosoma brucei: subcellular localization and differential expression in bloodstream and procyclic forms. *Int J Parasitol,* 36**,** 295-307.

Ben Amar, M. F., Pays, A., Tebabi, P., Dero, B., Seebeck, T., Steinert, M. & Pays, E. 1988. Structure and transcription of the actin gene of Trypanosoma brucei. *Mol Cell Biol,* 8**,** 2166-76.

Besteiro, S., Barrett, M. P., Riviere, L. & Bringaud, F. 2005. Energy generation in insect stages of Trypanosoma brucei: metabolism in flux. *Trends Parasitol,* 21**,** 185-91.

Besteiro, S., Biran, M., Biteau, N., Coustou, V., Baltz, T., Canioni, P. & Bringaud, F. 2002. Succinate secreted by Trypanosoma brucei is produced by a novel and unique glycosomal enzyme, NADH-dependent fumarate reductase. *J Biol Chem,* 277**,** 38001-12.

Bochud-Allemann, N. & Schneider, A. 2002. Mitochondrial substrate level phosphorylation is essential for growth of procyclic Trypanosoma brucei. *J Biol Chem,* 277**,** 32849-54.

Chaudhuri, M., Ott, R. D. & Hill, G. C. 2006. Trypanosome alternative oxidase: from molecule to function. *Trends Parasitol,* 22**,** 484-91.

Clayton, C. 1999. Genetic manipulation of kinetoplastida. *Parasitol Today,* 15**,** 372-378.

Clemencon, B., Rey, M., Dianoux, A. C., Trezeguet, V., Lauquin, G. J., Brandolin, G. & Pelosi, L. 2008. Structure-function relationships of the C-terminal end of the Saccharomyces cerevisiae ADP/ATP carrier isoform 2. *J Biol Chem,* 283**,** 11218-25.

Colasante, C., Alibu, V. P., Kirchberger, S., Tjaden, J., Clayton, C. & Voncken, F. 2006. Characterization and developmentally regulated localization of the mitochondrial carrier protein homologue MCP6 from Trypanosoma brucei. *Eukaryot Cell,* 5**,** 1194-205.

Colasante, C., Peña Diaz, P., Clayton, C. & Voncken, F. 2009. Mitochondrial carrier family inventory of Trypanosoma brucei brucei: Identification, expression and subcellular localisation. *Mol Biochem Parasitol,* 167**,** 104-17.

Coustou, V., Besteiro, S., Biran, M., Diolez, P., Bouchaud, V., Voisin, P., Michels, P. A. M., Canioni, P., Baltz, T. & Bringaud, F. 2003. ATP generation in the Trypanosoma brucei procyclic form: cytosolic substrate level is essential, but not oxidative phosphorylation. *J Biol Chem,* 278**,** 49625-35.

Coustou, V., Biran, M., Breton, M., Guegan, F., Riviere, L., Plazolles, N., Nolan, D., Barrett, M. P., Franconi, J. M. & Bringaud, F. 2008. Glucose-induced remodeling of intermediary and energy metabolism in procyclic Trypanosoma brucei. *J Biol Chem,* 283**,** 16342-54.

Drgon, T., Sabová, L., Nelson, N. & Kolarov, J. 1991. ADP/ATP translocator is essential only for anaerobic growth of yeast Saccharomyces cerevisiae. *FEBS Lett,* 289**,** 159-62.

Ebikeme, C., Hubert, J., Biran, M., Gouspillou, G., Morand, P., Plazolles, N., Guegan, F., Diolez, P., Franconi, J.-M., Portais, J.-C. & Bringaud, F. 2010. Ablation of succinate production from glucose metabolism in the procyclic trypanosomes induces metabolic switches to the glycerol 3-phosphate/dihydroxyacetone phosphate shuttle and to proline metabolism. *J Biol Chem,* 285**,** 32312-24.

Gawaz, M., Douglas, M. G. & Klingenberg, M. 1990. Structure-function studies of adenine nucleotide transport in mitochondria. II. Biochemical analysis of distinct AAC1 and AAC2 proteins in yeast. *J Biol Chem,* 265**,** 14202-8.

Gibson, W. C., Swinkels, B. W. & Borst, P. 1988. Post-transcriptional control of the differential expression of phosphoglycerate kinase genes in Trypanosoma brucei. *J Mol Biol,* 201**,** 315-325.

Hannaert, V., Bringaud, F., Opperdoes, F. R. & Michels, P. A. 2003a. Evolution of energy metabolism and its compartmentation in Kinetoplastida. *Kinetoplastid Biol Dis,* 2**,** 11.

Hannaert, V., Saavedra, E., Duffieux, F., Szikora, J.-P., Rigden, D. J., Michels, P. A. M. & Opperdoes, F. R. 2003b. Plant-like traits associated with metabolism of Trypanosoma parasites. *Proc Natl Acad Sci USA,* 100**,** 1067-71.

Heidkamper, D., Muller, V., Nelson, D. R. & Klingenberg, M. 1996. Probing the role of positive residues in the ADP/ATP carrier from yeast. The effect of six arginine mutations on transport and the four ATP versus ADP exchange modes. *Biochemistry,* 35**,** 16144-52.

Imboden, M. A., Laird, P. W., Affolter, M. & Seebeck, T. 1987. Transcription of the intergenic regions of the tubulin gene cluster of Trypanosoma brucei: evidence for a polycistronic transcription unit in a eukaryote. *Nucleic Acids Res,* 15**,** 7357-68.

Iwahashi, A., Ishii, A., Yamazaki, N., Hashimoto, M., Ohkura, K., Kataoka, M., Majima, E., Terada, H. & Shinohara, Y. 2008. Functionally important conserved length of C-terminal regions of yeast and bovine ADP/ATP carriers, identified by deletion mutants studies, and water accessibility of the amino acids at the C-terminal region of the yeast carrier. *Mitochondrion,* 8**,** 196-204.

Klingenberg, M. 2008. The ADP and ATP transport in mitochondria and its carrier. *BBA-Biomembranes,* 1778**,** 1978-2021.

Kohl, L., Drmota, T., Thi, C. D., Callens, M., Van Beeumen, J., Opperdoes, F. R. & Michels, P. A. 1996. Cloning and characterization of the NAD-linked glycerol-3-phosphate dehydrogenases of Trypanosoma brucei brucei and

Leishmania mexicana mexicana and expression of the trypanosome enzyme in Escherichia coli. *Mol Biochem Parasitol,* 76**,** 159-73.

Kolarov, J., Kolarova, N. & Nelson, N. 1990. A third ADP/ATP translocator gene in yeast. *J Biol Chem,* 265**,** 12711-6.

Lamour, N., Rivière, L., Coustou, V., Coombs, G. H., Barrett, M. P. & Bringaud, F. 2005. Proline Metabolism in Procyclic Trypanosoma brucei Is Down-regulated in the Presence of Glucose. *J Biol Chem,* 280**,** 11902-11910.

Lasorsa, F. M., Scarcia, P., Erdmann, R., Palmieri, F., Rottensteiner, H. & Palmieri, L. 2004. The yeast peroxisomal adenine nucleotide transporter: characterization of two transport modes and involvement in DeltapH formation across peroxisomal membranes. *Biochem J,* 381**,** 581-5.

Lawson, J., Gawaz, M., Klingenberg, M. & Douglas, M. 1990. Structure-function studies of adenine nucleotide transport in mitochondria. I. Construction and genetic analysis of yeast mutants encoding the ADP/ATP carrier protein of mitochondria. *J Biol Chem,* 265**,** 14195-14201.

Leroux, A. E., Maugeri, D. A., Opperdoes, F. R., Cazzulo, J. J. & Nowicki, C. 2011. Comparative studies on the biochemical properties of the malic enzymes from Trypanosoma cruzi and Trypanosoma brucei. *FEMS Microbiol Lett,* 314**,** 25-33.

Löytynoja, A. & Milinkovitch, M. C. 2001. Molecular phylogenetic analyses of the mitochondrial ADP-ATP carriers: the Plantae/Fungi/Metazoa trichotomy revisited. *Proc Natl Acad Sci USA,* 98**,** 10202-7.

Michels, P. A. & Opperdoes, F. R. 1991. The evolutionary origin of glycosomes. *Parasitol Today (Regul Ed),* 7**,** 105-9.

Michels, P. A. M., Bringaud, F., Herman, M. & Hannaert, V. 2006. Metabolic functions of glycosomes in trypanosomatids. *Biochim Biophys Acta,* 1763**,** 1463-77.

Mottram, J. C., McCready, B. P., Brown, K. G. & Grant, K. M. 1996. Gene disruptions indicate an essential function for the LmmCRK1 cdc2-related kinase of Leishmania mexicana. *Mol Microbiol,* 22**,** 573-83.

Müller, V., Basset, G., Nelson, D. R. & Klingenberg, M. 1996. Probing the role of positive residues in the ADP/ATP carrier from yeast. The effect of six arginine mutations of oxidative phosphorylation and AAC expression. *Biochemistry,* 35**,** 16132-43.

Overath, P., Czichos, J. & Haas, C. 1986. The effect of citrate/cis-aconitate on oxidative metabolism during transformation of Trypanosoma brucei. *Eur J Biochem,* 160**,** 175-82.

Palmieri, L., Rottensteiner, H., Girzalsky, W., Scarcia, P., Palmieri, F. & Erdmann, R. 2001. Identification and functional reconstitution of the yeast peroxisomal adenine nucleotide transporter. *EMBO J,* 20**,** 5049-5059.

Powell, S. J., Medd, S. M., Runswick, M. J. & Walker, J. E. 1989. Two bovine genes for mitochondrial ADP/ATP translocase expressed differences in various tissues. *Biochemistry,* 28**,** 866-73.

Rivière, L., Moreau, P., Allmann, S., Hahn, M., Biran, M., Plazolles, N., Franconi, J.-M., Boshart, M. & Bringaud, F. 2009. Acetate produced in the mitochondrion is the essential precursor for lipid biosynthesis in procyclic trypanosomes. *Proc Natl Acad Sci USA,* 106**,** 12694-9.

Rivière, L., van Weelden, S. W. H., Glass, P., Vegh, P., Coustou, V., Biran, M., van Hellemond, J. J., Bringaud, F., Tielens, A. G. M. & Boshart, M. 2004. Acetyl:succinate CoA-transferase in procyclic Trypanosoma brucei. Gene identification and role in carbohydrate metabolism. *J Biol Chem,* 279**,** 45337-46.

Robinson, A. J. & Kunji, E. R. S. 2006. Mitochondrial carriers in the cytoplasmic state have a common substrate binding site. *Proc Natl Acad Sci USA,* 103**,** 2617-22.

Saraste, M. & Walker, J. 1982. Internal sequence repeats and the path of polypeptide in mitochondrial ADP/ATP translocase. *FEBS Lett,* 144**,** 250-4.

Schneider, A., Charriere, F., Pusnik, M. & Horn, E. K. 2007. Isolation of mitochondria from procyclic Trypanosoma brucei. *Methods Mol Biol,* 372**,** 67-80.

Tielens, A. G. & Van Hellemond, J. J. 1998. Differences in energy metabolism between trypanosomatidae. *Parasitol Today (Regul Ed),* 14**,** 265-72.

Tielens, A. G. M. & van Hellemond, J. J. 2009. Surprising variety in energy metabolism within Trypanosomatidae. *Trends Parasitol,* 25**,** 482-90.

Van Hellemond, J., Opperdoes, F. & Tielens, A. 1998. Trypanosomatidae produce acetate via a mitochondrial acetate: succinate CoA transferase. *Proc Natl Acad Sci USA,* 95**,** 3036-3041.

van Roermund, C. W., Drissen, R., van Den Berg, M., Ijlst, L., Hettema, E. H., Tabak, H. F., Waterham, H. R. & Wanders, R. J. 2001. Identification of a peroxisomal ATP carrier required for medium-chain fatty acid beta-oxidation and normal peroxisome proliferation in Saccharomyces cerevisiae. *Mol Cell Biol,* 21**,** 4321-9.

Zíková, A., Schnaufer, A., Dalley, R. A., Panigrahi, A. K. & Stuart, K. D. 2009. The F(0)F(1)-ATP synthase complex contains novel subunits and is essential for procyclic Trypanosoma brucei. *PLoS Pathog,* 5**,** e1000436.#

Chapter V.

Study of the ADP/ATP-exchange function of MCP5: protein expression, purification, and reconstitution into liposomes

Table of Contents

Chapter V . Study of the ADP/ATP-exchange function of MCP5: protein expression, purification, and reconstitution into liposomes.

1. Introduction

The classical approach to study the transport function of MCF proteins consists of the isolation/purification of the respective metabolite carrier through affinity column chromatography, its reconstitution into liposomes, and the subsequent determination of its substrate specificity and transport kinetics via metabolite transport assays (Krämer and Klingenberg, 1977; Klingenberg *et al.*, 1995; Palmieri *et al.*, 1995). Key to this approach is the provision of a suitable *in vitro* membrane-like environment, which allows the MCF protein to arrange itself into its proper functional conformation and be capable of performing transport. This *in vitro* membrane-like environment, i.e. the liposome, forms a closed compartment, which is conveniently used to study the exchange of metabolites into and out of this compartment and enables the quantification of this transport process.

In this Chapter, a similar approach is described which was used for the study of the ADP/ATP exchange function of *T. brucei* MCP5. For this purpose, recombinant versions of MCP5 were expressed in various well-established heterologous expression systems, i.e. different *Escherichia coli* strains and the *Spodoptera frugiperda* Sf9 insect cell line. The recombinant MCP5 protein, either expressed in the prokaryotic *E. coli* or the eukaryotic *S. frugiperda* system, was isolated and purified from their respective hosts by using a range of techniques, including His-tag directed affinity chromatography, differential detergent extraction, and classical column chromatography. Once the MCP5 protein was isolated, it was subsequently reconstituted into liposomes, again by using different techniques. In an alternative approach, recombinant MCP5 protein was expressed in an *E. coli* strain, followed by *in vivo* metabolite transport assays, thereby omitting the isolation and reconstitution steps used in the classical approach.

Unfortunately, this Chapter described approaches that were only partially successful. Aim of this chapter was to give an overview of the many different techniques that have been tried for assessment of the ADP/ATP transport function of *T. brucei* MCP5. This information will be useful for future functional reconstitution attempts.

2. Results and Discussion

2.1. Heterologous expression of MCP5 in the prokaryotic *E. coli* system

Escherichia coli strain BL21 is one of the most common prokaryotic strains that are used for protein heterologous expression (Sorensen and Mortensen, 2005). The first expression trials were performed in *E. coli* strain BL21(DE3), using the commercially available pTrcHis expression vector (Invitrogen). IPTG-inducible expression from this vector is driven by the Ptrc promoter and will lead to the addition of a 6xHis-tag to the N-terminal end of the expressed protein. We initially used standard conditions for the expression of His-tagged MCP5. However, after many attempts, no expression of His-tagged MCP5 could be observed, even after changing all possible expression conditions, including the use of different culture media, the culture of *E. coli* strain BL21(DE3) at different (lower) temperatures, and the use of different IPTG concentrations.

This failure to express any *T. brucei* MCP5 protein in the commonly used *E. coli* strain BL21(DE3) lead to the hypothesis that the MCP5 gene maybe contained DNA codons that were rare in the used *E. coli* BL21(DE3) strain, therefore hampering its expression (Sharp and Li, 1987). To assess this possibility, a codon table was generated for *T. brucei* MCP5 (and other *T. brucei* MCF proteins), which was compared to those from other proteins that could readily be expressed in *E. coli*, like for example the *Saccharomyces cerevisiae* ADP/ATP carrier PET9. Codon-usage analysis was performed using the Graphical Codon Usage Analyzer 2.0 (Fuhrmann *et al.*, 2004). The outcome of this analysis indicated that the MCP5 sequence indeed contained most of the codons available for each of the amino acids in the genetic code, including a few which are less commonly used in *E. coli* (Figure 1). For example, the 6 different DNA codons coding for arginine (R) were all present in the MCP5 DNA sequence, whereas in *E. coli* only *2 out of 6 arginine codons* are commonly used.

Since some of the DNA codons used in the *T. brucei* MCP5 sequence could cause the observed expression problems, various other *E. coli* strains were tested for the expression of MCP5, including the Rossetta2(DE3)pLysS (Novagen®), Tuner(DE3)pLysS (Novagen®) and Rosetta-gami(DE3)pLysS (Novagen®) strains. These strains bear the pRARE plasmid, which codes for additional tRNAs codons that are usually rare (Novy *et al.*, 2001). Next to the different *E. coli* protein expression strains, also various plasmids harboring different promoters were tested.

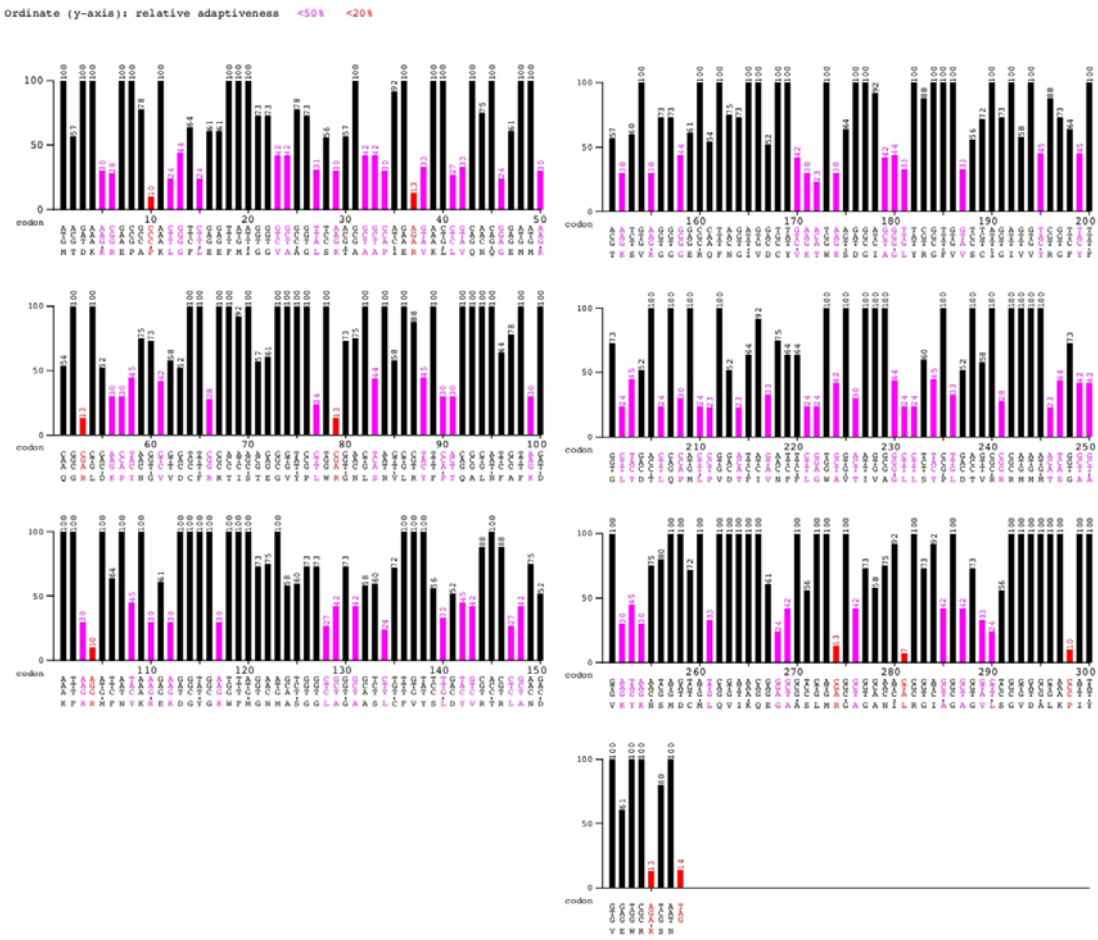

Figure 1. DNA codon usage analysis of the *T. brucei* MCP5 sequence, using the *Escherichia coli* DNA codon usage table for comparison. Residues in fuchsia and red represent codons with <50% or <20% adaptiveness of the host organism's protein production, respectively. Analysis was performed using the Graphical Codon Usage Analyzer 2.0 platform.

Western blotting revealed that some MCP5 could be expressed to very low levels (just above the detection limit for western blot analysis) within one hour of induction with IPTG. Shortly after, the *E. coli* cells would stop growing and eventually the culture would lyse (results not shown). Apparently, *E. coli* is not able to cope with the expression of *T. brucei* MCP5, both under standard conditions, which were successfully used for the expression of MCF proteins from other eukaryotes, and in the special *E. coli* Rosetta strains, which should compensate for the somewhat deviating DNA codon-usage of *T. brucei* proteins. These results indicated an additional problem, i.e. that the expression of *T. brucei* MCP5 might be toxic for *E. coli*.

Since it was possible to produce very low levels of *T. brucei* MCP5, but impossible to keep the *E. coli* cells long enough alive to isolate sufficient amounts of the protein, a different expression approach was tried: the so-called auto-induction procedure (Studier, 2005). This auto-induction procedure is based on the principle that protein expression is only induced upon shift of the *E. coli* culture from glucose metabolism to lactose metabolism. At the beginning of the auto-induction procedure, the *E. coli* expression strain is grown on glucose-containing medium (i.e. the non-induced condition), which will allow the selection of stable growing bacterial clones that are not affected by the possible leakage of toxic (i.e. MCP5) protein products. The obtained stable growing *E. coli* culture is subsequently transferred to a medium containing a low concentration of glucose and an excess of lactose as carbon/energy source. Upon depletion of the glucose, the *E. coli* cells will switch from glucose metabolism to lactose metabolism, which subsequently will lead to the induction of protein (i.e. MCP5) expression by lactose. Since the induction is triggered by lactose itself and not by IPTG, the concentration of the inductor reaching/entering the cells is controlled by a natural permease activity (Studier, 2005). Accordingly, the induction is much slower that when the membrane-soluble IPTG is added to the cells. A further advantage of this method is that the induction will start at higher cell densities: this will aid the large-culture expression of “toxic” proteins that only can be expressed in small cellular quantities, which is apparently the case for *T. brucei* MCP5.

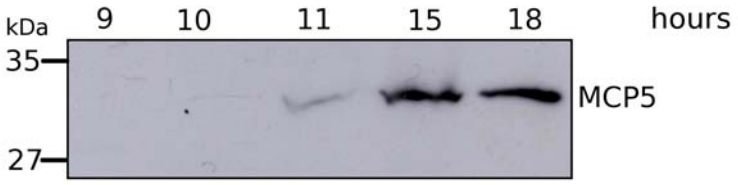

Figure 2. Western blot analysis showing the expression of *T. brucei* MCP5 in *E. coli* Rossetta2(DE3)pLysS, followed for 18 hours of culture in auto-induction medium. 40mg of total cell protein was loaded per well. A commercial His-tag antibody was used for the detection of the His-tagged MCP5 protein.

A typical result found for the auto-induced expression of *T. brucei* MCP5 in *E. coli* Rossetta2(DE3)pLysS is shown in Figure 2. Western blot analysis of the different culture samples taken in time revealed a maximum expression of *T. brucei* MCP5 at

15 hours of culture in the auto-induction medium. This result indicated that expression of His-tagged MCP5 is possible under these (auto-induction) conditions, although the quantity of total expressed MCP5 is still rather low. Despite the fact that MCP5 was able to express under the aforementioned conditions, the cell culture harboring the His-tagged MCP5 fails to grow further after auto-induction commences (Figure 3), a clear sign of the toxic effect this carrier has on *E. coli* cells.

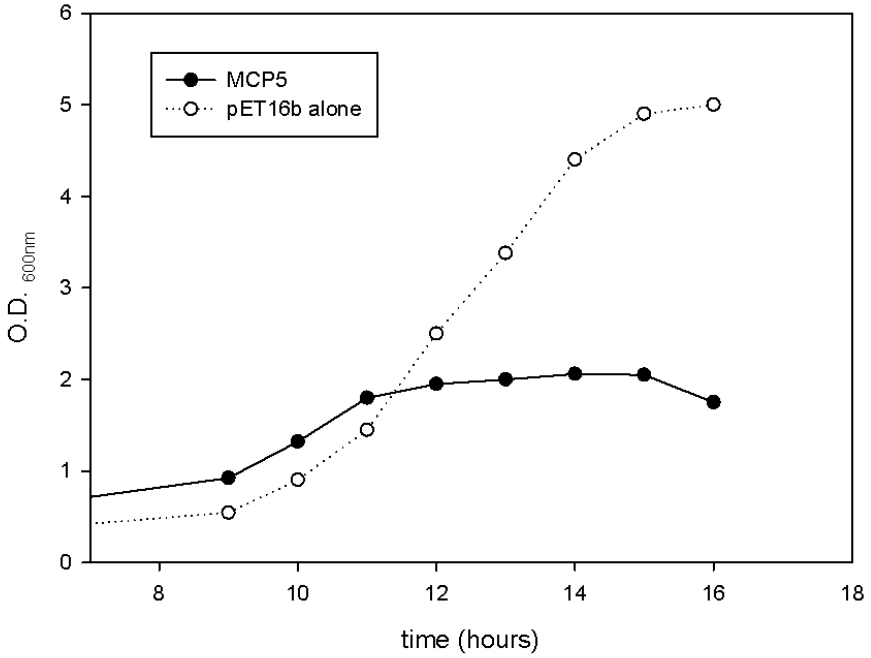

Figure 3. Growth curves for cell cultures of auto-induced *E. coli* Rossetta2(DE3)pLysS expressing His-tagged MCP5 (●) or the same *E. coli* strain but now containing an empty pET16b expression vector as control (o).

2.2. Heterologous expression of MCP5 in the eukaryotic *S. frugiperda* system

Several groups dealing with the biochemical characterization of membrane proteins from higher eukaryotes have recently reported misfolding issues and/or absence of post-translational modifications in commonly used prokaryotic heterologous expression systems that hampered the final functional reconstitution and activity of these proteins in liposomes (Heimpel *et al.*, 2001; Wagner *et al.*, 2006). Instead, some laboratories used different yeasts for the study of certain membrane proteins (Yadava and Ockenhouse, 2003; Cai and Gros, 2003), whereas others preferred to use insect cell lines for the expression of membrane proteins (Madeo *et al.*, 2009). Especially the insect cell expression system based on ovarian cell lines of the Fall Armyworm *Spodoptera frugiperda*, was found to be suitable for the expression of

"functional" MCF proteins. This expression system not only provides sufficient quantities of recombinant protein, but also allows the proper folding of the expressed proteins and eventual post-transcriptional modifications. More recently, successful expression and reconstitution was reported for an MCF protein from eel, i.e. the citrate carrier CIC, using the *S. frugiperda* insect cell line Sf9 for the expression of this protein (Madeo *et al*., 2009).

Recombinant expression of proteins in *S. frugiperda* insect cell lines is based on site-specific transposition of the MCP5-containing expression cassette into a baculovirus shuttle vector or bacmid (*Autographa californica* multiple nuclear polyhedrosis virus or AcMNPV), which can be propagated in *E. coli* cells. The resulting recombinant virus is then used for the transfection of different ovarian cell lines from *Spodoptera frugiperda*, i.e. Sf9 or Sf21, respectively. A simplified scheme showing an overview for the production of recombinant proteins using the insect cells baculovirus-infection system is shown in Figure 4.

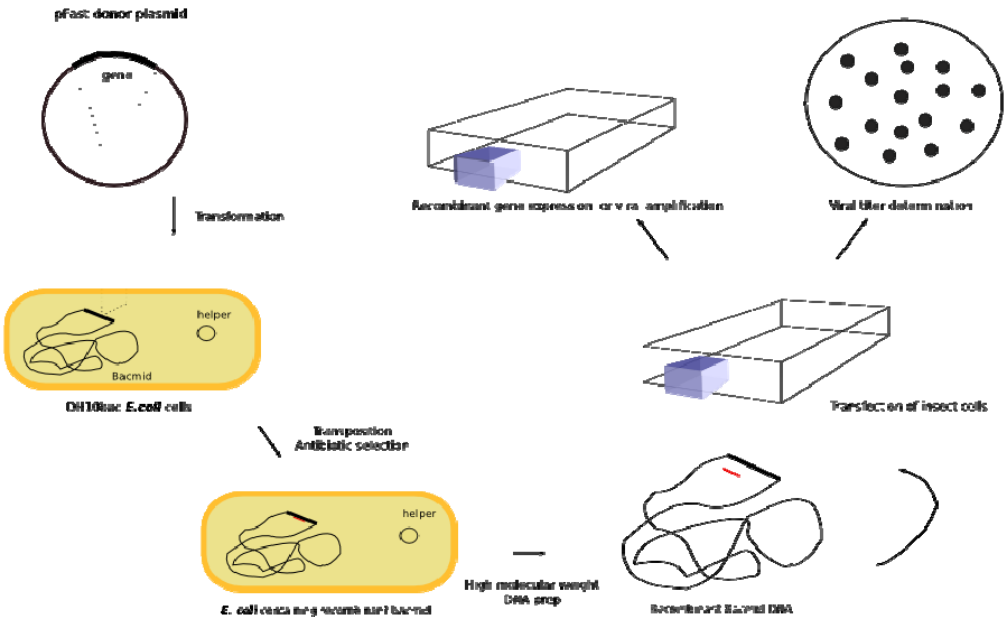

Figure 4. Schematic representation for the production of recombinant proteins using the insect cells baculovirus-infection system. pFastBac™ vector and the DH10bac™ vector are the major components of the baculovirus insect dell expression system kit developed by Invitrogen.

After the initial standardization of the required expression conditions, we were able to express low but sufficient quantities of *T. brucei* MCP5 protein using the *S. frugiperda* insect cell line Sf9. A representative western blot analysis is shown in Figure 5. For comparison, other *T. brucei* MCF proteins were expressed to multi-fold higher cellular concentrations than MCP5 when using *S. frugiperda* Sf9 and similar expression conditions. For example, *T. brucei* MCP12 was produced to 13-fold higher cellular concentrations than MCP5 (results not shown: C. Colasante, personal communication). This result indicated that MCP5, even when expressed in a eukaryotic heterologous expression system, could not be expressed to high cellular levels. Its unclear at this point, what causes this inherently low expression of the *T. brucei* MCP5 protein.

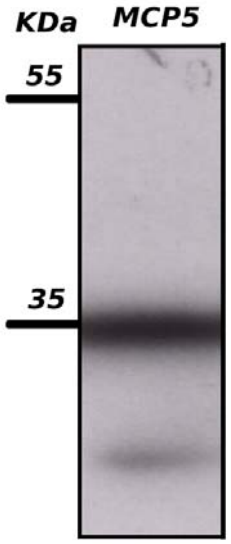

Figure 5. Western blot analysis showing the expression of *T. brucei* MCP5 in *S. frugiperda* Sf9. $2x10^6$ cells were loaded per well, and a commercial His-tag antibody was used for the detection of His-tagged MCP5. #

2.3. Purification of His-tagged MCP5 using affinity chromatography

The next step in the functional characterization of MCP5 was the solubilization and purification of this ADP/ATP carrier for its subsequent reconstitution into liposomes. Solubilization of membrane proteins refers to the removal and replacement of the natural membrane lipids, in which the proteins are embedded, by a detergent that at the same time keeps the protein in solution (Seddon *et al.*, 2004). By definition, a protein is regarded to be soluble if it remains in the supernatant after ultracentrifugation at 100,000xg for 1 hour (Staudinger and Bandres, 2003).

Most MCF proteins can be solubilized in the presence of mild non-ionic detergents, such as Triton X-100 and Triton X-114 (Palmieri *et al.*, 1995; Riccio *et al.*, 1975b;

Riccio *et al.*, 1975a; Krämer and Heberger, 1986). Multiple solubilization experiments revealed that the recombinant His-tagged MCP5 protein, whether expressed in different *E. coli* strains or *S. frugiperda* SF9*,* could not be solubilized in Triton X-100 and Triton X-114, even not in relatively high concentrations of these mild detergents (results not shown). These unexpected results indicated that more stringent conditions were required for the solubilization of the MCP5 protein.

More stringent solubilization conditions can be achieved by using either ionic-detergents or chaotropic agents like for example guanidinium-HCl (Creighton, 1990). Disadvantage of the application of more stringent solubilization conditions is that partial or complete unfolding (denaturation) of the protein occurs, which requires a subsequent re-folding (renaturation) step in order to achieve an active protein suitable for transport assays (Creighton, 1990).

We first tested the use of the chaotropic salt guanidinium-HCl as a more stringent solubilization condition. Experiments revealed that this chaotropic salt could only partially dissolve the bacterial expressed His-tagged MCP5 protein (results not shown). The with guanidinium-HCl solubilized MCP5 protein required a subsequent 5M urea dialysis step in order to eliminate the chaotropic salt and to keep the protein in solution for the final Ni-NTA or TALON affinity column chromatography purification step. Lowering of the urea concentrations below 5M resulted in immediate precipitation (aggregation) of MCP5. Unexpectedly, during Ni-NTA or TALON affinity column chromatography, His-tagged MCP5 was found exclusively in the effluent, suggesting that the protein could not bind to the affinity column matrices. Also the substitution of urea with various detergents did not result in an increased binding of the His-tagged MCP5 protein to the different affinity matrices. These results suggested that the N-terminal 6xHis-tag of MCP5 is not “available” for binding to the affinity matrices used for the final purification step. Why this is happening, is unclear at this point.

We finally resorted to the use of different ionic detergents instead, i.e. the polyoxyethylene detergent Brij 60, n-dodecyl-β-D-maltoside (DDM), and lauryl-sarcosine sulfate (Sarkosyl). A summary of the tested solubilization/purification conditions for recombinant His-tagged MCP5 (*E. coli* and Insect cells) and natural MCP5 (*T. brucei* PCF449) is shown in Table 1. Both Brij 60 and DDM failed to completely solubilize MCP5 (results not shown). Sarkosyl has previously been reported as an effective ionic detergent for the solubilization of some MCF proteins

(Fiermonte *et al.*, 1993; Heimpel *et al.*, 2001; Frankel *et al.*, 1991). Solubilization of recombinant 6xHis-tagged MCP5 with increasing concentrations of Sarkosyl revealed that the protein was completely solubilized (i.e. present in the supernatant fraction after high-speed centrifugation) in detergent concentrations of 0.5% w/v and above. The corresponding western blot analysis is shown in Figure 6.

During the solubilization experiments with Sarkosyl, two important observations were made. The first observation relates to the stability of the His-tagged MCP5 protein in the presence of this detergent: after extended incubations with 0.5% (w/v) Sarkosyl or alternatively shorter incubations but with higher (>0.5%) Sarkosyl concentrations, a rapid degradation of the protein was observed.

Carrier	**Expression method**	**Solubilized with**	**Affinity matrix used**	**Elution with**	**Result**
MCP5	*E. coli*	0.5% TX-100 (w/v)	Talon®	200mM imidazole	Not solubilized No binding
MCP5	*E. coli*	0.5% TX-114 (w/v)	Talon®	200mM imidazole	Not solubilized No binding
MCP5	*E. coli*	Brij60	-		Not solubilized
MCP5	*E. coli*	5M Guanidinium-HCL/ 5M Urea	Talon®	200mM imidazole	No binding
MCP5	*E. coli*	1.5% (w/v) Sarkosyl (overnight incubation, 4°C)	-		Protein degraded prior purification
MCP5	*E. coli*	5M Urea/2% (w/v) Sarkosyl (inclusion bodies isolation)	Ni-NTA	200mM imidazole	No binding
MCP5	*E. coli*	2% Sarkosyl (w/v)	Ni-NTA	200mM imidazole	No binding
MCP5	*E. coli*	0.5-1% DDM	-		Not solubilized
MCP5	Insect cells	Up to 2% (w/v) TX-100	-		Not solubilized
MCP5	Insect cells	TX-114	-		Not solubilized
MCP5	Insect cells	0.5% (w/v) Sarkosyl/ 2% (v/v) TX-100	Ni-NTA	200mM imidazole	Partially purified
MCP5	*T. brucei* PCF449	Extraction 1% (w/v) TX-114	CM Sephadex C-50	200mM NaCl	Partially purified

Table 1. Summary of the tested solubilization/purification conditions for recombinant His-tagged MCP5 (*E. coli* and Insect cells) and natural MCP5 (*T. brucei* PCF449). Ultracentrifugation was performed after solubilization to assess the solubility of the protein (supernatant contained the detergent solibilised protein).

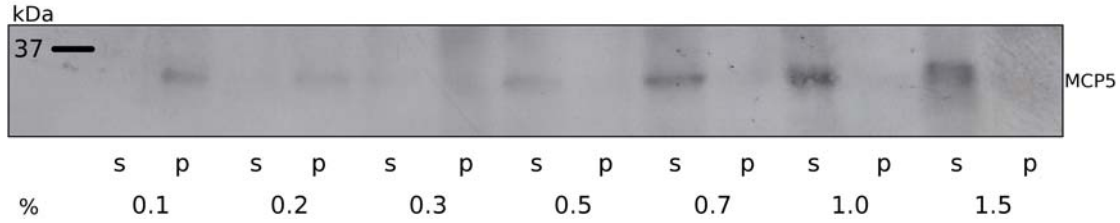

Figure 6. Solubilization of recombinant 6xHis-tagged MCP5 expressed in *S. frugiperda* SF9 with increasing concentrations of the ionic detergent Sarkosyl. After incubation with Sarkosyl, samples were ultracentrifuged (138000*xg*) and separated into supernatant (s: soluble) and pellet (p: insoluble) fractions. Detergent percentages are indicated in w/v. His-tagged MCP5 was detected using the His-tag antibody.

An example of Sarkosyl-directed protein degradation can be seen in Figure 6. When comparing the western blot results for 0.7% (w/v) and 1.5% Sarkosyl (w/v), a prominent smear of smaller His-antibody cross-reacting protein products was found below the main MCP5 protein band at the higher Sarkosyl concentration, indicating protein degradation. Prolonged incubation (> 1hour) with Sarkosyl eventually resulted in total lost of His-tagged MCP5 (results not shown).

The second important observation made during the Sarkosyl solubilization experiments was the significant increased detection of the His-tagged MCP5 protein with increasing Sarkosyl concentration. This phenomenon could also be observed in Figure 5: although solubilization experiments contained the same amount of protein at their start, an increased detection of His-tagged MCP5 protein was found. This result indicated that the N-terminal end of MCP5, which contains the 6xHis-epitope, became more and more accessible for the His-antibody with increasing Sarkosyl concentrations.

To avoid substantial Sarkosyl-directed degradation of His-tagged MCP5 protein during the further Ni-NTA affinity chromatography procedure, up to 2% (w/v) Triton X-100 was added to the solubilized protein. The presence of excess Triton-X100 (2% w/v) over Sarkosyl (0.5% w/v) was previously reported to prevent Sarkosyl-directed degradation of MCF proteins (Madeo *et al*., 2009). Addition of Triton X-100 (2% w/v) to the Sarkosyl-solubilized MCP5 protein fraction was indeed found to prevent further degradation of MCP5 (results not shown). Accordingly, all

subsequent Ni-NTA affinity chromatography steps were performed in presence of 2% (w/v) Triton X-100 (no Sarkosyl) in order to keep the protein soluble and to allow it to bind to the affinity matrix. Western blot analysis of the different protein fractions obtained during Ni-NTA chromatography of recombinant His-tagged MCP5 expressed in Sf9 insect cells, revealed that: (A) MCP5 now was able to bind to the Ni-NTA affinity matrix, and (B) that during elution with 200mM imidazole, only part of the protein could be eluted (Figure 7).

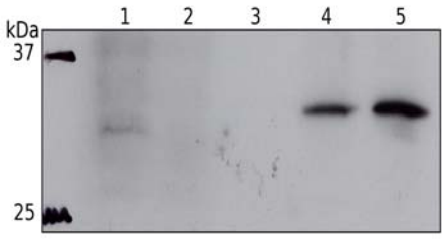

Figure 7. Western blot analysis of the different protein fractions obtained during Ni-NTA chromatography of recombinant His-tagged MCP5 expressed in *S. frugiperda* SF9. A commercial His-tag antibody was used for the detection of the protein. Legend: (1) cleared lysate after 2% (w/v) Sarkosyl treatment; (2) effluent containing the unbound protein fraction; (3) wash step to further remove unbound protein; (4) elution with 200mM imidazole; (5) Ni-NTA beads after elution with 200mM imidazole.

The partial elution of His-tagged MCP5 from the Ni-NTA affinity matrix, even at a very high concentrations of imidazole (up to 200mM), suggested that this protein is not only bound to the matrix via its His-tag. It is most probably also associated with the Sepharose matrix of the Ni-NTA column, which is not uncommon for hydrophobic proteins. That MCP5 is rather hydrophobic explained the requirement of a strong anionic detergent, i.e. Sarkosyl, for its solubilization. A similar behaviour was reported for the AAC from beef heart mitochondria when it was first solubilized and isolated (Riccio *et al*., 1975b).

2.4. In vivo transport assays in *Escherichia coli* Rossetta2(DE3)pLysS

As indicated in the introduction of this Chapter, two different approaches were used to determine the transport characteristics of the ADP/ATP carrier MCP5. The first approach is based on the expression of recombinant His-tagged MCP5 protein in *E. coli* Rossetta2(DE3)pLysS followed by *in vivo* metabolite transport assays in the

same strain. This approach was previously shown to be successful for the functional characterisation of different ADP/ATP carriers from other eukaryotes (Tjaden *et al*., 1998). It is based on the important fact that *E. coli* does not possess any ADP/ATP carriers: consequently measured ADP/ATP exchange activity would be solely due to the activity of the expressed eukaryotic ADP/ATP carrier. Transport activity requires the proper folding and insertion of the expressed ADP/ATP carrier in the *E. coli* membrane, which is apparently feasible (Tjaden *et al*., 1998). Further advantage of this approach is that the more troublesome isolation and reconstitution steps, used in the classical approach, will be omitted.

The *in vivo* transport assay in *E. coli* is based on the import of radioactive labeled substrates, i.e. ^{14}C or ^{32}P-labeled ADP and ATP, into those *E. coli* strains that express a functional eukaryotic ADP/ATP carrier. After a timed incubation of these cells with the various radioactive substrates, the cells were separated from the non-incorporated substrate through rapid filtration or centrifugation (Tjaden *et al.*, 1998). Measurement of the in *E. coli* incorporated radioactive substrates enables the quantification of ADP/ATP exchange.

As discussed in section 2.3, His-tagged MCP5 could be readily expressed, although at a low level, in the *Escherichia coli* Rossetta2(DE3)pLysS strain. We used the same *E. coli* strain for performing the *in vivo* transport assays. However, after many attempts, no ADP/ATP exchange could be observed even after varying all possible parameters. Major problem appeared to be the substantial lyses of the MCP5-expressing *E. coli* cells during the transport assay. The protocol is based on a Pi buffer for the transport assay (incubation step) and the subsequent removal (wash steps) of non-incorporated radioactive substrates (Tjaden *et al.*, 1998). To exclude eventual osmotic problems, iso-osmotic buffers were used instead, but again without success.

One possible explanation for the observed lyses could be that expression of His-tagged MCP5 resulted in “leakage” of the *E. coli* cells, which became detrimental upon transfer of the cells from the culture medium to the assay buffer. During the auto-induction experiments a significant decline in growth was observed upon induction with lactose (Figure 3). Such reduction in growth is usually a trait observed in *E. coli* cells that over-express a particular protein. However, in our case, MCP5 was always expressed at rather low cellular levels, excluding the possibility that over-expression is the cause of a reduced growth. Furthermore, over-expression of

MCP15 and MCP16 in *E. coli* Rossetta2(DE3)pLysS (Chapter VI) and MCP12 (personal communication with Dr. C. Colasante) in *E. coli* BL21(DE3), did not substantially affect cell growth. This observation is in agreement with the leakage of the *E. coli* cells and their subsequent lyses, possibly caused by the expression of MCP5.

2.5. Reconstitution of His-tagged MCP5 into liposomes and transport assays

This section summarizes the greater part of all the reconstitution work performed with MCP5. Unfortunately, the functional reconstitution of MCP5 in liposomes appeared to be “impossible”, at least with the conventional and well-established methods that seemed to work well for MCF proteins isolated from other eukaryotes.

The reconstitution of a metabolite transporter into liposomes refers to the integration of this protein into an enclosed artificial membrane-bound compartment, the so-called liposome, so that transport can occur only through the transport activity of this protein. The different reconstitution protocols used for the integration of MCP5 into liposomes and the subsequent transport assays were mainly based on methods previously published by Palmieri (Palmieri *et al*., 1995) and Klingenberg (Krämer and Klingenberg, 1977; Klingenberg *et al.*, 1995; Heimpel *et al.*, 2001). These methods were reported to be successful for the reconstitution of various MCF proteins from other eukaryotes. The protocols used for our work with MCP5 were essential the same or minimal modifications of these published methods. A schematic representation of the protocol used for the reconstitution of MCP5 is shown in Figure 8, whereas an overview of different attempted reconstitution conditions is shown in Table 2.

The artificial liposome membrane should resemble the natural membrane in that is formed by a particular mix of phospholipids, which permits the proper arrangement of the protein structure in order to perform transport (Seddon *et al*., 2004; Suzuki and Takeuchi, 2008). In most of the published protocols, egg yolk phosphatidylcholine (PC) was used as the main phospholipid for reconstitution (Klingenberg *et al.*, 1995; Palmieri *et al.*, 1995). Also asolectin, a mix of soybean phospholipids, and *E. coli* polar lipids were found to enable a successful reconstitution of several MCF proteins (Noël and Pande, 1986; Hutson *et al.*, 1990; Rück *et al.*, 1998; Kasamo, 1990; van der Giezen *et al.*, 2002). A number of

reconstitution studies indicated a further important role of cardiolipin for the successful reconstitution of ADP/ATP carriers (Chapter I). The presence of cardiolipin during reconstitution is essential for the stability of the ADP/ATP carrier and its ADP/ATP exchange activity (Krämer and Klingenberg, 1980; Heimpel *et al*., 2001; Klingenberg, 2009). The different phospholipids and variable mixtures of these, used for the functional reconstitution of MCP5, are shown in Table 2.

Virtually all of the reconstitution experiments were performed with freshly isolated 6xHis-tagged MCP5 protein in order to minimize its degradation once it was solubilized from the membrane. Prolonged storage of the isolated His-tagged MCP5 protein, on either ice or at -20^{o}C, invariably resulted in protein degradation, even in the presence of a broadband protease inhibitor mix (results not shown). In some cases, the cells or mitochondrial fractions were pre-incubated with the ADP/ATP carrier inhibitors ATR or CAT prior to the solubilization and isolation of MCP5. Both ATR and CAT were found to stabilize the structure of the beef heart AAC and protected it from rapid proteolytic degradation when solubilized out of its natural membrane environment (Riccio *et al.*, 1975b; Riccio *et al.*, 1975a; Klingenberg *et al.*, 1978; Klingenberg *et al.*, 1995). The formed ATR/AAC or CAT/AAC complexes further prevented the possible unfolding of the beef heart AAC, making it more stable for longer time periods. Since ATR-binding has been shown to be competitive to ADP, the addition of excess substrate would remove this inhibitor upon reconstitution, at which point the ADP/ATP carrier would be stabilized by its integration into the liposomal membrane (Krämer, 1986).

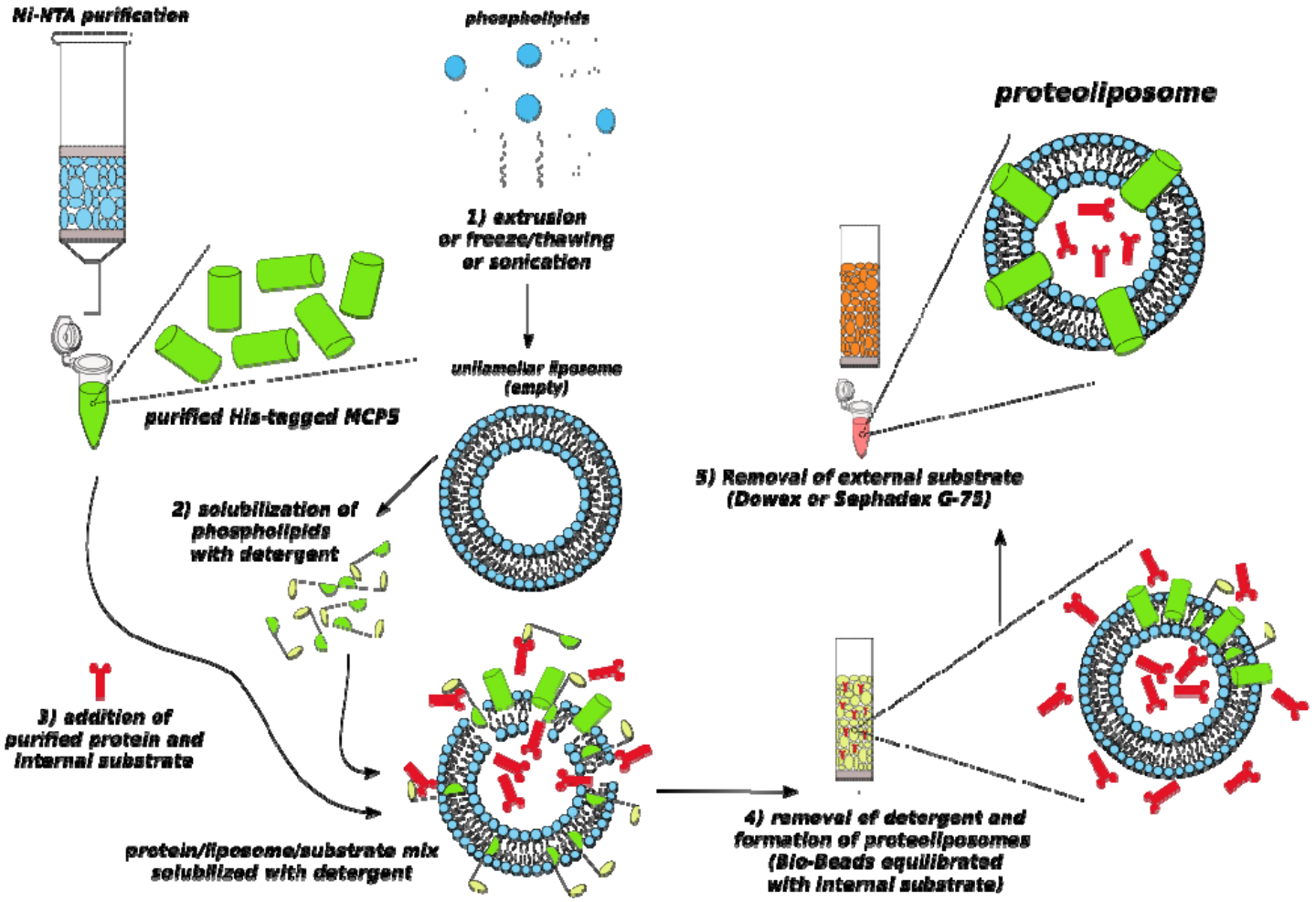

Figure 8. Schematic representation of His-tagged MCP5 reconstitution into liposomes. 1) The phospholipids are prepared by extrusion/or freeze-thawing/or sonication in order to obtain unilamellar liposomes. 2) The liposomes are solubilized with detergent and mixed with the purified protein and the internal substrate (shown in red, step 3) and subsequently loaded into Bio-beads columns for cyclic detergent removal, and formation of the proteoliposomes (4). 5) The sample is then cleaned of the external substrate by passage through Dowex or Sephadex G-75 columns.

#

PL	PL solubilization	Buffer	Salts	Reconstitution matrix	Clean-up column 1	Clean-up column 2
PC	1-1.3 % (v/v) TX-114	MOPS pH 7.0	10-30mM KCl	Amberlite XAD-2	Dowex AGI-X8	Dowex AGI-X8
PC/CL	1-1.3 % (v/v) TX-114	MOPS pH 7.0	-	Amberlite XAD-2	Dowex AGI-X8	Dowex AGI-X8
PC/CL	1-1.3 % (v/v) TX-114	Tris-HCl pH 7.5	10-30mM KCl	Amberlite XAD-2	Dowex AGI-X8	Dowex AGI-X8 - Sephadex G75
PC/CL	$C_{10}E_5$	Tris-HCl pH 7.5	-	Biobeads®	Sephadex G75	Sephadex G75
PC/CL	$C_{10}E_5$	Tris-HCl pH 7.5	10-100mM KCl	Biobeads®	Sephadex G75	Sephadex G75
PC/CL	$C_{10}E_5$	Tris-HCl pH 7.5	-	Amberlite XAD-2	Sephadex G75	Sephadex G75
PC/CL	$C_{10}E_5$	Tris-HCl pH 7.5	10-100mM KCl	Amberlite XAD-2	Sephadex G75	Sephadex G75
PC/CL	$C_{10}E_5$	Tris-HCl pH 7.5	10-50mM Na_2SO_4	Amberlite XAD-2	Sephadex G75	Sephadex G75
PC/CL	$C_{10}E_5$	Tris-HCl pH 7.5	10-50mM Na_2SO_4	Biobeads®	Dowex AGI-X8 - Sephadex G75	Sephadex G75
PC/CL	$C_{10}E_5$	Pipes pH 7.0	-	Biobeads®	Sephadex G75	Sephadex G75
PC/CL	$C_{10}E_5$	Pipes pH 7.0	10-50mM KCl	Biobeads®	Sephadex G75	Sephadex G75
PC/CL	$C_{10}E_5$	Pipes pH 7.0	10-50mM Na_2SO_4	Biobeads®	Sephadex G75	Sephadex G75
PC/CL	$C_{10}E_5$	Tricine pH 7.0	-	Biobeads®	Sephadex G75	Sephadex G75
PC/CL	1-1.3 % (v/v) TX-114	Tricine pH 7.0	10-50mM Na_2SO_4	Biobeads®	Sephadex G75	Sephadex G75
PC/CL	$C_{10}E_5$	Tricine pH 7.0	10-50mM Na_2SO_4	Biobeads®	Sephadex G75	Sephadex G75
Asol/CL	1-1.3 % (v/v) TX-114	Tris-HCl pH 7.5	-	Amberlite XAD-2	Dowex AGI-X8 - Sephadex G75	Sephadex G75
Asol/CL	1-1.3 % (v/v) TX-114	Tris-HCl pH 7.5	10-50mM KCl	Amberlite XAD-2	Dowex AGI-X8 - Sephadex G75	Sephadex G75
Asol/CL	1-1.3 % (v/v) TX-114	Tris-HCl pH 7.5	10-50mM KCl	Biobeads®	Sephadex G75	Sephadex G75
Asol/CL	$C_{10}E_5$	Tris-HCl pH 7.5	10-50mM KCl	Amberlite XAD-2	Sephadex G75	Sephadex G75
Asol/CL	$C_{10}E_5$	Tris-HCl pH 7.5	10-50mM KCl	Biobeads®	Sephadex G75	Sephadex G75
Asol/CL	$C_{10}E_5$	Tris-HCl pH 7.5	10-50mM Na_2SO_4	Biobeads®	Sephadex G75	Sephadex G75
Asol/CL	$C_{10}E_5$	Pipes pH 7.0	10-50mM Na_2SO_4	Biobeads®	Sephadex G75	Sephadex G75
Asol/CL	1-1.3 % (v/v) TX-114	Tricine pH 7.0	10-50mM Na_2SO_4	Biobeads®	Sephadex G75	Sephadex G75
Asol/CL	$C_{10}E_5$	Tricine pH 7.0	10-50mM Na_2SO_4	Biobeads®	Sephadex G75	Sephadex G75

Table 2. Summary of protocols used for MCP5 reconstitution into liposomes. PC= phosphatidylcholine from egg yolk; CL=cardiolipin; Asol=asolectin; $C_{10}E_5$= pentaethylene glycol monodecyl ether. Where dashes appear denotes one or other reagent used, except the salts, where it represents the concentration range. Slashes imply combination of reagents.

Another important parameter taken into account during the reconstitution of MCP5 was the previously reported requirement for particular ions at certain concentrations in the reconstitution mix, which seemed to be crucial for the establishment of an effective ADP/ATP exchange activity (Krämer, 1986). High ionic strength is regarded as an important factor in the solubilization process, but chlorides and phosphates seemed to be detrimental for the exchange activity (Krämer and Kürzinger, 1984; Krämer, 1986). Also the presence of magnesium decreased the ADP/ATP exchange activity considerably due to binding of this ion to ATP, preventing its entry into the binding pocket of the AAC (Krämer and Kürzinger, 1984; Krämer, 1986). A recent publication on the effect of chloride ions above concentrations of 150mM revealed a reduced ATP/ADP exchange activity due to binding of this negatively charged ion to the positive amino acid residues involved in substrate binding (Krammer *et al.*, 2009) Different ions were tested in the reconstitution of MCP5, at variable concentrations (see Table 2 for more information). Further, next to Tris-HCl as buffer, also tricine and pipes buffers were tested for the functional reconstitution of MCP5, although several publications indicated that the choice of buffer was not critical for the successful reconstitution of most carriers (Palmieri *et al*., 1995). Whenever a particular buffer was chosen for reconstitution, the same buffer would also be used during the purification of the MCP5 protein in order to minimize sudden physical changes in their environment.

Also the choice of detergent, which is used for the solubilization of the phospholipids prior to liposome formation, seemed to have an influence on the ADP/ATP exchange activity after reconstitution (Figure 8, step 2). For example, Palmieri and his co-workers used mainly Triton X-114 for the solubilization of phospholipids: invariably at a same concentration, i.e. 1.3% (v/v) (Palmieri *et al*., 1995; Fiermonte *et al*., 1993; Palmieri *et al*., 2000; Marobbio *et al*., 2002; Vozza *et al*., 2004; Palmieri *et al*., 2001; Todisco *et al*., 2006; Palmieri *et al*., 2006; Fiermonte *et al*., 2009; Iacopetta *et al*., 2010; Castegna *et al*., 2010). This is in contrast to Klingenberg and his co-workers, who reported that TX-100 and TX-114 both could not be used for phospholipid solubilization and the subsequent reconstitution of recombinant *Neurospora crassa* AAC expressed in *E. coli*: instead they used the detergent $C_{10}E_5$ in a specific PC/detergent ratio to accomplish a successful reconstitution and transport (Heimpel *et al*., 2001). Some other groups used mainly TX-100 to solubilize the phospholipids prior to the functional reconstitution of ADP/ATP carriers

(Geertsma *et al*., 2008). For solubilization of phospholipids and following reconstitution of MCP5 different detergents were used, i.e. TX-114 and $C_{10}E_5$, at variable concentrations (see Table 2 for further information). The detergent TX-100 was omitted from these experiments due to its previously observed failure to solubilize MCP5 (discussed in section 2).

The next two critical steps in the reconstitution of MCP5 were the formation of liposomes (contains no protein) and the subsequent formation of MCP5-containing proteoliposomes (Figure 8, steps 3 and 4). Phospholipids were solubilized as described above and indicated in Table 2, and were either extruded across a 100nm membrane or sonicated on ice for 10 minutes; both methods were previously shown to produce unilamellar membrane liposomes, which are required for the functional reconstitution of MCF proteins (Suzuki and Takeuchi, 2008; Hope *et al.*, 1986).

The formation of the MCP5-containing proteoliposomes is based on a partial re-solubilization of the extruded or sonicated liposomes, which results in micelles that allow the insertion of the proteins into the liposome structure. The slow removal of the detergent will ensure the closure of the proteoliposome with the MCF protein arranged on its surface. This process is called micelle-vesicle transition, and is essential for the formation of proteoliposomes (Ollivon *et al*., 2000). The different affinity matrices used for the removal of detergent during MCP5 reconstitution experiments are indicated in Table 2. In most cases, polystyrene beads (Biobeads) were used which are optimal for the removal of low “critical micelle concentration” (cmc) detergents. The phospholipid/detergent ratio is determined by the cmc of the detergent used, with cmc defined as the minimal detergent concentration required for micellar formation (Ollivon *et al.*, 2000; Seddon *et al.*, 2004). Detergents were most effectively removed by a method called “cyclic detergent removal”, i.e. the repeated passage (15-20x) of the proteoliposome/detergent mix over Biobeads® columns (Krämer, 1986; Krämer and Heberger, 1986; Klingenberg *et al.*, 1995; Ollivon *et al.*, 2000). The phospholipid/protein ratio used for the formation of proteoliposomes was also a key factor in the procedure: Klingenberg and his co-workers generally use a PC/protein ratio of 200 (Heimpel *et al*., 2001), whereas other authors used fixed volumes of phospholipid mixtures without establishing the phospholipid/protein ratios (Madeo *et al*., 2009).

Another essential prerequisite for the measurement of ADP/ATP exchange in proteoliposomes is the presence of ADP in the lumen, and the presence of its

counter ion, in this case radioactive labeled (^{3}H) ATP, on the outside of these artificial vesicles (Figure 9, steps 2 and 3). During proteoliposome formation, ADP is included in the reconstitution mix in order to act as an internal substrate for the later measurement of ADP/ATP exchange. To facility this exchange, ADP has to be removed from the outside of the formed proteoliposomes and has to be replaced by the radioactive counter ion, i.e. ^{3}H-ATP. If ADP/ATP exchange takes place, ^{3}H-ATP will be imported into the proteoliposomes in counter exchange with luminal ADP. In order to quantify this transport, non-imported ^{3}H-ATP has to be removed from the outside of the liposomes. Removal of external ADP and non-imported ^{3}H-ATP is accomplished by ion exchange chromatography. The different ion-exchangers used for this purpose are shown in Table 2. Initially Dowex AGI-X8 was used to both remove external ADP after the formation of MCP5 proteoliposomes and the removal of non-imported ^{3}H-ATP after the transport assay. However, control experiments with protein-free liposomes revealed that the binding capacity of Dowex AGI-X8 was insufficient and resulted in the presence of ^{3}H-ATP in the first eluate, which normally contains the proteoliposomes. Instead several other ion-exchangers and also different molecular sieves were tested. The best result for the removal of non-incorporated ^{3}H-ATP was obtained with Sephadex G75 (results not shown) (Krämer, 1986; Palmieri *et al.*, 1995). Sephadex G75 is a molecular sieve, which will separate the smaller molecules (substrates) from the larger particles (proteoliposomes) on a migration rate basis, without any electrostatic interactions intervening. Accordingly, Sephadex G75 was used for the removal of both ADP and ^{3}H-ATP during the different MCP5 reconstitution steps and following transport assays (Table 2).

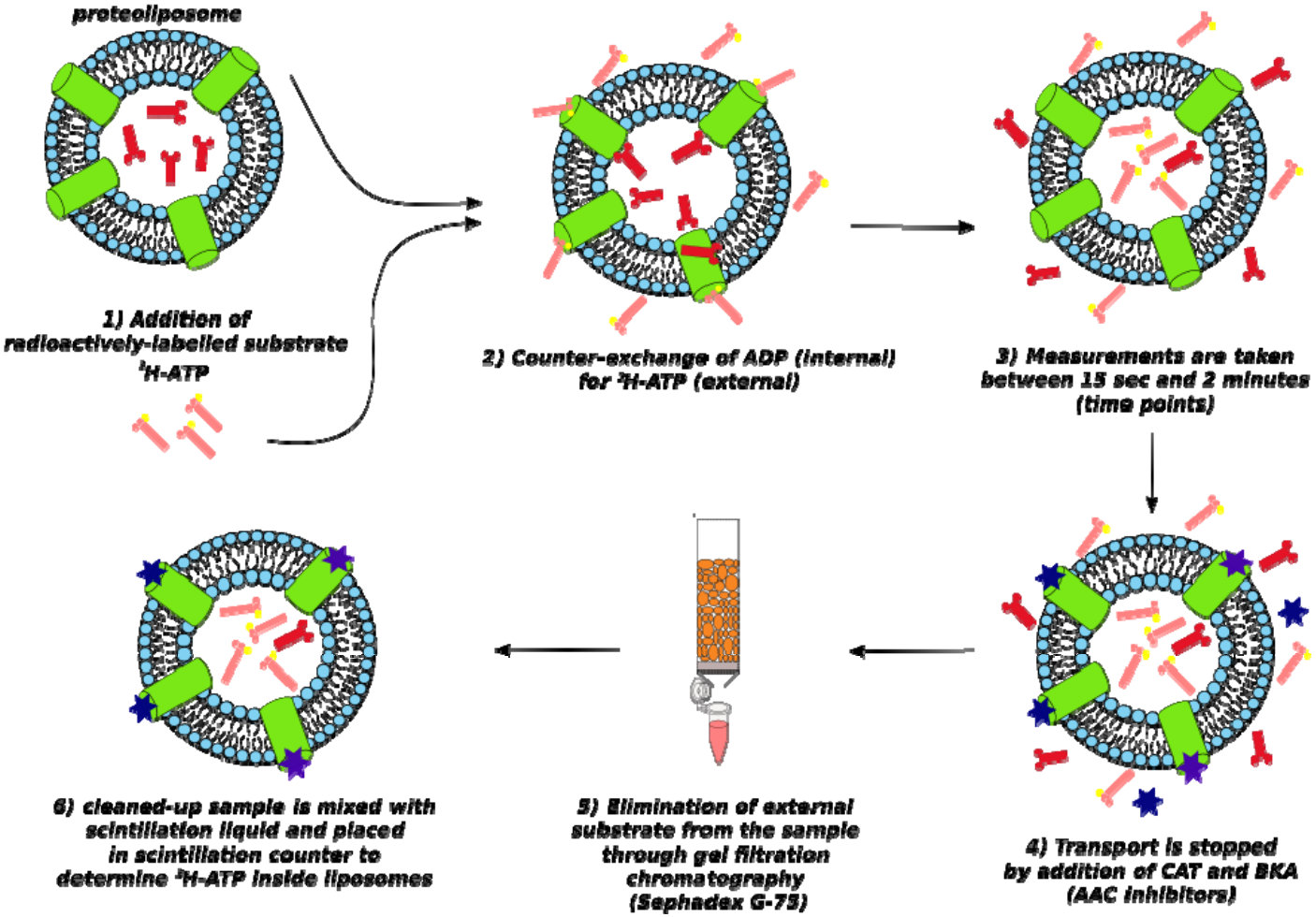

Figure 9. Schematic representation of the transport assays for MCP5 reconstituted into liposomes. ADP-filled proteoliposomes are mixed with ^{3}H-ATP (*ADP in red*, *^{3}H-ATP in pink*, step 1) and transport (step 2) is allowed to take place for 2 minutes (step 3). Time points are taken from the reaction and the samples are stopped with CAT and BKA (shown in dark blue and purple, step 4), before loading them into clean-up columns (step 5) for the elimination of non-transported substrate. Once external substrate is eliminated, the sample is placed in scintillation counter for determination of ^{3}H-ATP.

The actual presence of substrate in the lumen of the proteoliposomes was confirmed by a control experiment in which ATP was used as the internal substrate during liposome formation. Any external ATP was removed by ion exchange chromatography as indicated in table 2. Release of ATP, upon the addition of Triton X-100 to a final concentration of 0.1% (v/v), was measured by a hexokinase-coupled enzyme assay. As shown in Table 3 significant amounts of ATP were released upon addition of the detergent. This result indicated that the formed liposomes indeed contained substrate, as expected. Taking into account that the final concentration of ^{3}H-ATP in each time point aliquot was between 0.02-0.04 μmol/mL, the design was set up to force the reaction towards the counter-exchange of internal ADP for external ^{3}H-ATP. Table 3 also shows discrepancies in the amount of internal substrate found in the proteoliposomes depending on the detergent used for the solubilization of MCP5. Another reason to discard DDM as a detergent for the solubilization of His-tagged MCP5 was the apparent inefficiency of the Bio-beads to eliminate this detergent completely from the sample, which would have hampered even further the stability of the newly formed proteoliposome.

Liposome	**Protein treatment**	**ATP concentration after TX-100 solubilization**
No protein	-	0.797 μmol/mL
His-tagged MCP5	200mM TX-100	0.400 μmol/mL
His-tagged MCP5	200mM DDM	0.120 μmol/mL

Table 3. ATP concentrations measured in liposomes prepared under different conditions. ATP concentrations were measured using a spectrophometrically-assessed hexokinase coupled assay for the production of NADPH at 340nm (see Materials and Methods, Chapter II).

The presence of MCP5 in the proteoliposomes was confirmed by western blot analysis. The results shown in Figure 10 confirm the presence of His-tagged MCP5 in the final proteoliposomes used for the subsequent transport assays.

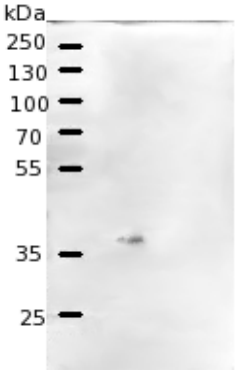

Figure 10. Western blot of His-tagged MCP5 reconstituted into liposomes. Detection was performed using His-tag antibody.

2.6. Further Discussion

Despite testing of all possible known variables (see Table 2), no ADP/ATP exchange activity could be detected upon the reconstitution of His-tagged MCP5 into proteoliposomes. Unfortunately, a similar negative result was also found for the functional reconstitution of MCP12 - a putative dicarboxylate carrier of *T. brucei* with significant sequence similarities to functionally characterized dicarboxylate carriers from other eukaryotes (Chapter III; personal communication Dr. C. Colasante). Also for MCP12, no dicarboxylate exchange could be detected upon liposome reconstitution and subsequent transport assays. For reconstitution of MCP12, essentially the same reconstitution protocols and conditions were used as described in this Chapter. However, mitochondrial metabolite transport assays for digitonin-permeabilised MCP12 double knockout cell lines of *T. brucei* confirmed the predicted di/tricarboxylate exchange function of MCP12 (personal communication Dr. C. Colasante). These results indicated that a yet unknown factor is hampering the successful reconstitution of *T. brucei* MCF proteins.

One of the common traits of the different functionally characterized MCF proteins is the presence of a 6xHis-tag at the N-terminal ends of these proteins. Our first thought was therefore that the added His-tag maybe affected the metabolite exchange function of the tested MCF proteins. However, this assumption was immediately discarded, since mitochondrial ATP production experiments and substrate/end product analyses of wildtype and knockout cell lines confirmed that the His-tagged versions of these MCF proteins were fully functional (Chapter IV for MCP5; personal communication Dr. C. Colasante for MCP12). This was further supported by the observation that removal of the His-tag from MCP12 did not lead to a restoration of the dicarboxylate-exchange activity upon reconstitution (C. Colasante, personal communication).

The other common trait of the analyzed MCF proteins is that they normally exist and function in the mitochondrial inner membrane of *T. brucei*. The only reconstitution condition, which has not taken been taken fully into account during our reconstitution experiments, is the lipid composition of the MCP5-containing proteoliposome. All of our reconstitution experiments have been done in either egg yolk PC or Asolectin (Table 2). The artificial liposome membrane should however resemble the natural membrane in order to permit the proper arrangement of the MCF protein structure in order to perform transport (Seddon *et al*., 2004; Suzuki and Takeuchi, 2008). However, nothing at all is known about the lipid composition of the *T. brucei* mitochondrial inner membrane. The only information available relates to the total phospholipid composition of trypanosomes. Phospholipid analysis of *T. brucei* cells indicated that PC and PE together represent approximately 70% of the total phospholipid composition in these parasites (Patnaik *et al*., 1993). This ratio is rather similar to the one found for mammalian cell lines, where PC represents approximately 40-50% and PE approximately 20-50% of total membrane phospholipid (Vance, 2008). However, the observed similarities in total PE and PC concentrations between *T. brucei* and other eukaryotes, does not exclude the possibility that the lipid composition of the *T. brucei* mitochondrial inner membrane could be different from that of other eukaryotes.

Another important observation is the prominent difference in mitochondrial structure and mitochondrial inner membrane organization when comparing trypanosomes and other (mostly higher) eukaryotes. For example, *T. brucei* contains only *a single mitochondrion*, which extends along the whole cell body (Matthews, 2005), whereas other eukaryotes often contain multiple and more ovoid- or short tubular-shaped mitochondria. Procyclic form *Trypanosoma brucei* presents an active mitochondrion, largely rich in cristae. Cristae play a key role in the structural and functional organization of the mitochondrial inner membrane (Zick *et al.*, 2009). Such a unique spatial organization of the single mitochondrion in procyclic form *T. brucei* implicates the presence of specific micro-domains in the mitochondrial membrane, which probably interact differently with the surrounding mitochondrial intermembrane space and the cytosol, depending on the position of that particular part of the mitochondrion in the cell. This organization of micro-domains in other organisms is mainly directed by the presence of specific phospholipids in these domains (Claypool *et al.*, 2008; Claypool, 2009). The most prominent of these phospholipids is cardiolipin, which was shown previously to be essential for the formation of

functional super-complexes in the mitochondrial inner membrane, like for example the discussed “respirasomes” in Chapter I (Mileykovskaya and Dowhan, 2009; Schlame and Ren, 2009). Depletion of cardiolipin was shown to result in disorganization of these super-complexes (Claypool *et al.*, 2008). Next to cardiolipin, also its precursor, phosphatidylglycerol (PG) and the phospholipid phosphatidylethanolamine (PE) have been reported to play a key role in the maintenance of mitochondrial structures, which in turn determine mitochondrial function (Gohil *et al.*, 2005; Trotter *et al.*, 1993; Ostrander *et al.*, 2001; Lasch *et al.*, 2003).

The mitochondrial membrane structure and lipid composition (and correspondingly the function of the mitochondrial membrane as a whole) are apparently tightly linked. Taking this into account, it is safe to assume that the lipid composition of the *T. brucei* mitochondrial inner membrane is different from that of other eukaryotes. This assumption is further supported by the rather hydrophobic character of MCP5, as was discovered during the purification of MCP5 by Ni-NTA affinity chromatography. A similar behaviour was also observed for MCP12 during its purification by Ni-NTA affinity chromatography (personal communication Dr. C. Colasante). This strong hydrophobic character was not observed for MCF proteins from other eukaryotes. The increased hydrophobicity of *T. brucei* MCF proteins would most probably be compensated by specific changes in the phospholipid composition of its mitochondrial membrane environment.

Biological membranes are per definition asymmetric, with important differences in lipid composition between the inner and outer leaflets of the lipid bilayer (Devaux and Morris, 2004; Devaux, 1991). In general, biological (and mitochondrial inner) membranes are more negatively charged on the inside due to the more abundant presence of negatively charged phospholipids, i.e. PE, in the inner leaflet of the lipid bilayer (Devaux, 1991). This phospholipid-directed charge difference creates a membrane potential, which is essential for many membrane-bound processes, including the insertion and orientation of membrane proteins (Ostrander *et al.*, 2001; Pfanner and Geissler, 2001). The most important pre-requisites for a successful reconstitution and subsequent measurement of transport activity of MCF proteins are their proper folding, and insertion and correct orientation in the proteoliposomal membrane.

Western blotting analysis indicated the presence of MCP5 in the generated proteoliposomes (Figure 10). However, it remained unclear whether MCP5 was properly inserted in the membrane or maybe remained in the lumen. It further remained unclear whether MCP5 was properly orientated in the proteoliposome membrane. The above-described differences in lipid composition and related membrane potential do not exist in artificially generated liposomes. Kramer and his co-workers described in 1986 an approximately 50/50 distribution of inside-out and right-side orientated AAC in proteoliposomes (Krämer, 1986). Such a 50/50 orientation of MCP5 would result in a rather futile counter-acting exchange, which might not be visible as transport activity during experiments with proteoliposomes. More recently, Klingenberg stated that the AAC re-orientates itself upon contact with its substrate, in this case ADP (Klingenberg, 2008). In case of a substrate-directed orientation of MCP5 in the proteoliposomal membrane, this orientation could change upon the decrease and/or depletion of the internal or external substrates with as a result a transport in the opposite direction. This transport would again not be visible if this exchange, and the reversal of this exchange, would occur at very high speeds.

2.7. Conclusion

The classical route of *in vitro* reconstitution and transport assays unfortunately did not lead to the confirmation of the proposed (Chapter IV) ATP/ADP exchange function of *T. brucei* MCP5. This result was somewhat unexpected since a His-tagged recombinant version of this MCF protein could be successfully expressed in both bacteria and insect cells, could be purified by Ni-NTA affinity chromatography, and most probably could be reconstituted in liposomes. Several observations made during the many different expression, solubilization, purification and liposome reconstitution experiments suggested however that the MCP5 protein is different from other prototypical ADP/ATP carriers: especially its inability to be solubilized by conventional mild non-ionic detergents and its very low cellular expression levels in different heterologous hosts are remarkable. This and other observed differences are important for future trypanosome-specific adaptations of the “standard” reconstitution protocol, which is apparently successful for MCF proteins from other eukaryotes.

3. References

Cai, J. & Gros, P. 2003. Overexpression, purification, and functional characterization of ATP-binding cassette transporters in the yeast, Pichia pastoris. *BBA-Biomembranes,* 1610**,** 63-76.

Castegna, A., Scarcia, P., Agrimi, G., Palmieri, L., Rottensteiner, H., Spera, I., Germinario, L. & Palmieri, F. 2010. Identification and functional characterization of a novel mitochondrial carrier for citrate and oxoglutarate in S. cerevisiae. *J Biol Chem*.

Claypool, S. M. 2009. Cardiolipin, a critical determinant of mitochondrial carrier protein assembly and function. *BBA - Biomembranes***,** 1-10.

Claypool, S. M., Oktay, Y., Boontheung, P., Loo, J. A. & Koehler, C. M. 2008. Cardiolipin defines the interactome of the major ADP/ATP carrier protein of the mitochondrial inner membrane. *J Cell Biol,* 182**,** 937-50.

Creighton, T. E. 1990. Protein folding. *Biochem J,* 270**,** 1-16.

Devaux, P. F. 1991. Static and dynamic lipid asymmetry in cell membranes. *Biochemistry,* 30**,** 1163-73.

Devaux, P. F. & Morris, R. 2004. Transmembrane asymmetry and lateral domains in biological membranes. *Traffic,* 5**,** 241-6.

Fiermonte, G., Paradies, E., Todisco, S., Marobbio, C. M. T. & Palmieri, F. 2009. A novel member of solute carrier family 25 (SLC25A42) is a transporter of coenzyme A and adenosine 3',5'-diphosphate in human mitochondria. *J Biol Chem,* 284**,** 18152-9.

Fiermonte, G., Walker, J. E. & Palmieri, F. 1993. Abundant bacterial expression and reconstitution of an intrinsic membrane-transport protein from bovine mitochondria. *Biochem J,* 294 (Pt 1)**,** 293-9.

Frankel, S., Sohn, R. & Leinwand, L. 1991. The use of sarkosyl in generating soluble protein after bacterial expression. *Proc Natl Acad Sci USA,* 88**,** 1192-6.

Fuhrmann, M., Hausherr, A., Ferbitz, L., Schodl, T., Heitzer, M. & Hegemann, P. 2004. Monitoring dynamic expression of nuclear genes in Chlamydomonas reinhardtii by using a synthetic luciferase reporter gene. *Plant Mol Biol,* 55**,** 869-81.

Geertsma, E. R., Nik Mahmood, N. A. B., Schuurman-Wolters, G. K. & Poolman, B. 2008. Membrane reconstitution of ABC transporters and assays of translocator function. *Nat Protoc,* 3**,** 256-66.

Gohil, V. M., Thompson, M. N. & Greenberg, M. L. 2005. Synthetic lethal interaction of the mitochondrial phosphatidylethanolamine and cardiolipin biosynthetic pathways in Saccharomyces cerevisiae. *J Biol Chem,* 280**,** 35410-6.

Heimpel, S., Basset, G., Odoy, S. & Klingenberg, M. 2001. Expression of the mitochondrial ADP/ATP carrier in Escherichia coli. Renaturation, reconstitution, and the effect of mutations on 10 positive residues. *J Biol Chem,* 276**,** 11499-506.

Hope, M., Bally, M., Mayer, L., Janoff, A. & Cullis, P. 1986. Generation of multilamellar and unilamellar phospholipid vesicles. *Chemistry and Physics of Lipids,* 40**,** 89-107.

Hutson, S. M., Roten, S. & Kaplan, R. S. 1990. Solubilization and functional reconstitution of the branched-chain alpha-keto acid transporter from rat heart mitochondria. *Proc Natl Acad Sci USA,* 87**,** 1028-31.

Iacopetta, D., Carrisi, C., De Filippis, G., Calcagnile, V. M., Cappello, A. R., Chimento, A., Curcio, R., Santoro, A., Vozza, A., Dolce, V., Palmieri, F. & Capobianco, L. 2010. The biochemical properties of the mitochondrial thiamine pyrophosphate carrier from Drosophila melanogaster. *FEBS J,* 277**,** 1172-81.

Kasamo, K. 1990. Mechanism for the Activation of Plasma Membrane H-ATPase from Rice (Oryza sativa L.) Culture Cells by Molecular Species of a Phospholipid. *Plant Physiol,* 93**,** 1049-52.

Klingenberg, M. 2008. The ADP and ATP transport in mitochondria and its carrier. *BBA-Biomembranes,* 1778**,** 1978-2021.

Klingenberg, M. 2009. Cardiolipin and Mitochondrial Carriers. *BBA - Biomembranes*, 1-38.

Klingenberg, M., Riccio, P. & Aquila, H. 1978. Isolation of the ADP, ATP carrier as the carboxyatractylate . protein complex from mitochondria. *Biochim Biophys Acta,* 503, 193-210.

Klingenberg, M., Winkler, E. & Huang, S. 1995. ADP/ATP carrier and uncoupling protein. *Methods Enzymol,* 260, 369-89.

Krämer, R. 1986. Reconstitution of ADP/ATP translocase in phospholipid vesicles. *Methods Enzymol,* 125, 610-8.

Krämer, R. & Heberger, C. 1986. Functional reconstitution of carrier proteins by removal of detergent with a hydrophobic ion exchange column. *Biochim Biophys Acta,* 863, 289-96.

Krämer, R. & Klingenberg, M. 1977. Reconstitution of adenine nucleotide transport with purified ADP, ATP-carrier protein. *FEBS Lett,* 82, 363-7.

Krämer, R. & Klingenberg, M. 1980. Enhancement of reconstituted ADP,ATP exchange activity by phosphatidylethanolamine and by anionic phospholipids. *FEBS Lett,* 119, 257-60.

Krämer, R. & Kürzinger, G. 1984. The reconstituted ADP/ATP carrier from mitochondria is both inhibited and activated by anions. *Biochim Biophys Acta,* 765, 353-62.

Krammer, E.-M., Ravaud, S., Dehez, F., Frelet-Barrand, A., Pebay-Peyroula, E. & Chipot, C. 2009. High-chloride concentrations abolish the binding of adenine nucleotides in the mitochondrial ADP/ATP carrier family. *Biophys J,* 97, L25-7.

Lasch, J., Weissig, V. & Brandi, M. 2003. Preparation of liposomes. *In:* TORCHILIN, V. & WEISSIG, V. (eds.) *Liposomes.* Second ed. Oxford: Oxford University Press.

Madeo, M., Carrisi, C., Iacopetta, D., Capobianco, L., Cappello, A. R., Bucci, C., Palmieri, F., Mazzeo, G., Montalto, A. & Dolce, V. 2009. Abundant

expression and purification of biologically active mitochondrial citrate carrier in baculovirus-infected insect cells. *J Bioenerg Biomembr,* 41**,** 289-97.

Marobbio, C., Vozza, A., Harding, M., Bisaccia, F., Palmieri, F. & Walker, J. 2002. Identification and reconstitution of the yeast mitochondrial transporter for thiamine pyrophosphate. *EMBO J,* 21**,** 5653-5661.

Matthews, K. R. 2005. The developmental cell biology of Trypanosoma brucei. *J Cell Sci,* 118**,** 283-90.

Mileykovskaya, E. & Dowhan, W. 2009. Cardiolipin membrane domains in prokaryotes and eukaryotes. *Biochim Biophys Acta,* 1788**,** 2084-91.

Noël, H. & Pande, S. V. 1986. An essential requirement of cardiolipin for mitochondrial carnitine acylcarnitine translocase activity. Lipid requirement of carnitine acylcarnitine translocase. *Eur J Biochem,* 155**,** 99-102.

Novy, R., Drott, D., Yaeger, K. & Mierendorf, R. 2001. Overcoming the codon bias of E. coli for enhanced protein expression. *inNovations. Newsletter of Novagen, Inc,* 12**,** 1-3.

Ollivon, M., Lesieur, S., Grabielle-Madelmont, C. & Paternostre, M. 2000. Vesicle reconstitution from lipid-detergent mixed micelles. *Biochim Biophys Acta,* 1508**,** 34-50.

Ostrander, D. B., Zhang, M., Mileykovskaya, E., Rho, M. & Dowhan, W. 2001. Lack of mitochondrial anionic phospholipids causes an inhibition of translation of protein components of the electron transport chain. A yeast genetic model system for the study of anionic phospholipid function in mitochondria. *J Biol Chem,* 276**,** 25262-72.

Palmieri, F., Indiveri, C., Bisaccia, F. & Iacobazzi, V. 1995. Mitochondrial metabolite carrier proteins: purification, reconstitution, and transport studies. *Methods Enzymol,* 260**,** 349-69.

Palmieri, L., Arrigoni, R., Blanco, E., Carrari, F., Zanor, M. I., Studart-Guimaraes, C., Fernie, A. R. & Palmieri, F. 2006. Molecular identification of an Arabidopsis S-adenosylmethionine transporter. Analysis of organ distribution, bacterial expression, reconstitution into liposomes, and functional characterization. *Plant Physiol,* 142**,** 855-65.

Palmieri, L., Rottensteiner, H., Girzalsky, W., Scarcia, P., Palmieri, F. & Erdmann, R. 2001. Identification and functional reconstitution of the yeast peroxisomal adenine nucleotide transporter. *EMBO J,* 20**,** 5049-5059.

Palmieri, L., Runswick, M. J., Fiermonte, G., Walker, J. E. & Palmieri, F. 2000. Yeast Mitochondrial Carriers: Bacterial Expression, Biochemical Identification and Metabolic Significance. *J Bioenerg Biomembr,* 32**,** 67-77.

Patnaik, P. K., Field, M. C., Menon, A. K., Cross, G. A., Yee, M. C. & Bütikofer, P. 1993. Molecular species analysis of phospholipids from Trypanosoma brucei bloodstream and procyclic forms. *Mol Biochem Parasitol,* 58**,** 97-105.

Pfanner, N. & Geissler, A. 2001. Versatility of the mitochondrial protein import machinery. *Nat Rev Mol Cell Biol,* 2**,** 339-49.

Riccio, P., Aquila, H. & Klingenberg, M. 1975a. Purification of the carboxy-atractylate binding protein from mitochondria. *FEBS Lett,* 56**,** 133-8.

Riccio, P., Aquila, H. & Klingenberg, M. 1975b. Solubilization of the carboxy-atractylate binding protein from mitochondria. *FEBS Lett,* 56**,** 192-32.

Rück, A., Dolder, M., Wallimann, T. & Brdiczka, D. 1998. Reconstituted adenine nucleotide translocase forms a channel for small molecules comparable to the mitochondrial permeability transition pore. *FEBS Lett,* 426**,** 97-101.

Schlame, M. & Ren, M. 2009. The role of cardiolipin in the structural organization of mitochondrial membranes. *Biochim Biophys Acta,* 1788**,** 2080-3.

Seddon, A. M., Curnow, P. & Booth, P. J. 2004. Membrane proteins, lipids and detergents: not just a soap opera. *Biochim Biophys Acta,* 1666**,** 105-17.

Sharp, P. M. & Li, W. H. 1987. The codon Adaptation Index--a measure of directional synonymous codon usage bias, and its potential applications. *Nucleic Acids Res,* 15**,** 1281-95.

Sorensen, H. P. & Mortensen, K. K. 2005. Advanced genetic strategies for recombinant protein expression in Escherichia coli. *J Biotechnol,* 115**,** 113-28.

Staudinger, R. & Bandres, J. C. 2003. Solubilization of Chemokine Receptors from Cell Membranes. *Methods Mol Biol,* 228.

Studier, F. W. 2005. Protein production by auto-induction in high-density shaking cultures. *Protein Expres Purif,* 41.

Suzuki, H. & Takeuchi, S. 2008. Microtechnologies for membrane protein studies. *Anal Bioanal Chem,* 391**,** 2695-702.

Tjaden, J., Schwöppe, C., Möhlmann, T., Quick, P. W. & Neuhaus, H. E. 1998. Expression of a plastidic ATP/ADP transporter gene in Escherichia coli leads to a functional adenine nucleotide transport system in the bacterial cytoplasmic membrane. *J Biol Chem,* 273**,** 9630-6.

Todisco, S., Agrimi, G., Castegna, A. & Palmieri, F. 2006. Identification of the mitochondrial NAD+ transporter in Saccharomyces cerevisiae. *J Biol Chem,* 281**,** 1524-31.

Trotter, P. J., Pedretti, J. & Voelker, D. R. 1993. Phosphatidylserine decarboxylase from Saccharomyces cerevisiae. Isolation of mutants, cloning of the gene, and creation of a null allele. *J Biol Chem,* 268**,** 21416-24.

van der Giezen, M., Slotboom, D., Horner, D., Dyal, P., Harding, M., Xue, G., Embley, T. & Kunji, E. 2002. Conserved properties of hydrogenosomal and mitochondrial ADP/ATP carriers: a common origin for both organelles. *EMBO J,* 21**,** 572-579.

Vance, J. E. 2008. Phosphatidylserine and phosphatidylethanolamine in mammalian cells: two metabolically related aminophospholipids. *J Lipid Res,* 49**,** 1377-87.

Vozza, A., Blanco, E., Palmieri, L. & Palmieri, F. 2004. Identification of the mitochondrial GTP/GDP transporter in Saccharomyces cerevisiae. *J Biol Chem,* 279**,** 20850-7.

Wagner, S., Bader, M. L., Drew, D. & de Gier, J.-W. 2006. Rationalizing membrane protein overexpression. *Trends Biotechnol,* 24**,** 364-71.

Yadava, A. & Ockenhouse, C. F. 2003. Effect of codon optimization on expression levels of a functionally folded malaria vaccine candidate in prokaryotic and eukaryotic expression systems. *Infect Immun,* 71**,** 4961-9.

Zick, M., Rabl, R. & Reichert, A. S. 2009. Cristae formation-linking ultrastructure and function of mitochondria. *BBA - Mol Cell Res,* 1793**,** 5-19.

Chapter VI.
Sequence analysis and functional characterization of the putative ADP/ATP carriers MCP15 and MCP16, and the putative GDP/GTP carrier MCP13

Table of Contents

#

Chapter VI . Sequence analysis and functional characterization of the putative ADP/ATP carriers MCP15 and MCP16, and the putative GDP/GTP carrier MCP13

1. Introduction

Next to MCP5, two other MCF proteins were identified with significant sequence similarities to prototypical ADP/ATP carriers, i.e. MCP15 and MCP16 (discussed in Chapters III of this thesis; Colasante *et al.* 2009). The presence of multiple putative ADP/ATP carrier-encoding genes in *T. brucei* is not unexpected. Virtually all eukaryotes contain multiple genes coding for ADP/ATP carriers (AACs). For example, the genome of *S. cerevisiae* contains 3 similar genes coding for different ADP/ATP carrier isoforms, i.e. AAC1, AAC2 and AAC3 (Adrian *et al.*, 1986; Kolarov *et al.*, 1990). More recently, another but less conserved AAC was discovered in *S. cerevisiae*, i.e. Sal1p. Knockout studies revealed that Sal1p could take over the role of AAC2 in yeast (Chen, 2004). Functional studies and mutation analysis in *S. cerevisiae* revealed further that each of the identified ADP/ATP carriers do play a different physiological role (Lawson *et al.*, 1990; Gawaz *et al.*, 1990; Kolarov *et al.*, 1990; Drgon *et al.*, 1991). Also in multicellular eukaryotes, like mammals and humans, multiple ADP/ATP carrier-encoding genes are found whose expression can be tissue-specific and their physiological function location-dependent (Powell *et al.*, 1989). The divergence of AACs into multiple tissue-dependent isoforms is most probably a direct consequence of the evolution to multicellular life forms (Löytynoja and Milinkovitch, 2001).

Reciprocal BLASTP searches and sequence analysis lead further to the identification of another remarkable MCF protein in *T. brucei*, i.e. MCP13 (Chapter III; Colasante *et al*. 2009). This MCF protein was not categorized as an ADP/ATP carrier, but showed significant sequence similarity to GGC1, the GDP/GTP carrier of *S. cerevisiae*. GGC1 is the first and only GDP/GTP carrier described to date, and homologues were so far only found in other yeasts and fungi, like *Aspergillus* and *Neurospora* (Vozza *et al.*, 2004). The absence of such a GDP/GTP carrier in higher eukaryotes, like plants and metazoans, was explained by the fact that higher eukaryotes possess a mitochondrial GTP-producing succinyl-CoA ligase (Vozza *et al*., 2004). This enzyme is involved in the tricarboxylic acid (TCA) cycle and

catalyses the conversion of succinyl-CoA to succinate with the concomitant production of mitochondrial GTP. Yeast and fungal mitochondria only produce ATP, therefore necessitating the import of GTP from the cytosol. This import is apparently catalysed by a GDP/GTP carrier, i.e. Ggc1p in *S. cerevisiae* (Przybyla-Zawislak *et al*., 1998). Knockout of GGC1 resulted in a defective iron regulation in yeast. It was suggested that this GDP/GDP-carrier was involved in the biogenesis of Fe-S clusters in mitochondria: in particular the iron-sulfur (Fe-S) cluster formation by Isu1p, which requires GTP, was affected by the knockout of GGC1 (Amutha *et al*., 2008). Isu proteins play a key role in the mitochondrial assembly of Fe-S clusters (Gerber *et al*., 2004). Fe-S clusters are essential cofactors required for the function of different mitochondrial and cytosolic proteins, like for example aconitase, ferredoxin and various proteins of the respiratory chain (Amutha *et al*., 2008; Stehling *et al*., 2009). Also the mitochondrion of *T. brucei* has been reported to be involved in the assembly of Fe-S clusters (Long *et al.*, 2008b; Long *et al.*, 2008a). Similar to yeast, trypanosomes also lack a mitochondrial GTP-producing succinyl-CoA ligase, therefore necessitating the presence of a GDP/GTP carrier in the mitochondrial inner membrane, here probably MCP13.

The main aim of this Chapter was the functional characterisation of (A) the putative ADP/ATP carriers MCP15 and MCP6, and (B) the putative GDP/GTP carrier MCP13. For the functional characterisation of these MCF proteins, a similar approach was used as described for MCP5 in the Chapters IV and V of this thesis. The predicted exchange functions of MCP15, MCP16 and MCP13 were further assessed by a more in-depth sequence analysis and phylogenetic reconstruction. Expression of these different MCPs in the bloodstream-form and the procyclic-form of *T. brucei* was analysed at the RNA level by northern blotting, whereas the subcellular localisation of the MCF proteins was determined by immunofluorescence microscopy. The different physiological role(s) of these putative ADP/ATP and GDP/GTP carriers was assessed by the generation of stable knockout cell lines in procyclic-form *T. brucei*. Finally, first steps were made towards the determination of their specific transport function by *in vitro* reconstitution in liposomes and subsequent transport assays.

2. Results and Discussion

2.1. Sequence analysis of MCP13, MCP15 and MCP16

Sequence analysis revealed that MCP15 displayed significant sequence similarities to prototypical ADP/ATP carriers from higher eukaryotes, with 45% and 47% similarity to human ANT and yeast AAC, respectively (Colasante *et al.*, 2009). A more in-depth sequence analysis revealed that the different substrate contact points (CPI-III), previously shown to be conserved in all ADP/ATP carriers (Colasante *et al*., 2009), were only partially conserved in MCP15 (Figure 1). For example, MCP15 contained the rather deviating "SxxxVxxxH" motif (with x representing any amino acid) instead of the expected CPI sequence motif "RxxxTxxxN" that is conserved in all functionally characterised AACs. CPII of MCP15 is only partially conserved: the "GI" amino acid duet, that has previously been proposed to provide a hydrophobic binding pocket for ADP in all ADP/ATP carriers, was replaced by a semi-conserved "GS" sequence motif in MCP15. Of the three different substrate contact points in MCP15, only CPIII, i.e. represented by a positive-charged arginine (R) residue, appeared to be conserved (Figure 1). Next to the substrate contact points, also the "RRRMMM" motif, which so far has been regarded as the hallmark of all ADP/ATP carriers, appeared to be slightly modified in MCP15, revealing a "RRRMMI" motif instead. The replacement of the hydrophobic methionine (M) residue at position 6 of the motif with the similar hydrophobic isoleucine (I) residue can be regarded as a conserved substitution, suggesting that the "RRRMMI" motif in MCP15 most probably functions in a similar way as the conserved "RRRMMM" motif found in other prototypical ADP/ATP carriers. Based on the (for a major part) conserved prototypical AAC sequence features and its significant homology to MCP5, it can be safely assumed that MCP15 most probably functions as an ADP/ATP carrier.

MCP16, on the other hand, appeared to be more divergent. Sequence analysis (Figure 2) revealed that MCP16 displayed an overall sequence similarity of 32% to both human and yeast AACs, which is significantly lower then found for MCP15 (Colasante *et al*., 2009). Instead of the expected "RRRMMM" motif, the less conserved "SRRMQL" motif was found in MCP16: the positively charged arginine (R) residue at position one of this motif has been replaced by an uncharged but polar serine (S) residue, whereas the hydrophobic methionine (M) residue at position five has been replaced by a positively charged glutamine (Q).

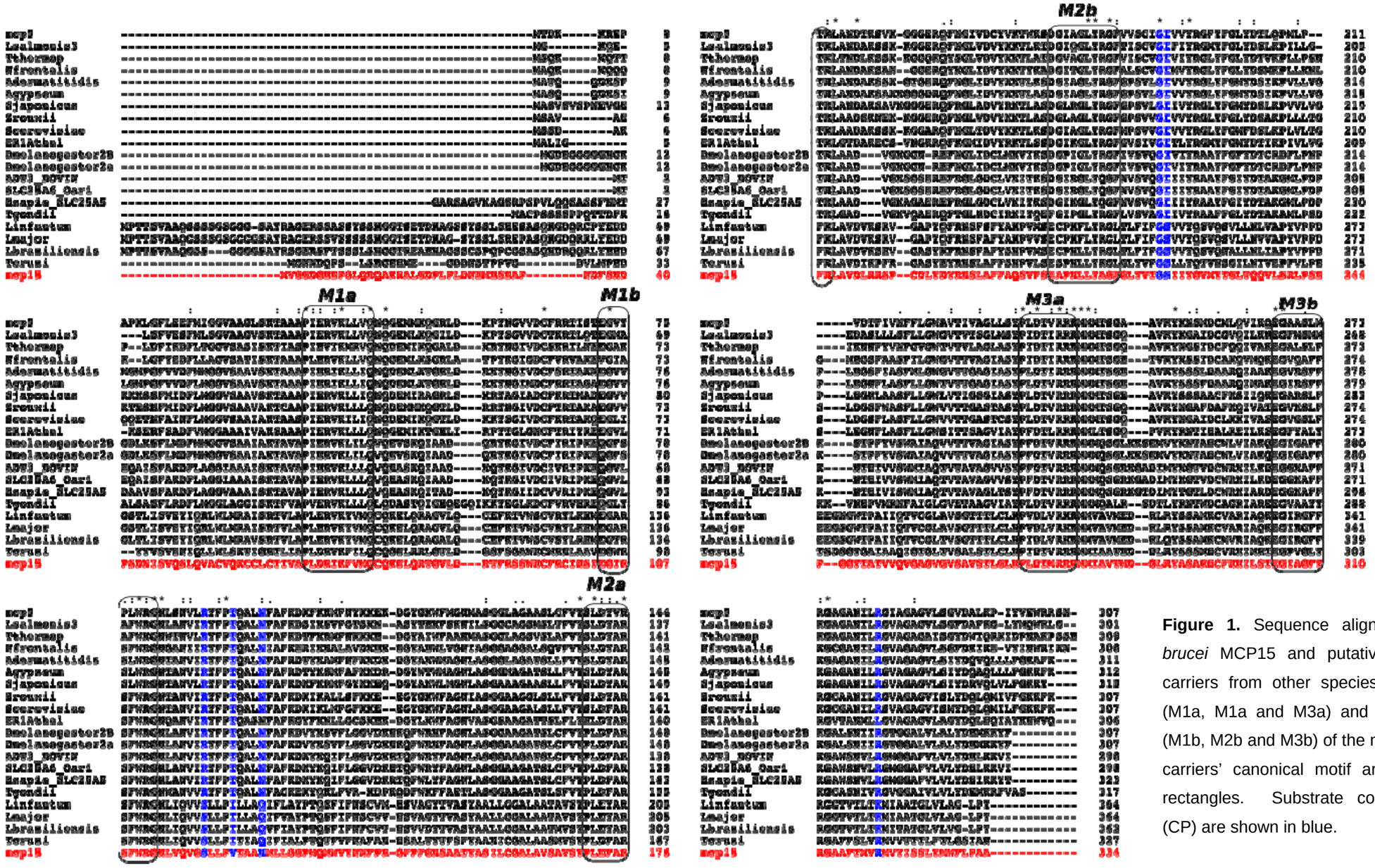

Figure 1. Sequence alignment of *T. brucei* MCP15 and putative ADP/ATP carriers from other species. The first (M1a, M1a and M3a) and second part (M1b, M2b and M3b) of the mitochondrial carriers' canonical motif are shown in rectangles. Substrate contact points (CP) are shown in blue.

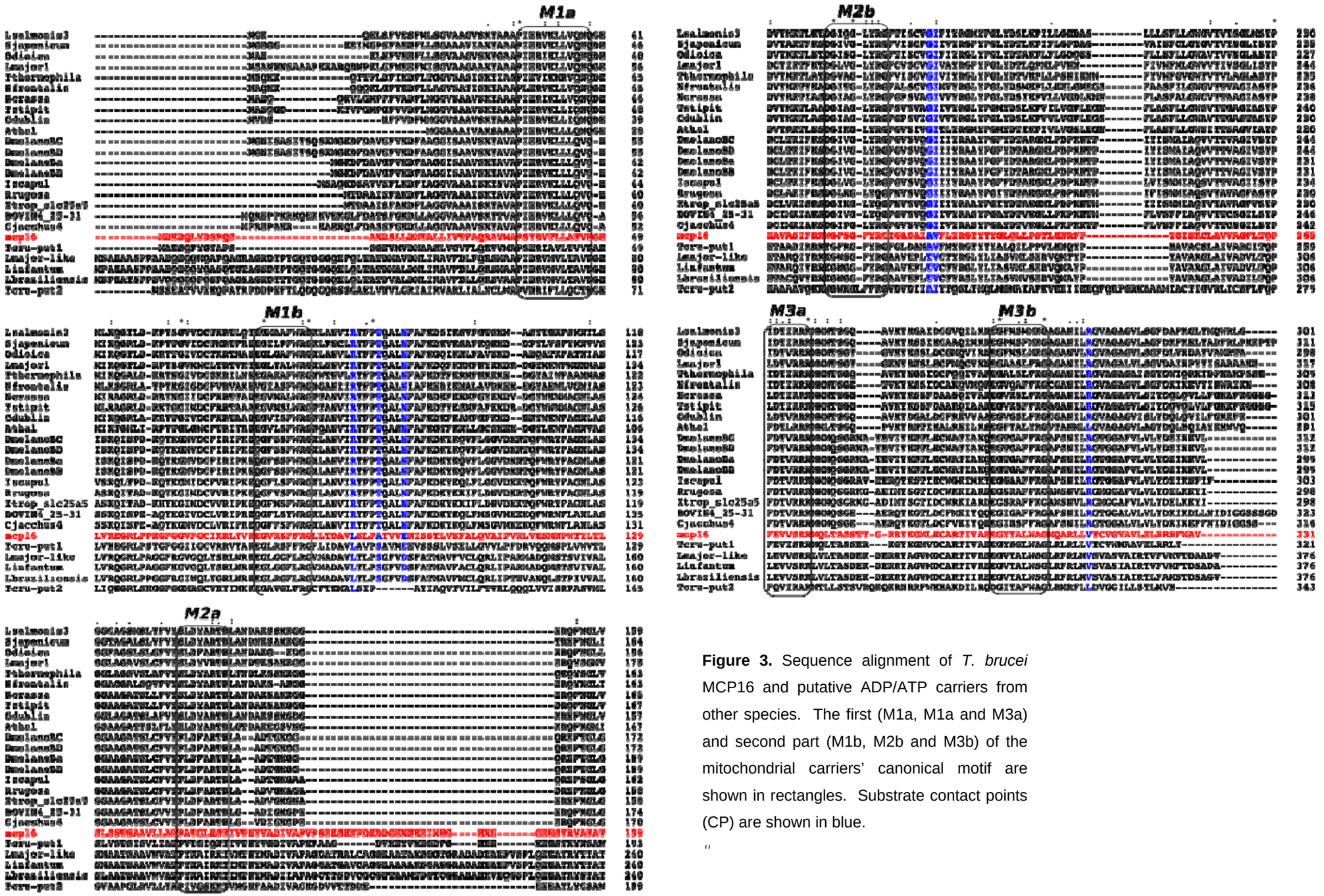

Figure 3. Sequence alignment of *T. brucei* MCP16 and putative ADP/ATP carriers from other species. The first (M1a, M1a and M3a) and second part (M1b, M2b and M3b) of the mitochondrial carriers' canonical motif are shown in rectangles. Substrate contact points (CP) are shown in blue.

"

Such non-conserved changes in the “RRRMMM” motif were previously shown to negatively affect OXPHOS activity. Mutation of the first R (R252I) in the “RRRMMM” motif of yeast AAC reduced OXPHOS activity to less than 50% of the wildtype version (Müller *et al*., 1996; Heidkamper *et al*., 1996).

The 3 positive charges amino acids in the “RRRMMM” motif has been proposed to be responsible for the neutralization of the 3 negative charges of ADP during ADP/ATP exchange (Heidkamper *et al*., 1996). Similar to the “RRRMMM” motif, also MCP16 contained in total 3 positive charged amino acids in its “SRRMQL” motif (Figure 2). Comparison of the MCP16 substrate contact points with those of known ADP/ATP carriers revealed some substantial differences. MCP16 contained the rather deviating “LxxxAxxxE” motif instead of the “RxxxTxxxN” CPI motif that is conserved in all functionally characterised AACs. For CPII, a more conserved substitution was found: the in prototypical ADP/ATP carriers conserved “GI” duet was in MCP16 replaced by two similar hydrophobic residues, i.e. alanine (A) and valine (V), respectively (Figure 2). The canonical positively charged arginine (R) residue in CPIII appeared not be conserved at all, and was in MCP16 replaced by the hydrophobic amino acid valine (V). Regarding the substantial substitution of amino acids in the different substrate contact points, and other deviations from conserved sequence features of ADP/ATP carriers, its unlikely that MCP16 will function as a prototypical ADP/ATP carrier.

Comparison of MCP13 with the yeast GDP/GTP carrier Ggc1p and related homologous sequences from other yeasts and fungi resulted in the prediction of putative substrate contact points for GDP/GTP carriers (Figure 3). The substrate contact points CPI and CPII, represented by respectively the sequence motif “YxxxQxxxK” and the amino acid duet “RN”, were both found to be conserved in MCP13 and other homologous GGC sequences (Robinson and Kunji, 2006). Also CPIII was found to be conserved among all putative GDP/GTP carriers: in yeast and fungal sequences a conserved threonine (T) residue was found, whereas in MCP13 and other kinetoplastid GGC homologues a conserved substitution was observed, i.e. the in yeast and fungi conserved threonine residue was in kinetoplastid sequences replaced by a similar serine (S) or phenylalanine (F) residue (figure 3).

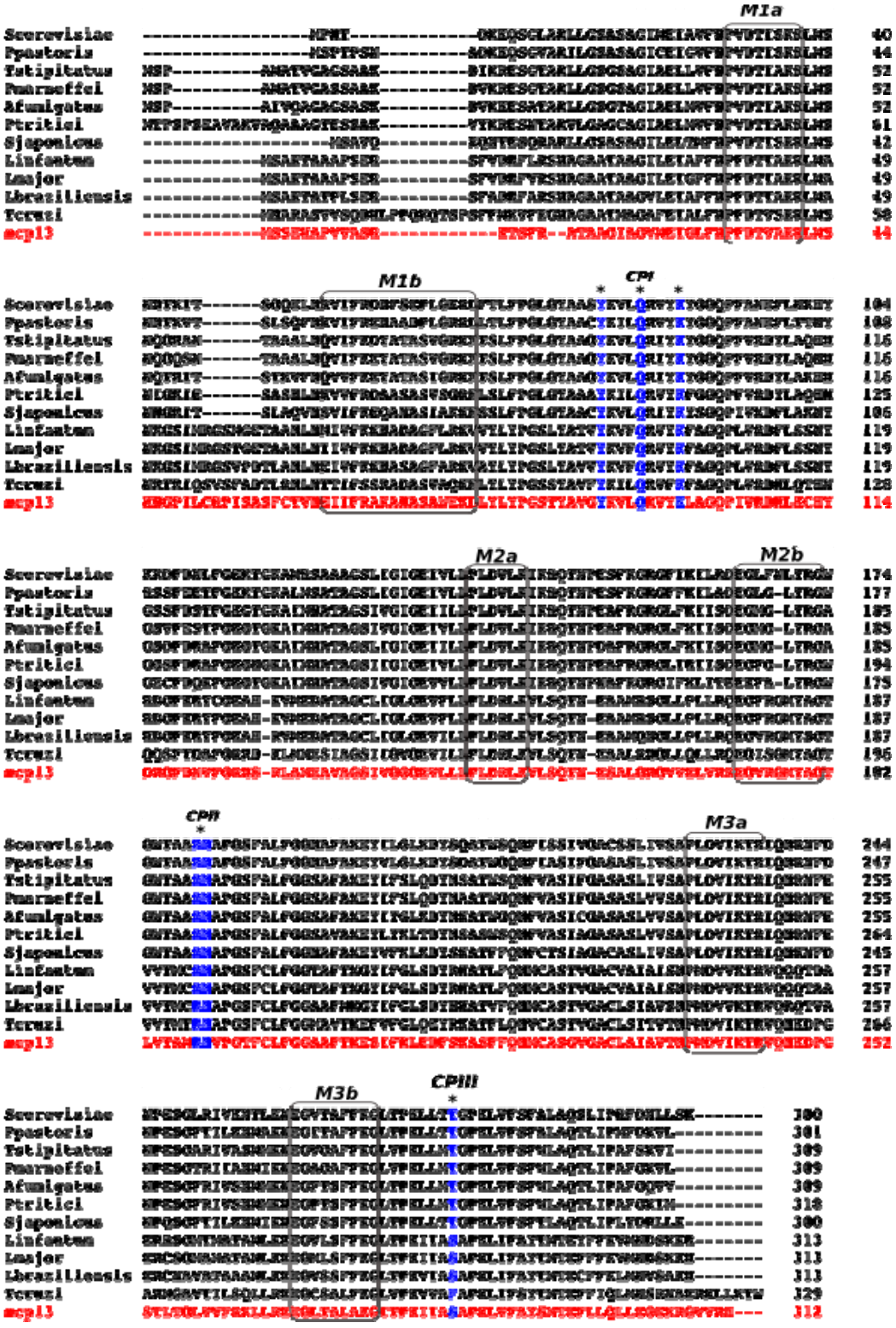

Figure 3. Sequence alignment of *T. brucei* MCP13, *S.cerevisiae* Ggc1p, and putative GDP/GTP carriers from yeasts and fungi. The first (M1a, M1a and M3a) and second part (M1b, M2b and M3b) of the mitochondrial carriers' canonical motif are shown in rectangles. Substrate contact points (CP) are shown in blue.

Phylogenetic reconstruction was subsequently used as a complementary approach to support the predicted exchange functions for MCP15 and MCP16. A similar phylogenetic analysis was performed as described in Chapter IV of this thesis. The resulting neighbor-joining tree is shown in Figure 4. The putative phosphate carriers MCP8 and MCP11 (Chapter III) and the putative ATP-Mg/Pi carrier MCP6 were included as references in this phylogenetic analysis, and, as reported previously, formed distinct functional groups during phylogenetic reconstruction (Chapter III; Colasante *et al*. 2009). Further, MCP5 clustered specifically in a single clade with different AACs from yeasts and plants, suggesting a common origin of these ADP/ATP carriers (see Chapter IV for further discussion). Similar to the results found in Chapter IV, also insect and metazoan ADP/ATP carriers appeared to form a separate evolutionary clade.

Unexpectedly, neither MCP15 nor MCP16 were found in either of these clades: instead, a novel clade was found which contained both MCP15 and MCP16, together with putative ADP/ATP carriers from other related Kinetoplastidae, like *Trypanosoma cruzi* and different *Leishmania* species. This result indicated a common origin of these MCF proteins, and further suggested that this particular clade branched off prior to the separation of the plant and fungi AACs on one hand and the metazoan and insect AACs on the other hand. Within this clade, MCP15 and MCP16 were found in two separate groups, suggesting an independent evolution of these MCF proteins. The grouping of MCP15 and MCP16 in a different clade than MCP5 suggested possible differences in ADP/ATP (or other substrates) exchange function.

Phylogenetic analysis revealed further that MCP13 was exclusively found present within a distinct clade, which included yeast GGC1 and other putative GDP/GTP carriers (predicted by sequence similarity) from yeasts and fungi (Figure 4). The grouping of MCP13 within the GDP/GTP carrier clade is supported by a high (100%) bootstrap value. Within the observed GDP/GTP-carrier clade, two distinct groups were found: MCP13 grouped specifically with putative GDP/GTP carriers from related Kinetoplastidae, whereas the yeast and fungal GDP/GTP carriers were found in the other group. The observed separation into two different groups of GDP/GTP carriers is further supported by the different CPIII sequences found in the kinetoplastid group and the yeast and fungi group, respectively.

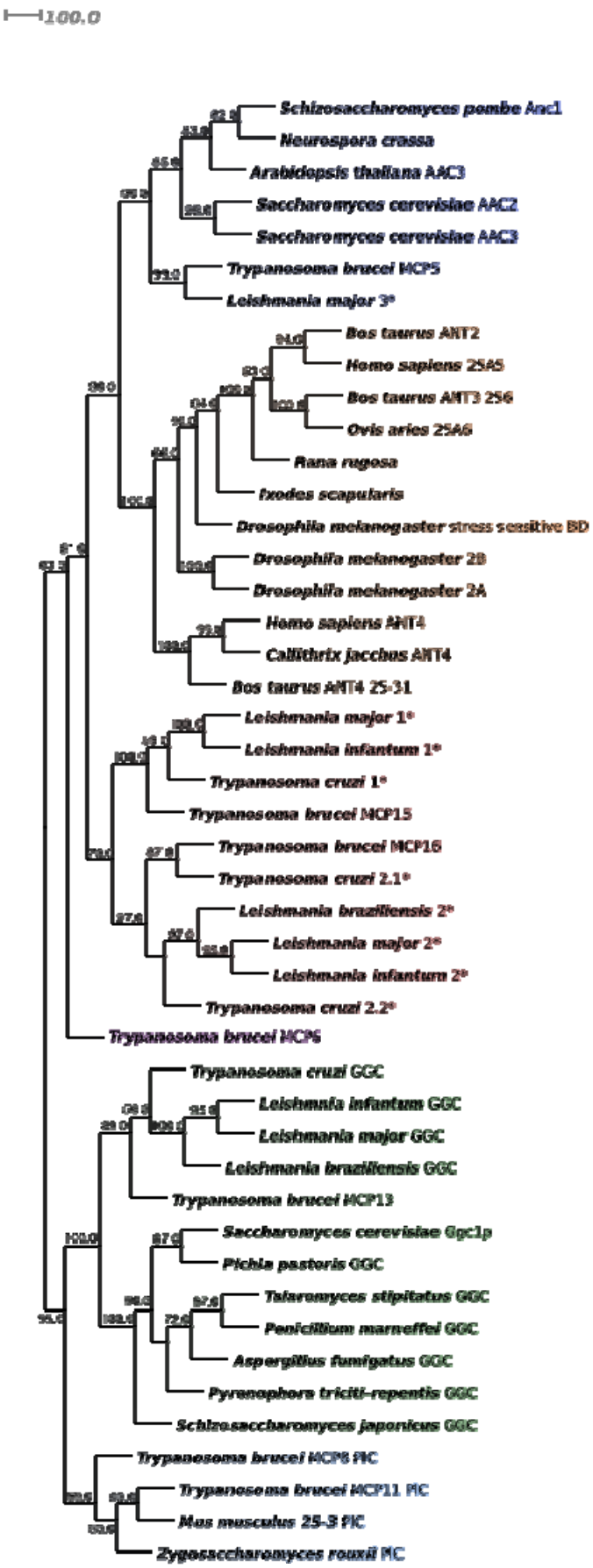

Figure 4. Neighbor-joining tree showing the evolutionary relationship between selected nucleotide and phosphate carriers from kinetoplastids with those of other species. Bootstraps values >50 are shown at each node. The NJ-Tree was constructed using Mobyle@Pasteur and its included Protdist and Neighbor-Joining programs. The consensus tree was constructed on the same platform, whereas the final tree was edited using SplitsTree V.

2.2. Expression of MCP13, MCP15 and MCP16, at the mRNA level

Expression of MCP13, MCP15 and MCP16, in the different life cycle stages of *T. brucei*, i.e. the procyclic- and the bloodstream-form, was exclusively assessed at the mRNA level, since there were no antibodies available for the immuno-detection of these MCF proteins.

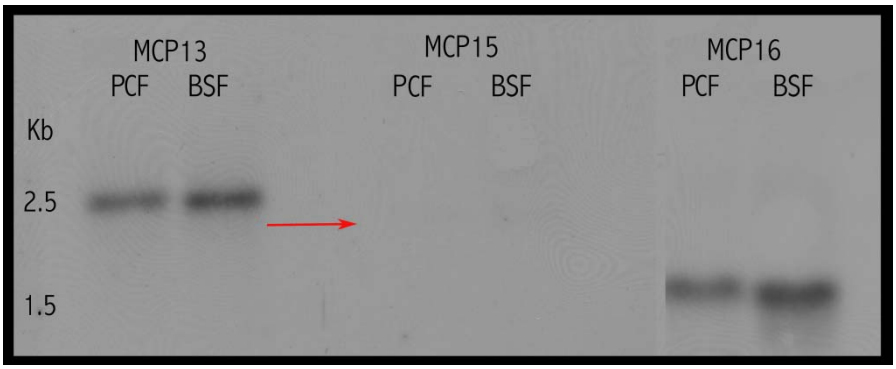

Figure 5. Northern blot analysis of *T. brucei* PCF449 and BSF449 total RNA. The respective open reading frames of MCP13, MCP15 and MCP16 were used as a DNA probe for detection. 10μg total RNA was loaded for each sample.

The results of the northern blot analysis are shown in Figure 5. For each of the tested MCPs, a single cross-reacting mRNA band was found with approximate size-lengths of 2.5kb (MCP13), 2.0kb (MCP15) and 1.5 kb (MCP16), respectively. The observed size-lengths are in agreement with (i.e. larger than) the expected minimum mRNA size corresponding to the open reading frame plus additional 5' and 3' untranslated (UTR) mRNA regions. Quantification revealed that there are no significant differences in expression (at the mRNA level) of the different analysed MCPs, when comparing PCF and BSF *T. brucei* (results not shown). This result suggested that the analysed MCPs are equally important, and probably expression to the same level (careful assumption), in both life cycle stages. Remarkable are the rather low mRNA quantities observed for MCP15, in comparison to the more abundant mRNA found for MCP13 and MCP16.

2.3. Subcellular localization studies of MCP13, MCP15 and MCP16.

Due to the lack of specific antibodies, the subcellular localization of the analysed MCPs had to be determined by the generation of specific *T. brucei* cell lines, i.e. *MCP13-nmyc*^{ti}, *MCP15-nmyc*^{ti}, and *MCP16-nmyc*^{ti}, respectively. Expression of the different myc-tagged versions of these MCPs was induced by the addition of tetracycline to the respective recombinant *T. brucei* cell lines: the expression of the recombinant myc-tagged protein products was subsequently confirmed by Western blot analysis (Figure 6). As expected, no myc-tagged proteins could be detected in the non-induced *T. brucei* cell lines, indicating a tight regulation of the promoter and operator used for inducible expression in these cell lines. Upon addition of tetracycline, single cross-reacting proteins were found in each of the cell lines (Figure 6). The molecular weights of the expressed MCF proteins were as expected: 36kDa for MCP13, 40kDa for MCP15, and 38kDa for MCP16 (taking into account the molecular weight of the added myc-tag*).*

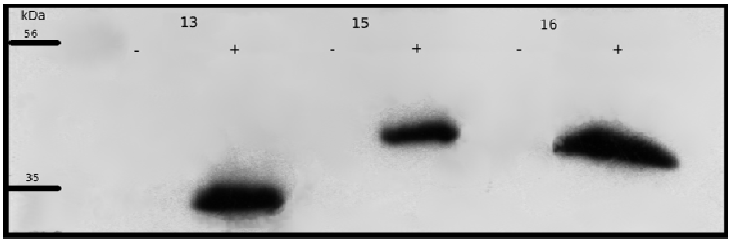

Figure 6. Western blot analysis showing the tetracycline-inducible expression of myc-tagged MCP13, MCP15 and MCP16 proteins in procyclic-form *T. brucei*. (-) induced; (+) induced with tetracycline.

The subcellular localization of the different myc-tagged proteins was subsequently determined by immunofluorescence microscopy using a commercial myc-tag antibody. The obtained results (Figure 7) revealed exclusive mitochondrial localization for all 3 tested MCPs.

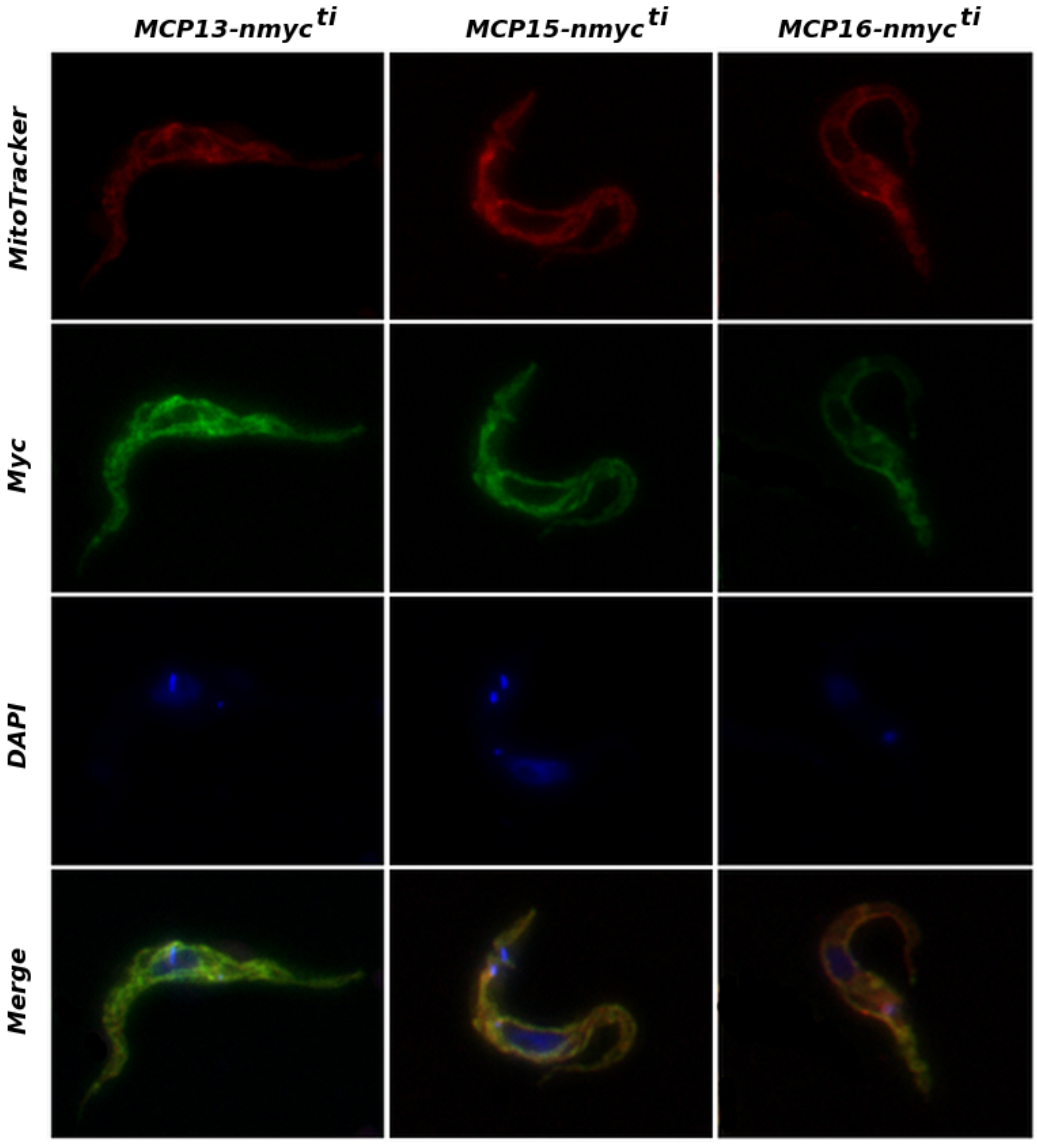

Figure 7. Immunofluorescence microscopy of different procyclic-form *T. brucei* cell lines respectively expressing myc-tagged MCP13, MCP15, or MCP6 (Myc, green). MitoTracker (red) was used as a mitochondrial marker, whereas DAPI was used to stain DNA (blue). Overlays are shown in the panels marked “Merge”.#

#
#
#
#
#
#
#
#
#
#
#
#
#

2.4. The generation of MCP13, MCP15 and MCP16 knockout cell lines

For the generation of the respective MCP13, MCP15 and MCP16 procyclic-form knockout cell lines, the same gene replacement technique was used which was proven successful for the generation of the previously discussed MCP5 double knockout cell line (Chapter IV). In contrast to MCP5, the in this section targeted MCPs are all single copy genes (Chapter III).

Similar to MCP5, we first attempted to generate conventional (no rescue copy) double knockout cell lines. However, no viable clones could be obtained after many attempts for either MCP13 or MCP16, indicating that these MCPs are essential for the survival of procyclic-form *T. brucei*. This in contrast to MCP15, for which a conventional double-knockout cell line could be obtained without any detrimental effect on trypanosome growth (not shown). This result indicated that MCP15 is apparently not essential for the survival of PCF *T. brucei.* The generated MCP15 double knockout cell line is hereafter called: *Δmcp15.* Southern blot analysis confirmed that the obtained *Δmcp15* cell line indeed lacked the MCP15-encoding gene: the observed hybridisation pattern indicated the replacement of the original MCP15 gene, i.e. the two diploid alleles, with the two different antibiotic resistance cassettes (Figure 8: panel B).

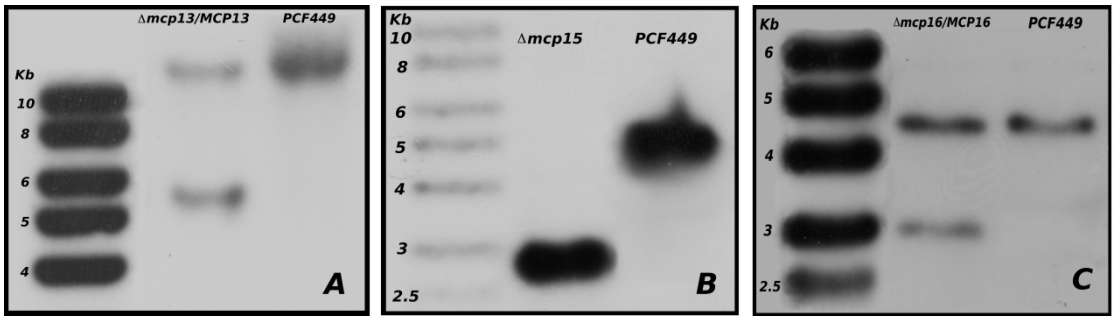

Figure 8. Southern blot analysis of (A) the conditional MCP13 half-knockout cell line *Δmcp13/MCP13/MCP13-nmyc*^{ti}, (B) the conventional MCP15 double knockout cell line *Δmcp15*, and (C) the conditional MCP16 half-knockout cell line *Δmcp16/MCP16/MCP16-nmyc*^{ti}. Each lane contains 10μg genomic DNA digested with BamHI. The respective 3'UTRs of MCP13, MCP15 and MCP16 were used as DNA probes.

As indicated above, no viable clones could be obtained after many attempts for either MCP13 or MCP16. After transfection with the various knockout-constructs,

viable cells could be observed after selection with the different antibiotics: however they invariably did not grow and ultimately died after prolonged cell culture. This lack of growth made it impossible to collect sufficient cell material for further analysis.

Like for MCP5 (Chapter IV), we instead attempted the generation of conditional knockout cell lines for both MCP13 and MCP16. The previously generated *MCP13-nmyc*^{ti} and *MCP16-nmyc*^{ti} cell lines were used as a starting point for this approach. Viable MCP13 and MCP15 half-knockout cell lines could be isolated, i.e. *Δmcp13/MCP13/MCP13-nmyc*^{ti} and *Δmcp16/MCP16/MCP16-nmyc*^{ti}, respectively. Southern blot analysis confirmed the true nature of the obtained MCP13 and MCP16 half-knockout cell lines (Figure 8: panels A and C, respectively): in both cases the natural MCP13 or MCP16 gene-containing genomic DNA fragments (BamHI digested) could still be observed next to the apparent replacement of one of the natural gene copies with the antibiotic resistance gene (represented by the low molecular weight hybridising genomic DNA band).

The obtained *Δmcp13/MCP13/MCP13-nmyc*^{ti} and *Δmcp16/MCP16/MCP16-nmyc*^{ti} half-knockout cell lines were subsequently used for the knockout of the remaining MCP13 or MCP16-encoding alleles. Unfortunately, it appeared to be impossible to obtain any "growing" conditional MCP13 or MCP16 double knockout cells: after transfection and subsequent antibiotic selection, viable cells could be observed by microscopy. These cells however were severely impaired in their growth, and invariably died after a fortnight of cell culture.

That the observed (surviving but not growing) cells indeed were of the expected genotype (i.e. *Δmcp13/MCP13-nmyc*^{ti} or *Δmcp16/MCP16-nmyc*^{ti}) was subsequently confirmed by PCR analysis. Southern blot analysis could not be used due to the lack of sufficient cell material. For the PCR analysis, the same approach was used as for the assessment of the *Δmcp5/MCP5-nmyc*^{ti} cell lines: i.e. the use of a specifically designed 5'-UTR forward primer, located upstream of the 5'UTR used for recombination, in combination with a reverse primer targeting the different antibiotic resistance cassettes (see Chapter IV). One example of such PCR analysis is shown in Figure 9. In case of the *Δmcp13/MCP13-nmyc*^{ti} cells, the second gene replacement round was performed with the NEO-construct. PCR analysis of two of the different (not growing but surviving) *Δmcp13/MCP13-nmyc*^{ti} clones confirmed that the second gene replacement round, using the NEO-knockout construct, was

indeed successful. In panels A and C of Figure 9, a PCR product was found of the expected size, i.e. approximately 2.0 kb, which indicated that he NEO-resistance cassette had properly recombined into the locus of the remaining MCP13 allele, thereby replacing it.

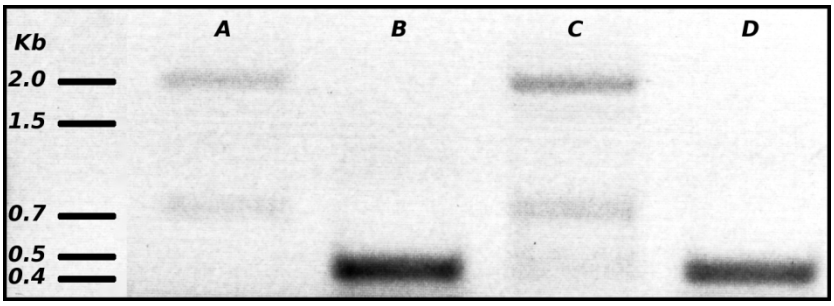

Figure 9. PCR assessment of the different *Δmcp13/MCP13-nmyc*^{ti} clones: PCR was performed with the designed forward primer, recognising a sequence upstream of the MCP13 5'-UTR target region used for homologous recombination, and the reverse primer selective for the NEO resistance cassette (lanes A and C). For the control PCR (lanes B and D), a primer set was used specific for the 5'UTR of MCP13. Approximately 2-4x10^4 cells were used as starting material for the PCR.

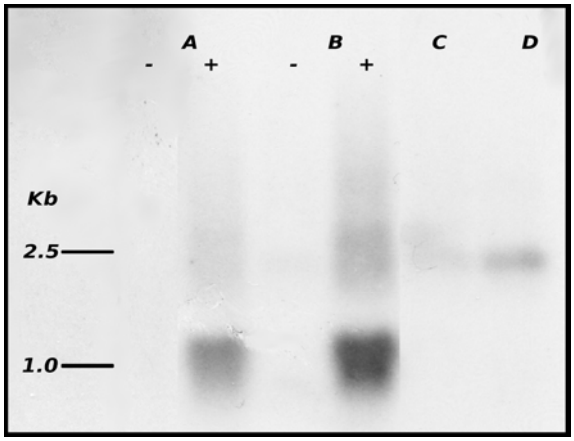

Figure 10. Northern blot analysis of two conditional *Δmcp13/MCP13*/*MCP13-nmyc*^{ti} half-knockout clones (A and B), grown in the presence (+) or absence (-) of tetracycline; the conventional *Δmcp13*/MCP13 half knockout cell line (lane C); and "wildtype" PCF449 (lane D). The MCP13 open reading frame was used as DNA probe for detection. The ~2.5Kb mRNA band represents the natural MCP13 gene, whereas the ~1.0Kb mRNA band represents rescue copy.

The inability to obtain growing MCP13 and MCP16 conditional knockout cell lines was rather unexpected. Possible explanations for this phenomenon could be that (A) the used (inducible) rescue copy of the respective MCPs was not functional or (B) that the used rescue copy was sufficiently not expressed to the appropriate level required for cell survival. The later explanation was assessed by Northern blot analysis. For this purpose, the obtained MCP13 and MCP16 half-knockout cell lines had to be used, since the double knockouts cell lines provided insufficient cell material for RNA isolation and detection. An example of such a Northern blot analysis is shown in Figure 10. Northern blot analysis of total RNA from the wildtype PCF449 cell line (Figure 10, lane D) or the conventional *Δmcp13/MCP13* half-knockout cell line (Figure 10, lane C) revealed the expected single 2.5kb hybridising mRNA band (compare to Figure 5). Comparison revealed further that remarkably less MCP13 mRNA was detected for the *Δmcp13/MCP13* half-knockout cell line when compared to the wildtype PCF449 cell line (approximately half mRNA signal). This result indicated that the MCP13 half-knockout was successful, leading to a concomitant reduction in MCP13 mRNA. Comparison of the northern blot results, obtained for the different induced and non-induced conditional *Δmcp13/MCP13*/*MCP13-nmyc*^{ti} half-knockout cell lines, confirmed the substantial over-expression of *MCP13-nmyc*^{ti} upon induction with tetracycline (Figure 10). *MCP13-nmyc*^{ti} mRNA is present in the induced *Δmcp13/MCP13*/*MCP13-nmyc*^{ti} cell lines approximately 4-5-fold the natural MCP13 mRNA (Figure 10). The observed abundance of the *MCP13-nmyc*^{ti} mRNA indicated that sufficient “rescue” MCP13 is present during the second gene-replacement round. This conclusion is based on the assumption that (A) the measured mRNA quantity is representative for the amount of expressed protein, and (B) that the added myc-tag does not negatively affect the function of MCP13.

Similar observations were made during the many attempts to generate a conditional MCP16 double-knockout cell line. PCR analysis of the surviving but not growing *Δmcp16/MCP16-nmyc*^{ti} cells confirmed that the second gene replacement round, in this case using the BLA-knockout construct, was indeed successful. In panels A and C of Figure 11, a PCR product was found of the expected size, i.e. 2.0 kb, which indicated that he BLA-resistance cassette had properly recombined into the locus of the remaining MCP16 allele, thereby replacing it.

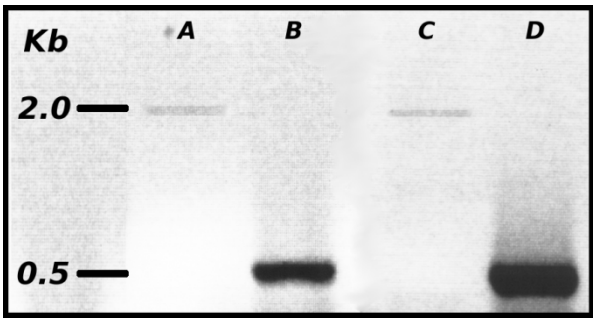

Figure 11. PCR assessment of the different *⊿mcp16/MCP16-nmyc*^{ti} clones: PCR was performed with the designed forward primer, recognising a sequence upstream of the MCP16 5'-UTR target region used for homologous recombination, and the reverse primer selective for the BLA resistance cassette (lanes A and C). For the control PCR (lanes B and D), a primer set was used specific for the 5'UTR of MCP13. Approximately 2-4x10^4 cells were used as starting material for the PCR.

The inability to generate viable and growing double-knockout cell lines for MCP13 and MCP16 indicated that these MCPs are essential for the survival of procyclic-form *T. brucei,* and implicated putative important roles of these MCF proteins in the mitochondrial metabolism of the parasite.

In contrast to MCP13 and MCP16, conventional MCP15 double-knockout cell lines could be generated without any negative effect on growth and survival of *T. brucei* (growth curves not shown). This result suggested a non-essential role of MCP15 in the mitochondrial metabolism of *T. brucei,* at least under laboratory culture conditions. A similar phenotype was also observed after the knockout of the AAC1 and/or AAC3 isoforms in *S. cerevisiae*, suggesting that these ADP/ATP carriers are not essential for mitochondrial oxidative phosphorylation and the concomitant survival of yeast (Drgon *et al.*, 1992; Smith and Thorsness, 2008; Drgon *et al.*, 1991). This in contrast to the knockout of *S. cerevisiae* AAC2, which had a detrimental effect on growth and survival of this yeast (Drgon *et al.*, 1992; Smith and Thorsness, 2008; Drgon *et al.*, 1991). Both AAC1 and AAC3 were further incapable of rescuing the AAC2 knockout-related growth phenotype in this organism, indicating different physiological roles of these AACs in *S. cerevisiae.* In analogy, different physiological roles can also be assumed for the putative ADP/ATP carriers MCP5 and MCP15 of *T. brucei*: MCP5 is essential for cell growth and survival of the procyclic-form parasite, whereas MCP15 is apparently not essential. The role of the putative ADP/ATP carrier MCP16 is unclear at this point.

2.5. Expression, purification and functional reconstitution of MCP13, 15 and 16.

As pointed out in Chapter V, the classical approach to study the transport function of MCF proteins consists of the isolation/purification of the respective metabolite carrier through affinity column chromatography, its reconstitution into liposomes, and the subsequent determination of its substrate specificity and transport kinetics via metabolite transport assays (Krämer and Klingenberg, 1977; Klingenberg *et al.*, 1995; Palmieri *et al.*, 1995). Similar to MCP5, a large number of different approaches were tested for the expression, isolation and functional reconstitution of MCP13, MCP15 and MCP16, respectively (see Chapter V for more information).

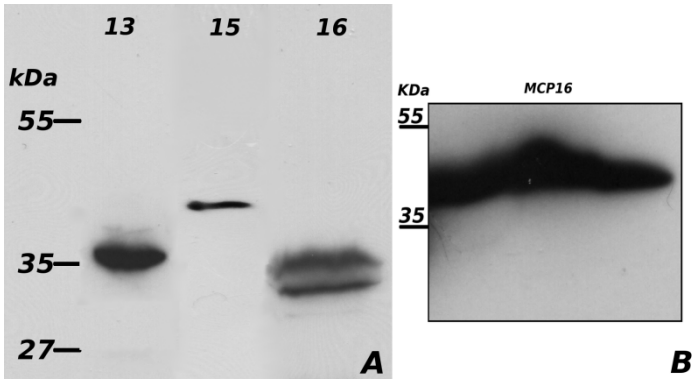

Figure 12. Western blot analysis of (A) *E. coli* Rossetta2-(DE3)-pLysS strains expressing His-tagged MCP13, MCP15 and MCP16, respectively, and (B) the *S. frugiperda* insect cell line Sf9 expressing His-tagged MCP16. A commercial His-antibody was used for detection.

The first step in this approach was the expression of His-tagged MCP13, MCP15 and MCP16 proteins in different heterologous systems. Similar to MCP5, both MCP13 and MCP16 could only be expressed in the *E. coli* Rossetta2(DE3)pLysS strain by using the previously discussed auto-induction procedure (Studier, 2005). However, in contrast to MCP5, MCP15 could be readily expressed in the same *E. coli* strain using conventional induction with IPTG instead. The corresponding western blot analysis results are shown in Figure 12. For MCP13 and MCP15, a single protein band with the expected molecular weight, i.e. approximately 36 kDa for MCP13 and 40 kDa for MCP15, was observed after detection with the His-tag antibody, whereas for MCP16, an unexpected double protein band was detected.

The reason for the appearance of a double His-tagged protein band during expression of MCP16 in *E. coli* Rossetta2(DE3)pLysS is unclear at this point, although a specific proteolytic cleavage of this protein in heterologous *E. coli* host could not be excluded. Instead MCP16 was expressed in the *S. frugiperda* cell line Sf9. Western blot analysis using the His-tag antibody revealed a single protein band of the expected molecular weight, i.e. 39 kDa.

The next step in the functional characterisation approach was the detergent solubilization and isolation of the His-tagged MCP13, MCP15 and MCP16 proteins with the aid of Ni-NTA affinity chromatography. The different tested conditions for detergent solubilization and affinity purification are summarised in Table 2. As is clear from this table, most of the conditions used for isolation of these MCPs were similar to those previously used for the successful isolation of His-tagged MCP5 (see Chapter V for more information).

MCP	Expressed in	Detergent used for solubilisation	Affinity Matrix used for Purification	Elution with	Result
MCP13	Bacteria	Up to 0.5% (w/v) TX-100	Talon®	200mM imidazole	Not binding
MCP13	Bacteria	Extraction 1% (w/v) TX-114	CM Sephadex C-50	50mM NaCl	Partially purified
MCP13	Bacteria	2% (w/v) Sarkosyl	Talon®	200mM imidazole	Partially purified
MCP13	Bacteria	0.5% (w/v) Sarkosyl	Ni-NTA	200mM imidazole	Partially purified
MCP15	Bacteria	0.5-2% (w/v) Sarkosyl	Talon®	200mM imidazole	Partially purified
MCP16	Bacteria	0.5-2% (w/v) Sarkosyl	Talon®	200mM imidazole	Partially purified
MCP16	Bacteria	Urea/0.5% Sarkosyl (w/v)/ 2% (w/v) TX-100 (inclusion bodies isolation)	Ni-NTA	200mM imidazole	Partially purified
MCP16	Insect cells	0.5% (w/v) Sarkosyl/ 2% (w/v) TX-100	Ni-NTA	200mM imidazole	Partially purified

Table 2. Summary of the different conditions used for solubilization and purification of MCP13, MCP15 and MCP16. After solubilization, an ultracentrifugation step was performed to assess the solubility of the protein.

The solubilisation and His-tag directed affinity purification a number of observations were made: (1) MCP13 was mostly present in inclusion bodies after expression in *E. coli* Rossetta2(DE3)pLysS and was found to be rather insoluble in non-ionic detergents: its solubilisation required the use of the strong anionic detergent Sarkosyl; (2) Over-expression of MCP15 and MCP16 did not lead to inclusion body formation: consequently they could be more easily solubilised with milder

detergents; (3), MCP15 and MCP16 were found to be degradation-resistant after solubilisation with Sarkosyl, whereas MCP13 (and MCP5, Chapter V) was rapidly degraded in the presence of this detergent; and (4) His-tagged MCP13, MCP15 and MCP16 protein could be completely eluted from the Ni-NTA affinity matrices when using 200mM imidazole: this was not possible for the previously characterised His-tagged MCP5 protein (Chapter V).

As indicated in table 2, all of the 3 analysed His-tagged MCPs could be partially purified after Ni-NTA affinity chromatography. Once the protein was eluted from the chromatography column, it was reconstitution immediately in order to further prevent further denaturation or degradation of the isolated proteins. Experiments revealed that repeated freeze-thawing of the isolated MCP preparations inevitable lead to protein degradation (results not shown). The protocols used for the reconstitution of MCP13, MCP15 and MCP16 are essentially the same as the ones described for MCP5 in Chapter V. Liposomes were generated with PC dissolved in the presence of variable concentrations of cardiolipin. ADP was used as the internal substrate for MCP15 and MCP16, whereas GDP was used in the case of MCP13 (Chapter II). For the formation of proteoliposomes, PC was dissolved with TX-114 or $C_{10}E_5$, mixed with the isolated His-tagged protein and the internal substrate, and passed through Biobeads columns in a cyclic manner until the detergent was completely removed. ^{14}C-ATP (MCP15 and MCP16) or ^{14}C-GTP (MCP13) was used as the external substrate for the assessment of transport activity.

Unfortunately, no exchange activity could be observed in any of the reconstitution experiments and subsequent transport assays. Please refer to Chapter V for further discussion and possible explanations for this lack of exchange activity after reconstitution of the different MCPs.

3. Further Discussion

Of the identified putative ADP/ATP carriers, it was MCP15 that showed the highest sequence similarity (32%) to MCP5 (Chapter III). Similar to MCP5, most of the conserved sequence features present in known AACs from other eukaryotes were also conserved in MCP16, although a few minor deviations were found for this MCF protein. Both sequence analysis and phylogenetic reconstruction predicted an ADP/ATP exchange function for MCP15. The above-described MCP15 double knockout experiments revealed that this MCF protein was not essential for the

survival of procyclic form *T. brucei*. This in contrast to MCP5: the generation of a conventional MCP5 knockout appeared to be impossible, indicating that this ADP/ATP exchanger indeed is essential for the survival of procyclic-form *T. brucei*. Intriguingly, the lack of MCP5 could not be compensated by the presence of MCP15 (Chapter III). This finding suggested that MCP5 and MCP15 do not have the same physiological roles in procyclic-form *T. brucei*, although both most probably function as mitochondrial ADP/ATP exchangers. This lack of complementation can also be explained in a different way. An important indication for this explanation is the detection of very low MCP15 mRNA levels in both procyclic-form and bloodstream-form *T. brucei*. One of the most important questions we have at the moment is whether MCP15 is expressed at all at the protein level. This question can yet not be answered due to the lack of a suitable MCP15 antiserum. It is further conceivable that MCP15 is not expressed or essential in the studied life stage of *T. brucei,* or is not expressed or essential due to the present laboratory culture conditions. This could however be different in another life cycle stage of the parasite (not studied here) or under different culture conditions. For that reason, it is important to determine what triggers the expression of MCP15 and under what conditions it becomes essential for trypanosome survival. One possible way to assess whether MCP15 is essential at all would be the passage of the procyclic-form *T. brucei* MCP15 double knockout parasites through its hosts, i.e. the Tsetse fly, with subsequent analysis of its survival rate.

The other predicted ADP/ATP carrier, i.e. MCP16, is rather divergent from MCP5 and MCP15, and lacks many of the conserved sequence features found in prototypical ADP/ATP carriers (section 2.1). Especially the absence (or non-conserved deviation) of the canonical “RRRMMM” motif, the hallmark of all AACs, raised doubts regarding the predicted function of a mitochondrial ADP/ATP exchanger. The alternative sequence motif present in MCP16, i.e. “SRRMQL”, resembled more that of ATP-Mg/Pi carriers, although the overall amino acid sequence of MCP16 is more similar to known ADP/ATP carriers (Colasante *et al*., 2006). Other indications for an ATP or ADP binding function were found during the analysis of the different substrate contact points. CPI and III, both conserved in MCP5 and MCP15 (Colasante *et al.*, 2009; Kunji and Robinson, 2006), have been proposed to complex with ADP in order to “neutralize” its charges (Heidkamper *et al*., 1996; Kunji and Robinson, 2006). Especially CPII, represented by the amino acid duet G-[IVLM] was found to be widely conserved in AACs, most probably due to its role in the formation of a hydrophobic binding pocket for the diterpenoid ring of

ADP. The same CPI amino acid duet is however also conserved in all nucleotide transporters. The conserved amino acid duet has used as a differentiation key for nucleotide carriers and other MCF subgroups like for example keto-acid and amino acid carriers (Kunji and Robinson, 2006). The conservation of these signature sequences in MCP16, and the lack of the canonical "RRRMMM" motif, suggests a putative role of this MCF protein as a nucleotide carrier (Chapter II; Colasante *et al*., 2006). This putative mitochondrial nucleotide-exchange role is apparently essential for the survival of procyclic form *T. brucei*, since no MCP16 double knockout cell lines could be generated at all.

Both sequence alignment and phylogenetic reconstruction predicted that *T. brucei* MCP13 most probably functions as a GDP/GTP carrier. GDP/GTP carrier-encoding genes are only found in yeast and fungi, and so far have not been found in any metazoans or plants. Apparently, such GDP/GTP carriers are also present in some protozoa, at least in this case in some members of the Kinetoplastidae (this Chapter). Genome database analysis revealed that in all of the kinetoplastid species of which the genome sequence has been determined to a larger extend, only a single gene could be identified with significant sequence similarities to Ggc1p: the functionally characterised *S. cerevisiae* GDP/GTP carrier (Vozza *et al.*, 2004). As discussed in the introduction, the *S. cerevisiae* GDP/GTP carrier was found to be essential for iron homeostasis and the biosynthesis of Fe-S clusters, which act as essential co-factors for several important proteins in the mitochondrion and the cytoplasm (Amutha *et al.*, 2008). The presence of such a mitochondrial GDP/GTP carrier in Kinetoplastida, and the absence of mitochondrial GTP succinyl-CoA ligases in the same protozoa, indicated that such a mitochondrial GDP/GTP exchanger is most probably essential for their survival. The inability to generate any MCP13 double knockout cell lines is in agreement with such an essential role in procyclic-form *T. brucei*.

4. Conclusion

Unfortunately, the classical route of *in vitro* reconstitutions and transport assays did not result in the confirmation of the different predicted ATP/ADP, GDP/GTP or nucleotide exchange functions, leaving the precise transport functions and associated physiological roles of MCP13, MCP15 and MCP16 yet answered.

5. References

Adrian, G. S., McCammon, M. T., Montgomery, D. L. & Douglas, M. G. 1986. Sequences required for delivery and localization of the ADP/ATP translocator to the mitochondrial inner membrane. *Mol Cell Biol,* 6**,** 626-34.

Amutha, B., Gordon, D. M., Gu, Y., Lyver, E. R., Dancis, A. & Pain, D. 2008. GTP is required for iron-sulfur cluster biogenesis in mitochondria. *J Biol Chem,* 283**,** 1362-71.

Chen, X. J. 2004. Sal1p, a calcium-dependent carrier protein that suppresses an essential cellular function associated With the Aac2 isoform of ADP/ATP translocase in Saccharomyces cerevisiae. *Genetics,* 167**,** 607-17.

Colasante, C., Alibu, V. P., Kirchberger, S., Tjaden, J., Clayton, C. & Voncken, F. 2006. Characterization and developmentally regulated localization of the mitochondrial carrier protein homologue MCP6 from Trypanosoma brucei. *Eukaryot Cell,* 5**,** 1194-205.

Colasante, C., Peña Diaz, P., Clayton, C. & Voncken, F. 2009. Mitochondrial carrier family inventory of Trypanosoma brucei brucei: Identification, expression and subcellular localisation. *Mol Biochem Parasitol,* 167**,** 104-17.

Drgon, T., Sabová, L., Gavurniková, G. & Kolarov, J. 1992. Yeast ADP/ATP carrier (AAC) proteins exhibit similar enzymatic properties but their deletion produces different phenotypes. *FEBS Lett,* 304**,** 277-80.

Drgon, T., Sabová, L., Nelson, N. & Kolarov, J. 1991. ADP/ATP translocator is essential only for anaerobic growth of yeast Saccharomyces cerevisiae. *FEBS Lett,* 289**,** 159-62.

Gawaz, M., Douglas, M. G. & Klingenberg, M. 1990. Structure-function studies of adenine nucleotide transport in mitochondria. II. Biochemical analysis of distinct AAC1 and AAC2 proteins in yeast. *J Biol Chem,* 265**,** 14202-8.

Gerber, J., Neumann, K., Prohl, C., Muhlenhoff, U. & Lill, R. 2004. The yeast scaffold proteins Isu1p and Isu2p are required inside mitochondria for maturation of cytosolic Fe/S proteins. *Mol Cell Biol,* 24**,** 4848-57.

Heidkamper, D., Muller, V., Nelson, D. R. & Klingenberg, M. 1996. Probing the role of positive residues in the ADP/ATP carrier from yeast. The effect of six arginine mutations on transport and the four ATP versus ADP exchange modes. *Biochemistry,* 35**,** 16144-52.

Klingenberg, M., Winkler, E. & Huang, S. 1995. ADP/ATP carrier and uncoupling protein. *Methods Enzymol,* 260**,** 369-89.

Kolarov, J., Kolarova, N. & Nelson, N. 1990. A third ADP/ATP translocator gene in yeast. *J Biol Chem,* 265**,** 12711-6.

Krämer, R. & Klingenberg, M. 1977. Reconstitution of adenine nucleotide transport with purified ADP, ATP-carrier protein. *FEBS Lett,* 82**,** 363-7.

Kunji, E. R. S. & Robinson, A. J. 2006. The conserved substrate binding site of mitochondrial carriers. *BBA - Bioenergetics,* 1757**,** 1237-1248.

Lawson, J., Gawaz, M., Klingenberg, M. & Douglas, M. 1990. Structure-function studies of adenine nucleotide transport in mitochondria. I. Construction and genetic analysis of yeast mutants encoding the ADP/ATP carrier protein of mitochondria. *J Biol Chem,* 265**,** 14195-14201.

Long, S., Jirku, M., Mach, J., Ginger, M. L., Sutak, R., Richardson, D., Tachezy, J. & Lukes, J. 2008a. Ancestral roles of eukaryotic frataxin: mitochondrial frataxin function and heterologous expression of hydrogenosomal Trichomonas homologues in trypanosomes. *Mol Microbiol,* 69**,** 94-109.

Long, S., Vavrova, Z. & Lukes, J. 2008b. The import and function of diatom and plant frataxins in the mitochondrion of Trypanosoma brucei. *Mol Biochem Parasitol,* 162**,** 100-4.

Löytynoja, A. & Milinkovitch, M. C. 2001. Molecular phylogenetic analyses of the mitochondrial ADP-ATP carriers: the Plantae/Fungi/Metazoa trichotomy revisited. *Proc Natl Acad Sci USA,* 98**,** 10202-7.

Müller, V., Basset, G., Nelson, D. R. & Klingenberg, M. 1996. Probing the role of positive residues in the ADP/ATP carrier from yeast. The effect of six arginine mutations of oxidative phosphorylation and AAC expression. *Biochemistry,* 35**,** 16132-43.

Palmieri, F., Indiveri, C., Bisaccia, F. & Iacobazzi, V. 1995. Mitochondrial metabolite carrier proteins: purification, reconstitution, and transport studies. *Methods Enzymol,* 260**,** 349-69.

Powell, S. J., Medd, S. M., Runswick, M. J. & Walker, J. E. 1989. Two bovine genes for mitochondrial ADP/ATP translocase expressed differences in various tissues. *Biochemistry,* 28**,** 866-73.

Przybyla-Zawislak, B., Dennis, R. A., Zakharkin, S. O. & McCammon, M. T. 1998. Genes of succinyl-CoA ligase from Saccharomyces cerevisiae. *Eur J Biochem,* 258**,** 736-43.

Robinson, A. J. & Kunji, E. R. S. 2006. Mitochondrial carriers in the cytoplasmic state have a common substrate binding site. *Proc Natl Acad Sci USA,* 103**,** 2617-22.

Smith, C. P. & Thorsness, P. E. 2008. The molecular basis for relative physiological functionality of the ADP/ATP carrier isoforms in Saccharomyces cerevisiae. *Genetics,* 179**,** 1285-99.

Stehling, O., Sheftel, A. D. & Lill, R. 2009. Chapter 12 Controlled expression of iron-sulfur cluster assembly components for respiratory chain complexes in mammalian cells. *Methods Enzymol,* 456**,** 209-31.

Studier, F. W. 2005. Protein production by auto-induction in high-density shaking cultures. *Protein Expres Purif,* 41.

Vozza, A., Blanco, E., Palmieri, L. & Palmieri, F. 2004. Identification of the mitochondrial GTP/GDP transporter in Saccharomyces cerevisiae. *J Biol Chem,* 279**,** 20850-7.

#
#

#

Chapter VII.
General Discussion and Conclusions

Chapter VII. General Discussion and Conclusions

The ADP/ATP carrier is the mitochondrial ATP gateway out of the mitochondrion. This protein in *Trypanosoma brucei* is represented by MCP5, and its role was proved by sequence analysis, phylogenetic reconstruction, gene knockout studies and mitochondrial ATP production assays with digitonin-permeabilized *T. brucei*.

In a mitochondrion the size of the one in the procyclic form of *Trypanosoma brucei*, seems obvious that the AAC must be quite ubiquitous and abundant. MCP5 depletion from the procyclic form of the parasite seems to be deleterious, as observed by the impossibility to obtain a conventional knockout. This conditional knockout would loose the repression of its tetracycline rescue copy, just a few days after depletion. Moreover, the carbon consumption and metabolites production profiles present a shift in the fermentative process that not just confirms the redirection of carbons out of the mitochondrion, but also implies alternative pathways that produce ATP for cellular processes as well as the maintenance of the redox and energy balance inside the glycosome and the mitochondrion.

It has been proved that glucose remodels the energy metabolism of these parasites and, it is apparent that in-vitro conditions the parasite prefers the carbohydrate to proline when in presence of both (Coustou *et al.*, 2008). In this remodelling, glucose is mainly metabolized via glycosome, re-entering the organelle for PEPCK and PPDK activity, and the ultimate production of succinate (Ebikeme *et al.*, 2010; Coustou *et al.*, 2008). It is also widely accepted that the TCA cycle does not function as a cycle and that its main function does not mainly imply energy generation (van Weelden *et al*., 2005). Despite some inconsistencies in the statistical significance of the excretion of succinate profile for GDMP, the data for succinate production in the MCP5 KO grown in NMP and MPglu, suggest a shift in the metabolites excretion pattern that seems to be modulated by the presence of glucose. The fact that succinate is still produced under low-glucose conditions raises the question to whether this succinate is produced in the mitochondrion or the glycosome. Since in our experimental design, there is no way of determining the site of origin of this metabolite, no final conclusions can be derived. However, the fact that there is no MCP5 in the uninduced MCP5 KO, leads to think that a redirection of carbons might be taking place in the cell, as there would be no way for the mitochondrial metabolism to continue if there is no flux of the ATP produced in the organelle. We propose that the only way the carbons can be redirected in the mitochondrion,

without the ultimate production of succinate inside this organelle (which would be impaired because of the ATP/ADP blockage) is through the TCA cycle in reverse mode, towards the formation of malate, and its subsequent export into the cytosol. An ideal methodology in order to determine the site of origin of the succinate in the cell would be the use of radioactively labelled proline, for the subsequent detection of excretion products through ^{13}C NMR spectroscopy (Coustou *et al.*, 2008).

The other hypothesis produced out of these results is the highly possible implication of gluconeogenesis. Since there is no glucose in the media the parasite has an absolute requirement to continue glycosomal pathways functioning, as well as the maintenance of the redox balance. Also, the parasite requires carbohydrates for the production of sugar nucleotides involved in the remodelling of GPI anchors, essential for procyclins production.

The KO growth curves in presence of glucose reveal the mutant cell line consumes as much glucose as the WT, whereas its growth rate is never achieved, even when in presence of an active rescue copy of the transporter. This growth arrest might be structurally related to the rescue copy of MCP5. The conditional KO bears an active rescue copy with a myc-tag in its n-terminus, which might be involved in protein interactions signalling that cannot be attained. The ADP/ATP carrier has been characterized in various protein complexes, structurally interacting with proteins and lipids. As discussed before a mitochondrion the size of the one found in procyclic form *T. brucei* must be interacting with other structures for the efficient transport of metabolites and intermediates. The structural changes that the myctag might attain could result in a lack of recognition in protein-protein interactions key for signalling, independently of the protein activity. This behaviour could also result in probable microenvironments for the AAC, for protein-protein interaction and channelling to occur. This phenomenon makes sense in such a big mitochondrion where diffusion of substrates would ablate rapid metabolic shifts, therefore making very feasible the existence of membrane microdomains that gather known protein complexes for channelling (Zhang *et al*., 2002). This has been proved in other organisms, from yeast to humans and particularly involving the AAC, in view of its very important metabolic energy-providing role as well as in apoptosis and programmed cell death (Beutner *et al.*, 1996; Vyssokikh *et al.*, 2001; Crompton, 1999; Chiara *et al.*, 2008).

The structural differences of the mitochondrion of procyclic form *T. brucei* also indicate towards the composition of its membranes, very important data for the

future reconstitution of the carriers into liposomes. Although the activity of the AAC in this work was demonstrated via mitochondrial assays, the ultimate assay to demonstrate the carrier's activity requires an isolated purified protein. This implies that a substantial change in the methodological approach for the assessment of the isolated carried must be undertaken. Klingenberg (2001) demonstrated that the AAC from *Neurospora crassa* expressed in *Escherichia coli* presented challenges for reconstitution. Moreover, drastic results could be obtained depending whether different strains of the same bacteria were used. These data posses as an example of the great amount of factors involved in the reconstitution process, many of which are determined from the production of the protein itself. The appropriateness of the insect cells for the expression of eukaryotic membrane proteins, particularly mitochondrial carrier proteins, has been demonstrated before (Madeo *et al.*, 2009). However, the approach did not seem suitable for the AAC of *Trypanosoma brucei*. As stated before, the composition and structure the mitochondrion of *Trypanosoma brucei* has never been studied. Several factors like phospholipid composition and redox state of the proteins might be playing a key role in the functional insertion of proteins in the membrane of this mitochondrion that are unknown to date.

All the points raise in the above paragraph imply the need to work with the mitochondrial membranes of *T. brucei* itself. The use of *T. brucei* originated material would solve the need for futile tryouts of conditions that otherwise might take excruciating efforts to bare results, without mentioning that there is very little evidence of the active state of the protein. This approach can be overtaken in two possible ways: 1) isolating mitochondrial-enriched fractions, by differential centrifugation, followed by continuous or discontinuous isopycnic gradients. These mitochondrial-enriched fractions may be used as starting material for the reconstitution process. The reconstitution process here would be a "fused-membranes" approach, and has been done in the past by other authors (van der Giezen *et al.*, 2002). 2) Using *T. brucei* mitochondrial-enriched fractions for purification of the natural protein, under native conditions. Although the main purification method that Klingenberg used for the isolation of the AAC from beef heart mitochondria (Klingenberg *et al.*, 1995), i.e. hydroxyapatite chromatography, does not seem to be effective for MCP5 (results not shown), other chromatography methods like hydrophobic chromatography (phenyl or octyl sepharose chromatography) in combination with gel filtration chromatography, might serve the purpose of protein isolation from the parasite. It is however known that natural protein purification is a very difficult and unpredictable process, that might take

years to achieve as well as implies the need for great amounts of staring material to achieve detectable concentrations of protein useful for subsequent reconstitution.

Although the protein-protein interactions described to date for known AACs mostly involve members of the respiratory chain and components of the Mitochondrial Transition Pore, as well as some very well documented affiliation with the phospholipid cardiolipin, it should not be discarded the possibility that MCP5 might be interacting with other MCF proteins as well. The relationship with the phosphate carrier (Traba *et al*., 2009) has been documented in yeast, but the since *Trypanosoma brucei* mitochondrion differs greatly from those organelles in other species, this possibility might be even wider. MCP15 and MCP16 have not had a role attained yet, but the possibility of their involvement in procyclic form *T. brucei* metabolism should not be discarded. MCP16 particularly, with its high divergence from classic AACs, as well as the impossibility to obtain a double KO of this protein, place it in a very special place regarding metabolic regulation and/or signalling. Although this role remains to be evidenced, it opens great possibilities for metabolic pathway regulation, in the procyclic form and other life stages of the parasite.

References

Beutner, G., Ruck, A., Riede, B., Welte, W. & Brdiczka, D. 1996. Complexes between kinases, mitochondrial porin and adenylate translocator in rat brain resemble the permeability transition pore. *FEBS Lett,* 396**,** 189-95.

Chiara, F., Castellaro, D., Marin, O., Petronilli, V., Brusilow, W. S., Juhaszova, M., Sollott, S. J., Forte, M., Bernardi, P. & Rasola, A. 2008. Hexokinase II detachment from mitochondria triggers apoptosis through the permeability transition pore independent of voltage-dependent anion channels. *PLoS ONE,* 3**,** e1852.

Coustou, V., Biran, M., Breton, M., Guegan, F., Riviere, L., Plazolles, N., Nolan, D., Barrett, M. P., Franconi, J. M. & Bringaud, F. 2008. Glucose-induced remodeling of intermediary and energy metabolism in procyclic Trypanosoma brucei. *J Biol Chem,* 283**,** 16342-54.

Crompton, M. 1999. The mitochondrial permeability transition pore and its role in cell death. *Biochem. J.,* 341**,** 233-249.

Ebikeme, C., Hubert, J., Biran, M., Gouspillou, G., Morand, P., Plazolles, N., Guegan, F., Diolez, P., Franconi, J.-M., Portais, J.-C. & Bringaud, F. 2010. Ablation of succinate production from glucose metabolism in the procyclic trypanosomes induces metabolic switches to the glycerol 3-phosphate/dihydroxyacetone phosphate shuttle and to proline metabolism. *J Biol Chem,* 285**,** 32312-24.

Heimpel, S., Basset, G., Odoy, S. & Klingenberg, M. 2001. Expression of the mitochondrial ADP/ATP carrier in Escherichia coli. Renaturation, reconstitution, and the effect of mutations on 10 positive residues. *J Biol Chem,* 276**,** 11499-506.

Klingenberg, M., Winkler, E. & Huang, S. 1995. ADP/ATP carrier and uncoupling protein. *Methods Enzymol,* 260**,** 369-89.

Madeo, M., Carrisi, C., Iacopetta, D., Capobianco, L., Cappello, A. R., Bucci, C., Palmieri, F., Mazzeo, G., Montalto, A. & Dolce, V. 2009. Abundant expression and purification of biologically active mitochondrial citrate carrier in baculovirus-infected insect cells. *J Bioenerg Biomembr,* 41**,** 289-97.

Traba, J., Satrústegui, J. & Arco, A. d. 2009. Transport of adenine nucleotides in the mitochondria of Saccharomyces cerevisiae: Interactions between the ADP/ATP carriers and the ATP-Mg/Pi carrier. *Mitochondrion,* 9**,** 79-85.

van der Giezen, M., Slotboom, D., Horner, D., Dyal, P., Harding, M., Xue, G., Embley, T. & Kunji, E. 2002. Conserved properties of hydrogenosomal and mitochondrial ADP/ATP carriers: a common origin for both organelles. *EMBO J,* 21**,** 572-579.

van Weelden, S. W. H., van Hellemond, J. J., Opperdoes, F. R. & Tielens, A. G. M. 2005. New functions for parts of the Krebs cycle in procyclic Trypanosoma brucei, a cycle not operating as a cycle. *J Biol Chem,* 280**,** 12451-60.

Vyssokikh, M. Y., Katz, A., Rueck, A., Wuensch, C., Dörner, A., Zorov, D. B. & Brdiczka, D. 2001. Adenine nucleotide translocator isoforms 1 and 2 are differently distributed in the mitochondrial inner membrane and have distinct affinities to cyclophilin D. *Biochem J,* 358**,** 349-58.

Zhang, M., Mileykovskaya, E. & Dowhan, W. 2002. Gluing the respiratory chain together. Cardiolipin is required for supercomplex formation in the inner mitochondrial membrane. *J Biol Chem,* 277**,** 43553-6.

Appendix

1. MEM-Pros (Minimum Essential Medium for procyclic Trypanosomes)

	g/10L
$CaCl_2$ x $2H_2O$	2.65
KCl	4.0
$MgSO_4$ x $7H_2O$	2.0
NaCl	68.0
NaH_2PO_4 x H_2O	1.40
HEPES	71.40
L-Arg-HCl	1.26
L-Cys-Cys	0.24
L-Gln	2.92
L-His-HCl x H_2O	0.42
L-Ile	0.52
L-Leu	0.52
L-Lys	0.73
L-Met	0.15
L-Phe	1.0
L-Thr	0.48
L-Try	0.10
L-Tyr	1.0
L-Val	0.46
L-Pro	6.0
Adenosin	0.12
Ornithin-HCl	0.10

Components are dissolved in 4 L ultra-pure H_2O. pH is adjusted to 7.4 with NaOH. 100 mL MEM non-essential amino acids, 100 mL MEM-vitamins and 0.1 g Phenol Red are then added to the preparation. pH is measured again and the media is brought to 10 L volume with ultra pure H_2O. After filter-sterilizing, the media is divided in 450 mL aliquots in sterile glass bottles and placed at 4°C.

2. Hemin stock preparation

250 mg hemin are dissolved in 100mL NaOH and autoclaved. Stock is kept at 4°C.

3. HMI-9 medium. Bloodstream trypanosomes culture media.

g/10L	
Iscove's modified Dulbecco's medium	176.6
Sodium carbonate	30.24
Hypoxanthine	1.36
Sodium pyruvate	1.10
Thymidine	0.39
Bathocopper sulfonate	0.28

Components are mixed and brought to pH 6.3. The media is filter-sterilized, divided in 400 mL aliquots in sterile glass bottles and kept at -20°C. Before use, the medium is completed with 40 mL FCS, 5mL 150mM L-Cysteine solution, 5 mL 0.14% β-mercaptoethanol solution and 5 mL Penicillin/Streptomycin stock (5000 U/mL, 5mg/mL).

4. Oligos used for all cloning procedures in this work

oHU	Oligo name	Sequence	Construct designed for	Gene or target region	Restric. Site
20	5prsacMCP25koFor	agggtgagctctttcacacgtattgacgggaacaaatgagtg	KO constructs	5' UTR MCP15	SacI
21	5prSpeMCP25koRev	acctgcaactagtctgtccctctgctcatagccccgcattc	KO constructs	5' UTR MCP15	SpeI
22	3prBamMCP25koFor	ctcaccaggatcccttgtgtgtgatgggtcctgtgctgag	KO constructs	3' UTR MCP15	BamHI
23	3prApaMCP25koRev	ccttgggcccgagacaaggcgacgaagaacagaacagg	KO constructs	3' UTR MCP15	ApaI
31	5prSacTbcp5koFor	agggtgagccgttctcagaagtgacttctgtcgcc	KO constructs	5' UTR MCP5	SacI
32	5prSpeTbcp5koRev	acctgcaacagtcatctttttttcttgtagccacg	KO constructs	5' UTR MCP5	SpeI
33	3prBamTbcp5koFor	ctcaccaggatccgtgccgttgctggtttttatttg	KO constructs	3' UTR MCP5	BamHI
34	3prApaTbcp5koRev	ccttgggcccctcctcaggcacagccttaccgtttt	KO constructs	3' UTR MCP5	ApaI
46	MCP27_5UTR_FOR	ccgagctcacgtaactacagagtgtttccggttgctgtct	KO constructs	5' UTR MCP16	SacI
47	MCP27_5UTR_REV	cgcactagtactcgccgagatctgaattgatgacagat	KO constructs	5' UTR MCP16	SpeI
48	MCP27_3UTR_FOR	atgggatccagttgttagtcgccgcatgcaactcactgatt	KO constructs	3' UTR MCP16	BamHI
49	MCP27_3UTR_REV	tatagggcccgatcatcaagacttgtacgcactatcga	KO constructs	3' UTR MCP16	ApaI
50	25_forw_NdeI_orf	taacatatggttggtggcgatggtgaggagcccgggct	pET16b (his-tag expression)	MCP15 orf	NdeI
51	25_rev_BamHI_orf	tatggatcctcaggagccggtaaaaaccacatatagag	pET16b (his-tag expression)	MCP15 orf	BamHI
52	27_forw_NdeI_orf	tatcatatggatcacgatcaactatagactctccc	pET16b (his-tag expression)	MCP16 orf	NdeI
53	27_rev_BamHI_orf	taggatccgaactgcatcgccatttctgggccgtttag	pET16b (his-tag expression)	MCP16 orf	BamHI
106	cp5_sacI_fw	atgagctcagatgacggataaaaagcgg	ptrcHisA (his-tag expression)	MCP5 orf	SacI
107	cp5_ecorI_rev	acgaattcctaattcgatctgcgccact	ptrcHisA (his-tag expression)	MCP5 orf	EcoRI
108	cp13_sacI_fw	atgagctcagatgtcatccgaacacgcacc	ptrcHisA (his-tag expression)	MCP13 orf	SacI
109	cp13_ecorI_rev	acgaattcttaatgccgaaccacccctct	ptrcHisA (his-tag expression)	MCP13 orf	ecoRI
110	cp25_sacI_fw	atgagctcagatggttggtggcgatggtga	ptrcHisA (his-tag expression)	MCP15 orf	SacI
111	cp25_ecorI_rev	acgaattctcaggcagccggtaaaaacca	ptrcHisA (his-tag expression)	MCP15 orf	EcoRI
112	cp27_sacI_fw	atgagctcagatggatcacgatcaactatac	ptrcHisA (his-tag expression)	MCP16 orf	SacI
113	cp27_ecorI_rev	acgaattcctaaacggcccagaaatggcg	ptrcHisA (his-tag expression)	MCP16 orf	EcoRI
114	cp5_sacI_fw_new	tatgagctcatgacggataaaaagcgg	ptrcHisA (his-tag expression)		SacI
115	cp25_sacI_fw_new	tatgagctcatggttggtggcgatggtga	ptrcHisA (his-tag expression)		SacI

116	mcp27_fw_bamHI_o	aatggatccgaatggatcacgatcaactatacgactct	ptrcHisC (his-tag expression)	MCP16 orf	BamHI
117	mcp27_rv_hindIII	ccgaagcttctaaacggcccagaaatggcgatgc	ptrcHisC (his-tag expression)	MCP16 orf	HindIII
118	mcp13_fw_BamHi_o	aatggatccgaatgtcatccgaacacgcaccggtg	ptrcHisC (his-tag expression)	MCP13 orf	BamHI
119	mcp13_rv_EcorRi_o	cgcgaattcttaatgccgaaccacccctctttttt	ptrcHisC (his-tag expression)	MCP13 orf	HindIII
120	forw_mcp13_pcr	tatgggatcgctacaagcacaacaacat	upstream 5'utr target region	MCP13 5'UTR (upstream)	-
121	forw_mcp5_pcr	gcattgtttcacccgttttcaggttctcagaagt	upstream 5'utr target region	MCP5 5'UTR (upstream)	-
122	forw_mcp25_pcr	cttaaggtgtcatattggtttgctgcaggggcct	upstream 5'utr target region	MCP15 5'UTR (upstream)	-
123	forw_mcp27_pcr	gtggacgtaactacagcgagatgttcattgttaccgg	upstream 5'utr target region	MCP16 5'UTR (upstream)	-
124	13_3utr_apaI_rev	tatgggcccattaacgtacccccctccctc	KO constructs	MCP13 3'UTR	ApaI
125	13_3utr_bamhI_fw	tctggatccgaggatcaagtcatgtgatacga	KO constructs	MCP13 3'UTR	BamHI
126	13_5utr_sacI_fw	catgagctccgcatacgtgtgagtgtgtgac	KO constructs	MCP13 5'UTR	SacI
127	13_5utr_speI_rev	cgcactagttcacgtgctgaacgatcccttccttt	KO constructs	MCP13 5'UTR	SpeI
128	5_ef	tctgaattcatgacggataaaaagcgggaaccg	pac28 (his-tag expression)	MCP5 orf	EcoRI
129	5_hr	ttgaagcttctaattcgatctggccactccac	pac28 (his-tag expression)	MCP5 orf	HindIII
130	13_bf	gacggatccatgtcaccgaacacgcaccggtggta	pac28 (his-tag expression)	MCP13 orf	BamHI
131	13_sr	gcggtcgacttaatgccgaaccacccctctt	pac28 (his-tag expression)	MCP13 orf	SalI
132	5_pIvex_bHI_rv	aatggatccctaattcgatctgcgccactccac	pIvex2.4 (his-tag expression)	MCP5 orf	BamHI
133	5_pIvex_NotI_fw	aatgcggcgcacggataaaagcgggaaccggcc	pIvex2.4 (his-tag expression)	MCP5 orf	NotI
134	13_pIvex_NotI_fw	tatgcggccgctcatccgaacacgcaccggtggtag	pIvex2.4 (his-tag expression)	MCP13 orf	NotI
135	13_pIvex_BHI_rv	tagggatccttaatgccgaaccacccctctt	pIvex2.4 (his-tag expression)	MCP13 orf	BamHI
177	pFASTBacHT For	cggattattcataccgtcccaccatc	pFastBac HT		
178	pFASTBacHT Rev	caagtaaaacctctacaaatgtggtatgg	pFastBac HT		
182	pUC/M13fw	cccagtcacgacgttgtaacagg	Bacmid insert detection		
183	pUC/M13rv	agcggataacaatttcacacagg	Bacmid insert detection		
	TbCP5-BamHI-Rev	gcttgcaggatccattcgatctgcgccactccacataaatgg	pHD1701 (myc-tag expression)	MCP5 orf	BamHI
	TbCP5a-HindIII-For	ggacggaagcttaccatggcggataaaaagcgggaaccgg	pHD1701 (myc-tag expression)	MCP5 orf	HindIII
	TbCP5a-NdeI-For	ggacttcatatgacggataaaaagcgggaaccgg	pET16b (his-tag expression)	MCP5orf	NdeI
	TbCP13-HpaI-For	ggacgggttaacatggcatccgaacacgcaccggtggtagc	pHD1700 (myc-tag expression)	MCP13 orf	HpaI
	TbCP13-BamHI-Rev	gcttgcaggatccatgccgaaccacccctctttttcc	pHD1700 (myc-tag expression)	MCP13 orf	BamHI
	TbCP25-HindIII-For	ggacggaagcttaccatggttggtggcgatggtgaggag	pHD1701 (myc-tag expression)	MCP15 orf	HindIII

	TbCP25-HpaI-Rev	gcttgcagttaacggcagccggtaaaaaccacatatagagtgac	pHD1701 (myc-tag expression)	MCP15 orf	HpaI
	TbCP27a-BamHI-Rev	gcttgcaggatccaacggcccagaaatggcgatgcagttccag	pHD1701 (myc-tag expression)	MCP16 orf	BamHI
	TbCP27a-HindIII-For	ggacggaagcttaccatggatcacgatcaactatacgactctccc	pHD1701 (myc-tag expression)	MCP16 orf	HindIII

Acknowledgements

I did not perform this work in a vacuum. I owe a great deal of gratitude to a number of people who, in one way or another, contributed to the realization of this work.

Many thanks go to:

Dr. Frank Voncken, my boss. I greatly appreciate all the time and effort you invested in putting up with my chaotic mind. It has been an honour sharing the bench with you.

Dr. Claudia Colasante, colleague and friend. Thanks for all the muffins, sausage rolls, cakes, breads, pizza, discussions, fights, shouting and shopping trips. We'll make it to those carnivals someday.

Mrs. Cath Wadforth, our lab mother. Pipetting away would have never been as great without your elephant jokes, the smell of fish and the Thursday donuts. You're awesome.

Fei Gao, Chan Kuan Yoow, Wen Liu, Mohammed Bessat and Klaus Ersfeld for sharing the lab and the laughter.

Dr. Camille Ettellaie, for kindly lending us her lab's luminometer.

Dr. Graham Scott, Head of Department, for dealing wisely with bureaucracy.

Ms. Maggie Harley for all the support with the re-activation of the hot lab. Mrs. Joy Miller for always sharing a smile and Chris Park for always sharing a bad joke. Extra special thanks to Ms. Val Fairhurst, the washing machine and the autoclaves have never been the subject of so much amusement.

Sir Stuart McKay, for all your amazing stories and ever-so encouraging words. You rock.

My family, for all their support and trust.

Tim Morgan, for being there.

To Science, for being so much like science-fiction.

#